GEOLOGY, GEOCHEMISTRY AND METALLOGENY OF THE ARCHEAN FLORENCE LAKE GROUP AND ASSOCIATED ULTRAMAFIC AND TRONDHJEMITIC ROCKS, NAIN PROVINCE, LABRADOR

TERRY D. BRACE, B.Sc. (Honours)

NOTICE

The quality of this microform is heavily dependent upon the quality of the original thesis submitted for microfilming. Every effort has been made to ensure the highest quality of reproduction possible.

If pages are missing, contact the university which granted the degree.

Some pages may have indistinct print especially if the original pages were typed with a poor typewriter ribbon or if the university sent us an inferior photocopy.

Reproduction in full or in part of this microform is governed by the Canadian Copyright Act, R.S.C. 1970, c. C-30, and subsequent amendments.

AVIS

La qualité de cette microforme dépend grandement de la qualité de la thèse soumise au microfilmage. Nous avons tout fait pour assurer une qualité supérieure de reproduction.

S'il manque des pages, veuillez communiquer avec l'université qui a conféré le grade.

La qualité d'impression de certaines pages peut laisser à désirer, surtout si les pages originales ont été dactylographiées à l'aide d'un ruban usé ou si l'université nous a fait parvenir une photocopie de qualité inférieure.

La reproduction, même partielle, de cette microforme est soumise à la Loi canadienne sur le droit d'auteur, SRC 1970, c. C-30, et ses amendements subséquents.

Geology, Geochemistry and Metallogeny of the Archean Florence Lake Group and Associated Ultramafic and Trondhjemitic Rocks, Nain Province, Labrador

By

Terry D. Brace, B.Sc. (Honours)

A thesis submitted to the School of Graduate Studies
in partial fulfillment of the requirements for the degree of
Master of Science

Department of Earth Sciences
Memorial University of Newfoundland
(December, 1990)

St. John's Newfoundland

ISBN 0-315-65325-6

ABSTRACT

The Florence Lake Group (FLG) forms a 65 km-long northeast-trending greenstone belt within the southernmost Archean Nain Province, Labrador. The FLG contains a bimodal volcanic sequence consisting dominantly of mafic metavolcanic schists, flows and pillow lavas, and minor synvolcanic sills. Felsic metavolcanic and siliceous metasedimentary rocks are less extensive. The FLG is intruded by elongate bodies of strongly serpentinized peridotite, which have undergone various degrees of carbonatization. Massive, gneissic and mylonitic trondhjemite and tonalite of the Kanairiktok Intrusive Suite envelop and intrude both the FLG and the metaperidotites. All units are folded and have undergone middle greenschist facies metamorphism. Post-tectonic Proterozoic diabase and gabbro dykes, informally referred to as the Florence Lake (FL) dykes, cut all other lithologies.

Based on the relative depletion of LREE, FLG basalts can be divided into two groups: (1) Group 1 has flat chondrite-normalized REE patterns; (2) Group 2 is slightly LREE-depleted. The FLG basalts are similar to typical N-MORB, whereas the felsic supracrustal rocks and Kanairiktok trondhjemites display classic arc (or continental crust) signatures. Both lithological and geochemical characteristics are consistent with the FLG having been deposited subaqueously in a back-arc basin which lay proximal to a volcanic arc and/or continental margin.

The Proterozoic FL diabase and gabbro dykes appear to be of two ages: (1) an older set of north- to northeasterly-

trending gabbro dykes, viz., the FL gabbro dykes; and (2) an apparently younger set of east-west-trending smaller diabase dykes, viz., the FL diabase dykes. The FL gabbro dykes may be equivalent to the Harp dykes further to the north; however, the FL diabase dykes are chemically more evolved than other Proterozoic mafic suites in Labrador, with the exception of the Nain HP (high P_2O_5) dykes, with which they are very similar.

The metaperidotites which intrude the FLG are enriched in Mg, Ni and Cr, and appear to consist dominantly of serpentinized dunites. Fe-Ni-Cu (+ minor PGE) sulphides hosted by meta-ultramafic rocks at the Baikie showings are interpreted to be magmatic in origin, and concentrations of PGE, Ni and Cu indicate that the metaperidotites south of Florence Lake and the meta-ultramafic xenoliths at the Baikie showing are komatiitic.

Magnesite-quartz rocks southeast of Florence Lake are chemically similar to the metaperidotites. The alteration is somewhat similar to that associated with Archean lode gold deposits. However, abundant quartz veins which infill tension gashes in the rocks appear to have formed in situ due to the carbonatization process, and shear-related silicification and/or sulphidation is absent.

Although metavolcanic and metasedimentary rocks of the FLG host many thin syngenetic pyrite horizons and several small base-metal sulphide occurrences, no significant mineralization has been discovered.

ACKNOWLEDGEMENTS

Financial support for this project was provided by the Geological Survey of Canada through the Canada-Newfoundland Mineral Development Agreement Project "Metallogeny of the Central Mineral Belt of Labrador". Additional financial support was provided through a Northern Scientific Training Program (NSTP) grant to the author. Logistical support was provided by the Newfoundland Department of Mines and Energy through W. Tuttle in Goose Bay and M. Batterson at Moran Lake.

The author would especially like to acknowledge John Clarke, a hard working field assistant who showed a keen eye and maintained his interest under oftentimes adverse working conditions. M. Dredge and M. O'Dea also assisted on several traverses. I am grateful to Dr. Derek Wilton who originally suggested the project to me, and helped with discussions and suggestions throughout the course of the study. M. Batterson and his crew at Moran Lake are thanked for several home-cooked meals, and a special thanks goes out to A. Simpson who willingly shared his potent home brew to a thirsty Florence Lake crew.

S. Gandhi supplied copies of I. Ermanovics and M. Raudsepp's (1979) GSC map and other pertinent background material for the study. Thanks go out to I. Ermanovics for his useful suggestions prior to the study, and Dr. D. Wilton, S. Gandhi, R. Wardle, J. Clarke and A. Simpson for discussions during the field season. Geochemical analyses at MUN were carried out by G. Andrews (major elements - AA), G. Veinott (trace elements - XRF), D. Healy (REE - ICP-MS) and S. Jackson (PGE and Au - ICP-MS).

Finally, I would especially like to thank my parents and family for their support and encouragement.

TABLE OF CONTENTS

LIST OF FIGURES

Figure

LIST OF TABLES

Table

LIST OF PLATES

PLATE

CHAPTER 1. INTRODUCTION

1.1. LOCATION AND ACCESS

The study area is located near the coastal portion of central Labrador, approximately 170 km north-northwest of Goose Bay and 80 km southwest of the coastal village of Hopedale (Figure 1.1). The area covers approximately 100 km^2 within NTS map sheet 13 K/15, and is bounded by latitudes 54°45'N and 54°57'N, and longitudes 60°43'W and 60°54'W.

Access can be gained by helicopter, or small fixed-wing aircraft equipped with floats or skis, all of which can be chartered in Goose Bay. Ice break-up on lakes in the area usually begins around mid-June. Summers are short and generally cool; however, daily temperatures can reach maximums in excess of 30°C.

The best location for a campsite in the vicinity of the study area is on a small sandy spit near the southern end of Florence Lake; the shorelines of lakes and rivers elsewhere are invariably scattered with large boulders. Relatively large northeast-trending ridges located northwest and southeast of Florence Lake make access to these areas somewhat difficult.

1.2. PHYSIOGRAPHY, VEGETATION AND OUTCROP

The map area is generally characterized by two northeast-trending outcrop upland areas dissected by the Florence Lake valley. The area is bounded to the east by the broad low-lying Kanairiktok River valley, and to the west by the Ugjoktok

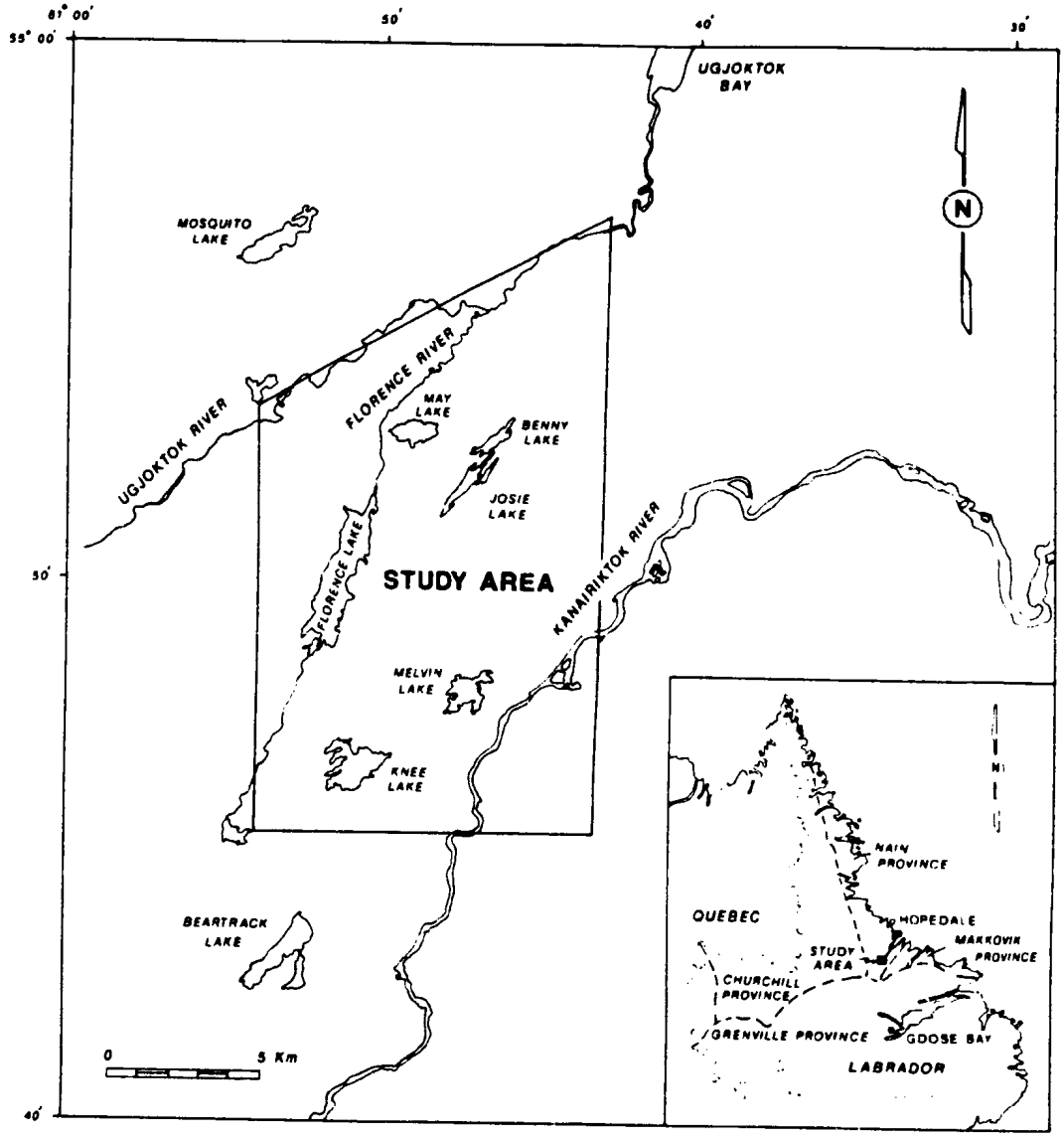

Figure 1.1. Location and extent of the Florence Lake study area. Insert map shows the tectonic province subdivisions (after Taylor, 1971) of the Labrador portion of the Canadian Shield.

River valley (Figure 1.1). Florence Lake lies at an elevation of 115 m above sea level, while upland areas generally rise 100 to 200 m above the lake (i.e., 200-300 m above sea level). A ridge west of Florence Lake maintains the maximum elevation in the map area (340 m above sea level).

The Kanairiktok River is the largest river in the area and meanders in a general northeasterly direction through the Kanairiktok River valley, which is located approximately 8 km east of Florence Lake. The Ugjoktok and Florence rivers merge about 7 km northeast of Florence Lake and then flow northeastward into Ugjoktok Bay.

Areas underlain by granitoids of the Kanairiktok Intrusive Suite are invariably less vegetated than those underlain by the Florence Lake Group, and geological contacts between the two units can generally be traced with confidence on aerial photographs. The Kanairiktok Intrusives are very well exposed, commonly only covered by low bushes and mosses, with isolated small boggy areas between outcrop ridges. In contrast, the Florence Lake Group is less well exposed, and appears on aerial photographs as a distinct, partially tree-covered, wedge-shaped area bounded to the east by the Kanairiktok Valley and to the west by the relatively barren Kanairiktok intrusives. The area underlain by the Florence Lake Group east of Florence Lake consists of alternating outcrop ridges and hills, and spruce and moss-covered hillsides and valleys. Thick alder groves are common on hillsides and around streams.

During the Pleistocene Wisconsin glaciation, ice flow directions were northeastward, and Batterson et al. (1988) note that north of the Kanairiktok Valley, these latest flow directions are often the only ones recorded. According to Batterson et al. (1988), individual sections in the Kanairiktok Valley expose outwash sand and gravel in excess of 20 m thick. Red-coloured, rhymically layered marine sediments believed to have been derived from the Seal Lake Group mudstones to the southwest (Thompson and Klassen, 1986), underlie these outwash sediments. Abundant outwash sands and gravels, and large boulders are also abundant south of Florence Lake.

1.3. PREVIOUS WORK

In 1959, Lundberg Exploration Limited, on behalf of British Newfoundland Exploration Limited (BRINEX), conducted a 777 km² airborne magnetometer and electromagnetic survey that included the Florence Lake area (Wilson, 1959). Flight lines were orientated northwest-southeast with 400 m spacings.

In evaluating the airborne survey, Wilson (1959) considered areas of low, moderate, and high magnetic intensity to roughly correlate with areas underlain by granitic, mafic volcanic, and ultramafic rocks, respectively. Magnetic anomalies which cross the regional trend were considered to represent diabase dykes. Numerous small EM conductors were recognized however none of those considered to be sulphide-bearing were very large, and most of the conductivity was

believed to be caused by pyrite. Wilson suggested that there might be some chalcopyrite and/or gold in pyritic zones, and in fractures and shear zones, and that the magnetic conductors might contain asbestos. Ultimately, Wilson (1959) concluded that there was little likelihood of locating a significant base-metal deposit within the area surveyed.

Following the airborne survey, between 1959 and 1962 BRINEX in joint venture with Asbestos Corporation carried out an extensive exploration program throughout the 'Florence Lake' or 'Ugjoktok' greenstone belt (Roderick, 1959a,b; Hansuld, 1959; Ellingwood, 1959; Mayor and Mann, 1960; Piloski, 1960, 1962, 1963). This work included geological mapping, prospecting, soil and stream sediment sampling, and ground geophysical surveys.

Roderick (1959a) carried out ground follow-up work on a number of conductors, including geophysical surveys (vertical loop EM and SP), geological investigations and prospecting, and limited soil sampling. This work partially supported the general conclusion of Wilson (1959) that the small conductors were generally due to gossanous pyritic bands within the greenstones, and of limited economic potential. Roderick (1959b) also interpreted a detailed ground magnetometer survey over part of the 'Ugjoktok' serpentinite belt located south of Florence Lake (see map - back pocket).

Hansuld (1959) carried out a geochemical exploration program including semi-reconnaissance stream sediment and soil sampling in the Knee Lake area, and detailed soil sampling. A

total of 1029 samples were analyzed for Cu, Zn, U and Mo. These surveys effectively outlined areas of known Cu mineralization in the Knee Lake area, as well as several other areas of interest north of Shark Lake, and northwest of Benny Lake. The survey in the Knee Lake area showed Cu values to be the most anomalous and widespread of the entire survey, with the highest values coinciding with either pyritic bands and/or known Cu mineralization. The Zn values were less homogeneous and of lower contrast than the Cu values, and the only notable Zn anomalies were confined to two areas of known Cu mineralization located southeast and southwest of Knee Lake, and appeared absent over barren pyritic bands. This suggests that the numerous pyritic bands outlined on Ellingwood's (1959) geological map of the area contained variable base-metal contents.

Piloski (1960) carried out detailed geological examinations of several of the showings discovered in 1959, as well as additional geological mapping and prospecting. The Robin Lake asbestos showing located south of Florence Lake, which was discovered in 1958, and mapped and magnetically surveyed in 1959 (Roderick, 1959b), was trenched in 1960. Trenching showed slip fibre with abundant associated magnetite in seams of apparent random orientation, but also revealed good cross fibre in very thin fractures (up to 3 mm). The mineralization was considered to be of no economic significance. During the latter stages of the 1960 field season, Mr. F. Baikie discovered an outcrop containing nickel

and copper sulphides (Main Baikie showing) while prospecting northwest of Florence Lake. Interestingly, this mineralization had not been detected on the airborne survey. A chip sample across the exposed 2.4 m outcrop assayed 1.18% Ni and 0.10% Cu, however a grab sample of massive sulphide returned 6.6% Ni. Additional prospecting in the area resulted in the discovery of another small outcrop with disseminated sulphides located approximately 38 m southwest of the discovery outcrop.

Mayor and Mann (1960) mapped an area extending from southwest of Knee Lake to north-northwest of Florence Lake, and they tentatively suggested that the greenstones west of Florence Lake may form the western limb of a major structure, and that the greenstones east of Florence Lake form the complimentary eastern limb.

In 1961, a grid was cut over the Baikie showing and the area was mapped at a scale of 1"=100' (Piloski, 1962). A ground magnetometer survey was carried out, and the showing was stripped, sampled, and subsequently drilled (6 packsack drill holes totalling 42 m). An area around Sunfish Lake located southeast of Florence Lake, where a sulphide showing and massive sulphide float had been discovered, was also examined in some detail. Geophysical work and prospecting in this area as well as several others did not produce any encouraging results.

In 1962, a limited exploration program including geological mapping, prospecting, geophysics, and geochemistry was carried out in two areas, north of the Ugjoktok River to

the northwest of Florence Lake, and north of the Baikie showing over two favourable airborne anomalies (13A and 13B) (Piloski, 1963). The discouraging results of exploration in these areas led BRINEX to delay the geochemical sampling of low priority airborne anomalies which had received no previous attention. Piloski (1963) also noted anomalous geochemical values in Ni and sometimes Cu proximal to talcose, sericitic and chloritic alteration zones within the greenstones. Copper appeared to be associated with nickel but in lesser amounts. Piloski (1963) suggested that a general soil and stream sediment sampling survey for both Ni and Cu might be useful, as previous surveys were more detailed and determinations for Ni did not begin until 1962. He also recommended that a patterned sampling of the greenstones and ultramafic rocks be carried out to measure Ni/S ratios, which might act as a useful exploration guide to more detailed work.

Stream sediment sampling over the area in 1963 revealed anomalous Ni values throughout the Florence Lake greenstone belt, most notably around Klotz and Benny Lakes to the east of Florence Lake (Bondar, 1963).

In 1964, Cliffs of Canada in joint venture with BRINEX carried out an exploration program involving prospecting of approximately 777 km^2 and stream sediment sampling of 1295 km^2 (Earthrowl, 1964). Earthrowl outlined several areas that should be investigated in more detail. He suggested that the most important types of mineralization present in the area were sulphide replacements (pyrrhotite, pyrite and

chalcopyrite) in the volcanic and metasedimentary rocks. Stream sediment sampling included analysis of Ni, Cu, Zn and Mo. The sampling program did not reveal any well defined areas strongly anomalous in Ni or Cu, and Zn and Mo values were very low.

Sutton (1970, 1971) mapped an area northwest of Florence Lake and another south of Ugjoktok Bay at a scale of 1:24000. His main objective was to investigate the nature of the granite-greenstone contact. Sutton (1970) noted that in most of the area northwest of Florence Lake the contact between the granite and greenstone is sharp and obviously intrusive, with stringers and lenses of granodiorite in greenstone, and xenoliths of greenstone within granodiorite. In the area of the Baikie Showing however, he describes the contact zone as a 500 m wide zone of mixing between granodiorite-greenstone. He notes that the greenstones and granodiorite are intensely modified by post-intrusion, syn-foliation deformation and shearing, to talc and actinolite schists, and to quartz feldspar phyllonites respectively, and that these fabrics within the tectonized rocks grade outward into those typical of the granodiorite and greenstone. Sutton (1970) suggested that detailed geological mapping might be warranted in areas with similar 'early' tectonic granite-greenstone contacts, and he concurred with previous workers that no further exploration should be done on the numerous small pyritic gossans within the greenstones.

In 1978 the Geological Survey of Canada under the

direction of Ingo Ermanovics commenced a four year geological study of the Hopedale Block in eastern Labrador, covering an area of approximately 12000 km² (Ermanovics and Raudsepp, 1979a, 1979b; Ermanovics, 1980; Ermanovics and Korstgård, 1981; Ermanovics et al., 1982). Ermanovics and Raudsepp (1979a, 1979b) carried out 1:50000 scale geological mapping of the area containing the 'Florence Lake' or 'Ugjoktok' greenstone belt, renaming it the Florence Lake Group. Within the Florence Lake Group, they defined three formations considered to represent mafic, intermediate and felsic successions: (i) the Schist Lakes Formation, mafic flows and sills with minor felsic rocks; (ii) the Adlatok Formation, pyroclastic rocks with associated sedimentary rocks; and (iii) the Lise Lake Formation, tuffs with minor chert. All formations were reported to contain impure marbles and calc-silicate rocks (Ermanovics and Raudsepp, 1979b).

In 1982-1983 BP Minerals and Billiton Canada Limited carried out a joint venture exploration program, including an airborne magnetic-VLF-EM survey to determine the potential for base-metal and gold mineralization within the Florence Lake Group (Guthrie, 1983; Stewart, 1983). The survey covered 2000 line km, with northwest-southeast directed flight lines at 200 m spacings. Ground follow-up work in 1982 included geological mapping, prospecting, and VLF (EM-16) surveys to locate airborne conductors on the ground. A rock suite was collected for petrographic studies and major and trace element analysis. Geological mapping and prospecting continued in 1983 (Stewart,

1983). Numerous small conductors (generally less than 1 m wide) consisting of gossanous pyrite horizons within felsic rocks were detected. These were interpreted to represent cherty tuffaceous and metapelitic beds with minor syngenetic pyrite and carbonaceous material. Stewart (1983) considered the relative lack of felsic volcanic rocks within the area, and the non-spatial association of geophysical anomalies and felsic volcanic rocks as discouraging, and downgraded the base-metal potential of the Florence Lake Group. Guthrie (1983) and Stewart (1983) also described zones of intense carbonatization associated with major faults parallel to regional strike, with almost complete replacement of ultramafic rocks and adjacent lithologies. Stewart (1983) reported negligible sulphide mineralization or gold associated with either the carbonatized rocks or the small pyritic zones.

Reusch (1987) whilst conducting a reconnaissance exploration program for platinum in the Harp Lake area for Platinum Exploration Canada Inc., collected three grab samples at the Main Baikie showing which revealed anomalous platinum-group element (PGE) concentrations of up to 497 ppb Pt and 1020 ppb Pd. Platinum Exploration Canada Inc. subsequently map staked the Baikie property in late 1986 and early 1987.

Arengi (1987) produced a preliminary report noting zones with similar magnetic features to the Baikie showings in the same area. He suggested an initial program of detailed geological examination, complemented by trenching and sampling to determine the nature of the PGE distribution within the

altered zones. Subsequent work (Wilton, 1987; Brace and Wilton, 1990), however, has led to a downgrading of the potential of the Baikie showings due to the podiform nature of the mineralization.

1.4. PRESENT STUDY - PURPOSE AND SCOPE

The Florence Lake Group forms a 65 km-long Late Archean volcanosedimentary supracrustal sequence, or 'greenstone belt', within the southernmost Nain Structural Province, central Labrador.

Archean greenstone belts are an integral component of Precambrian cratons around the world. They have generally been extensively studied, and are well-known for their abundant and economically important mineral deposits (viz., banded iron formations, volcanogenic massive Fe-Cu-Zn sulphide deposits, komatiite-related Fe-Ni-Cu (+ minor PGE) sulphide deposits and epigenetic lode Au deposits).

The mineral potential of the Florence Lake Group has been evaluated by several exploration companies (e.g., Piloski, 1962; Stewart, 1983; Arengi, 1987), but none of this information has been published. In fact, the only published comprehensive geological information on the Florence Lake Group results from regional studies by the Geological Survey of Canada (Ermanovics and Raudsepp, 1979a,b), whereas published geochemical data for the Florence Lake Group are non-existent. This study attempts to review the petrographic, geochemical and metallogenic characteristics of the

southernmost portion (30 km) of the Florence Lake Group. It should be noted from the outset that this is not a detailed stratigraphic and/or structural study of the Florence Lake Group. It is hoped that information contained herein will complement that of I. Ermanovics and coworkers, which is expected to be published as a Geological Survey of Canada memoir sometime around 1992 (Ermanovics, 1989, per. comm.).

Field work for the present study involved regional 1:50000 scale geological mapping, which was carried out during the summer of 1987. An estimated 20 ground traverses and 2 helicopter traverses were carried out throughout the area, concentrating most intensely on the areas southeast and east of Florence Lake, where the most extensive exposures of the Florence Lake Group outcrop.

Laboratory work has included: geochemical analyses (major, trace and rare earth elements), precious metal and base-metal analyses, petrographic studies, and electron microprobe and SEM analyses for mineral identification.

CHAPTER 2. GENERAL GEOLOGY

2.1. REGIONAL GEOLOGICAL SETTING

The Nain Province in Labrador occupies a relatively narrow (maximum 80-90 km wide) coastal area extending from northern to central Labrador (Figure 2.1), and forms the southwestern extremity of the North Atlantic craton, which is also exposed in East and West Greenland and in northwest Scotland (Bridgewater et al., 1973). At the southern margin of the Nain Province, Archean granitoids of the Kanairiktok Intrusive Suite (Ermanovics and Raudsepp, 1979a) are unconformably overlain by Early Proterozoic volcanic and sedimentary rocks of the Moran Lake Group (Ryan, 1984; Wilton et al., 1988) in the foreland zone of the Makkovik Province (Wardle et al., 1986). To the west, the Nain Province is bounded by the Churchill Province and Middle Proterozoic Elsonian intrusions of the Nain, Harp Lake, and Flowers River Igneous Complexes (Ermanovics et al., 1982).

2.2. GEOLOGY OF THE SOUTHERN NAIN PROVINCE

The geology and structural evolution of the southern portion of the Archean Nain Province and the adjacent Proterozoic Makkovik Province to the south, has been studied by Ermanovics and Raudsepp (1979a,b); Ermanovics (1980); Ermanovics and Korstgård (1981); and Ermanovics et al. (1982). Korstgård and Ermanovics (1984, 1985) have reviewed the structural and tectonic evolution of the southern Nain and

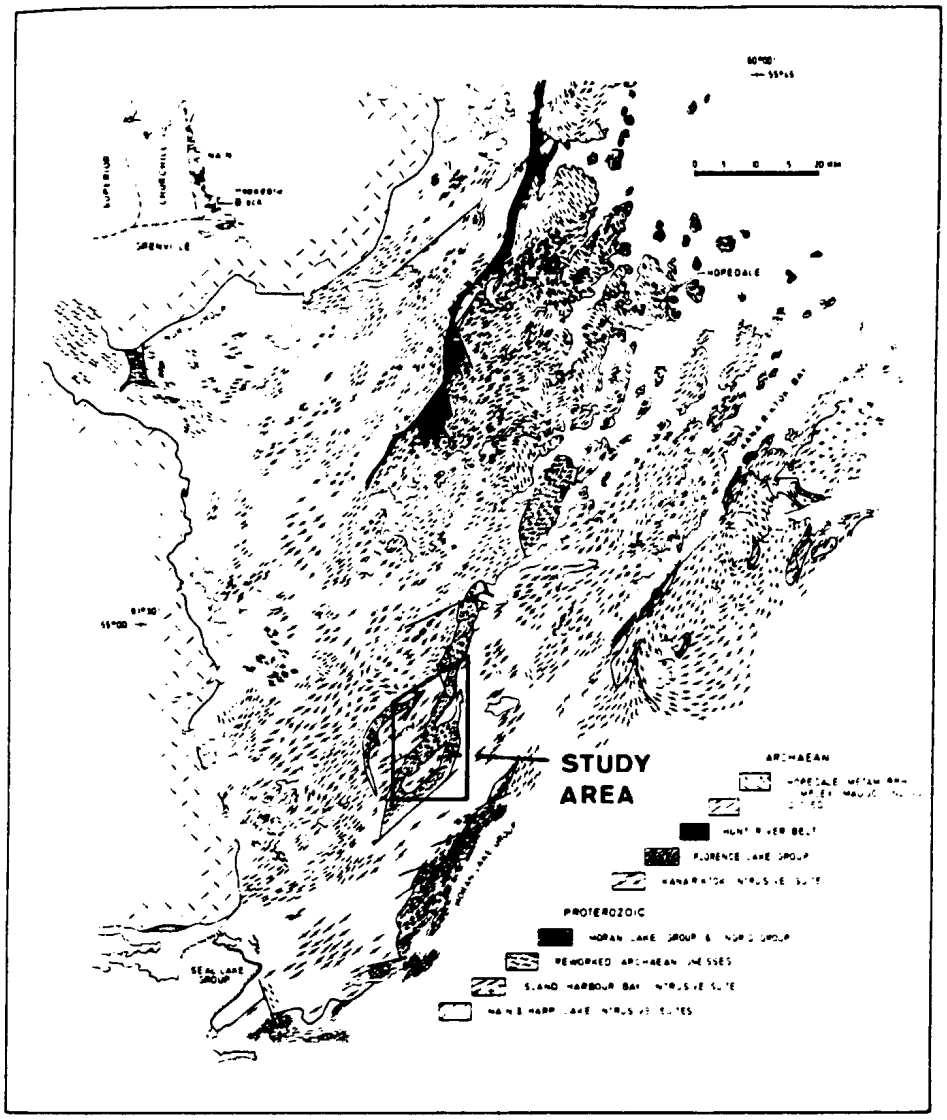

Figure 2.1. Structural and lithological sketch map of the southern part of the Archean Nain Province and the adjacent Proterozoic Makkovik Province (after Korstgård and Ermanovics, 1985).

Makkovik provinces.

Table 2.1 shows the major lithological units recognized by Ermanovics and Raudsepp (1979a) within the southern Nain Province. The oldest rocks as part of the Weekes Amphibolite (Ermanovics and Raudsepp, 1979a) occurs as rafts and inclusions (up to hundreds of square metres in area) within layered granoblastic grey gneiss of the Maggo Gneiss (Ermanovics and Raudsepp, 1979a). The Weekes Amphibolites are characteristically coarse-grained, metamorphically layered (10-100 cm thick) rocks. They locally contain meta-ultramafic layers, garnet-rich quartzofeldspathic gneiss and orthopyroxene-bearing units. The amphibolites are considered to represent mafic volcanic or layered mafic intrusive rocks, and because they are the oldest rocks recognized in the area, workers (Ermanovics and Raudsepp, 1979a; Korstgård and Ermanovics, 1985) have generally correlated them with similar rocks in the 80 km-long Hunt River belt (Collerson et al., 1976; Jesseau, 1976) (see Figure 2.1). However, Korstgård and Ermanovics (1985) have pointed out that age relations are inconclusive, and the Weekes Amphibolite could represent basement to the Hunt River belt. A U-Pb zircon age of 3105 +6/-9 Ma (Loveridge et al., 1987) and a Rb-Sr whole rock isochron age of 3011 ± 110 Ma (Voner, 1985) are minimums for an igneous precursor to the Maggo Gneiss.

The Maggo Gneiss is a medium-grained, granoblastic grey tonalite to granodioritic gneiss which appears to intrude the Weekes Amphibolite. As a unit it is highly variable in

Table 2.1. Table of formations for major rock units recognized in the southern part of the Nain Province (after Ermanovics and Raudsepp, 1979a).

Table of Formations

Eon	Map Unit	Lithology
Proterozoic	Undivided dykes: diabase and gabbro	Harp Lake dykes: olivine and mauve-coloured augite; 5 to 15% altered; post 1.45 Ga. Kikkertavak dykes: pigeonite (± augite) and rims of hornblende on pyroxene; 40 to 70% altered to actinolite, carbonate, chlorite, zoisite, sericite-muscovite and leucoxene.
	Intrusive contact	
?		
Archean or Early Proterozoic	Kanairiktok intrusive suite	Foliated, grey to pale pink, coarse and medium grained, biotite/hornblende, granodiorite, tonalite and minor pink granite; mafics altered to actinolite/tremolite, epidote, chlorite, muscovite and calcite (M_2-metamorphism).
	Intrusive contact	
	Meta-ultramafic suite	Serpentinite, metapyroxenite, minor metagabbro.
	Intrusive contact	
	Florence Lake group	M_2-metamorphism.
	Lise Lake formation	Felsic (colour index <15-20) tuff, lapilli tuff, lappilistone; poorly sorted, locally banded; generally not reworked; disseminated sulphides and rare cherty pyrite horizons; generally grades to aphanitic members containing blue quartz clasts; includes 20% intermediate rocks.
	Adlatok formation	Intermediate (colour index 15-20 – 35-40) pyroclastic rocks with minor argillaceous sandstone and siltstone; tuff, lapilli tuff, volcanic breccia; poorly sorted but locally finely layered; porphyritic sills; includes 30% mafic and felsic rocks; quartz veins with blue Cu stain.
	Schist Lakes formation	Mafic (colour index 35-40 – 70) layered flows and sills intercalated with 20% intermediate and felsic rocks; sills reflect composition of host rocks; minor ferruginous metachert sulphide facies.
?		
	? Unconformity ?	
Archean		M_1 + M_2-metamorphism
	Maggo gneiss	Medium grained, granoblastic, mafic hornblende-andesine dykes; layered, leucocratic, biotite-tonalite gneiss with sparse garnet; abundant felsic lit-par-lit aplite and hornblende-bearing pegmatite.
	Weekes amphibolite	Remnants of presumed Hunt River group amphibolite probably intruded by tonalite; coarse grained, layered hornblende + plagioclase + garnet (± pyroxene and M_2 biotite, epidote and actinolite); medium grained, granoblastic hornblende gneiss.

composition, ranging from medium-grained hornblende-plagioclase-quartz leucotonalite to coarse-grained porphyroblastic granodiorite. Metamorphic layering in the Maggo Gneiss is locally cut by elongate pods of amphibolite which are interpreted to represent recrystallized and tectonically thinned dykes called the Hopedale Dykes (Ermanovics et al., 1982). Korstgård and Ermanovics (1985) referred to the Weekes Amphibolite, Maggo Gneiss and Hopedale Dykes collectively as the Hopedale Metamorphic Complex. It should be noted that rocks of the Hopedale Metamorphic Complex do not crop out within the map area of this study.

The Florence Lake Group forms a volcanosedimentary supracrustal sequence which unconformably overlies the Hopedale Metamorphic Complex (Ermanovics and Raudsepp, 1979a). The Florence Lake Group (after Brace and Wilton, 1989) consists predominantly of mafic metavolcanic rocks, and less extensive siliceous metasedimentary and felsic metavolcanic rocks. Intensely serpentinized peridotites which have undergone variable carbonatization form elongate, regionally concordant intrusive bodies within the Florence Lake Group.

The Florence Lake Group is intruded by the Kanairiktok Intrusive Suite (Ermanovics and Raudsepp, 1979a) which comprises massive, gneissic and mylonitic trondhjemite-tonalite. A U-Pb zircon age of 2838 Ma (Loveridge et al., 1987) for the Kanairiktok Intrusive Suite serves as a minimum age for the Florence Lake Group. However, Ermanovics (per. comm., 1989) has pointed out that the Kanairiktok Intrusive

Suite may comprise rocks with a range of ages, and hence, this may not necessarily be a minimum age for the Florence Lake Group. The Florence Lake Group, the meta-ultramafic rocks and the Kanairiktok Intrusive Suite, have all been deformed and metamorphosed to middle greenschist facies (Ermanovics and Raudsepp, 1979a).

All lithologies are cut by undeformed Proterozoic diabase and gabbro dykes of at least two ages. These dykes strike between north-south and east-west.

2.3. FLORENCE LAKE GROUP

Ermanovics and Raudsepp (1979a,b) divided the Florence Lake Group (**FLG**) into three formations based largely on colour index (CI) and characteristic textures (Table 2.1). These are the Lise Lake (CI < 15-20), Adlatok (CI=15-20 to 35-40) and Schist Lakes (CI=35-40 to 70) formations, which generally correspond to a felsic, intermediate, and mafic volcanic association respectively. Each formation contains varying proportions of lithologies that are characteristic of the other formations. For example, the Adlatok Formation is reported to contain 50% combined mafic and felsic rocks (Table 2.1). The stratigraphic top and bottom of the FLG is unknown; however, Ermanovics and Raudsepp (1979a) tentatively indicated that the sequence may progress upwards (?) from mafic flows and sills (Schist Lakes Formation) into intermediate (Adlatok Formation) and felsic (Lise Lake Formation) pyroclastic rocks.

Classification of the FLG on a regional 1:50000 scale is

difficult because the sequence is generally thinly intercalated, and intense deformation and metamorphism have resulted in non-preservation of primary textures and structures. Within the map area of this study, the author concluded that it is impossible to effectively distinguish between the Schist Lakes and Adlatok formations (viz., mafic and intermediate suites) in the field. Therefore, in this study the FLG has been divided into a mafic (Unit 1) and felsic (Unit 2) unit (see map - back pocket). Unit 1 generally corresponds to the Schist Lakes and Adlatok formations collectively, and Unit 2 corresponds to the Lise Lake Formation. However, it must be stressed that, as originally suggested by Ermanovics and Raudsepp (1979a,b), Units 1 and 2 each contain varying proportions of the lithologies which characterize the other.

Within the map area, dark-to-medium green mafic metavolcanic schists, and minor mafic pillow lavas and flows (Unit 1) are by far the most abundant lithologies (see map - back pocket). White and pale pink and green, fine-grained siliceous metasedimentary and felsic metavolcanic rocks (Unit 2) are also present, but are less abundant.

2.3.1. Mafic Metavolcanic Rocks (Unit 1)

2.3.1.1. Field Description

Mafic and minor intermediate metavolcanic rocks are by far the most abundant lithologies within the FLG. These are generally preserved as medium-to-dark green, fine-grained

schists, thinly banded flows and minor pillow lavas. Massive, fine-to-medium grained rocks of similar composition, but lacking a pronounced foliation, are interpreted to represent either massive flows and/or synvolcanic sills. The entire mafic metavolcanic sequence is interstratified with thin (centimetres to a few metres) beds of siliceous metasedimentary and felsic metavolcanic rocks.

In the field, the mafic metavolcanic rocks vary considerably in appearance. Mafic flows are locally thinly banded on a centimetre scale with alternating medium-to-dark green layers (Plate 2.1). In highly deformed areas, the rocks have a strong penetrative cleavage and are commonly converted to tightly folded actinolite-epidote-chlorite schists (Plate 2.2). Mafic pillow lavas are locally well developed immediately west of Benny Lake and east of the southern end of Florence Lake. Undeformed pillows are generally less than 1 metre long in their maximum dimension (Plate 2.3); however, in more highly deformed areas, individual pillows are variably stretched and elongated (Plate 2.4).

Massive, fine- to medium-grained mafic rocks comprising both flows and synvolcanic sills lack the pronounced foliation typically displayed by the fine-grained mafic metavolcanic schists. Approximately 1.25 km southeast of Florence Lake, massive medium-grained porphyritic metavolcanic sills contain numerous large (up to 2 cm in diameter) anhedral plagioclase (?) phenocrysts (Plate 2.5). These phenocrysts are locally segregated into thin layers several centimetres thick. One

Plate 2.1. Thinly banded mafic metavolcanic flows [1 km SE of Florence Lake].

Plate 2.2. Tight angular folds in mafic metavolcanic actinolite-chlorite schists [1.5 km N of Benny Lake].

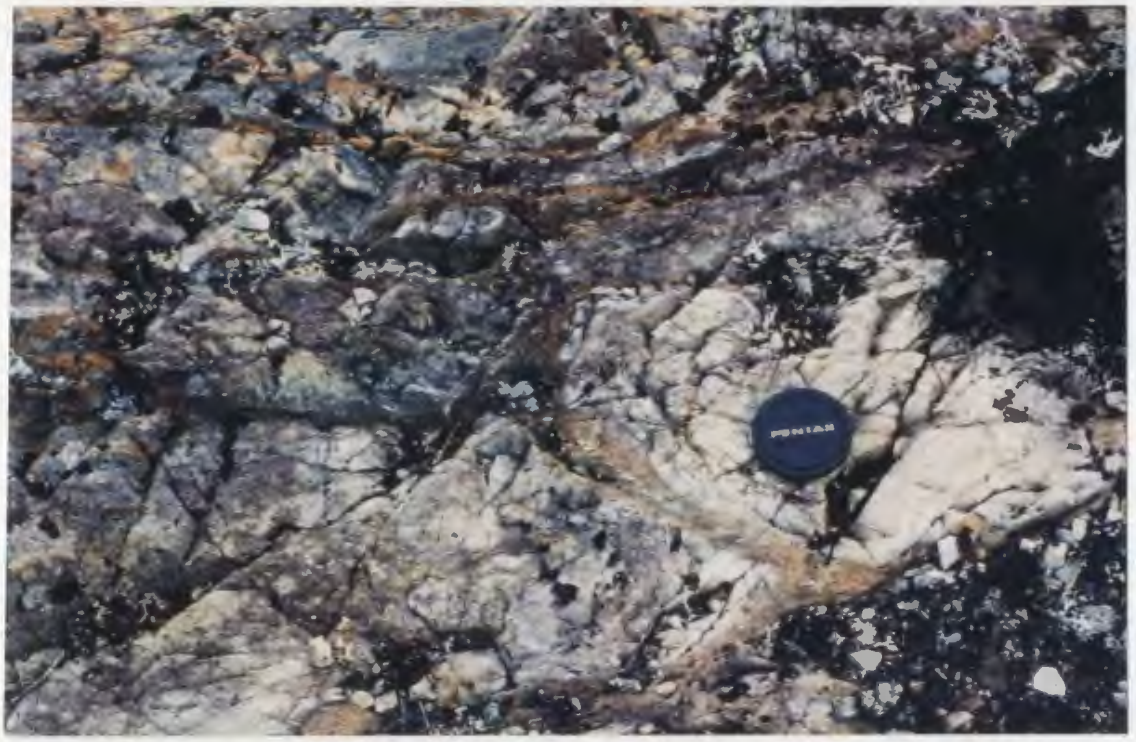

Plate 2.3. Relatively little deformed mafic pillow lavas with brown-weathering rinds outlining individual pillows [1 km E of southern end of Florence Lake].

Plate 2.4. Highly 'stretched' mafic pillow lavas [100 m W of Benny Lake].

Plate 2.5. Massive plagioclase (?) (totally saussuritized) porphyritic mafic metavolcanic sill. Note the segregation of phenocrysts [1.25 km SE of Florence Lake].

Plate 2.6. Thin (2 m thick) carbonate (ankerite)-quartz lens within mafic metavolcanic schists. Note the thin milky white quartz veins within the carbonate lens [1 km E-SE of Florence Lake].

distinctive lithology observed in several outcrops is a massive, medium-grained leucocratic rock comprising roughly equal proportions of plagioclase and long prismatic amphibole (up to 5-6 mm long). The relationship of these rocks to other lithologies is unknown.

Carbonate is ubiquitous throughout the entire metavolcanic sequence, and occurs in a variety of forms: (1) thin (mm's) cross-cutting calcite veinlets; (2) thin (mm's-cm's) bands parallel to foliations; and (3) lenses up to several metres thick within the mafic metavolcanics (Plate 2.6). These carbonate lenses are brown-weathering, and contain variable amounts of fine-grained quartz and thin (cm's) discontinuous milky-white quartz veinlets (Plate 2.6). Ermanovics and Raudsepp (1979a,b) described these carbonate lenses as impure limestones (marbles) and calc-silicate rocks.

Metamorphic grade increases from middle greenschist to amphibolite facies near intrusive contacts with the Kanairiktok Intrusive Suite, where mafic metavolcanic rocks of the FLG are converted to amphibolites. The amphibolites are intruded by, and occur as xenoliths and rafts (few centimetres to hundreds of metres), within the Kanairiktok trondhjemites. In the vicinity of the Baikie showings (see map - back pocket), mafic metavolcanic rocks are injected by trondhjemitic melts (Plate 2.7). In one outcrop near the contact zone immediately east of Benny Lake, intensely folded milky-white quartz veins, with intervening amphibolite layers, occur within the Florence Lake amphibolites (Plate 2.8).

Plate 2.7. Trondhjemitic melts intruding mafic metavolcanic schists [several metres SW of the Main Baikie showing].

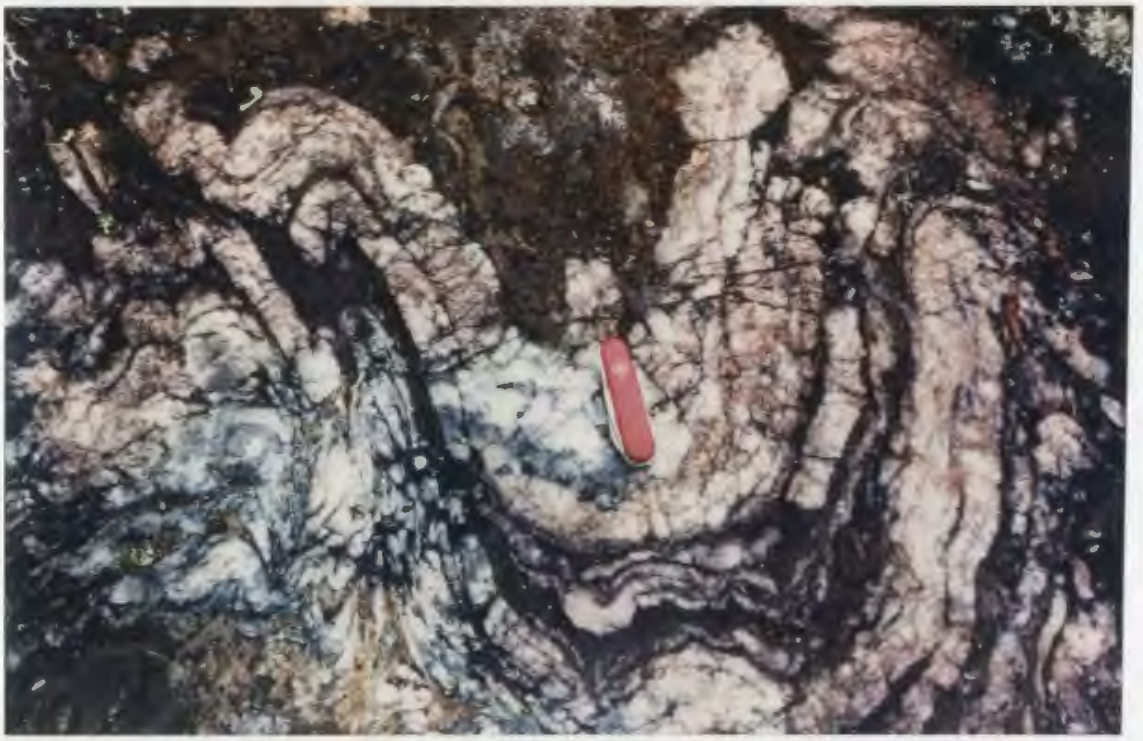

Plate 2.8. Folded milky-white quartz veins with intervening amphibolite layers (dark) near the contact between the Florence Lake Group and Kanairiktok Intrusive Suite. [300 m E of Benny Lake).

2.3.1.2. Petrography

The mafic metavolcanic rocks lack primary igneous textures, and primary phases are completely replaced by a middle greenschist metamorphic assemblage. The rocks are invariably very fine-grained, and for the most part are non-descript.

The fine-grained rocks are strongly foliated and contain varying proportions of actinolite, epidote, chlorite, quartz and calcite. The most common rocks are actinolite-epidote-chlorite schists consisting predominantly of fibrous actinolite (0.1-1 mm long) in a very fine-grained matrix of epidote and minor chlorite (Plate 2.9). Chlorite-quartz-epidote schists are less common, and consist of roughly equal proportions of green chlorite and recrystallized quartz (elongated parallel to the foliation), epidote and calcite (Plate 2.10).

The fine- to medium-grained massive flows and/or sills are of similar composition, and contain relatively equigranular amphibole crystals in a fine-grained matrix comprising predominantly epidote, and minor quartz, chlorite and carbonate. In fine-grained samples, amphibole crystals are generally between 0.25-0.75 mm in diameter (Plate 2.11), and quartz, if present, is highly strained with strong undulatory extinction. In medium-grained samples, amphibole is slightly coarser (1-3 mm in diameter) and quartz appears to be more abundant, but again is highly strained. The porphyritic sills (see Plate 2.5) are similar, but contain large anhedral,

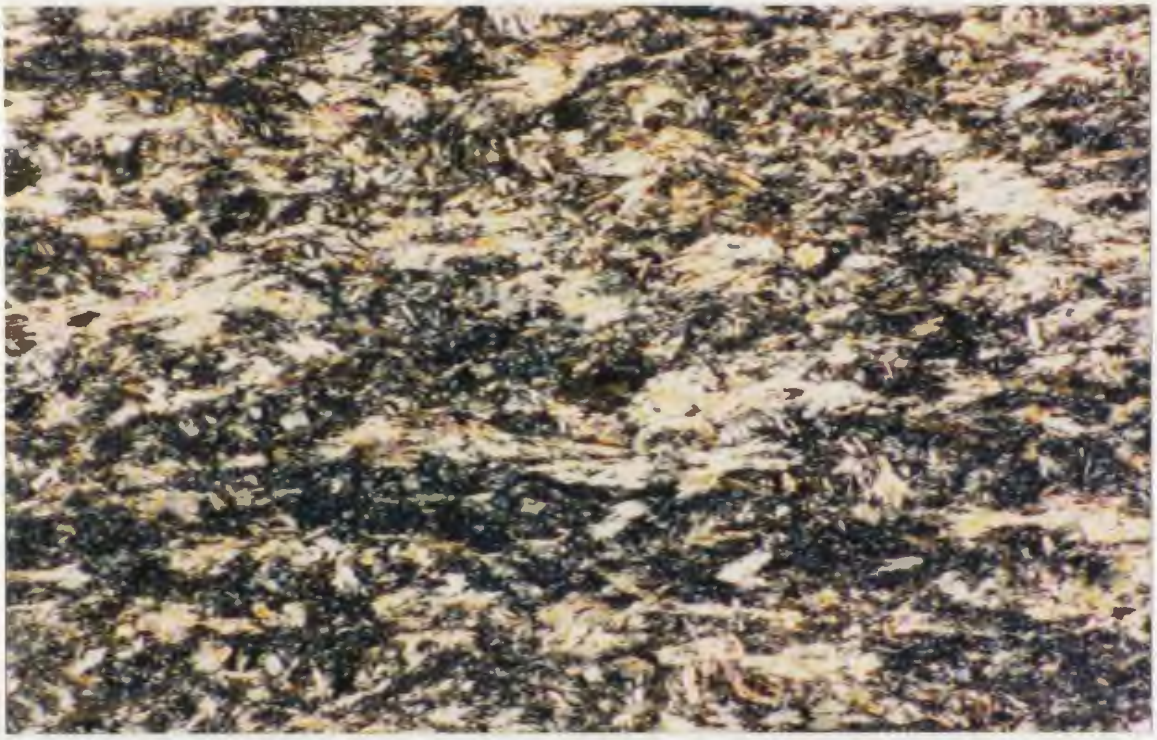

Plate 2.9. Fine-grained mafic metavolcanic schist comprising actinolite-chlorite-epidote [87-139, 30x, XN].

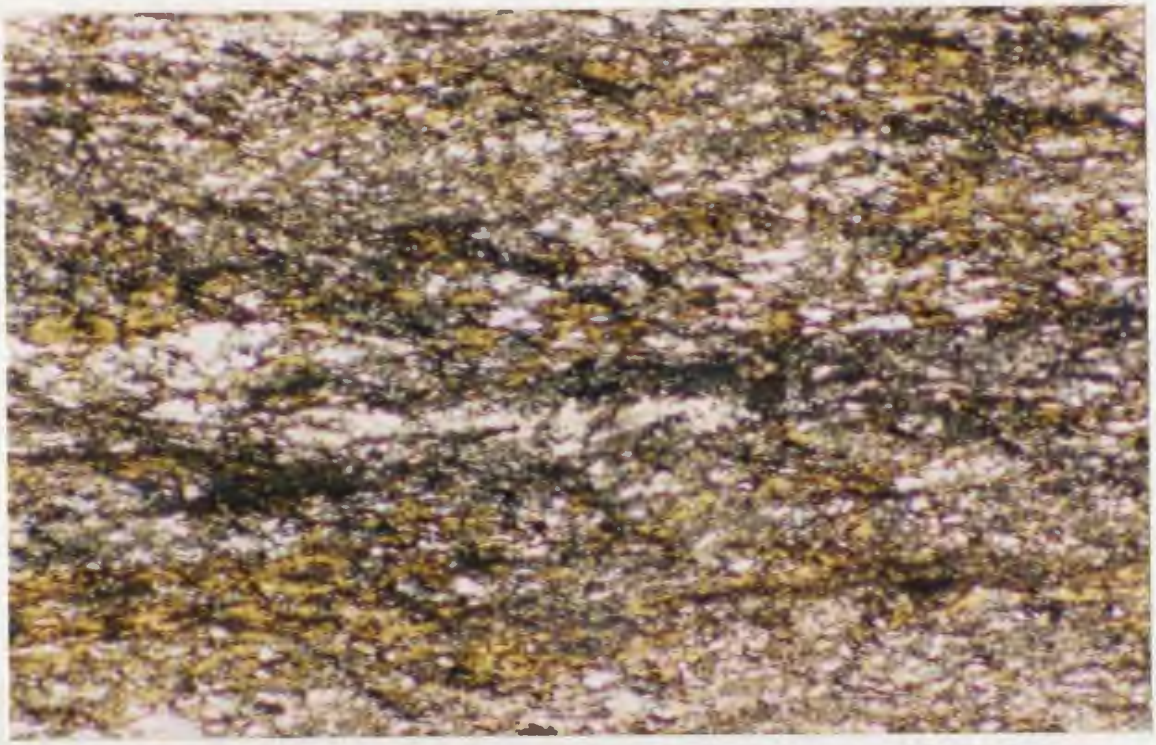

Plate 2.10. Fine-grained mafic metavolcanic schist comprising chlorite-quartz-carbonate-epidote [87-149A, 45x, XN].

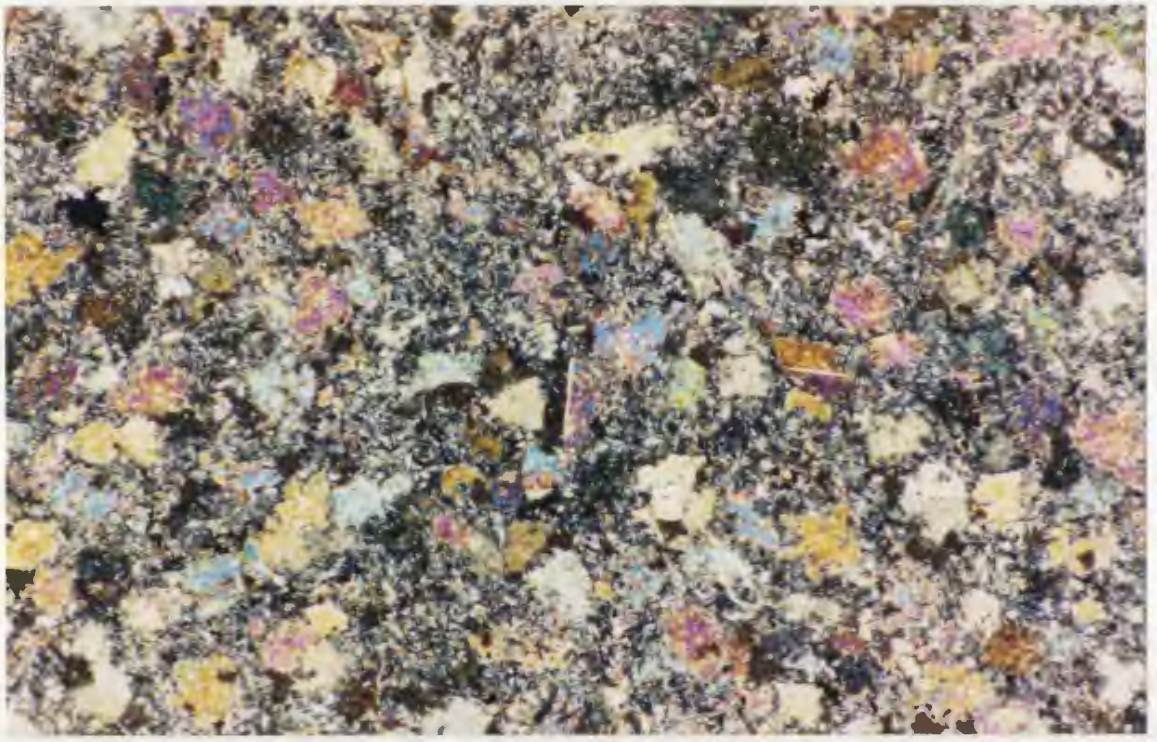

Plate 2.11. Massive fine-grained mafic metavolcanic flow/sill (?) comprising actinolite-epidote-chlorite [87-230D, 20x, XN].

Plate 2.12. Medium-grained metavolcanic sill (?) comprising prismatic amphibole aggregates (1-5 mm long), totally saussuritized plagioclase and quartz. Note the myrmekitic texture of plagioclase/quartz at middle and top center [87-126, 10x, XN).

completely saussuritized, plagioclase phenocrysts up to 2 cm in diameter.

The distinctive, leucocratic plagioclase-amphibole rocks are medium-grained, and contain long amphibole crystals up to 5 mm long which have been replaced by fine-grained fibrous amphibole aggregates (Plate 2.12). Plagioclase is completely sausseritized. Strained quartz with undulose extinction and myrmekitic intergrowths between quartz and saussuritized plagioclase are also present (Plate 2.12).

The amphibolites near intrusive contacts with the Kanairiktok Intrusive Suite, are fine-grained (0.1-0.5 mm) and comprise hornblende, saussuritized plagioclase, recrystallized plagioclase and quartz, epidote, calcite and Fe-oxides.

2.3.2. Felsic Metavolcanic/Metasedimentary Rocks (Unit 2)

2.3.2.1. Field Description

The felsic supracrustal rocks weather white and pink, to pale green, and are readily distinguished from the mafic metavolcanic rocks by their inherent leucocratic colour. In the field, classification of these rocks as strictly volcanic (flows and/or pyroclastic) or sedimentary (clastic and/or volcaniclastic) is difficult, owing to their fine grain size and lack of primary structures and textures. Ermanovics and Raudsepp (1979a) described the felsic lithologies as a variety of pyroclastic rocks; however, following detailed petrographic studies, Ermanovics (per. comm., 1987, 1990) now believes that many of the felsic rocks containing plagioclase and quartz

fragments are actually metagreywackes.

The felsic metavolcanic/sedimentary rocks form mappable units throughout the study area, and are also thinly (several centimetres to several metres thick) intercalated with the considerably more voluminous mafic metavolcanic rocks. Contacts between the felsic and mafic rocks are generally quite sharp. In areas of strong folding, competency contrasts between relatively massive felsic lithologies containing plagioclase and quartz fragments, and schistose mafic units, result in variations in fold styles. In these areas, mafic rocks are characterized by tight angular folds, whereas the felsic rocks are characterized by open parallel folds (Plate 2.13). In one outcrop located approximately 1.25 km southeast of Florence Lake, the contact between a porphyritic rhyolite (87-057, see Table 3.2.1) and mafic metavolcanic schists is highly irregular (Plate 2.14), and appears to be either erosional or intrusive, although no chilling is preserved.

In the field, felsic lithologies can generally be divided into two groups based on the presence or absence of plagioclase and/or quartz fragments. Very fine-grained siliceous rocks with variable, although generally minor, mafic phases are very common. Quartz-sericite schists are the most abundant, although quartz-hornblende schists occur locally. Although sedimentary structures and textures are generally absent, these fine-grained quartz-rich lithologies are interpreted to represent siliceous metasedimentary rocks since they are totally devoid of fragments or phenocrysts. Some of

Plate 2.13. Variation of fold styles in interstratified mafic metavolcanic schists (tight, angular) and felsic porphyritic rocks (concentric) [1.5 km north of Benny Lake].

Plate 2.14. Irregular contact between relatively massive felsic porphyritic rocks (top) and mafic metavolcanic schists (bottom) [1.25 km SE of Florence Lake].

the very fine-grained varieties may be recrystallized metacherts. Locally, abundant very fine-grained sericite gives the rocks a characteristic pale green colour. Thin (several mm's to 1 m thick) gossanous pyrite horizons which appear to be parallel to the original bedding (?), are common within these siliceous metasedimentary rocks (Plate 2.15).

Felsic metavolcanic flows and/or tuffs with small quartz and plagioclase phenocrysts (up to 1-2 mm) form thin (10's of centimetres to a few metres) beds interstratified with mafic metavolcanic rocks of Unit 1. These are generally massive, and lack the pronounced foliation commonly displayed by the fine-grained siliceous metasedimentary rocks. A distinctive pale green tuffaceous lithology with rounded blue quartz eyes up to 3-4 mm in diameter was noted in several outcrops.

The hill immediately east of the carbonatized ultramafic rocks (Map Unit 3a) southeast of Florence Lake is underlain by massive, medium-grained leucocratic rocks comprising plagioclase, quartz and chlorite. According to Ermanovics and Raudsepp (1979b), the area is underlain by felsic pyroclastic rocks of the Lise Lake Formation; however, a cursory examination during this study indicates that the rocks are trondhjemitic.

2.3.2.2. Petrography

Petrographically the felsic rocks vary from very fine-grained sericite/hornblende-quartz schists to relatively massive plagioclase-quartz porphyritic rocks.

Plate 2.15. Thin, rusty pyrite horizon within fine-grained siliceous metasedimentary schists [1.25 km SE of Florence Lake].

Petrographic examination of porphyritic samples collected during this study indicates that the rocks are volcanogenic. The only fragments recognized are anhedral to euhedral plagioclase and quartz, which show a complete range in their relative proportions. No lithic fragments of any kind have been identified, although admittedly these are commonly incorporated into the matrix of greywackes during deformation and metamorphism. The matrices of the samples are very felsic and generally do not contain large proportions of mafic minerals, indicating that if the rocks are sedimentary, they did not contain significant quantities of mafic and/or ultramafic detritus.

The matrix of the porphyritic rocks consists of very fine-grained, partially recrystallized quartz (generally < 0.01 mm, max. 0.05 mm) and minor sericite and rarely chlorite. The proportion of phenocrysts varies from 5-30 vol.%, and consists of varying proportions of strained quartz with undulose extinction, and twinned, invariably saussuritized, plagioclase. Sample 87-149B contains a relatively high proportion of phenocrysts (25-30 vol.%), comprising predominantly subhedral to anhedral twinned plagioclase (0.1-3 mm in diameter) and minor quartz (< 5 vol.%) (Plate 2.16). The matrix consists of very fine-grained recrystallized quartz and minor chlorite. Samples 87-130A and 87-178B (Plates 2.17 and 2.18 respectively) provide additional unequivocal evidence that these rocks are volcanic in origin. Sample 87-130A contains approximately 20-25 vol.% euhedral, saussuritized

Plate 2.16. Felsic porphyritic tuff comprising subhedral to anhedral plagioclase phenocrysts within a very fine-grained recrystallized quartz-plagioclase matrix. Mafic minerals include very minor chlorite and trace epidote [87-149B, 15x, XN].

Plate 2.17. Felsic porphyry with euhedral plagioclase phenocrysts within a very fine-grained quartz-plagioclase matrix. Mafic minerals include minor chlorite and epidote, and trace muscovite [87-130A, 10x, XN].

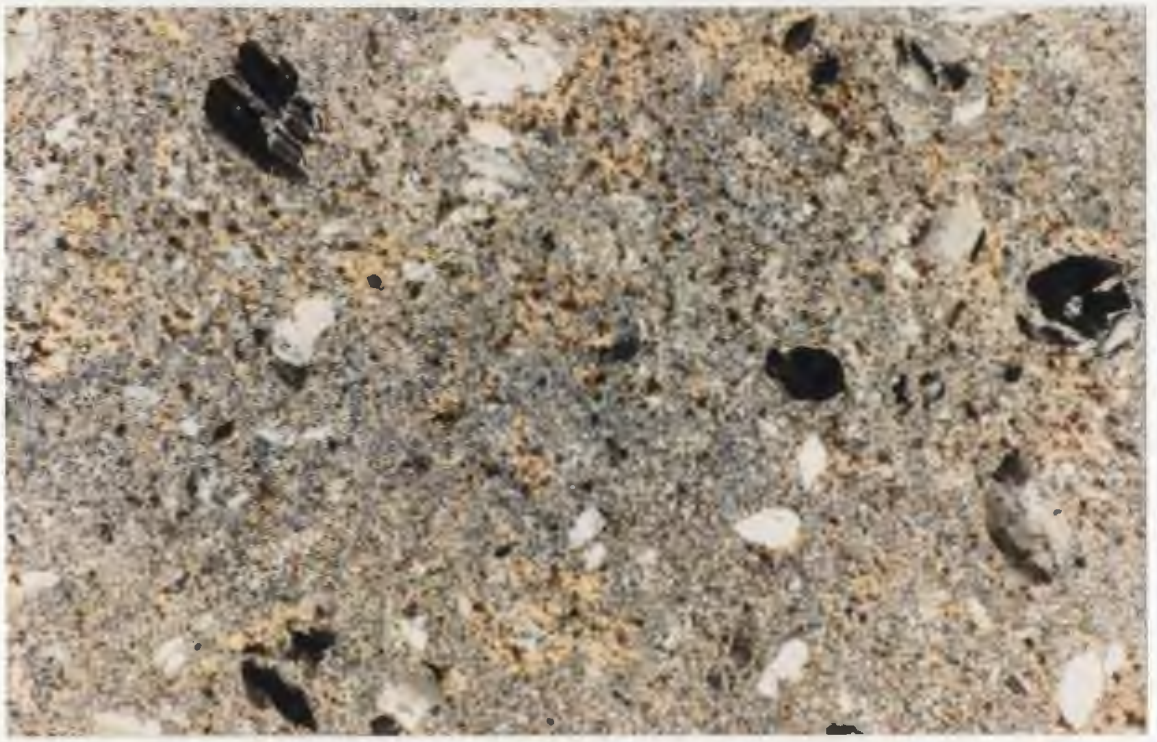

Plate 2.18. Euhedral quartz phenocrysts in a rhyolite porphyry. Note the embayed and euhedral volcanic quartz at extreme middle right and top center and left. The very fine-grained yellow mineral is sericite [87-178B, 15x, XN].

Plate 2.19. Elongated quartz phenocrysts in a boudinaged rhyolite porphyry (see Plate 2.38). The very fine-grained foliation-forming mineral is sericite [87-247B, 10x, XN].

plagioclase phenocrysts (up to 2-4 mm long) within a matrix comprising recrystallized quartz, minor plagioclase, and sericite and epidote (Plate 2.17). Minor 'clotty' chlorite (blue in thin section), carbonate, and epidote are also present. Sample 87-178B contains abundant euhedral and embayed quartz phenocrysts (0.5-1.5 mm) and very minor twinned plagioclase phenocrysts (Plate 2.18). The matrix is again comprised of very fine-grained recrystallized quartz and sericite. Approximately 1.5 km southeast of Florence Lake, a discontinuous boudinaged layer of rhyolite porphyry (see Plate 2.38) is enveloped by carbonatized ultramafic rocks. The rhyolite is strained, and contains elongated quartz phenocrysts up to 2 mm long in a fine-grained matrix of recrystallized quartz and sericite (Plate 2.19).

The retention of delicate volcanic features such as embayed quartz, and euhedral plagioclase and quartz phenocrysts, indicates that for the most part these rocks are volcanogenic and are proximal to their source areas. The author believes that based on petrography and geochemistry (see Section 3.2), these particular rocks are best termed felsic porphyries and/or tuffs, as Ermanovics and Raudsepp (1979a) originally described them. The term 'greywacke' seems inappropriate for rocks totally devoid of lithic fragments and lacking in mafic phases.

The very fine-grained siliceous metasediments are quartz-dominated schists containing sericite and minor chlorite and epidote. Plagioclase is generally absent, and if present is

minor (< 5 vol.%). The rocks are predominantly quartz-sericite schists (Plate 2.20), although quartz-hornblende schists (Plate 2.21) are present locally. The quartz-sericite schists consist of very fine-grained (0.05-0.1 mm) recrystallized polygonal quartz and sericite. The quartz-hornblende schists are fine-grained, metamorphically layered rocks containing predominantly hornblende (up to 1 mm long) and recrystallized quartz (0.05-0.2 mm), with minor plagioclase, epidote, biotite and chlorite. Foliations are defined by aligned hornblende, minor biotite, and elongated quartz. Hornblende contains very small (< 0.01 mm) inclusions of quartz, and plagioclase is 'fresh' and recrystallized.

2.4. META-ULTRAMAFIC ROCKS (Unit 3)

2.4.1. Field Description

South of Florence Lake, serpentinized peridotites form elongate northeast-trending intrusive bodies within the FLG (see map - back pocket). Their intrusive nature is not readily apparent in the field because contacts with the FLG are rarely exposed; however, several outcrops indicate that the peridotites are intrusive. In one outcrop, a peridotite 'plug' intrudes mafic metavolcanic schists (Plate 2.22) of the FLG, while in another outcrop, a mafic metavolcanic xenolith several metres in diameter is completely enveloped by peridotite. Although the peridotites are intrusive, and hence are younger than adjacent volcanosedimentary rocks of the FLG, they nevertheless form an integral part of the greenstone

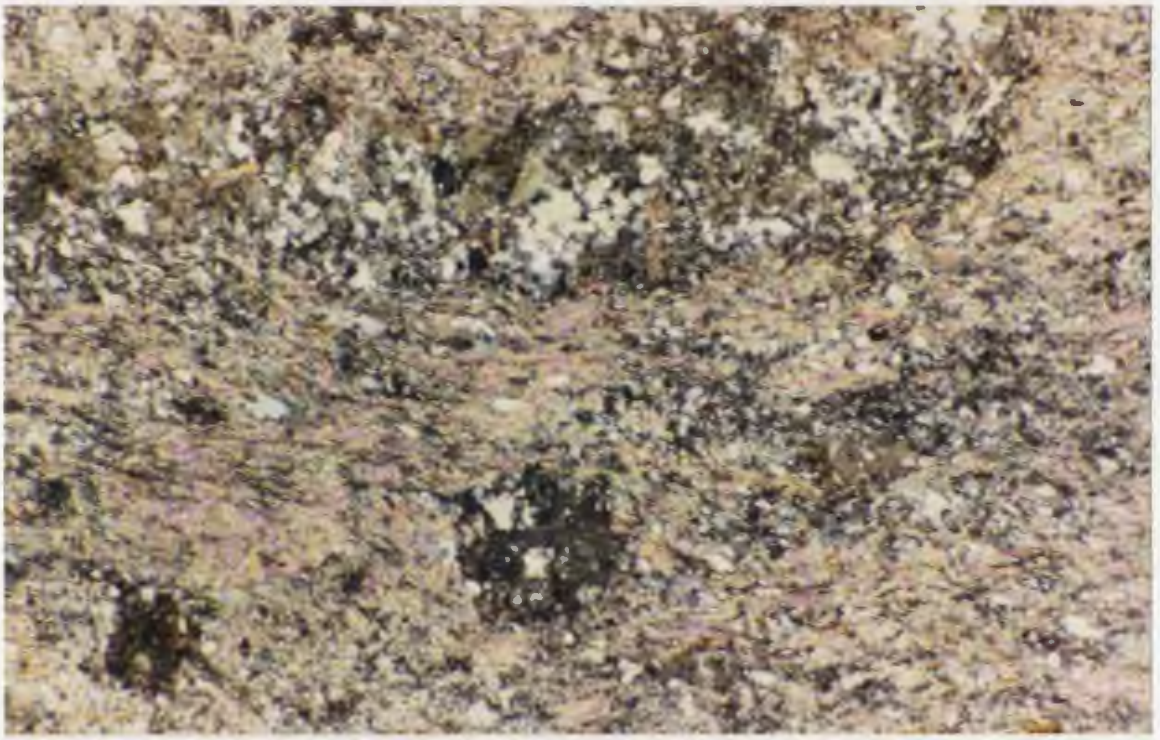

Plate 2.20. Fine-grained siliceous metasedimentary schist comprising abundant sericite and recrystallized quartz, with small (up to 0.5 mm) carbonate fragments (lower center) [87-267, 35x, XN].

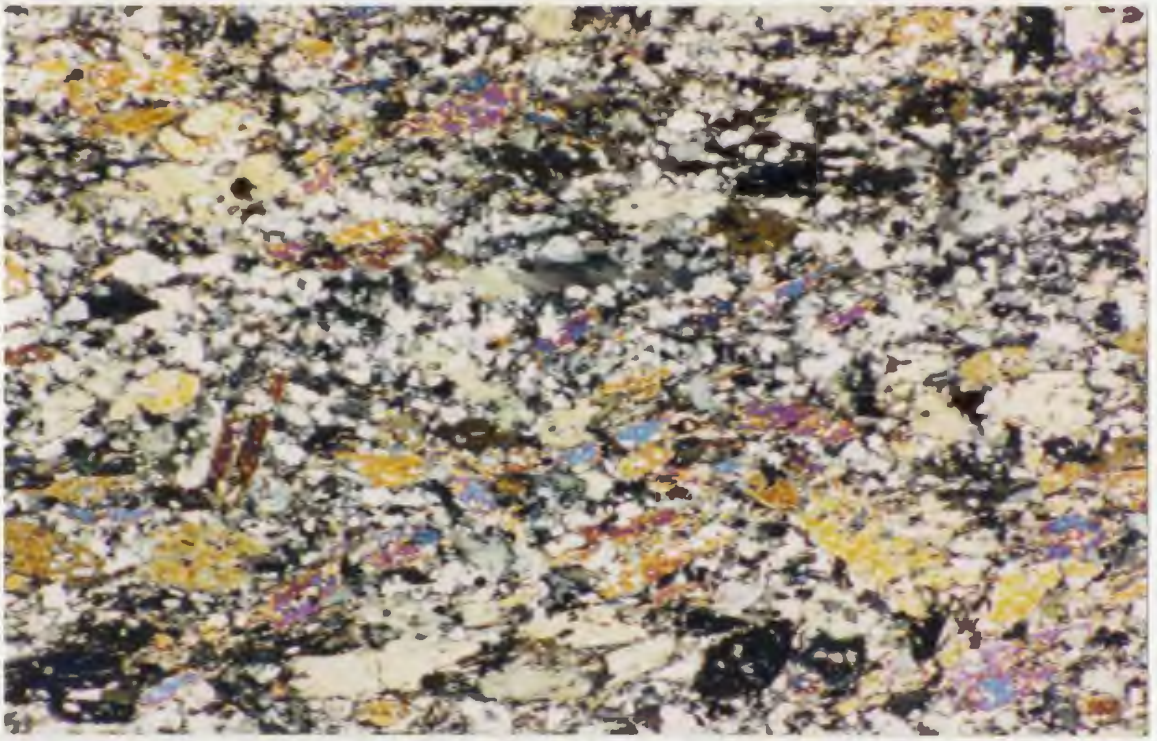

Plate 2.21. Fine-grained, metamorphically layered, metasedimentary schist with abundant amphibole (hornblende), recrystallized quartz and plagioclase, and epidote [87-077A, 30x, XN].

Plate 2.22. Small meta-ultramafic 'plug' intruding mafic metavolcanic schists of the Florence Lake Group [1 km W of Shark Lake].

Plate 2.23. Massive serpentinized peridotites. Note the colour contrast between weathered (red-brown) and fresh surfaces (dark green) [200 m S of Shark Lake].

belt.

The serpentinized peridotites are naturally very magnetic because of their high magnetite content, and are clearly defined on airborne magnetic surveys (Jagodits, 1983).

In the field, the peridotites show a wide range in appearance due largely to variations in the intensity of deformation and alteration. They range from relatively massive, to tightly folded and strongly cleaved. All rocks are serpentinized and are generally medium-to-dark green on fresh surfaces. Weathered surfaces are predominantly various shades of reddish-brown to tannish-brown.

Massive varieties generally weather red but are dark green on fresh surfaces due to intense serpentinization (Plate 2.23). Variations in alteration and weathering sometimes produce weathering rinds on rounded outcrop surfaces. These resemble infolding of red- into brown-weathered peridotite, and were initially interpreted as such (Plate 2.24). Primary igneous layering was observed only locally where clinopyroxene is still preserved; however, thin carbonate bands up to several centimetres thick sometimes mimic primary igneous layering (Plate 2.25). Small resistant magnetite and chromite grains (generally < 1 mm in diameter) are common and 'stand out' against the weathered serpentine.

As noted above, the peridotites are completely serpentinized, but they have also undergone variable degrees of carbonatization (± talc). Locally blocks of serpentinized peridotite are completely engulfed by talc-magnesite schists

Plate 2.24. Variations in weathering of metaperidotite outcrops result in weathering rinds which mimic 'infolding' [1 km W of Shark Lake].

Plate 2.25. Carbonate layers mimicking primary igneous layering in metaperidotites [1 km W of Shark Lake].

(Plate 2.26). Cross-cutting magnetite and coarse rhombohedral carbonate veinlets are also common. In areas where the rocks are tightly folded, they are converted to pale green serpentinite schists (Plate 2.27), and develop a strong cleavage which is crenulated in fold hinge areas. A small asbestos occurrence consisting of slip-fibre in serpentinites was observed about 4.5 km south of Florence Lake (see map - back pocket).

In the southern part of the map area southwest of Knee Lake, highly weathered medium- to coarse-grained serpentinized peridotites form large talus slopes which are readily visible from the air (Plate 2.28). In one outcrop located on a prominent east-northeast-trending linear about 3 km northeast of Shark Lake, the meta-ultramafic rocks are sheared and converted to chlorite-carbonate schists (Plate 2.29).

2.4.2. Petrography

The ultramafic rocks are petrographically variable, and range from strongly foliated, talc-carbonate schists to relatively massive medium-grained, serpentinized peridotites.

Only one sample (87-135) was observed to contain a primary igneous silicate phase, that being clinopyroxene in an otherwise serpentinized peridotite (Plate 2.30). The most abundant rocks are medium-grained (0.5-5 mm), completely serpentinized peridotites which commonly display relict cumulate textures. Serpentine pseudomorphs after olivine and/or orthopyroxene are effectively outlined by magnetite

Plate 2.26. Blocks of red-weathering metaperidotite engulfed by talc-carbonate rocks [500 m NNW of Shark Lake].

Plate 2.27. Tightly folded and crenulated pale green serpentinite schists [200 m N of Shark Lake].

Plate 2.28. Talus slopes formed by highly-weathered green sepentinites [6.5 km S of Florence Lake].

Plate 2.29. Sheared chlorite-carbonate meta-ultramafic schists [2.25 km E-SE of Florence Lake].

Plate 2.30. Medium-grained clinopyroxene-bearing serpentinized peridotite [87-135, 10x, XN].

Plate 2.31. Medium- to coarse-grained serpentinized peridotite with magnetite in intercumulate areas outlining relict crystals pseudomorphed by serpentine [87-019A, 10x, XN].

(Plate 2.31) or more rarely carbonate (Plate 2.32) in intercumulate areas. Relict crystals can also be identified when they are pseudomorphed by pale yellow serpentine, which is coarser grained than the very fine-grained blue serpentine matrix (Plate 2.33). Chromite occurs as small anhedral to subhedral grains (0.1-0.75 mm) which are locally rimmed by magnetite. Besides rimming chromite and outlining relict crystals, magnetite also occurs as small anhedral grains throughout the serpentinites. Traces of millerite and pentlandite have also been identified in several samples.

The intensity of carbonatization varies considerably. Some samples have only traces of carbonate while others show near complete replacement (> 95 vol.%) of the rock (Plate 2.34). In these cases, igneous textures are totally obliterated, and only a replacement assemblage of carbonate and serpentine remain. Talc-carbonate schists consist of a very fine-grained assemblage of turbid granular magnesite and talc (Plate 2.35). Magnetite and chromite form anhedral grains generally 0.1-0.5 mm in diameter.

2.5. CARBONATE ROCKS (Unit 3a)

2.5.1. Field Description

Approximately 1.5 km southeast of Florence Lake, a belt of carbonate rocks appears to form a northeastern extension of the main ultramafic body (see map - back pocket). This belt is quite extensive and extends along strike for approximately 1.25 km, in contrast to the much smaller carbonate lenses

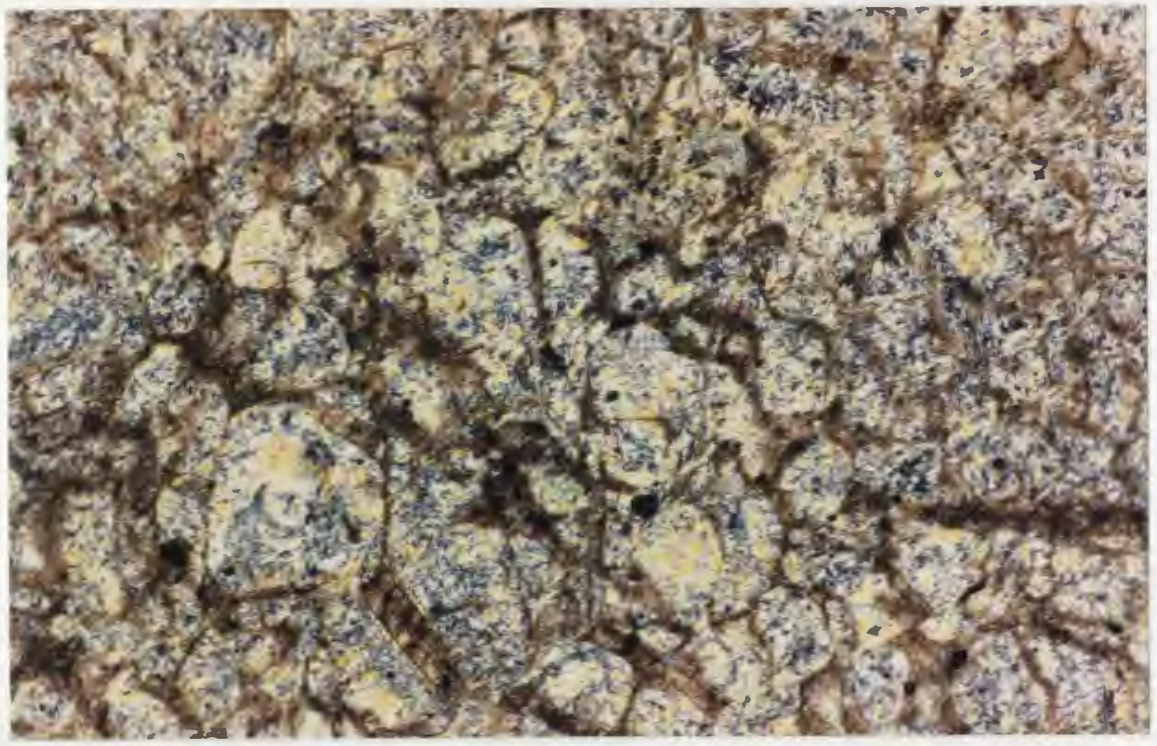

Plate 2.32. Medium-grained serpentinized peridotite with carbonate outlining relict crystals pseudomorphed by serpentine [87-198C, 15x, XN].

Plate 2.33. Relict crystals pseudomorphed by yellow serpentine in a very fine-grained blue serpentine matrix [87-174, 15x, XN].

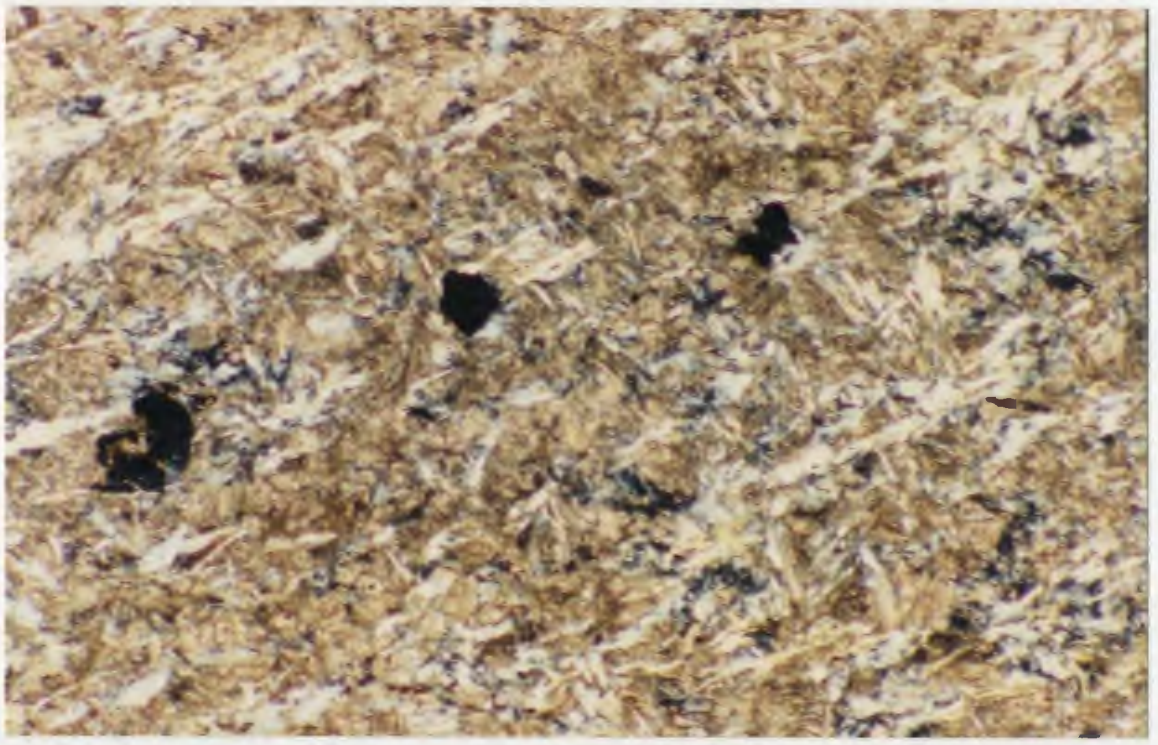

Plate 2.34. Pervasive magnesite and minor serpentine (fibrous) in an intensely carbonatized meta-ultramafic rock [87-018, 45x, XN].

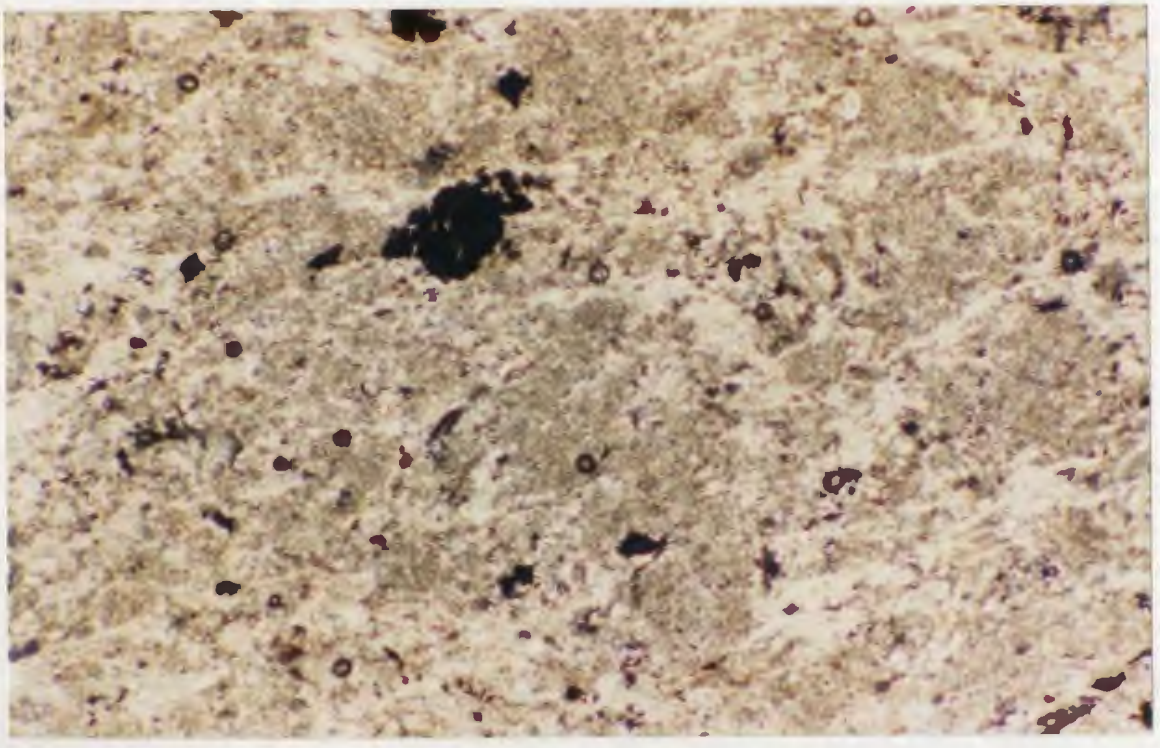

Plate 2.35. Meta-ultramafic rock is totally replaced by fine-grained granular magnesite and talc. The opaque minerals are magnetite and chromite [87-185C, 45x, XN].

within the mafic metavolcanic schists (see Plate 2.6).

These carbonatized ultramafic rocks are generally fine- to medium-grained granular rocks which are grey to cream-coloured on fresh surfaces, but weather red to brown. Magnesite is by far the most abundant phase, but variable amounts of quartz, talc, chlorite, chromite and magnetite are also present. The rocks are commonly cut by abundant milky-white quartz veins which characteristically infill tension gashes. The nature of the veins indicate that they formed in situ as a result of the carbonatization process (Plate 2.36).

In one outcrop, folded quartz-rich layers within the carbonates (Plate 2.37) give the rocks a 'bedded' sedimentary appearance (i.e., siliceous marbles); however, whole-rock and mineral chemistry (see Section 3.4) clearly show that these are indeed carbonatized ultramafic rocks. In the same area, the carbonatized rocks are layered and envelop a discontinuous boudinaged layer of rhyolite porphyry (Plate 2.38).

Although the carbonates invariably contain minor amounts of fine-grained recrystallized quartz, it is not readily apparent in the field. Talc and chlorite are common and occur both as foliation-forming minerals and also as small patches up to several centimetres in diameter. In one outcrop which was blasted by BP Minerals Limited, chromium-rich chlorite and talc define a strong foliation, and give the rocks a characteristic deep green colour (Plate 2.39). On another outcrop, small resistant albite porphyroblasts (up to 2 mm in diameter) stand out against weathered carbonate (Plate 2.40).

Plate 2.36. Northeast-trending sequence of magnesite-quartz-talc meta-ultramafic rocks cut by abundant milky white quartz veins [1.5 km SE of Florence Lake].

Plate 2.37. Folded quartzitic layers in northeast-trending magnesite-quartz-talc meta-ultramafic rocks locally give the rocks a sedimentary appearance; however, petrography and chemistry show that the rocks are ultramafic in origin. Note the thin quartz veins generally parallel to axial planes [1.5 km SE of Florence Lake].

Plate 2.38. Boudinaged felsic porphyritic tuff (white) within layered carbonate-quartz-talc meta-ultramafic rocks. Layers consist of alternating fine- and medium-grained carbonate [1.5 km SE of Florence Lake].

Plate 2.39. An outcrop of carbonate-quartz-talc meta-ultramafic schists which was blasted by BP Minerals Ltd. during their 82/83 exploration program. Note the deep green chlorite (Cr-rich) defining the foliation, and the milky white quartz veins cutting the carbonates [1.5 km SE of Florence Lake].

Plate 2.40. Resistant albite porphyroblasts stand out in contrast to weathered carbonate in a completely carbonatized ultramafic rock [1.5 km SE of Florence Lake].

This resembles the 'hob-nail' texture of many peridotites, where resistant pyroxene crystals stand out against weathered olivine. Small chromite and magnetite grains (< 1mm) are also common within the carbonatized ultramafic rocks.

2.5.2. Petrography

The carbonatized ultramafic rocks are generally fine-grained granular rocks containing in excess of 90% magnesite. They vary from massive to well-foliated and layered, and comprise the mineralogy ferroan-magnesite (see Section 3.4.1), quartz, chlorite, talc, chromite and magnetite. The ferroan-magnesite is invariably fine-grained and granular (0.1-0.5 mm in diameter), while quartz is very fine-grained (≤ 0.1 mm) and recrystallized with sutured grain boundaries. Chlorite and talc define the foliation (Plate 2.41), although locally chlorite and talc may be patchy, quartz absent, and carbonate coarser-grained (1-2 mm). Chromite and magnetite form anhedral grains about 0.1 mm in diameter, and trace millerite was identified in one sample (87-065). Some layered varieties consist of alternating fine- and medium-grained carbonate layers (Plate 2.42). Sample 87-264A contains relatively large albite porphyroblasts up to 4-5 mm in diameter (see Plate 2.40), and has the mineral assemblage ferroan-magnesite + quartz + albite + fuchsite (trace) + chromite + magnetite. The albite is both twinned and untwinned, and contains numerous micro-inclusions of rutile, which was identified by SEM analysis.

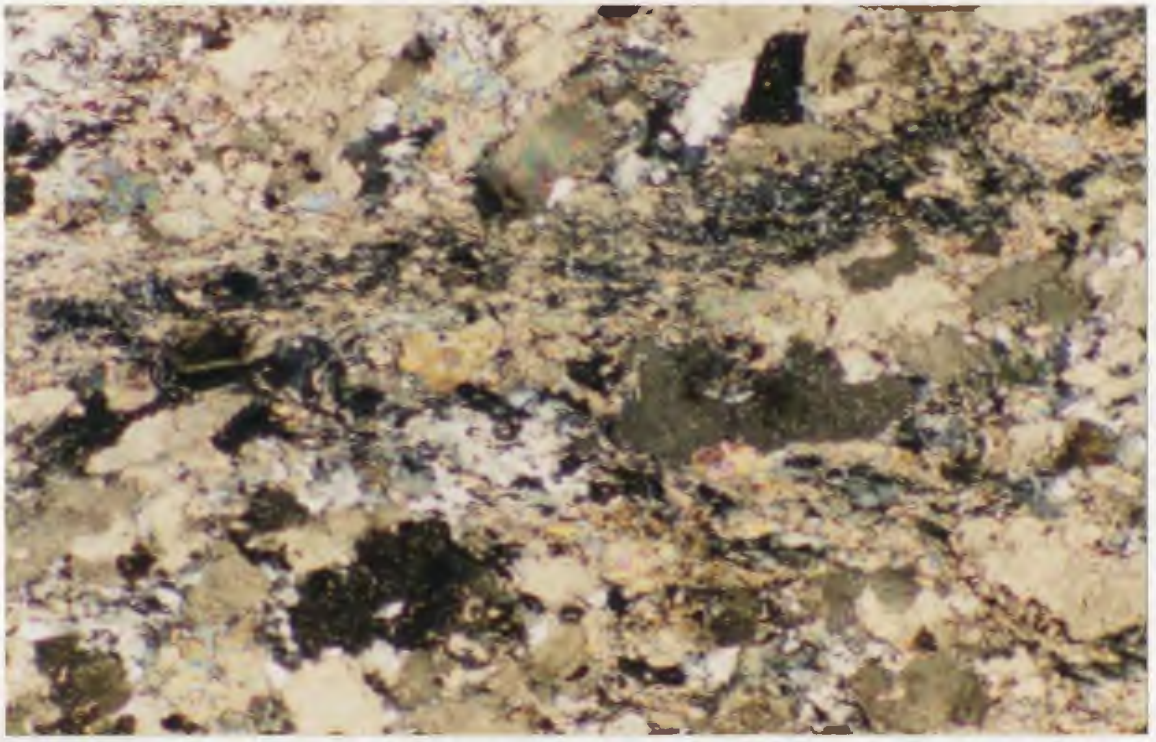

Plate 2.41. Foliated magnesite-quartz-talc-chlorite (Cr-rich) meta-ultramafic rock [87-063-2, 45x, XN].

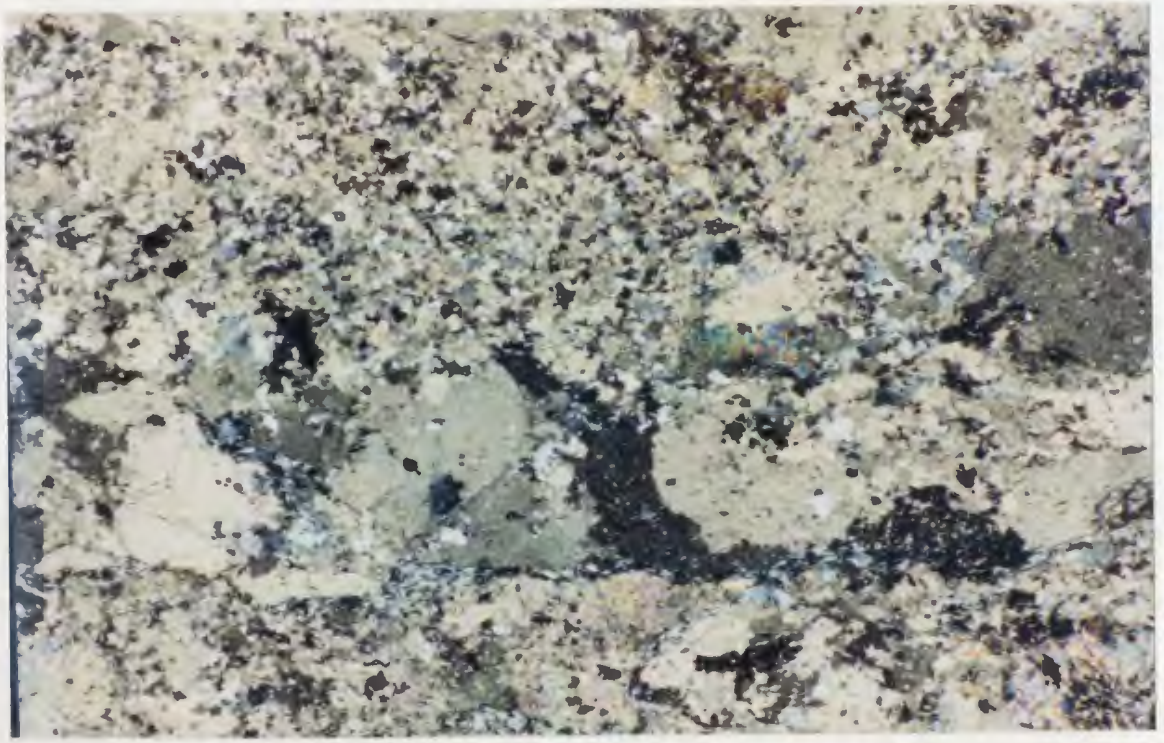

Plate 2.42. Alternating fine- and medium-grained layers (see Plate 2.38) in a magnesite-quartz meta-ultramafic rock [87-262, 20x, XN].

2.6. KANAIRIKTOK INTRUSIVE SUITE (Unit 4)

2.6.1. Field Description

The Kanairiktok Intrusive Suite consists of trondhjemitic rocks which envelop and intrude the FLG (see map - back pocket). The trondhjemites are medium-grained, leucocratic rocks which weather white to pink, and vary from massive to mylonitic, depending on the degree of deformation (Plates 2.43 and 2.44). Plagioclase and quartz generally comprise greater than 90% of the rock, while mafic minerals (mostly chlorite and muscovite) define the foliation.

Contacts with the FLG are generally sharp; however, commonly the contacts are marked by zones where trondhjemite contains numerous xenoliths and rafts (centimetres to hundreds of metres) of mafic metavolcanic rocks (amphibolites). Thin veinlets of trondhjemitic melt are commonly injected into the amphibolites. South and southwest of Florence Lake, the trondhjemites are relatively massive and display only a very weak fabric defined by aligned chlorite and muscovite. However, northeast and east of Florence Lake, the trondhjemites are strongly deformed gneisses and mylonites comprising alternating layers of ribbon quartz and plagioclase (Plate 2.44). Despite the large strain gradient variation between the massive and mylonitic trondhjemites, they are nevertheless interpreted to represent a single magmatic event.

Northwest of Florence Lake in the vicinity of the Baikie showings, the trondhjemites are relatively massive with a very weak fabric, and angular xenoliths and rafts of mafic

Plate 2.43. An east-west-trending, fine-grained diabase dyke (left) cutting relatively undeformed, massive leucocratic Kanairiktok trondhjemite [2 km S of Florence Lake].

Plate 2.44. Tight angular folds in highly deformed Kanairiktok mylonitic trondhjemite characterized by alternating bands of ribbon quartz (white, high relief) and plagioclase. Note the folded thin (2 cm) quartz band [300 m E of Benny Lake].

metavolcanic (and minor meta-ultramafic) rocks are so numerous within the trondhjemites that the they are more properly termed agmatites (see Plate 4.7).

2.6.2. Petrography

The Kanairiktok trondhjemites are medium-grained and contain plagioclase and quartz which comprise greater than 90 vol.% of the rock. Minor mafic minerals help to define the foliation, and include chlorite (after biotite), muscovite, epidote and minor biotite.

The trondhjemites display a complete range in deformation, from essentially undeformed massive rocks to strongly deformed mylonitic rocks with alternating layers of ribbon quartz and plagioclase. The least deformed samples are medium-grained rocks which exhibit hypidiomorphic textures with euhedral to subhedral plagioclase, and anhedral quartz (Plate 2.45). Plagioclase is unaltered and forms subhedral, compositionally zoned crystals (average 1-3 mm, up to 5 mm in diameter) with albite, pericline and Carlsbad twinning. Quartz shows slight undulose extinction, is only weakly strained, and forms anhedral crystals approximately 0.5-3.0 mm in diameter. Plagioclase locally contains small round inclusions of quartz (0.1 mm) and epidote (0.05 mm). The foliation is very weak and is defined by aligned pale green chlorite (after biotite), biotite (almost completely replaced), muscovite and epidote porphyroblasts (0.5-1.5 mm). Locally, a reduction in the grain size of quartz along foliation planes indicates minor brittle

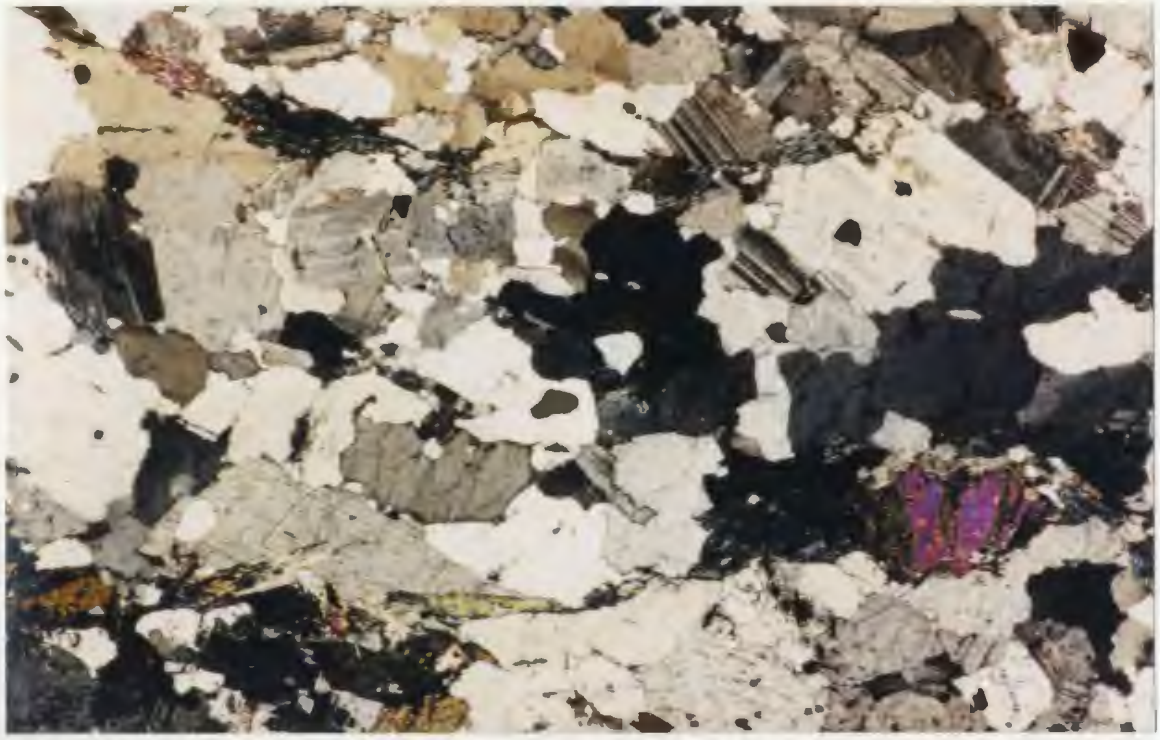

Plate 2.45. Massive, undeformed Kanairiktok trondhjemite comprising quartz and plagioclase with minor epidote (lower right), chlorite (left of epidote), muscovite (bottom center) and biotite (extreme bottom center) [87-013, 15x, XN].

Plate 2.46. Strongly deformed Kanairiktok mylonitic trondhjemite comprising alternating layers of recrystallized ribbon quartz (elongated quartz grains) and plagioclase. Mafic minerals are chlorite and muscovite [87-237, 10x, XN].

deformation.

In areas of high strain the rocks are mylonitic, and are characterized by alternating layers (2-5 mm wide) of highly strained and recrystallized ribbon quartz and plagioclase (Plate 2.46). These pinch and swell to form augens up to 1 cm in length. Plagioclase is strongly saussuritized and forms anhedral crystals between 0.25-0.5 mm in diameter. Quartz is highly strained and elongated parallel to the foliation. Grain boundaries are commonly sutured with small (< .01 mm) recrystallized quartz crystals concentrated along grain boundaries. Chlorite and muscovite are generally confined to the plagioclase layers and/or boundaries between these layers and ribbon quartz. In contrast to the relatively undeformed trondhjemites, epidote or biotite have not been observed in these highly deformed mylonites, and chlorite is brown in thin section.

2.7. PROTEROZOIC DIABASE AND GABBRO DYKES (Unit 5)

2.7.1. Field Description

Undeformed Proterozoic diabase and gabbro dykes cut all other lithologies in the map area (see Plate 2.43). These dykes are subvertical and range in thickness from only a few centimetres to greater than 100 m. Most small dykes appear to strike roughly east-west; however, a series of wider and more continuous gabbro dykes strikes between north-south and northeast-southwest.

One of the large gabbro dykes outcrops on a ridge

immediately west of Florence Lake (see map - back pocket). Mayor and Mann (1960) reported that small diabase dykes cut this large gabbro dyke, thus indicating that at least two periods of magmatism existed. Based on airborne magnetic data, Jagodits (1983) considered the small east-west-trending dykes to represent the last intrusive event in the area. The dykes show a very strong magnetic contrast with adjacent lithologies due to their relatively high contents of ilmenite and minor pyrrhotite and/or pyrite.

In the field, the dykes are very easy to identify since they are undeformed and essentially unaltered. They are massive rocks and lack the strong foliation typically displayed by other lithologies. Contacts with country rocks are very sharp, and dykes of significant width exhibit fine-grained diabasic margins and medium- to coarse-grained gabbroic cores. The gabbro dykes generally weather brown, but are dark green on fresh surfaces. Some of the gabbro dykes contain large subhedral plagioclase phenocrysts up to 2 cm long.

2.7.2. Petrography

The mineralogy and textures of dykes vary slightly between fine- and coarse-grained varieties. Fine-grained east-west-trending diabase dykes contain clinopyroxene (titanaugite), plagioclase (labradorite), ilmenite, apatite and minor pyrite and/or pyrrhotite. These dykes are relatively equigranular with respect to clinopyroxene and plagioclase,

with both phases generally less than 1 mm in maximum dimension (Plate 2.47). Titanaugite is strongly pleochroic (lilac to pale brown) and occurs both as anhedral stubby (<0.1 mm) and elongated crystals (≤ 1 mm long). Titanaugite crystals partially enclose twinned, variably saussuritized plagioclase laths (0.25-0.50 mm long) to form subophitic textures; however, some of the smaller stubby crystals lie between plagioclase laths and form intergranular textures. Plagioclase locally forms larger anhedral phenocrysts up to 5 mm long. Plagioclase shows variable degrees of sericitization and saussuritization. Ilmenite forms long needles (≤1 mm) and small discrete anhedral crystals (0.1-0.2 mm) (Plate 2.47). Apatite occurs as both small euhedral hexagonal (basal) crystals, and as long prismatic needles (longitudinal) with cleavage traces perpendicular to their length. Secondary amphibole, chlorite, biotite, epidote and quartz occur in the groundmass.

The medium- and coarse-grained gabbro dykes contain clinopyroxene (titaniferous augite), plagioclase (labradorite) and ilmenite, but no apatite. Large titaniferous augite oikocrysts up to 2 cm in diameter partially to totally enclose much smaller twinned plagioclase laths (0.5-2.0 mm) to form subophitic and ophitic textures (Plate 2.48). The coarse-grained gabbro dykes generally have a higher modal proportion of plagioclase than the fine-grained diabase dykes. Plagioclase shows slight compositional zoning and is relatively unaltered, although local sericitization and

Plate 2.47. Fine-grained diabase dyke with relatively equigranular clinopyroxene and plagioclase. Note the small equant and long prismatic habit of ilmenite crystals [87-056, 45x, XN].

Plate 2.48. Medium- to coarse-grained gabbro dyke with large clinopyroxene oikocrysts enclosing euhedral plagioclase laths. Note the anhedral ilmenite crystals (top left) [87-101, 15x, XN].

saussuritization is not uncommon. Locally plagioclase forms large (up to 1.5-2.0 cm long) subhedral phenocrysts which are considerably larger than those enclosed by the titaniferous augite. Ilmenite forms anhedral crystals generally less than 1 mm in diameter; however the long prismatic ilmenite crystals which are typical of the fine-grained diabase dykes are absent. Although the titaniferous augite is generally unaltered, locally rims are replaced by amphibole and chlorite.

2.8. STRUCTURE AND METAMORPHISM

2.8.1. Structural and Tectonic Evolution of the Southern Nain Province

Korstgård and Ermanovics (1984, 1985) have reviewed the structural and tectonic evolution of the southern Nain Province and adjacent Proterozoic Makkovik Province to the south. The sequence of Archean and Proterozoic events are summarized in Table 2.2.

Based on the parallelism of planar and linear structures, Korstgård and Ermanovics (1984, 1985) recognized two major structural domains within the southern Nain Province, viz., the Hopedale and Fiord structural domains. The Hopedale domain, which is restricted to a relatively small (20 x 40 km) area around the coastal village of Hopedale, contains the oldest (ca. 3015 Ma, Grant et al., 1983) regional structures. Planar structures strike northwest (see Figure 2.1) and dip steeply to the southwest; linear structures plunge gently to

Table 2.2. Summary of Archean and Early Proterozoic events in the southern Nain Province and adjacent Makkovik Province (modified after Korstgård and Ermanovics, 1985).

PROTEROZOIC

12) Intrusion of dioritic sills and dykes, *Kokkovik Dykes* (ca. 1635 Ma)

11) Intrusion of *Island Harbour Bay Intrusive Suite*. Early phases are syntectonic to Makkovikian deformation; the main phase is post-tectonic at ca. 1810 Ma, but was followed by shearing in Kanairiktok Bay.

10) *Makkovikian* deformation and metamorphism at lower amphibolite facies.

9) Deposition of shallow-water, basinal sediments and lava flows, of *Moran Lake Group*, and subaerial lava flows and conglomerates of *Ingrid Group*.

8) Intrusion of doleritic to gabbroic dykes, *Kikkertavak Dykes* (ca. 2200 Ma).

ARCHEAN

7) *Fiordian* deformation and metamorphism at lower amphibolite facies.

6) Intrusion of *Kanairiktok granitoid rocks* (ca. 2830 Ma).

5) Deposition of mafic to felsic volcanic rocks, *Florence Lake Group*.

4) *Hopedalian* deformation and metamorphism at upper amphibolite facies (ca. 3015 Ma).

3) Intrusion of dolerite dykes, *Hopedale Dykes*.

2) (?) Intrusion of tonalite and porphyritic granodiorite, *Maggo Gneiss*, followed by deformation and metamorphism.

1) (?) Deposition of mainly basaltic supracrustal rocks, *Weekes Amphibolite* (= Hunt River belt?), and intrusion of gabbro-anorthositic rocks.

---

* All ages are Rb-Sr whole rock ages from Grant et al. (1983).

the southeast. These Hopedalian structures are deformed into northeast-trending structures in the much more extensive Fiord domain, which is characterized by north to northeast-trending subvertical planar structures, and shallow northeast-plunging linear structures. Locally, older Hopedalian structures are preserved within the Fiord structural domain.

Following Hopedalian deformation and migmatization, and before Fiordian deformation, the terrane was cratonized and the Florence Lake Group was deposited unconformably on the Hopedale Metamorphic Complex. Before and possibly during Fiordian deformation, elongate northeast-trending plutons of the Kanairiktok Intrusive Suite were emplaced at 2838 Ma (Loveridge et al., 1987). After Fiordian deformation and metamorphism, the Archean block was cut by several generations of basic dykes.

Korstgård and Ermanovics (1984, 1985) proposed a simple shear model for the evolution for the Hopedale and Fiord domains. The Fiord structural domain is considered to represent part of a major ductile shear belt with a north-northeast-striking subvertical shear plane; movement direction was subhorizontal and the sense of shear sinistral as indicated by the deflection of Hopedalian structures.

2.8.2. Structure

All lithologies within the map area, except the Proterozoic diabase and gabbro dykes, have been affected by intense Fiordian deformation.

In intensely deformed areas, the style of folding is locally a reflection of the lithology present. For example, competency contrasts between relatively massive felsic and schistose mafic metavolcanic rocks, locally result in concentric, parallel folds in the former and tight, angular folds in the latter (Plate 2.13). The serpentinized peridotites are locally tightly folded with a strong penetrative cleavage, and around fold hinge areas crenulation cleavage is well-developed (Plate 2.27). In highly deformed areas the Kanairiktok trondhjemites are converted to well-foliated gneisses (Plate 2.44).

Planar structures including cleavage, schistosity and gneissosity are invariably northeast-trending and subvertical, with both northwest and southeast dipping directions (Figure 2.2). These prominent northeast-trending structures are most evident around Benny and Josie Lakes.

Several prominent linears, interpreted to be regional faults, are visible on aerial photographs. The contact between the FLG and the Kanairiktok Intrusive Suite south of Florence Lake, is marked by a major northeast-trending (030°) linear which appears to be at least locally fault-controlled. Ultramafic rocks are intensely sheared and converted to carbonate-chlorite schists along a prominent east-northeast-trending (060°) linear southeast of Florence Lake (Plate 2.29). In another outcrop, intensely carbonatized ultramafic rocks have undergone ductile deformation and envelop a

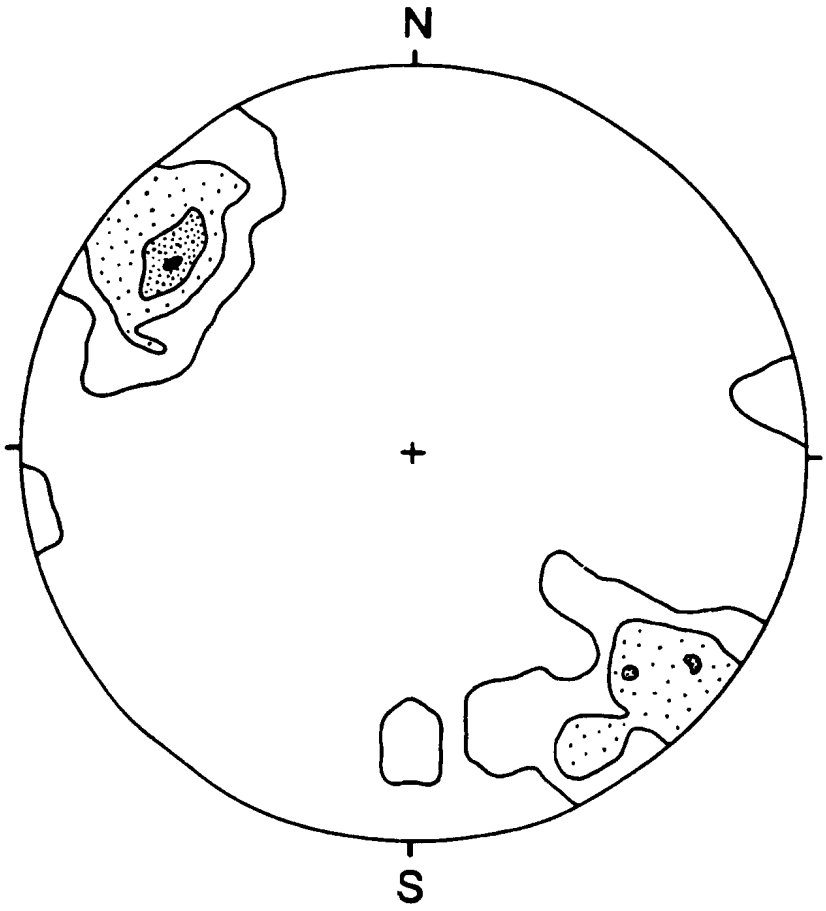

Figure 2.2. Orientation of poles to planar structures (cleavage, schistosity, gneissosity) in the study area; 32 poles. Contours at 1, 6, 12 and 18% per 1% area; maximum value 18.7%.

discontinuous boudinaged layer of rhyolite porphyry (Plates 2.38, 2.19).

Many of the rocks within the Florence Lake area have undergone intense ductile deformation along high strain zones, raising the possibility that the stratigraphy may be tectonic in nature, resulting from thrust imbrication. This important question points to the obvious need for detailed structural and stratigraphic studies within the FLG.

2.8.3. Metamorphism

All lithologies within the study area, except the Proterozoic diabase and gabbro dykes, were metamorphosed during regional Fiordian deformation. The FLG contains the metamorphic assemblage actinolite + epidote + chlorite + sericite + calcite ± biotite + plagioclase + quartz. Ermanovics and Raudsepp (1979a) noted that this assemblage is characteristic of middle greenschist facies metamorphism. Near intrusive contacts with the Kanairiktok Intrusive Suite, mafic metavolcanic rocks of the FLG are commonly metamorphosed to amphibolites, containing the assemblage hornblende + plagioclase + quartz ± epidote ± calcite. In one outcrop located several metres south of the Main Baikie showing northwest of Florence Lake (see map - back pocket), a small garnet-amphibolite xenolith contains the assemblage hornblende + garnet (almandine) + quartz (polygonal texture) + epidote + calcite.

During metamorphism of ultramafic rocks, addition of H_2O converts ultramafic rocks to serpentinites, whereas addition of H_2O and CO_2 converts serpentinites to talc-carbonate rocks.

The 'typical' meta-ultramafic rocks south of Florence Lake consist of serpentinized peridotites containing the assemblage serpentine ± magnesite ± talc + magnetite + chromite. Serpentine is stable only at very small values of X_{CO2} (see Figure 2.3), and its presence indicates X_{CO2} values < 10 mole% (Winkler, 1979), otherwise serpentine would be converted to magnesite + quartz (reaction 5) or to magnesite + talc (reaction 3). Conversion of the peridotites to serpentinites can be explained by the reaction:

2 forsterite + 3 H_2O = 1 serpentine + 1 brucite (6)

Although brucite has not been observed, Moody (1976) notes that "brucite may not be identified in thin section studies of serpentinized rocks because it is often fine-grained and intimately intergrown with lizardite and/or chrysotile". The serpentinite samples were not X-rayed for brucite. Many of the samples contain the assemblage serpentine + magnesite, which can be formed by the addition of CO_2 in addition to H_2O according to the reaction:

2 forsterite + $2H_2O$ +$1CO_2$ = 1 serpentine + 1 magnesite (1)

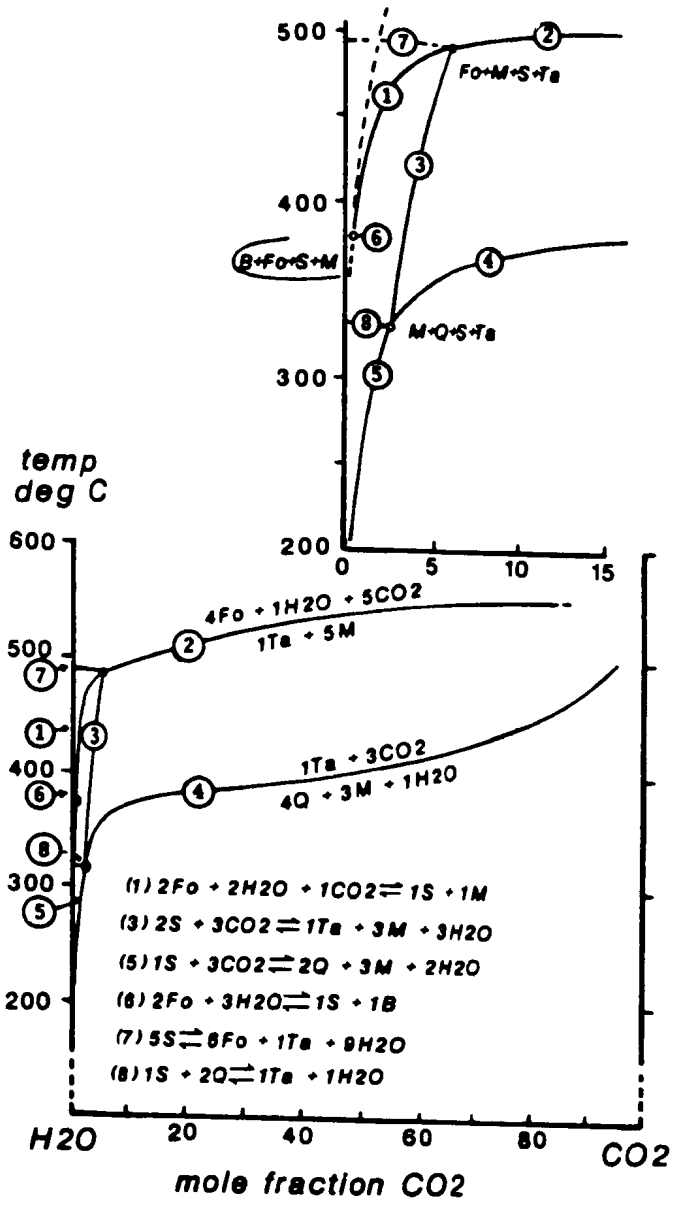

Figure 2.3. Isobaric equilibrium curves in the system MgO-SiO_2-H_2O-CO_2 (after Winkler, 1979). Note that the assemblages observed in the meta-ultramafic rocks within the Florence Lake area can be explained by reactions 1 through 6 at low to moderate values of X_{CO2}. Fluid pressure (P_f) = 2 Kb. Mineral abbreviations: Fo = forsterite; B = brucite; S = serpentine; M = magnesite; Ta = talc; Q = quartz.

The talc-carbonate schists can be produced by the reactions:

$$4 \text{ forsterite} + 1\ H_2O + 5\ CO_2 = 1 \text{ talc} + 5 \text{ magnesite} \quad (2)$$

$$2 \text{ serpentine} + 3CO_2 = 1 \text{ talc} + 3 \text{ magnesite} + 3\ H_2O \quad (3)$$

Rivers (1991, pers. comm.) suggests that formation of magnesite according to reactions 1 and 2 is unlikely, and notes that magnesite generally develops from serpentine (reaction 3), not olivine.

Serpentine is absent within the completely carbonatized meta-ultramafic rocks southeast of Florence Lake, and the rocks contain the assemblage magnesite + quartz + chlorite (Mg-Cr-rich) ± talc ± fuchsite + magnetite + chromite. This assemblage clearly indicates that X_{CO2} values within these rocks were higher than in the serpentinites further south. The assemblages observed in the carbonatized ultramafic rocks can be explained in terms of the reactions:

$$4 \text{ quartz} + 3 \text{ magnesite} + 1\ H_2O = 1 \text{ talc} + 3\ CO_2 \quad (4)$$

$$1 \text{ serpentine} + 3\ CO_2 = 2 \text{ quartz} + 3 \text{ magnesite} + 2\ H_2O \quad (5)$$

If X_{CO2} values are very high, anthophyllite + magnesite or enstatite + magnesite assemblages will be produced (Figure 2.3), and these have not been observed.

During serpentinization, iron in olivine may be redistributed and enter the structure of serpentine or brucite, or form discrete opaque phases including magnetite,

awaruite, pentlandite, ferrit-chromite, etc. (Ashley, 1975). Magnetite is formed according to the reaction:

$$3\ Fe_2SiO_4 + 2\ O = 2\ Fe_3O_4 + 3\ SiO_2$$

and occurs both as rims on chromite grains and as independent grains.

The presence of Al_2O_3 results in the formation of Mg (Cr)-rich chlorite, and the extremely low CaO content in all the metaperidotites (except 87-135) and intensely carbonatized meta-ultramafic rocks (see Section 3.3.1) indicates that clinopyroxene was a very minor phase in these rocks. However, albite porphyroblasts and traces of fuchsite in sample 87-264A indicate that saline, metasomatic fluids carrying Na^+ and K^+ were locally important within the intensely carbonatized ultramafic rocks.

2.9. DISCUSSION

Recent field mapping in the southernmost portion of the FLG (this study) confirms that volcanic rocks in the succession are bimodal; however, the author suggests that in the Florence Lake area, the mafic sequence appears to be comprised almost entirely of rocks of basaltic composition, with rocks of andesitic composition rare. The felsic rocks can generally be divided into two groups based on the presence or absence of plagioclase and/or quartz fragments. Fine-grained quartz-rich schists are herein interpreted to be fine-grained

clastic (volcaniclastic ?) metasedimentary rocks, whereas more massive lithologies containing plagioclase and quartz fragments intercalated with mafic metavolcanic rocks, are interpreted to be felsic porphyries and tuffs. As originally noted by Ermanovics and Raudsepp (1979a), felsic rocks which can be definitively classified as volcanic flows have not been recognized.

Ermanovics and Raudsepp (1979a,b) described the carbonate rocks within the metavolcanic rocks as impure limestones (marbles) and calc-silicate rocks, and cited the calcareous character of the felsic and intermediate pyroclastic rocks as evidence for exhalative volcanic activity. However, Ermanovics and Raudsepp did not comment on the extensive zone of intensely carbonatized meta-ultramafic rocks southeast of Florence Lake. Guthrie (1983) and Stewart (1983) first brought attention to these carbonatized rocks, and they related intense carbonatization to major regional faults. The carbonatized ultramafic rocks southeast of Florence Lake appear to form a northeastern extension of the main ultramafic body (see map - back pocket), and the assemblages contained within these rocks can be explained in terms of a series of metamorphic and metasomatic reactions at low to moderate X_{CO2} values, with X_{CO2} values increasing northeastward.

Ermanovics and Raudsepp (1979a) recognized Proterozoic diabase and gabbro dykes of at least two ages within the southern portion of the Nain Province. The oldest and apparently most abundant dykes are the Kikkertavak dykes,

which trend between 025°-045°. These dykes are reported to contain abundant (40-70%) secondary epidote, actinolite, chlorite and carbonate. The author has not identified any dykes within the Florence Lake area which match the description of the Kikkertavak dykes (Ermanovics and Raudsepp, 1979a). An apparently younger set of dykes strike between 045°-070°. These are much less altered and typically contain distinctive mauve titanaugite and up to 20% olivine. Ermanovics and Raudsepp (1979a) noted similarities between these younger dykes and those to the east and west of the Nain Province, namely the Aillik and Harp dykes, respectively. Ryan (1984) suggested that these may represent part of the Harp dyke suite (Meyers and Emslie, 1977).

The east-west-trending diabase dykes of this study area do not contain olivine, and the dykes are also chemically distinct from the Harp dykes (see Section 3.7). However, the larger north-south to northeast-southwest-trending gabbro dykes may be correlative to the Harp dykes. Although olivine has not been observed in these dykes, Ermanovics (per. comm., 1989) has indicated that gabbroic Harp Dykes rarely contain olivine and when they do, it is often in the chilled margins or in flow bands within the dykes.

CHAPTER 3. GEOCHEMISTRY

3.1. INTRODUCTION

Prior to the preliminary results of the present study (Brace and Wilton, 1989), published geochemical data for the Florence Lake Group (FLG) were non-existent. The only available data consisted of unpublished results (BP Minerals Ltd.) comprising major element and selected trace element analyses of FLG metavolcanic rocks. Therefore, one of the main goals of this study was to determine the geochemical affinities of the FLG utilizing a complete geochemical data set comprising major, trace and rare earth element (REE) analyses.

Although this study concentrates primarily on the FLG and meta-ultramafic rocks within the volcanosedimentary sequence, a small number of samples of the Kanairiktok Intrusive Suite and Proterozoic diabase and gabbro dykes have also been included for analysis.

In the following tables of analyses, total iron is expressed as Fe_2O_3*, and in discrimination diagrams FeO* has been calculated from Fe_2O_3* assuming $Fe^{+3}/Fe^{+2} = 0.15$ (Brooks, 1976). In all diagrams, analyses have been recalculated to 100% anhydrous unless otherwise stated. Hf and Ta values for mafic rocks (Table 3.1) only, are recalculated from Zr and Nb concentrations using the ratios Zr/Hf=37 and Nb/Ta=17 (after Jochum et al., 1986). The reasoning for this, is that the samples were pulverized in a tungsten carbide bowl, making Ta

values suspect due to contamination problems, and measured Hf values were unrealistically low relative to expected values based on Zr contents. This can be attributed to analytical problems in measuring Hf by the ICP-MS method at MUN (Jenner, 1990, per. comm.). Hf and Ta values elsewhere are analytical, but for reasons cited above should be regarded with caution. Analytical procedures are described in Appendix 1.

3.2. FLORENCE LAKE GROUP

Thirty-eight samples of FLG mafic (Table 3.1) to felsic (Table 3.2) supracrustal rocks were analyzed for major and trace elements, and over half of these were also analyzed for REE.

Before discussing the geochemistry of the FLG, it is essential to establish whether the analyzed samples are metavolcanic or metasedimentary in origin. This can sometimes be difficult in deformed and metamorphosed rocks.

Such a determination of the protolithology is generally not a problem for the mafic schists, since these have bulk compositions indistinguishable from established mafic volcanic rocks. However, the felsic rocks pose a greater problem. As noted previously, Ermanovics (per. comm., 1987, 1990) believes that many of the rocks containing plagioclase and/or quartz fragments are metagreywackes. In Table 3.3, the chemical compositions of greywackes of various ages (from Taylor and McLennan, 1985) are presented along with the average composition of FLG felsic porphyritic samples. The most

Table 3.1.1. Chemical analyses of mafic metavolcanic schists, flows, and pillow lavas, Florence Lake Group.

	TB-87-028	87-032	87-051	87-071	87-089A	87-103	87-108
SiO2 (wt. %)	48.70	49.30	50.60	48.40	45.80	48.40	51.10
TiO2	0.56	0.60	1.12	0.92	0.80	0.76	0.48
Al2O3	14.60	14.10	17.00	14.50	16.50	13.80	13.80
Fe2O3*	8.31	11.72	9.88	12.08	12.86	12.25	10.26
MnO	0.19	0.21	0.16	0.19	0.18	0.17	0.16
MgO	6.22	6.92	4.88	8.05	7.02	7.70	7.11
CaO	6.98	10.10	8.76	8.98	8.70	8.66	12.12
Na2O	4.12	1.66	2.89	3.02	0.44	1.79	1.89
K2O	0.00	0.03	0.12	0.02	0.22	0.01	0.03
P2O5	0.08	0.03	0.08	0.05	0.04	0.05	0.02
LOI	9.01	3.80	4.51	2.82	5.71	5.06	1.76
Total	98.77	98.47	100.00	99.03	98.27	98.65	93.73
Cr (ppm)	339	255	333	304	333	428	296
Ni	82	76	133	110	161	92	129
Sc	38.73	58.72	51.52	42.51	41.74	48.54	37.71
V	325	278	335	276	294	275	219
Cu	84	95	59	38	34	90	100
Zn	74	64	96	77	111	72	51
Rb	0.30	0.31	2.19	0.19	10.44	0.06	0.52
Ba	84	62	55	53	62	37	27
Sr	23.09	84.82	153.01	118.89	175.86	103.30	110.57
Ga	15	13	16	15	19	11	14
Nb	1.71	1.35	2.80	2.42	2.32	2.08	1.07
Zr	66	38	63	56	54	54	30
Y	5.44	15.47	20.65	19.09	18.78	17.22	12.34
Ta^	0.10	0.08	0.16	0.14	0.14	0.12	0.06
Hf^	1.78	1.03	1.70	1.51	1.46	1.46	0.81
Pb	0.79	2.35	3.27	1.39	1.78	1.48	1.43
Th	0.23	0.20	0.27	0.25	0.32	0.23	0.09
U	0.03	0.07	0.11	0.10	0.09	0.06	0.07
La (ppm)	2.40	1.73	2.82	2.76	2.60	2.49	1.21
Ce	7.04	4.59	8.24	7.84	7.16	6.89	3.44
Pr	1.13	0.70	1.34	1.21	1.14	1.16	0.59
Nd	5.13	3.23	6.57	6.08	5.62	5.45	2.85
Sm	1.62	1.36	2.38	2.17	2.05	1.98	1.16
Eu	0.42	0.47	0.79	0.78	0.77	0.69	0.53
Gd	1.42	1.78	2.91	2.69	2.55	2.56	1.52
Tb	0.25	0.39	0.61	0.52	0.51	0.52	0.31
Dy	1.40	2.73	4.15	3.59	3.56	3.55	2.09
Ho	0.26	0.63	0.89	0.77	0.76	0.73	0.47
Er	0.68	1.94	2.56	2.37	2.30	2.16	1.47
Tm	0.09	0.26	0.38	0.31	0.33	0.31	0.20
Yb	0.56	1.82	2.42	2.02	2.00	1.83	1.33
Lu	0.08	0.27	0.34	0.26	0.27	0.23	0.19

Note: Hf^ and Ta^ concentrations recalculated from Zr and Nb respectively, using the ratios Zr/Hf=37 and Nb/Ta=17 (after Jochum et al., 1986). nd = not detected.

Table 3.1.1 (continued).

	87-114A	87-139	87-149A	87-150	87-175A	87-189B	87-247C
SiO2 (wt. %)	49.60	46.40	48.80	43.80	54.80	56.60	47.70
TiO2	0.96	0.60	0.96	1.04	1.00	1.20	1.16
Al2O3	13.50	14.90	13.80	14.70	12.90	12.70	12.90
Fe2O3*	13.34	11.01	13.22	15.55	13.42	11.51	15.52
MnO	0.19	0.17	0.16	0.24	0.16	0.22	0.21
MgO	5.65	9.21	7.47	6.36	4.22	3.48	5.43
CaO	11.60	11.02	5.58	12.36	8.22	9.54	7.92
Na2O	1.40	1.90	1.34	1.18	1.81	1.20	1.39
K2O	0.07	0.01	0.27	0.02	0.24	0.06	0.22
P2O5	0.05	0.03	0.06	0.08	0.10	0.09	0.09
LOI	2.84	3.14	6.41	3.19	2.21	2.06	6.26
Total	99.20	98.39	98.07	98.52	99.08	98.66	98.80
Cr (ppm)	186	359	307	289	nd	173	29
Ni	54	138	85	140	nd	55	45
Sc	46.54	30.42	45.74	44.30	31.30	---	---
V	321	249	349	319	313	349	337
Cu	103	47	57	30	nd	3	87
Zn	76	55	73	95	32	135	101
Rb	0.94	0.07	8.97	0.15	4.10	nd	3
Ba	60	39	34	nd	129	11	nd
Sr	148.59	131.60	98.31	139.22	230.41	139	106
Ga	15	13	16	18	20	18	17
Nb	2.55	1.41	2.32	5.94	4.00	5	7
Zr	62	45	57	59	104	81	80
Y	20.33	11.37	20.63	18.65	24.13	31	25
Ta^	0.15	0.08	0.14	0.35	0.24	0.29	0.41
Hf^	1.68	1.22	1.54	1.59	2.81	---	---
Pb	1.48	1.44	1.41	1.10	2.54	---	---
Th	0.24	0.15	0.28	0.19	1.17	---	---
U	0.09	0.07	0.07	0.07	0.36	---	---
La (ppm)	2.93	1.69	2.93	2.51	8.73	---	---
Ce	8.32	4.68	8.08	7.03	19.36	---	---
Pr	1.28	0.74	1.29	1.13	2.75	---	---
Nd	6.16	3.80	6.23	5.68	11.53	---	---
Sm	2.32	1.42	2.27	2.00	3.37	---	---
Eu	0.85	0.53	0.73	1.07	1.26	---	---
Gd	2.84	1.72	2.70	2.52	4.00	---	---
Tb	0.56	0.37	0.56	0.53	0.71	---	---
Dy	3.87	2.42	3.75	3.68	4.93	---	---
Ho	0.83	0.53	0.82	0.77	0.95	---	---
Er	2.54	1.53	2.45	2.35	2.73	---	---
Tm	0.35	0.23	0.34	0.33	0.39	---	---
Yb	2.42	1.42	2.19	2.16	2.32	---	---
Lu	0.32	0.19	0.30	0.31	0.35	---	---

Note: Hf^ and Ta^ concentrations recalculated from Zr and Nb respectively, using the ratios Zr/Hf=37 and Nb/Ta=17 (after Jochum et al., 1986). nd = not detected.

Table 3.1.2 Chemical analyses of mafic metavolcanic massive flows and sills, Florence Lake Group.

	87-081	87-087A	87-175B	87-230C	87-261A
SiO2 (wt. %)	52.20	51.10	51.20	46.90	47.20
TiO2	0.52	1.36	0.84	0.76	0.96
Al2O3	12.80	12.30	13.40	15.60	14.20
Fe2O3*	8.50	15.97	13.99	11.20	13.03
MnO	0.14	0.24	0.20	0.16	0.20
MgO	6.56	5.02	5.75	8.74	7.08
CaO	14.06	9.38	8.22	9.78	10.92
Na2O	1.06	3.76	1.94	1.56	1.46
K2O	0.05	0.07	0.23	0.23	0.03
P2O5	0.03	0.14	0.09	0.05	0.09
LOI	3.84	1.35	2.75	3.48	3.87
Total	99.76	100.69	98.61	98.46	99.04
Cr (ppm)	267	nd	nd	356	235
Ni	49	4	11	174	97
Sc	---	---	---	---	---
V	256	405	293	240	331
Cu	nd	80	nd	62	88
Zn	24	45	91	64	75
Rb	nd	nd	1	4	nd
Ba	nd	20	63	55	1
Sr	115	305	152	108	117
Ga	12	23	20	12	15
Nb	5	7	5	4	2
Zr	31	117	77	46	54
Y	13	38	22	18	20
Ta^	0.29	0.41	0.29	0.24	0.12
Hf^	---	---	---	---	---
Pb	---	---	---	---	---
Th	---	---	---	---	---
U	---	---	---	---	---
La (ppm)	---	---	---	---	---
Ce	---	---	---	---	---
Pr	---	---	---	---	---
Nd	---	---	---	---	---
Sm	---	---	---	---	---
Eu	---	---	---	---	---
Gd	---	---	---	---	---
Tb	---	---	---	---	---
Dy	---	---	---	---	---
Ho	---	---	---	---	---
Er	---	---	---	---	---
Tm	---	---	---	---	---
Yb	---	---	---	---	---
Lu	---	---	---	---	---

Note: Hf^ and Ta^ concentrations recalculated from Zr and Nb respectively, using the ratios Zr/Hf=37 and Nb/Ta=17 (after Jochum et al., 1986). nd = not detected.

Table 3.1.3. Chemical analyses of mafic metavolcanic amphibolites, Florence Lake Group.

	87-120	87-155	87-156A	87-233A	87-2388	87-252
SiO2 (wt. %)	45.90	48.50	47.60	50.00	49.00	49.10
TiO2	1.24	0.96	1.20	0.92	1.32	0.84
Al2O3	15.50	13.90	13.60	15.40	13.70	13.90
Fe2O3*	13.20	12.89	16.81	10.66	15.80	13.03
MnO	0.30	0.21	0.22	0.18	0.22	0.22
MgO	8.24	7.51	7.88	5.54	5.98	8.03
CaO	9.52	10.64	8.98	9.84	9.30	9.72
Na2O	2.66	1.94	2.13	2.09	1.97	1.74
K2O	0.39	1.18	0.63	0.93	0.67	0.34
P2O5	0.05	0.06	0.15	0.05	0.09	0.07
LOI	1.72	1.78	1.74	2.63	1.15	1.19
Total	98.72	99.57	100.94	98.24	99.20	98.18
Cr (ppm)	203	218	54	334	55	285
Ni	94	151	46	126	61	103
Sc	55.32	30.42	---	45.78	---	27.26
V	465	262	407	316	452	313
Cu	79	106	58	100	144	14
Zn	124	81	97	70	137	83
Rb	8.59	53.63	10	38.60	14	2.96
Ba	172	139	43	112	44	38
Sr	132.32	119.87	103	221.65	107	50.12
Ga	17	18	17	14	18	15
Nb	2.51	3.29	7	2.48	6	1.77
Zr	87	60	77	54	81	48
Y	21.82	17.76	25	18.76	30	11.80
Ta^	0.15	0.19	0.41	0.15	0.35	0.10
Hf^	2.35	1.62	---	1.46	---	1.30
Pb	10.36	7.15	---	2.56	---	2.78
Th	0.37	0.33	---	0.20	---	0.14
U	0.16	0.11	---	0.08	---	0.07
La (ppm)	3.87	3.51	---	2.09	---	1.90
Ce	10.62	9.23	---	5.78	---	5.48
Pr	1.79	1.41	---	1.03	---	0.88
Nd	8.11	7.25	---	5.24	---	4.47
Sm	2.86	2.16	---	1.91	---	1.52
Eu	0.85	0.88	---	0.69	---	0.59
Gd	3.35	2.66	---	2.44	---	1.90
Tb	0.69	0.50	---	0.52	---	0.41
Dy	4.69	3.45	---	3.47	---	2.70
Ho	1.01	0.68	---	0.73	---	0.54
Er	2.87	1.86	---	2.17	---	1.72
Tm	0.41	0.28	---	0.31	---	0.24
Yb	2.60	1.79	---	1.99	---	1.49
Lu	0.39	0.25	---	0.33	---	0.25

Note: Hf^ and Ta^ concentrations recalculated from Zr and Nb respectively, using the ratios Zr/Hf=37 and Nb/Ta=17 (after Jochum et al., 1986). nd = not detected.

Table 3.2.1. Chemical analyses of plagioclase and quartz porphyritic felsic supracrustal rocks Florence Lake Group.

	87-057	87-130A	87-149B	87-178B	87-247B
SiO2 (wt. %)	72.50	72.30	68.60	79.00	73.90
TiO2	0.28	0.40	0.12	0.08	0.08
Al2O3	14.20	14.00	14.80	12.20	14.10
Fe2O3*	2.78	2.71	2.96	0.78	0.64
MnO	0.04	0.05	0.04	0.01	0.00
MgO	0.74	0.78	1.22	0.57	0.79
CaO	1.44	3.08	1.90	0.10	0.24
Na2O	4.39	4.95	4.84	2.80	5.43
K2O	1.56	0.67	1.70	3.20	1.62
P2O5	0.11	0.09	0.21	0.05	0.08
LOI	1.74	1.20	2.69	1.30	1.41
Total	99.78	100.23	99.08	100.09	98.29
Cr (ppm)	nd	nd	nd	nd	nd
Ni	nd	nd	nd	nd	nd
Sc	5.98	6.69	4.41	2.66	2.04
V	31	27	49	nd	30
Cu	4	12	4	nd	nd
Zn	27	6	34	nd	nd
Rb	47.91	16.04	43.55	86.03	43.72
Ba	688	316	534	421	281
Sr	76.68	204.00	188.09	26.05	164.15
Ga	18	16	20	17	20
Nb	4.83	4.75	0.22	3.03	0.11
Zr	165	174	129	65	101
Y	11.28	12.57	4.93	8.51	1.29
Ta	0.83	1.17	0.61	0.24	0.85
Hf	3.67	4.20	3.36	2.94	2.43
Pb	2.66	4.34	4.28	1.91	3.05
Th	5.99	5.73	4.72	5.95	1.56
U	1.32	1.22	0.88	1.49	0.50
La (ppm)	27.35	33.02	39.36	10.54	6.20
Ce	53.83	61.91	78.98	24.96	11.38
Pr	6.06	7.03	9.60	2.92	1.25
Nd	20.06	22.71	32.37	8.88	4.29
Sm	3.44	3.70	4.31	1.79	0.86
Eu	0.76	0.87	1.00	0.13	0.21
Gd	3.02	2.86	2.40	1.44	0.65
Tb	0.41	0.43	0.28	0.27	0.09
Dy	2.25	2.34	1.27	1.55	0.37
Ho	0.43	0.45	0.19	0.31	0.04
Er	1.26	1.23	0.48	0.98	0.08
Tm	0.18	0.19	0.07	0.13	0.01
Yb	1.11	1.20	0.43	0.87	0.08
Lu	0.16	0.17	0.06	0.15	0.01

Note: nd = not detected.

Table 3.2.2. Chemical analyses of fine-grained siliceous supracrustal rocks, Florence Lake Group.

	TB-87-054A	87-074	87-077A	87-092	87-153	87-250A	87-257	87-267
SiO2 (wt. %)	70.40	64.20	64.20	66.40	62.50	70.80	65.70	70.20
TiO2	0.16	0.56	0.48	0.16	0.64	0.20	0.56	0.16
Al2O3	13.20	16.10	13.00	17.40	14.90	15.80	16.20	16.00
Fe2O3*	2.69	5.38	7.83	4.56	5.07	1.12	3.36	1.54
MnO	0.05	0.07	0.10	0.05	0.09	0.02	0.05	0.02
MgO	1.01	2.44	3.28	1.11	3.75	0.86	1.66	2.13
CaO	3.26	2.86	5.02	1.40	5.24	1.64	4.10	1.40
Na2O	4.54	4.96	2.14	1.87	3.22	2.68	6.18	0.39
K2O	1.28	0.44	0.71	1.83	2.04	4.13	0.52	4.07
P2O5	0.09	0.12	0.25	0.21	0.06	0.11	0.13	0.06
LOI	3.45	1.55	2.41	3.59	1.69	2.04	1.26	3.77
Total	100.13	98.68	99.42	98.58	99.20	99.40	99.72	99.74
Cr (ppm)	nd	53	82	23	68	19	nd	1
Ni	nd	30	43	2	44	3	2	2
Sc	5.96	13.31	---	13.32	15.70	---	---	2.23
V	37	94	98	142	108	64	75	5
Cu	4	nd	nd	nd	nd	nd	6	1
Zn	27	58	61	6	42	nd	11	14
Rb	35.52	13.61	25	42.41	50.29	63	12	87.51
Ba	374	120	143	403	567	931	221	532
Sr	101.14	117.81	110	102.10	227.23	145	145	96.97
Ga	15	20	16	18	14	17	15	17
Nb	1.33	5.47	7	1.40	4.72	7.00	6.00	0.48
Zr	152	158	125	156	142	144	131	79
Y	8.40	13.09	13	7.42	14.60	12	12	1.49
Ta	0.77	1.07	---	0.47	1.20	---	---	0.26
Hf	3.80	1.75	---	3.73	1.17	---	---	1.98
Pb	2.71	3.76	---	3.06	4.89	---	---	2.81
Th	4.84	2.36	---	2.24	2.27	---	---	0.47
U	1.05	0.46	---	0.57	0.51	---	---	0.27
La (ppm)	21.01	19.54	---	7.82	16.48	---	---	2.41
Ce	41.42	38.12	---	17.34	34.40	---	---	5.65
Pr	4.55	5.12	---	2.01	4.20	---	---	0.67
Nd	14.85	17.94	---	7.81	15.51	---	---	2.45
Sm	2.49	3.62	---	1.58	3.09	---	---	0.47
Eu	0.50	0.94	---	0.43	0.81	---	---	0.12
Gd	1.93	3.22	---	1.59	3.40	---	---	0.54
Tb	0.28	0.49	---	0.23	0.48	---	---	0.06
Dy	1.65	2.74	---	1.42	2.93	---	---	0.27
Ho	0.32	0.53	---	0.27	0.59	---	---	0.05
Er	0.94	1.35	---	0.80	1.74	---	---	0.14
Tm	0.14	0.17	---	0.15	0.26	---	---	0.02
Yb	0.99	0.96	---	1.00	1.67	---	---	0.12
Lu	0.15	0.11	---	0.15	0.24	---	---	0.02

Note: nd = not detected.

Table 3.3. Chemical compositions of selected Phanerozoic and Archean greywackes (after Taylor and McLennan, 1985) and felsic porphyries of the FLG.

	GREYWACKES						LITHIC WACKE	AVERAGE FLG PORPHYRIES
	PHANEROZOIC			ARCHEAN				
	M277	MK64	MK97	DD9	YK2	KH44	YK28	
SiO2 (wt.%)	56.35	68.28	81.13	65.8	67.79	69.76	65.55	73.26
TiO2	1.39	1.00	0.62	0.52	0.56	0.52	0.44	0.19
Al2O3	16.19	12.95	10.01	15.9	15.44	13.79	10.94	13.86
FeO	11.22	6.94	2.76	5.36	5.94	7.79	8.44	1.97
MnO	0.19	0.21	0.03	0.07	0.07	0.02	0.16	0.03
MgO	4.06	2.22	1.44	3.56	2.54	2.91	3.83	0.82
CaO	5.22	4.50	0.26	2.87	1.9	1.27	7.34	1.35
Na2O	4.59	2.96	1.69	3.65	4.26	1.78	2.14	4.48
K2O	0.55	0.83	1.93	2.17	1.4	2.11	1.06	1.75
P2O5	0.24	0.12	0.14	0.11	0.09	0.05	0.1	0.11
LOI	3.50	6.10	1.85	2.88	1.62	6.23	11.29	1.67
Cr (ppm)	31	109	51	--	144	110	96	*nd
Ni	14	20	19	--	59	95	70	*nd
Co	31	11	13	--	--	30	--	--
Sc	37	25	10	--	--	16	--	4
V	350	172	57	--	116	72	124	27
Cu	190	9	11	--	46	680	25	4
Zn	--	95	53	--	72	--	55	13
Rb	--	36	91	--	50	52	27	45
Ba	85	150	400	566	418	790	393	448
Sr	190	222	44	457	357	93	259	128
Cs	0.41	--	--	--	--	1.3	--	--
Nb	--	10	11	--	7	6	10	2.59
Zr	105	175	384	--	130	113	81	126.8
Y	19	22	32	--	17	12	13	11.2
Hf	1.8	3.8	10.1	--	--	2.8	--	3.32
Pb	--	13	16	--	--	--	--	3.25
Th	0.88	6.96	16.4	--	9.6	6.3	5.8	4.79
U	0.32	1.33	3.42	--	--	1.6	--	1.08
La (ppm)	10	25	43	--	18	17	20	23.29
Ce	18	53	83	32.6	41	33	38	46.21
Pr	2.2	5.8	12	--	4.7	4.4	3.9	5.37
Nd	10	22	42	14.8	19	17	17	17.66
Sm	2.8	4.5	7.1	2.68	3.9	3.1	3	2.82
Eu	0.97	0.9	1	0.785	1.1	1.1	0.9	0.59
Gd	3.4	3.5	5.6	2.24	3	3.2	2.3	2.07
Tb	0.52	0.6	0.88	--	--	0.49	--	0.30
Dy	3.1	3.6	4.7	1.74	2.4	3.1	1.6	1.56
Ho	0.79	0.8	1	--	--	0.64	--	0.28
Er	2.2	2.2	2.9	0.913	1.2	1.8	1	0.81
Yb	2.3	2	2.9	0.845	1	1.6	0.4	0.74
Lu	--	--	--	0.14	--	--	--	0.11

Note: nd = not detected.

striking difference between FLG porphyritic samples and the greywackes are the considerably higher Cr and Ni concentrations in the latter. In fact, none of the FLG samples containing phenocrysts (or framework grains), which might be classified as 'metagreywacke', contain any detectable Cr or Ni (Table 3.2.1). Some of the fine-grained siliceous schists which contain higher concentrations of mafic minerals (e.g., sericite, chlorite, amphibole) have variable, although generally low Cr and Ni concentrations (Table 3.2.2). This suggests that if these rocks are sedimentary in origin, they must have been derived from a source area essentially devoid of mafic and/or ultramafic lithologies.

Several workers have devised geochemical discrimination diagrams to distinguish between meta-igneous and metasedimentary rocks. On Tarney's (1977) TiO_2-SiO_2 discrimination diagram, 31 of 38 FLG samples plot in the igneous field (Figure 3.1A). Only one of the felsic samples and six of the mafic samples plot in the sedimentary field. However, it is well known that SiO_2 is highly mobile during metamorphism and alteration, and the usefulness of this diagram is limited. Winchester et al. (1980), recognizing the problem of SiO_2 mobility in metamorphosed and altered rocks, developed a discrimination diagram utilizing relatively immobile elements (Zr, Ti and Ni) to distinguish between meta-igneous and metasedimentary rocks. In the Zr/Ti-Ni diagram (Figure 3.1B), only one of the mafic samples and three of the felsic samples plot in the sedimentary field. One of the

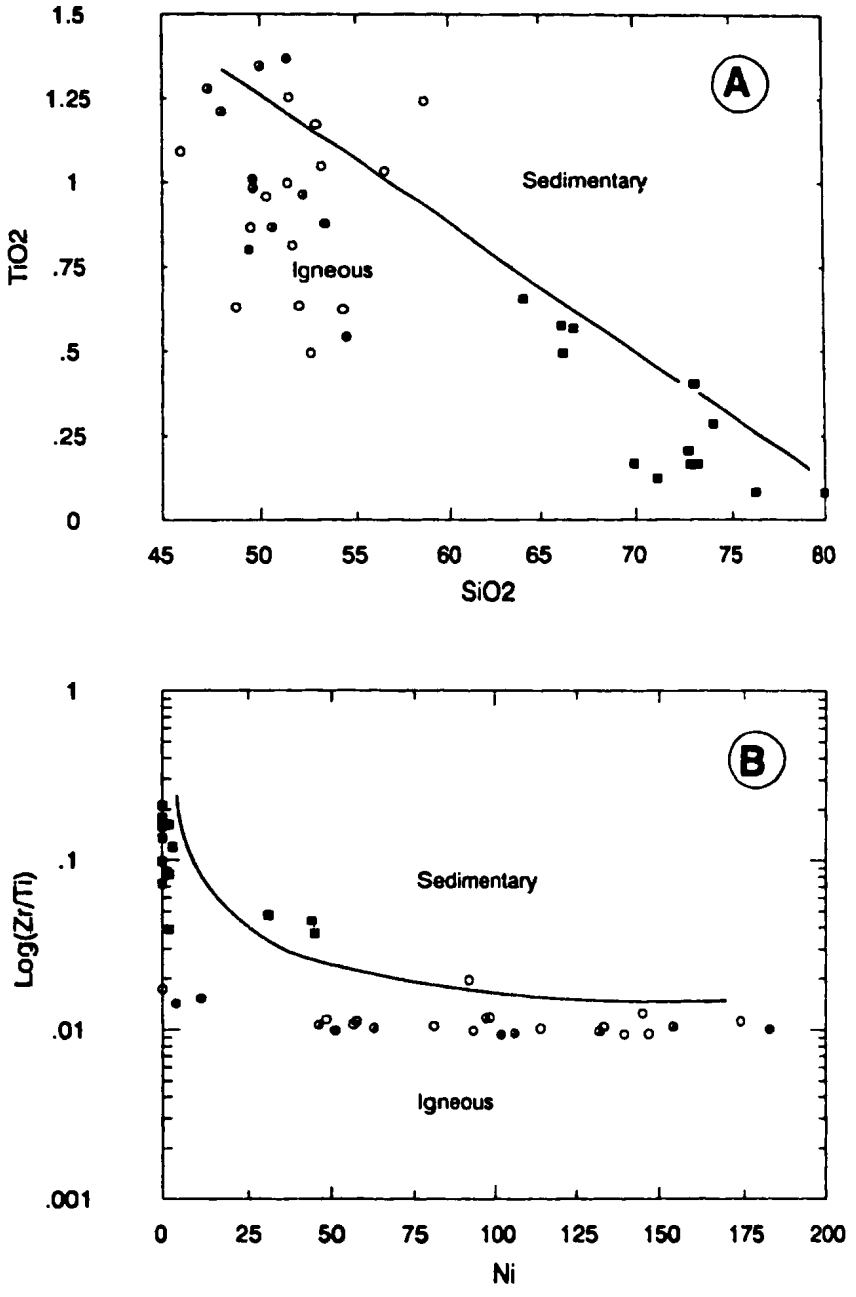

Figure 3.1. Discrimination diagrams which distinguish between igneous and sedimentary rocks. (A) TiO_2 versus SiO_2 (after Tarney, 1977); and (B) Zr/Ti versus Ni (after Winchester et al., 1980). Symbols: open circle = mafic schists, flows and pillow lavas; solid circles = mafic massive flows and/or sills; half-filled circles = mafic amphibolites; solid squares = felsic supracrustal rocks.

felsic samples (87-153) which plots in the sedimentary field was also analyzed for REE, and has a chondrite-normalized pattern which is indistinguishable from other samples which are clearly volcanic.

Therefore, based on igneous/sedimentary discrimination diagrams, the extremely low transition element (Cr, Ni) contents of felsic samples, and the similarity of chondrite-normalized REE patterns between samples of clearly volcanic and sedimentary origin, the FLG felsic rocks are herein collectively grouped as "undivided felsic supracrustal" rocks.

3.2.1. Major Elements

As noted previously, field mapping indicates that volcanic rocks of the FLG are bimodal in the Florence Lake area. This is supported by the SiO_2 histogram in Figure 3.2, which clearly shows a bimodal distribution with most of the samples containing between 46-56 wt.% SiO_2 (anhydrous).

One of the main problems encountered in studies of volcanic rock geochemistry is the degree to which the rocks have been chemically modified by metamorphism and/or secondary alteration. This is particularly important in studies of Archean greenstone volcanic suites, which are commonly metamorphosed to greenschist or amphibolite facies, and are chemically altered to some degree. In this respect, the FLG is no exception.

Several approaches have been proposed to evaluate the effects of metamorphism and alteration on major elements in

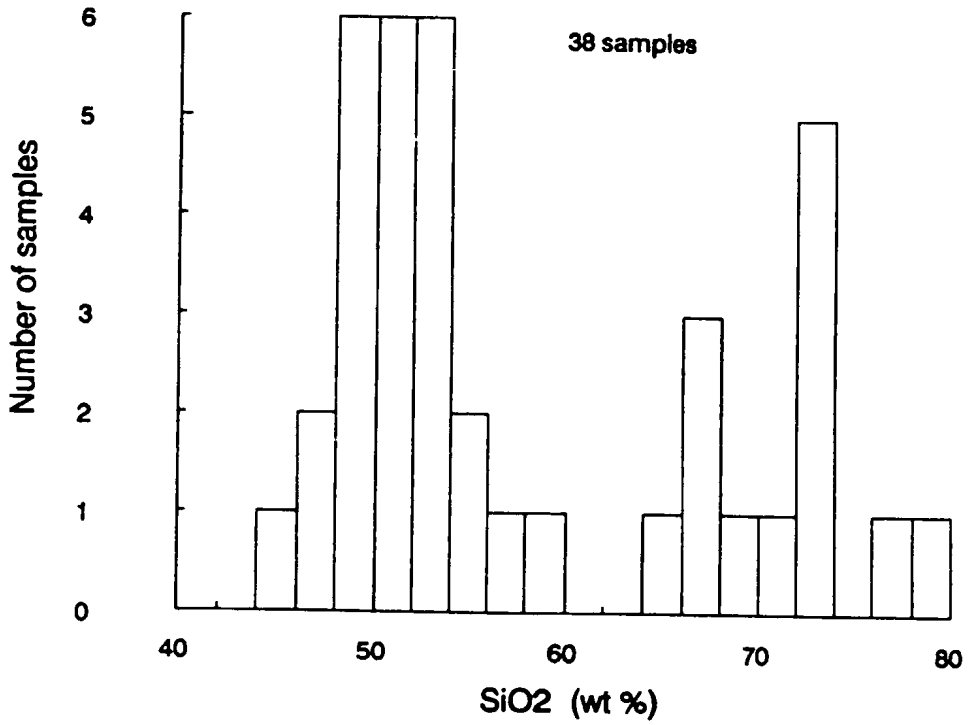

Figure 3.2. Histogram illustrating the bimodal SiO_2 distribution in the Florence Lake Group. Note that SiO_2 contents are recalculated to 100% anhydrous.

volcanic rocks. A common practice is to assume that those rocks in a given suite which exhibit the best preservation of primary mineralogy and textures are least altered. These 'least altered' rocks are then used as a standard for chemical comparison with more highly altered rocks. A major weakness with this approach is that these 'least altered' rocks are often modified to some extent. In the case of the FLG, all samples are metamorphosed to greenschist or amphibolite facies, and secondary carbonate alteration is widespread.

The approach taken here is to plot major elements against Y to test their mobility during metamorphism and secondary alteration (Figure 3.3). Y was chosen because it can act as an immobile fractionation index, and shows a significant range in values between samples. A wide scatter of data points should indicate major element mobility. In the mafic rocks, all the major elements show weak to moderate trends, but generally there is considerable scatter. The felsic rocks do not display any common trend, and samples show a large scatter both in terms of Y and major element contents.

As a further test of alkali element mobility, the FLG data have also been plotted on the 'Hughes diagram' (Figure 3.4). Hughes (1973) determined that all common igneous rocks plot inside an envelope, referred to as the 'igneous spectrum', and samples which plot outside this envelope indicate either Na- or K-metasomatism. It should be stressed that samples which do plot inside the 'igneous spectrum' may nevertheless have undergone mobilization of Na and/or K, with

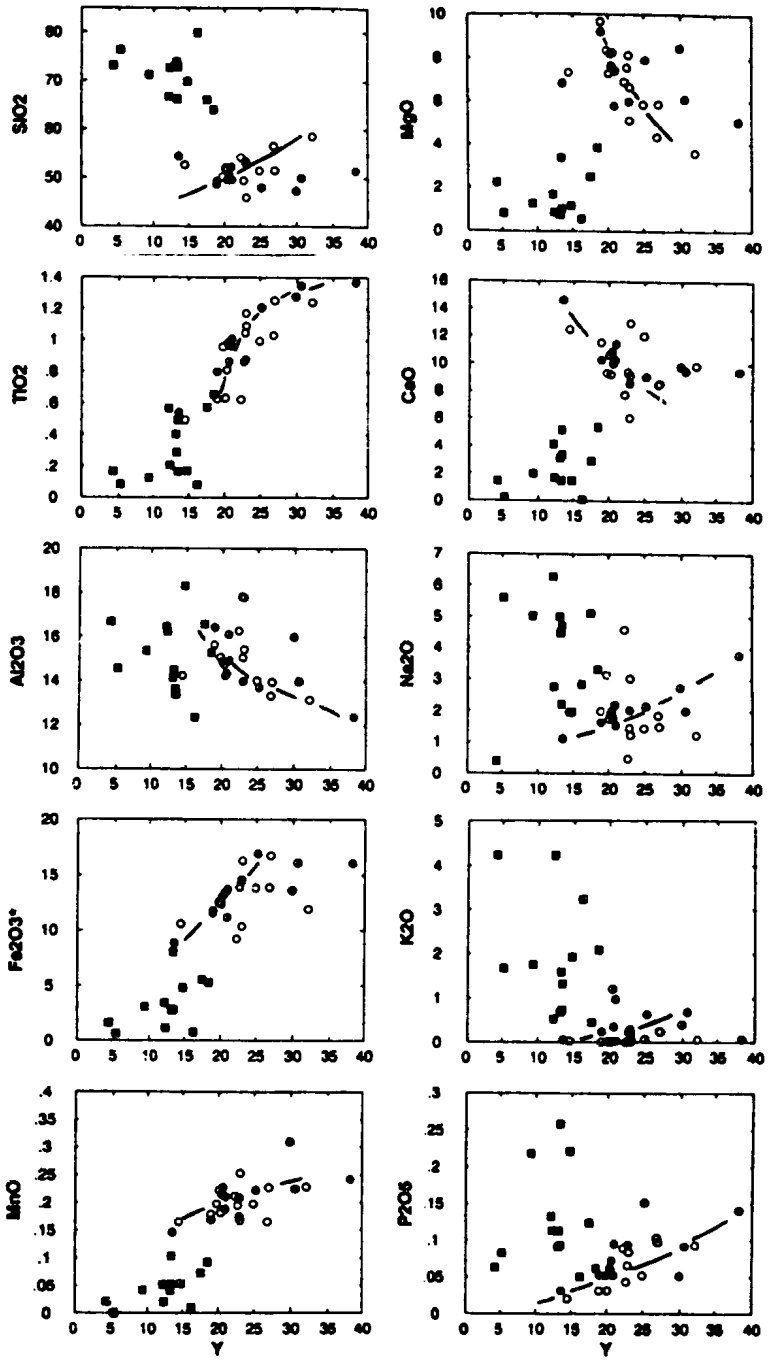

Figure 3.3. Major elements versus Y as a fractionation index. Note that the mafic metavolcanic rocks display weak to moderate trends (dashed lines), whereas the felsic supracrustal rocks show a large overall scatter both in terms of Y and major elements, and there appears to be no common trend. Symbols as for Figure 3.1.

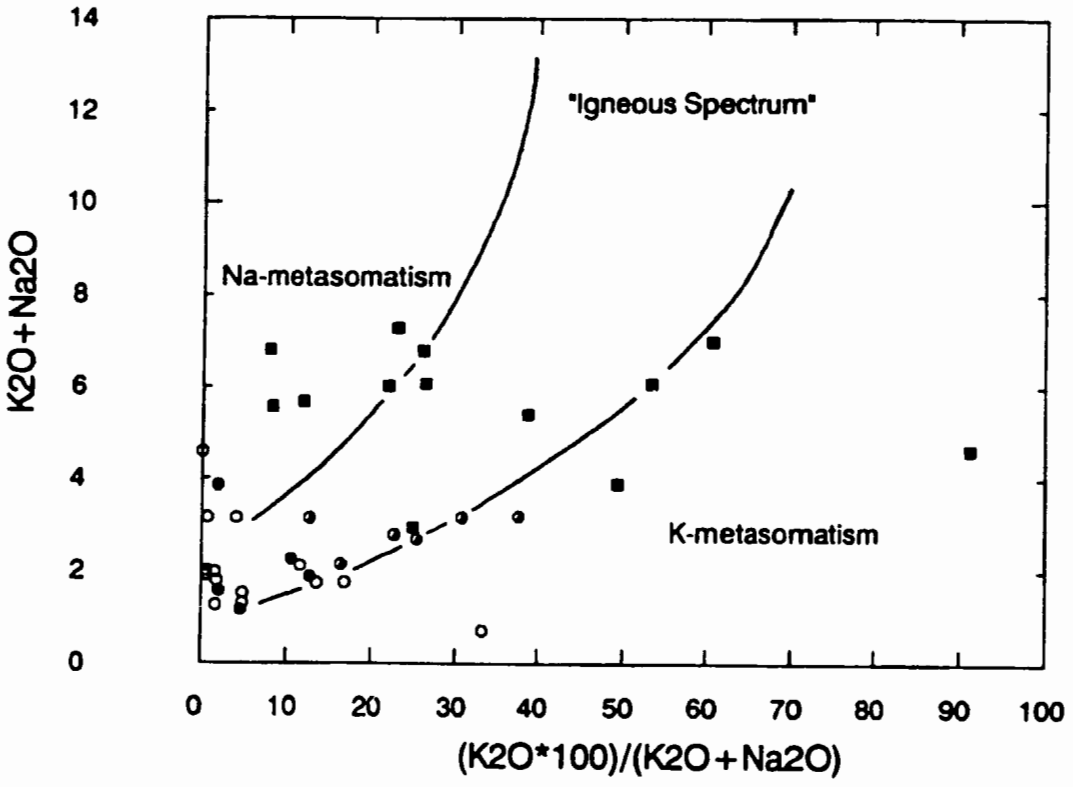

Figure 3.4. Hughes (1973) diagram showing alkali element mobility in Florence Lake Group supracrustal rocks. Symbols as for Figure 3.1.

data points having moved up or down within the envelope. Figure 3.4 shows that most of the FLG samples plot within the spectrum, but with many samples straddling the lower boundary. Stauffer et al. (1975) suggested that this lower boundary should be extended downwards slightly, to incorporate island arc tholeiites. A significant number of the felsic rocks plot outside the spectrum, indicating both Na- and K- metasomatism.

Despite the obvious mobility of major elements, classification diagrams employing them to identify magma series generally give consistent results. The FLG is classified as subalkaline (tholeiitic and/or calc-alkaline) on the total alkalies versus SiO_2 diagram (Figure 3.5). On the AFM diagram (Figure 3.6), the mafic rocks are classified as tholeiitic whereas the felsic rocks are calc-alkaline, although the latter show a much wider scatter. On the Jensen (1976) cation plot (Figure 3.7), which has the added advantage of discriminating between rock types as well as magma series, the mafic samples plot in the high-Fe tholeiite field, whereas the felsic rocks range from tholeiitic to calc-alkaline andesites through to rhyolites. Andesites and dacites are less common than rhyolites.

3.2.2. Trace Elements and Rock Classification

Saunders et al. (1979) divided the incompatible trace elements (excluding REE) into two groups based on the ionic character of the elements. Elements with large ionic radii and low charges, and hence high radius/charge ratios, were called

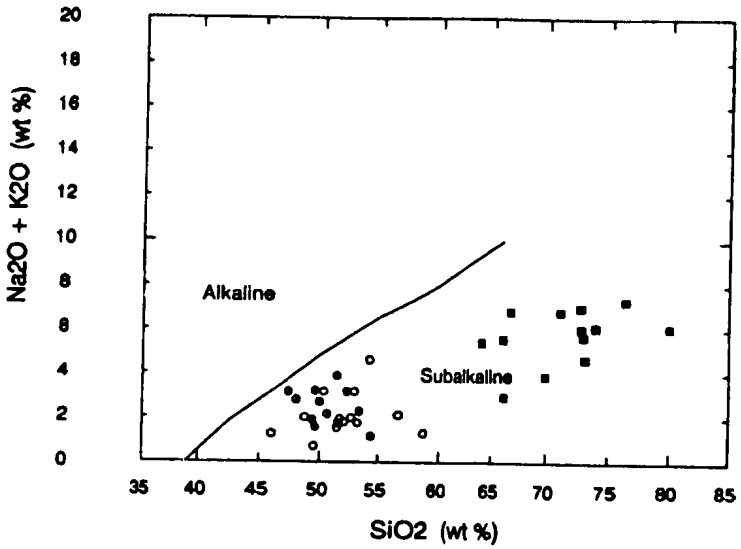

Figure 3.5. Total alkalis versus SiO_2 diagram for Florence Lake Group supracrustal rocks. Dividing line between alkaline and subalkaline fields (after Irvine and Baragar, 1971). Symbols as for Figure 3.1.

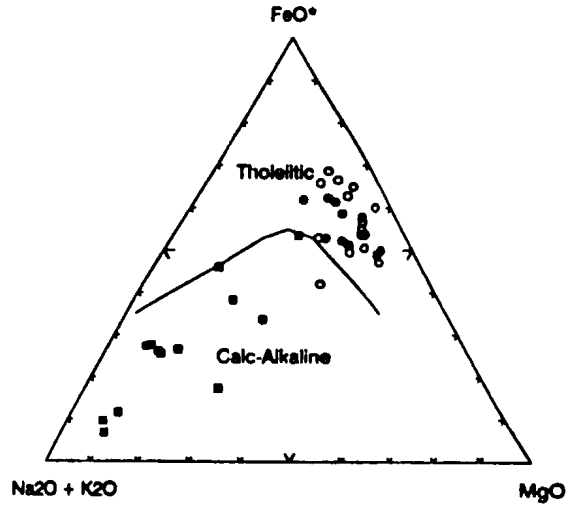

Figure 3.6. AFM diagram for Florence Lake Group supracrustal rocks. Dividing line between tholeiitic and calc-alkaline fields (after Irvine and Baragar, 1971). Symbols as for Figure 3.1.

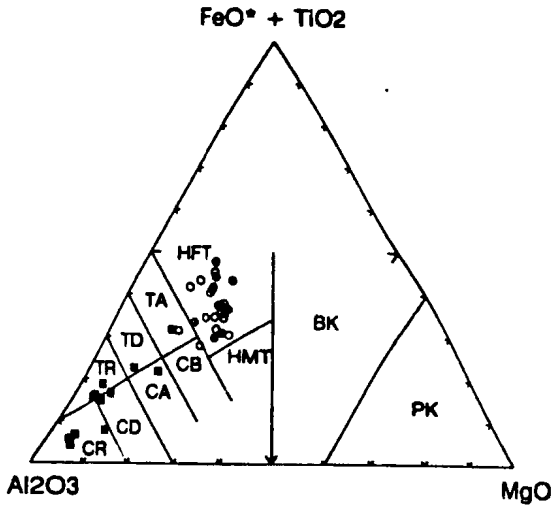

Figure 3.7. Jensen (1976) cation plot showing distribution of Florence Lake Group supracrustal rocks. Abbreviations: T = tholeiitic; C = calc-alkaline; R = rhyolite; D = dacite; A = andesite; B = basalt; HFT = high-Fe tholeiite; HMT = high-Mg tholeiite; BK = basaltic komatiite; and PK = peridotitic komatiite. Symbols as for Figure 3.1.

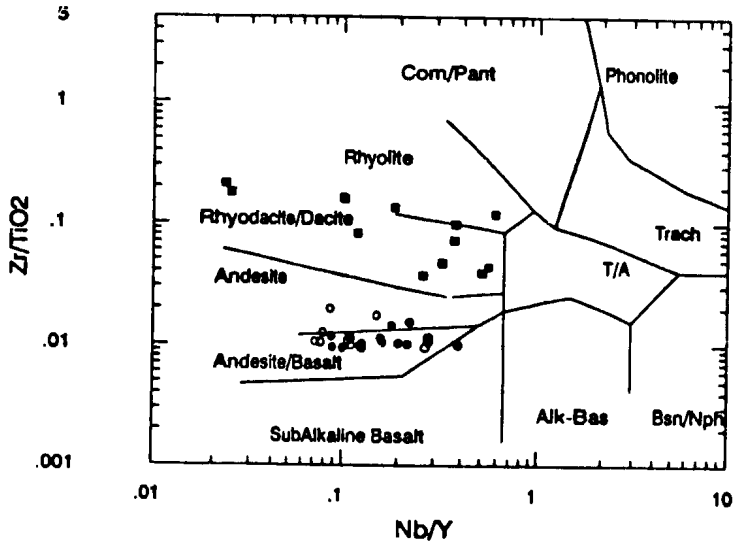

Figure 3.8. Zr/TiO_2-Nb/Y diagram (after Winchester and Floyd, 1977) showing the distribution of Florence Lake Group supracrustal rocks. Abbreviations: Trach = trachytes; T/A = trachyandesites; Alk-Bas = alkali basalts, hawaiites, mugearites, trachybasalts; Bsn/Nph = basanites, trachybasanites, nephelinites. Symbols as for Figure 3.1.

low field strength elements (LFS elements or LFSE). These include Cs, Rb, K, U, Th, Sr and Ba. Highly charged elements with small ionic radii, and hence low radius/charge ratios, were called high field strength elements (HFS elements or HFSE), and include Ti, P, Zr, Hf, Nb and Ta.

The LFSE are mobile during secondary processes, and cannot be used reliably in the classification and discrimination of metamorphosed and altered volcanic rocks; hence, these elements will not be used in discussions of the geochemistry of the FLG. However, Th is generally considered to be relatively immobile during low-grade metamorphism (e.g., Saunders and Tarney, 1984), and can be used as an indicator of relative LFSE enrichment or depletion. In contrast, the HFSE are considered to be relatively immobile during secondary processes (e.g., Pearce and Cann, 1973; Winchester and Floyd, 1977), and along with the REE are used extensively in classification and discrimination diagrams of metamorphosed and altered volcanic rocks.

Winchester and Floyd (1977) used covariations between the immobile element ratios Zr/TiO_2 and Nb/Y to classify metavolcanic rocks. In this discrimination diagram, Zr/TiO_2 acts as a differentiation index and Nb/Y as an alkalinity index, so that alkaline and subalkaline rocks, and individual rock types are effectively classified on the same diagram. The FLG mafic metavolcanic rocks plot predominantly in the andesite/basalt field (Figure 3.8), with only four samples falling within the andesite-only field. The felsic rocks plot

within the rhyodacite/dacite and rhyolite fields. The scarcity of data points in the andesite-only field supports the contention that volcanic rocks of the FLG are bimodal.

3.2.3. Rare Earth Elements

Rare earth element (REE) concentrations for FLG samples are presented in Tables 3.1-3.2, and chondrite-normalized REE diagrams are displayed in Figures 3.9-3.10.

3.2.3.1. Mafic Metavolcanics

The FLG basalts can be divided into two groups based on the relative depletion of LREE. Group 1 basalts (Figure 3.9A) have very flat chondrite-normalized REE profiles with LREE and HREE concentrations approximately 10x chondrite (La_n/Lu_n=0.8-1.4). Group 2 basalts (Figure 3.9B) have lower and slightly depleted LREE (La=3.6-6.2x chondrite) and comparable HREE (La_n/Lu_n=0.6-0.9) relative to Group 1. Generally the basalts do not exhibit Eu anomalies, although two samples have positive anomalies (87-150, 87-108) while another has a negative anomaly (87-120). It is unclear whether these Eu anomalies are due to plagioclase fractionation or alteration.

Chondrite-normalized REE patterns for two samples which are more fractionated (La_n/Lu_n=2.5-3.2) than those of the 'typical' basalts are displayed in Figure 3.9C. Compared to the typical FLG basalts, sample 87-028 displays a pronounced HREE-depletion (Lu=2.2x chondrite). Its chondrite-normalized pattern is somewhat irregular, characterized by a fairly

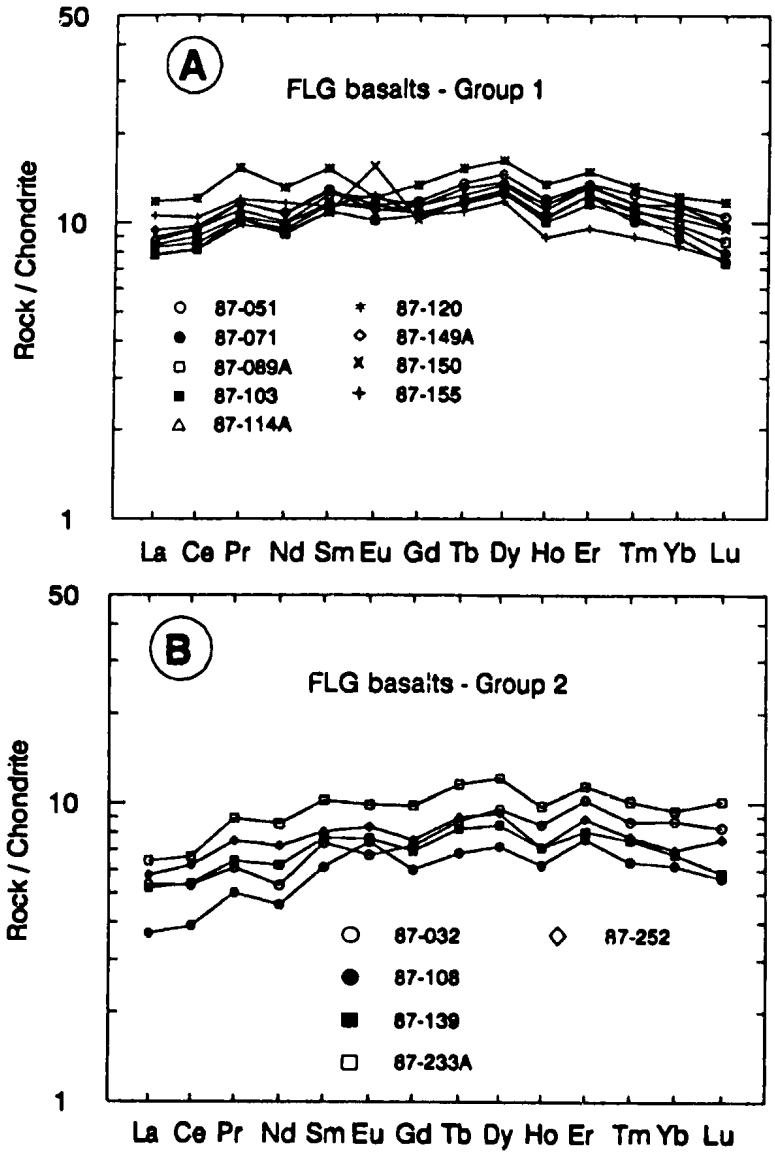

Figure 3.9. Chondrite-normalized REE diagrams for Florence Lake Group (FLG) mafic metavolcanic rocks and other Archean tholeiites. (A) FLG Group 1 basalts; (B) FLG Group 2 basalts; (C) FLG andesites; and (D) other Archean tholeiites: 5053 (Jahn et al., 1982), S145 (Jahn et al., 1980), KA1 (Arndt and Jenner, 1986), Rh-73-210 (Hawkesworth and O'Nions, 1977), Orkney (Crow and Condie, 1988), TH1 and TH2 (Condie, 1981). Abbreviations: DAT = depleted Archean tholeiite; EAT = enriched Archean tholeiite. Chondrite normalizing values are from Wakita et al. (1971): La (0.34), Ce (0.91), Pr (0.121), Nd (0.64), Sm (0.195), Eu (0.073), Gd (0.26), Tb (0.047), Dy (0.30), Ho (0.078), Er (0.2C), Tm (0.032), Yb (0.22) and Lu (0.034).

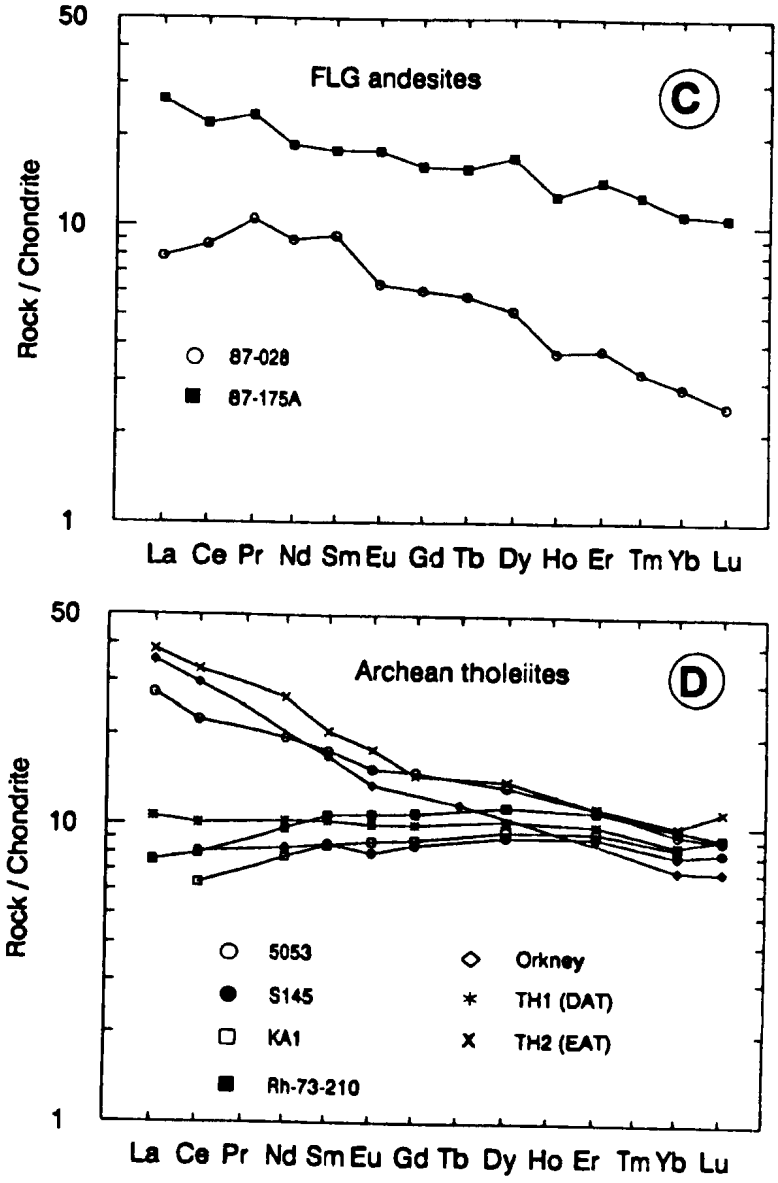

Figure 3.9. (continued).

fractionated slope from Lu to Pr, but a marked depletion in Ce and La. Petrographic examination of this sample shows that it is highly altered and contains up to 10 modal % carbonate (L.O.I.=9.01), and the REE may have been remobilized in this sample during carbonatization. Sample 87-175A contains comparable HREE concentrations to the typical FLG basalts, but is notably LREE-enriched (La=25.7x chondrite). This sample does not contain any detectable Cr or Ni, and is more siliceous (54.80 wt.%) than other samples. Both samples plot in the andesite-only field on the Winchester and Floyd (1977) diagram (Figure 3.8), which may explain their more fractionated chondrite-normalized REE patterns. However, sample 87-028 may also represent a highly altered basalt from which the HREE have been mobilized and lost.

Condie (1976, 1981) proposed a two-fold classification of Archean tholeiites based on chondrite-normalized REE patterns: (1) TH1 is characterized by flat REE patterns with concentrations approximately 10x chondrite; and (2) TH2 is LREE-enriched with fractionated patterns. In addition, other workers (e.g., Jahn et al., 1982; Arndt and Jenner, 1986) have recognized Archean tholeiites which are slightly LREE-depleted, thus constituting a third type of Archean tholeiite. Chondrite-normalized REE patterns for several tholeiites (including TH1 and TH2) from other Archean greenstone belts are plotted in Figure 3.9D for comparison with FLG basalts. With the exception of sample 87-175A, the FLG basalts lack the strong LREE-enrichment displayed by TH2 tholeiites; however,

the REE patterns of FLG Group 1 basalts are very similar to the flat patterns of TH1 tholeiites, and FLG Group 2 basalts have slightly LREE-depleted patterns similar to those described elsewhere (e.g., Jahn et al., 1982).

3.2.3.2. Felsic Metavolcanic/Metasedimentary Rocks

Whereas almost all (14 of 16 samples) of the mafic metavolcanic rocks show similar chondrite-normalized REE patterns, the felsic rocks show more variability.

The most common REE patterns for FLG felsic supracrustal rocks (5 of 10 samples) are displayed in Figure 3.10A. The patterns are fractionated (La_n/Lu_n=6.8-19) with LREE concentrations 50-100x chondrite and HREE concentrations 3-7x chondrite. Most of the samples show a very slight negative Eu anomaly.

The patterns for three samples which differ from this common trend are displayed in Figure 3.10B. Compared to the typical patterns, samples 87-092 and 87-178B have similar concentrations of MREE and HREE, but LREE are more depleted (La=23-31x chondrite), and sample 87-178B has a very pronounced negative Eu anomaly. Sample 87-149B has a significantly more fractionated pattern (La_n/Lu_n=64.5), with high LREE (La=116x chondrite) and low HREE concentrations (Lu=2x chondrite).

Samples 87-247B and 87-267 (Figure 3.10C) also have fractionated patterns (La_n/Lu_n=12-77.5), but REE concentrations are much lower than the other felsic supracrustal rocks

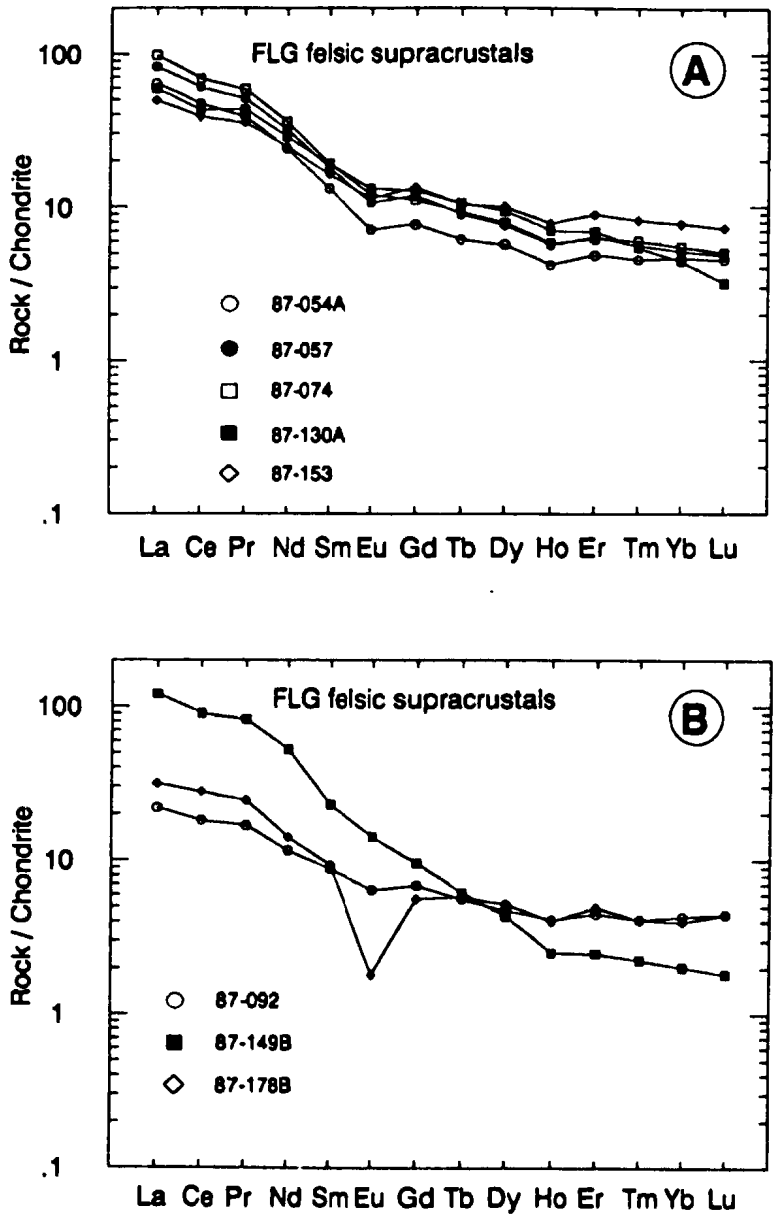

Figure 3.10. Chondrite-normalized REE diagrams for (A, B and C) Florence Lake Group felsic supracrustal rocks and (D) various types of Archean felsic volcanic rocks recognized by Condie (1976, 1981) and greywackes (after Taylor and McLennan, 1985). Legend: D-RD = dacite-rhyodacite; RHY = rhyolite. Chondrite normalizing values as for Figure 3.9 (after Wakita et al., 1971).

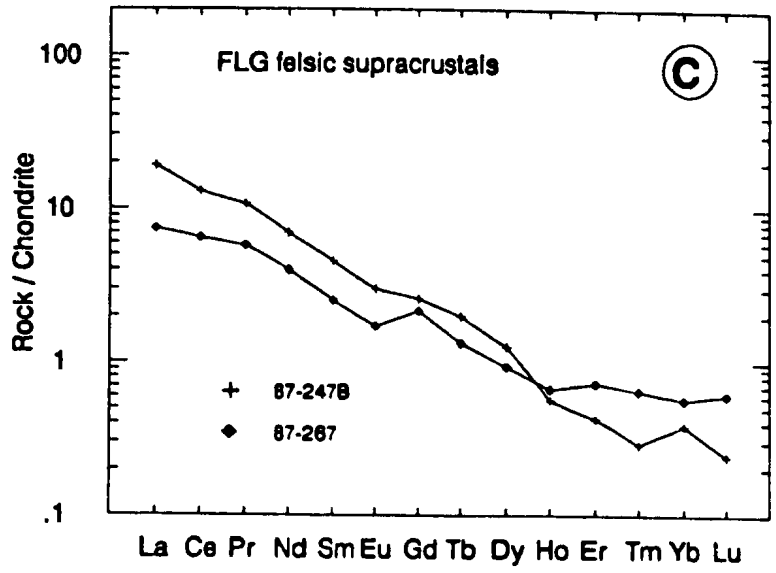

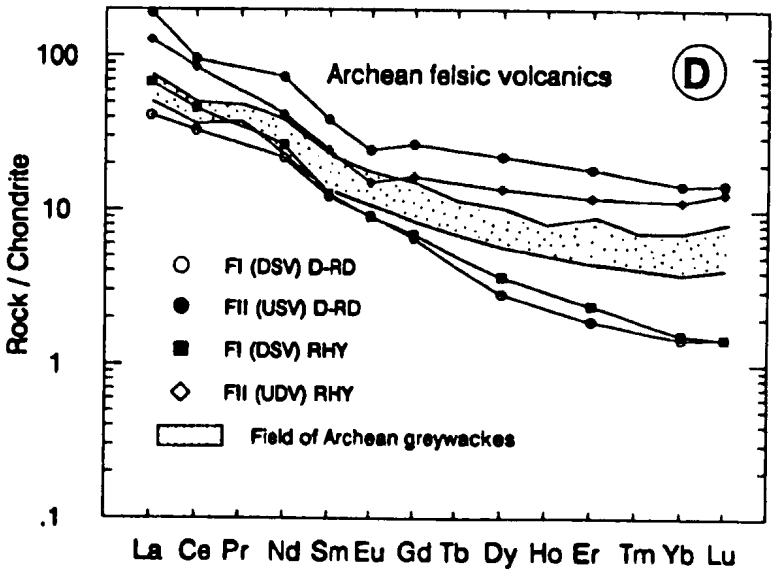

Figure 3.10. (continued)

(La=7-18x chondrite, Lu=0.2-0.6x chondrite).

Condie (1976, 1981) divided Archean felsic volcanic rocks into two groups based on chondrite-normalized REE patterns: (1) FI is strongly HREE-depleted; and (2) FII is not HREE-depleted. Chondrite-normalized patterns for FI and FII felsic volcanic rocks, as well as the field outlined by several Archean greywackes (after Taylor and McLennan, 1985), are plotted in Figure 3.10D for comparison with FLG felsic rocks. The typical FLG felsic rocks (Figure 3.10A) have REE patterns which are intermediate between Condie's FI and FII felsic volcanics, which also characterizes Archean greywackes. Taylor and McLennan (1985, p. 133) noted that "In spite of the differing sources," (of Archean greywackes) "the REE patterns are remarkably similar with no or very slight depletion in europium". Therefore, although the FLG felsic rocks differ from Archean greywackes in that the former contain negligible transition element (Cr and Ni) concentrations, their REE concentrations are remarkably similar. This may indicate that the FLG felsic supracrustal rocks represent volcaniclastic rocks which were derived from a source area essentially devoid of mafic or ultramafic lithologies.

The strong HREE-depletion of many Archean felsic volcanic rocks and trondhjemites-tonalites-granodiorites cannot be produced by fractional crystallization of basaltic magma. Arth and Hanson (1975) suggested that Archean tonalites and trondhjemites with strong HREE-depletion, were generated by partial melting of eclogite at mantle depths, and Arth and

Barker (1976) showed that partial melting of amphibolites at crustal depths can produce similar REE patterns.

3.2.4. Tectonic Discrimination Diagrams (Mafic Metavolcanics)

Since the pioneering work of Pearce and Cann (1973), numerous empirical tectonic discrimination diagrams have been constructed using geochemical data from relatively young (Mesozoic and younger) basaltic volcanic suites. These diagrams invariably utilize immobile trace elements (e.g., Pearce and Cann, 1973; Wood et al., 1979; Meschede, 1986).

On the Ti-Zr-Y diagram (Figure 3.11) the FLG basalts are tightly clustered in the field of overlap between ocean-floor basalts (OFB), low-potassium tholeiites (LKT) and calc-alkaline basalts (CAB). None of the samples have within-plate characteristics. On the Zr-Nb-Y diagram (Figure 3.12), the FLG basalts plot in the field of overlap between normal mid-ocean ridge basalts (N-MORB) and volcanic arc basalts (VAB).

The La/Nb ratio is a very useful criterion for distinguishing between MORB and VAB, since VAB are notably depleted in Nb relative to La, resulting in a higher La/Nb ratio. In the La/Nb versus Y diagram (see Winchester et al., 1987), the FLG basalts plot predominantly in the back-arc basin field, well below the area outlined by island arc tholeiites (Figure 3.13). This reflects the lack of a Nb depletion in the FLG basalts. The FLG basalts have lower Y concentrations compared to typical N-MORB.

Myers and Breitkopf (1989) pointed out that large

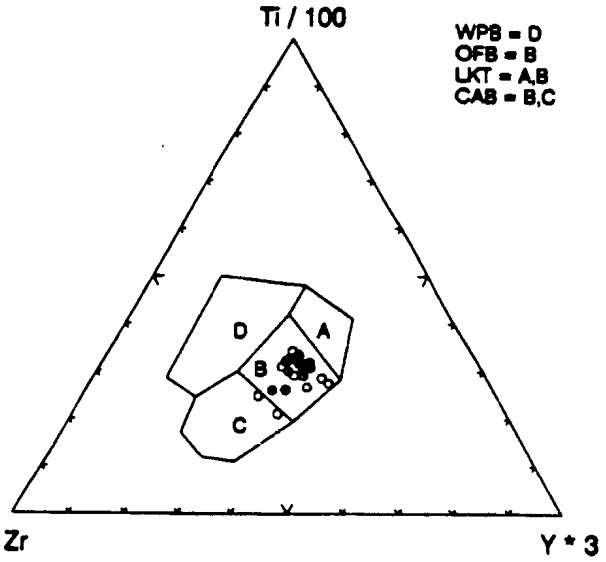

Figure 3.11. Zr-Ti/100-Y tectonic discrimination diagram (after Pearce and Cann, 1973) for Florence Lake Group mafic metavolcanic rocks. Abbreviations: OFB = ocean-floor basalts; LKT = low-potassium tholeiites; CAB = calc-alkaline basalts; WPB = within-plate basalts. Symbols as for Figure 3.1.

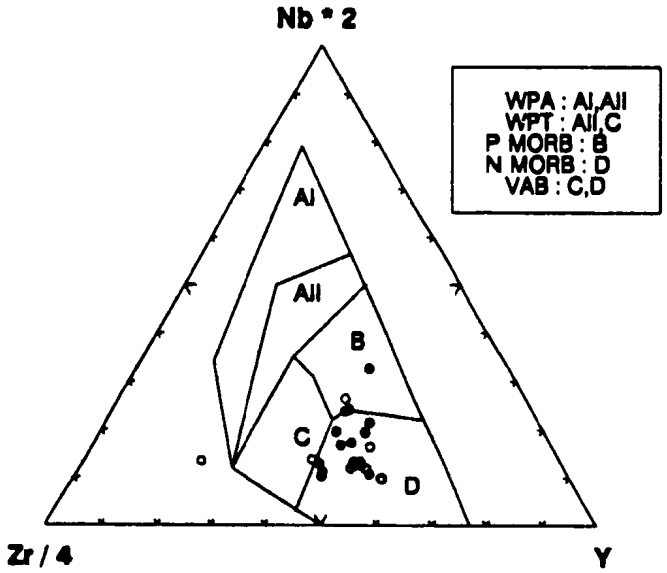

Figure 3.12. Zr/4-Nb*2-Y tectonic discrimination diagram (after Meschede, 1986) for Florence Lake Group mafic metavolcanic rocks. Abbreviations: WPA = within-plate alkali basalts; WPT = within-plate tholeiites; P MORB = plume mid-ocean ridge basalts; N MORB = normal mid-ocean ridge basalts; VAB = volcanic arc basalts. Symbols as for Figure 3.1.

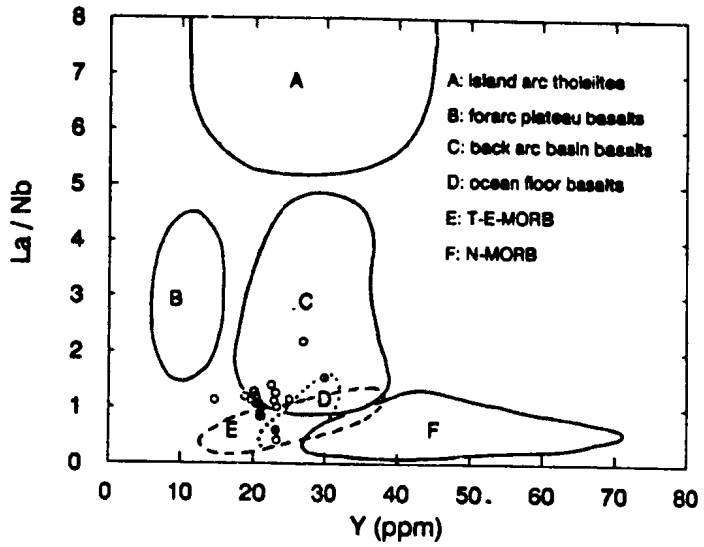

Figure 3.13. La/Nb-Y tectonic discrimination diagram (see Winchester et al., 1987) for Florence Lake Group mafic metavolcanic rocks. Symbols as for Figure 3.1.

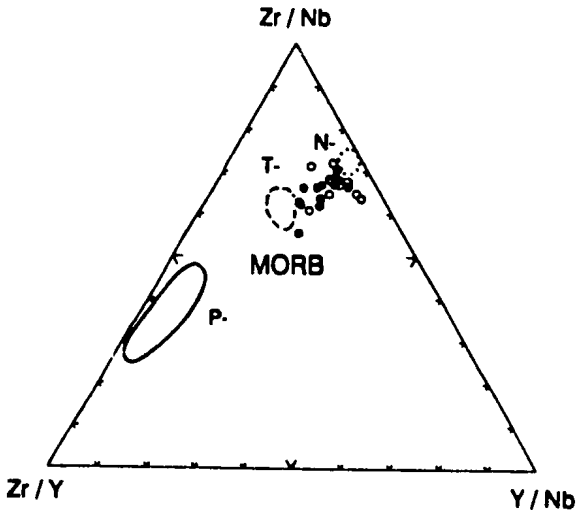

Figure 3.14. Zr/Y-Zr/Nb-Y/Nb MORB discrimination diagram (after Fodor and Vetter, 1984) for Florence Lake Group mafic metavolcanic rocks. Fields are N-, T- and P-MORB for the Southwest Indian Ridge (data from le Roex et al., 1983). Symbols as for Figure 3.1.

variations in HFSE ratios, which are incompatible during early fractionation of olivine, pyroxene and plagioclase, indicate a non-differentiation process or processes such as mantle heterogeneity. On the Zr/Y-Zr/Nb-Y/Nb diagram of Fodor and Vetter (1984), the FLG basalts show a relatively tight clustering of data intermediate between N-MORB and T-MORB (Figure 3.14), indicating that most of the variation in the FLG basalts can be attributed to differentiation processes.

3.2.5. Spider Diagrams

Numerous workers (e.g., Sun, 1980; Gill, 1981; Pearce, 1983) have noted that volcanic rocks derived from subduction-related magmatism at destructive plate margins, show a pronounced depletion in Nb relative to the LREE (La) and the LFSE (Th). Although the cause of this 'arc signature' is not well understood and is highly controversial (e.g., Morris and Hart, 1986; Perfit and Kay, 1986), it is generally attributed to contamination by subducted sediment and/or altered oceanic crust. In contrast, tholeiitic basalts erupted at normal mid-ocean ridge segments (N-MORB) lack this relative Nb-depletion.

The FLG data are plotted on MORB-normalized spider diagrams in Figures 3.15-3.16. Because the LFSE (Rb, Ba, K, Sr) are mobile during secondary processes, they have been excluded from the diagrams since they give erratic and meaningless results. However, Th is considered to be relatively immobile during secondary processes (e.g., Saunders and Tarney, 1984), and is used here as an indicator of

relative LFSE enrichment or depletion.

3.2.5.1. Mafic Metavolcanics

MORB-normalized spidergrams for FLG Group 1 and 2 basalts are presented in Figures 3.15A and 3.15B respectively. Although element concentrations are slightly lower in Group 2 basalts, the patterns for both are similarly flat with negligible Nb anomalies. These flat patterns confirm that the FLG basalts are MORB-like and distinctly non-arc, although the FLG basalts are notably enriched in Th (i.e., LFSE) relative to N-MORB. Several samples (87-103, 87-149A, 87-032, 87-139) show very slight negative Nb anomalies relative to La and Th; however, only sample 87-120 (1 of 14 samples) displays a pronounced negative Nb anomaly (i.e., arc signature). Sample 87-150 has a strong positive Nb anomaly (Figure 3.15A), however, since the overall spidergram is identical to the other samples, this feature is considered to be the result of an analytical problem.

Spidergrams for the two andesite samples (87-028, 87-175A) are displayed in Figure 3.15C. The patterns for these samples are more fractionated than those of the basalts, and both samples show Th enrichment and Nb depletion relative to La. Sample 87-028 has a very erratic profile, with a pronounced 'spike' in Zr relative to the MREE. The irregular pattern may be due at least in part to intense secondary carbonate alteration (Section 3.2.3.1).

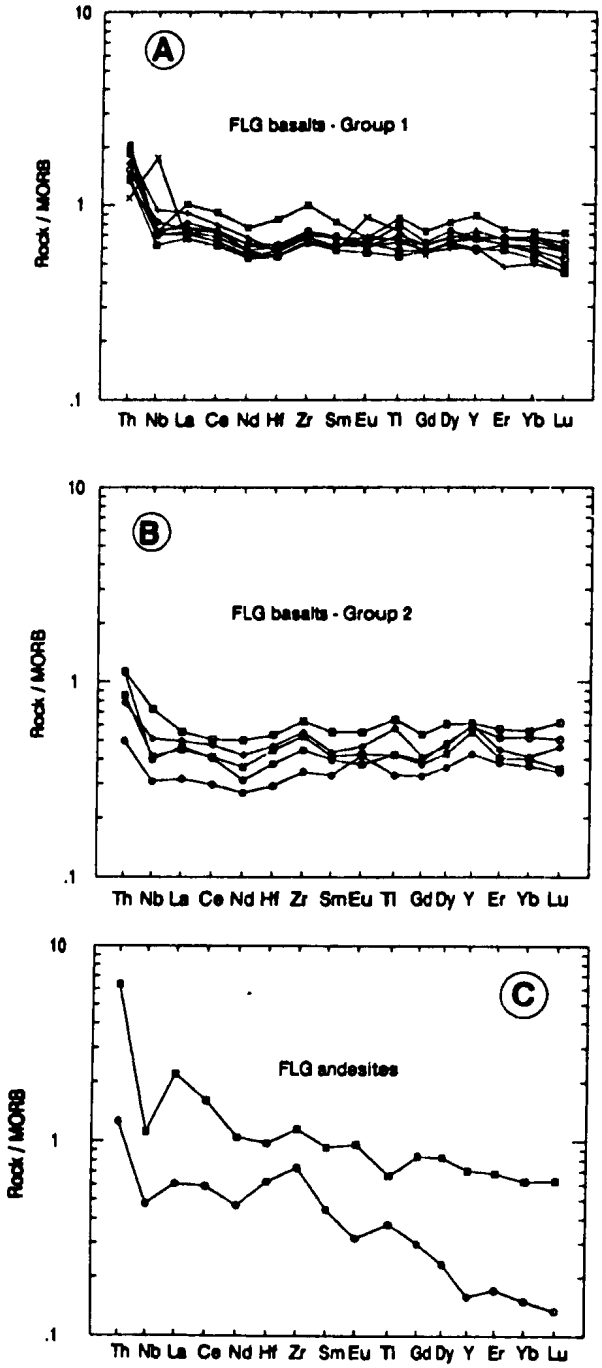

Figure 3.15. MORB-normalized spider diagrams for Florence Lake Group mafic metavolcanic rocks. (A) Group 1 basalts; (B) Group 2 basalts; and (C) andesites. Symbols as for Figure 3.9. MORB normalizing values are from NEWPET (1990): Th (0.185), Nb (3.58), La (3.96), Ce (11.97), Nd (10.96), Hf (2.87), Zr (90), Sm (3.62), Eu (1.31), Ti (9000), Gd (4.78), Dy (5.98), Y (34.2), Er (3.99), Yb (3.73) and Lu (0.56).

3.2.5.2. Felsic Metavolcanic/Metasedimentary Rocks

MORB-normalized spidergrams for the FLG felsic rocks are displayed in Figure 3.16, and all samples display classic arc (or continental crust) signatures. The patterns for 'typical' FLG felsic rocks (Figure 3.16A) are very consistent, and show a pronounced negative Nb anomaly relative to La and Th, and a Ti-depletion relative to the MREE.

Samples 87-092, 87-149B and 87-178B display similar spidergrams, but have been plotted separately because of their greater overall variability (Figure 3.16B). Sample 87-092 shows a large Zr 'spike' relative to the MREE, and the pronounced negative Eu anomaly of sample 87-178B is also quite evident.

Spidergrams for samples 87-247B and 87-267 are displayed in Figure 3.16C. Both samples show similar patterns with strong depletion in the HREE, pronounced negative Nb anomalies, and large Zr 'spikes' relative to the REE.

3.3. META-ULTRAMAFIC ROCKS

Chemical analyses of meta-ultramafic rocks are presented in Table 3.4. Since these rocks have undergone intense serpentinization and/or carbonatization, loss on ignitions (L.O.I.) are extremely high (up to 43.60 wt.%). Therefore, on the following diagrams, analyses are not recalculated on an anhydrous basis since this results in unrealistic element concentrations.

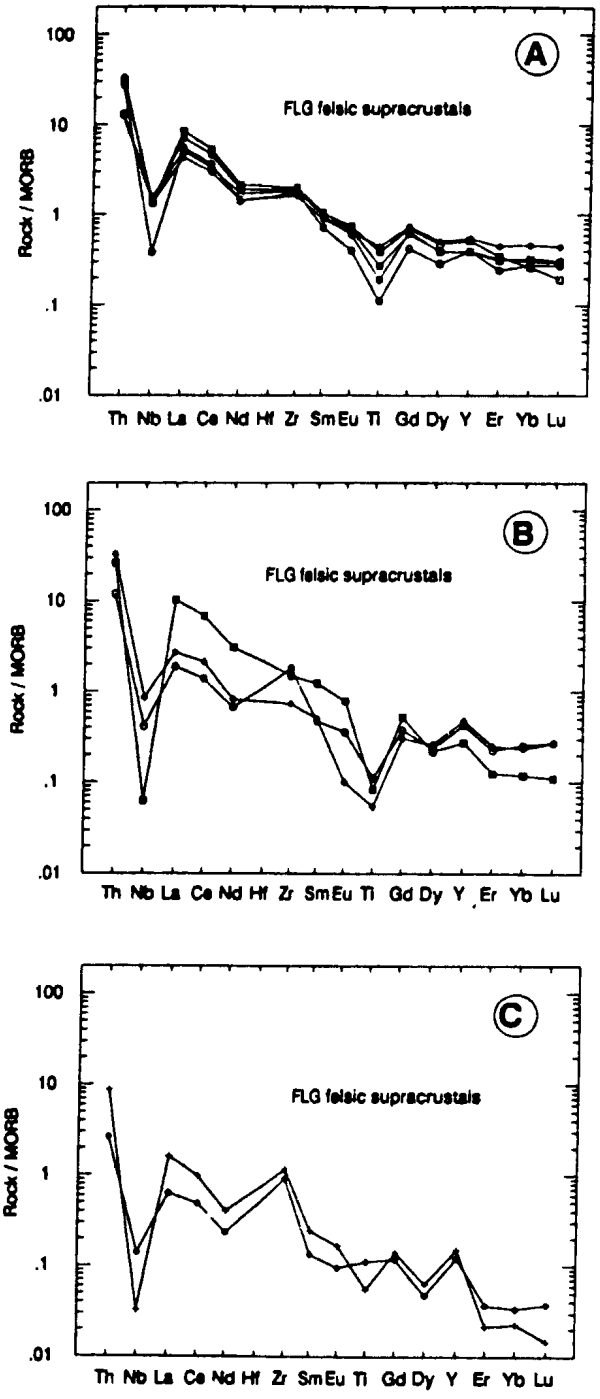

Figure 3.16. MORB-normalized spider diagrams for Florence Lake Group felsic supracrustal rocks. Symbols as for Figure 3.10. MORB normalizing values as for Figure 3.15 (from NEWPET, 1990).

Table 3.4. Chemical analyses of meta-ultramafic rocks, Florence Lake area.

	TB-87-135	87-157A	87-173	87-174	87-179	87-180C	87-181
SiO2 (wt. %)	46.80	39.60	39.80	41.40	38.60	38.10	37.90
TiO2	0.08	0.32	0.12	0.08	0.12	0.12	0.08
Al2O3	0.34	6.74	2.22	2.33	0.72	0.61	0.72
Fe2O3*	7.46	11.66	8.40	4.66	11.28	11.56	9.01
MnO	0.20	0.18	0.07	0.08	0.06	0.07	0.12
MgO	28.30	12.62	37.45	40.50	38.05	37.10	40.05
CaO	9.26	14.14	0.18	0.04	0.56	0.56	0.00
Na2O	0.02	0.00	0.00	0.00	0.00	0.01	0.00
K2O	0.00	0.00	0.01	0.01	0.00	0.00	0.00
P2O5	0.04	0.05	0.02	0.02	0.01	0.00	0.00
LOI	6.67	14.94	11.10	11.65	11.39	11.40	11.30
Total	99.17	100.25	99.37	100.77	100.79	99.53	99.18
Cr (ppm)	2421	1308	3065	1665	1373	1153	1308
Ni	866	2649	2229	2373	2972	3311	2649
Sc	20.80	---	---	---	---	---	9.29
V	61	39	60	63	39	40	39
Cu	62	0	nd	nd	nd	nd	nd
Zn	19	32	25	20	23	19	32
Ga	1	2	4	4	2	1	2
Rb	0.05	nd	nd	nd	nd	nd	0.10
Ba	6	0	nd	nd	nd	nd	nd
Sr	6.25	2	4	3	21	4	6.01
Nb	0.03	2	2	2	2	2	1.37
Zr	nd	5	12	12	7	7	5
Y	0.81	1	2	3	2	nd	1.45
Ta	0.09	---	---	---	---	---	2.86
Hf	0.02	---	---	---	---	---	0.30
Pb	1.73	---	---	---	---	---	1.02
Th	0.01	---	---	---	---	---	0.09
U	0.02	---	---	---	---	---	0.04
La (ppm)	0.04	---	---	---	---	---	0.39
Ce	0.09	---	---	---	---	---	1.13
Pr	0.02	---	---	---	---	---	0.17
Nd	0.13	---	---	---	---	---	0.72
Sm	0.08	---	---	---	---	---	0.21
Eu	0.02	---	---	---	---	---	0.07
Gd	0.08	---	---	---	---	---	0.20
Tb	0.03	---	---	---	---	---	0.04
Dy	0.16	---	---	---	---	---	0.26
Ho	0.04	---	---	---	---	---	0.06
Er	0.10	---	---	---	---	---	0.16
Tm	0.02	---	---	---	---	---	0.03
Yb	0.10	---	---	---	---	---	0.21
Lu	0.02	---	---	---	---	---	0.03

Note: nd = not detected.

Table 3.4. (continued).

	87-184A	87-184B	87-185A	87-185B	87-189A	87-195	87-198B
SiO2 (wt. %)	37.10	37.50	31.60	38.80	31.80	27.30	31.10
TiO2	0.12	0.12	0.00	0.08	0.08	0.00	0.08
Al2O3	1.04	1.15	0.61	0.61	0.83	0.19	0.40
Fe2O3*	7.90	7.02	6.81	7.28	7.85	10.45	7.55
MnO	0.11	0.10	0.12	0.02	0.10	0.13	0.14
MgO	38.50	38.85	38.70	41.25	40.55	40.30	39.05
CaO	0.06	1.60	0.00	0.00	0.04	0.00	0.02
Na2O	0.00	0.00	0.00	0.00	0.00	0.00	0.00
K2O	0.00	0.00	0.00	0.00	0.00	0.00	0.00
P2O5	0.01	0.02	0.00	0.01	0.01	0.00	0.00
LOI	15.80	14.34	21.21	12.58	19.52	21.78	22.19
Total	100.64	100.70	99.05	100.63	100.78	100.15	100.53
Cr (ppm)	2925	2110	1136	1183	1146	1127	2330
Ni	2148	2187	2276	2397	2437	2692	2639
Sc	---	---	3.79	5.91	---	---	---
V	34	30	23	16	30	6	20
Cu	nd	nd	nd	nd	nd	nd	nd
Zn	20	19	31	14	16	2	28
Ga	2	2	nd	nd	nd	nd	nd
Rb	nd	nd	0.40	0.18	nd	nd	nd
Ba	nd	nd	nd	nd	nd	nd	nd
Sr	3	7	6.75	5.16	3	2	4
Nb	2	2	0.13	0.12	1	1	2
Zr	5	5	2	4	3	2	3
Y	1	1	0.62	0.56	2	1	2
Ta	---	---	0.08	0.15	---	---	---
Hf	---	---	0.17	0.07	---	---	---
Pb	---	---	1.93	0.96	---	---	---
Th	---	---	0.07	0.04	---	---	---
U	---	---	0.04	0.01	---	---	---
La (ppm)	---	---	0.16	0.09	---	---	---
Ce	---	---	0.40	0.25	---	---	---
Pr	---	---	0.07	0.04	---	---	---
Nd	---	---	0.25	0.20	---	---	---
Sm	---	---	0.08	0.06	---	---	---
Eu	---	---	0.01	0.00	---	---	---
Gd	---	---	0.11	0.05	---	---	---
Tb	---	---	0.02	0.02	---	---	---
Dy	---	---	0.13	0.10	---	---	---
Ho	---	---	0.03	0.02	---	---	---
Er	---	---	0.09	0.07	---	---	---
Tm	---	---	0.01	0.01	---	---	---
Yb	---	---	0.07	0.10	---	---	---
Lu	---	---	0.01	0.01	---	---	---

Note: nd = not detected.

Table 3.4. (continued).

	87-198C	87-199A	87-248	"87-264A	"87-271	#87-277	#MBS-CTUM
SiO2 (wt. %)	31.10	32.20	38.90	28.80	8.18	42.70	37.80
TiO2	0.08	0.08	0.00	0.00	0.00	0.00	0.00
Al2O3	0.17	0.51	1.20	0.99	0.15	1.41	1.89
Fe2O3*	6.52	7.40	5.45	6.53	9.60	6.43	9.29
MnO	0.14	0.10	0.07	0.08	0.14	0.07	0.13
MgO	41.15	40.45	37.30	25.56	36.45	34.65	28.60
CaO	0.06	0.28	1.74	0.70	0.16	1.58	3.38
Na2O	0.00	0.00	0.00	0.28	0.01	0.01	0.01
K2O	0.00	0.00	0.00	0.04	0.00	0.00	0.00
P2O5	0.01	0.01	0.00	0.29	0.02	0.01	0.01
LOI	21.01	19.68	14.51	32.92	43.60	12.07	17.08
Total	100.24	100.71	99.17	96.19	98.31	98.93	98.19
Cr (ppm)	1399	1385	2197	2768	3931	1710	1615
Ni	2744	2620	1983	1832	1934	2052	2020
Sc	---	---	---	3.45	4.67	7.92	9.70
V	8	19	24	23	29	40	31
Cu	nd	nd	nd	nd	nd	nd	27
Zn	31	19	13	26	244	28	32
Ga	3	2	3	4	nd	3	2
Rb	nd	nd	nd	1.58	0.19	0.06	0.13
Ba	nd	nd	nd	158	nd	nd	nd
Sr	3	5	9	9.50	5.50	22.76	33.08
Nb	1	2	2	0.02	0.01	0.08	1.00
Zr	1	3	5	5	3	2	4
Y	nd	3	1	0.72	0.47	0.81	0.87
Ta	---	---	---	0.07	0.05	0.06	0.02
Hf	---	---	---	0.10	0.05	0.00	0.02
Pb	---	---	---	2.48	2.75	0.21	3.92
Th	---	---	---	0.09	0.07	0.05	0.04
U	---	---	---	0.19	0.08	0.01	0.03
La (ppm)	---	---	---	0.46	0.52	0.11	0.17
Ce	---	---	---	1.07	1.16	0.32	0.39
Pr	---	---	---	0.14	0.15	0.05	0.05
Nd	---	---	---	0.52	0.61	0.24	0.24
Sm	---	---	---	0.16	0.12	0.08	0.09
Eu	---	---	---	0.04	0.03	0.01	0.02
Gd	---	---	---	0.14	0.11	0.12	0.12
Tb	---	---	---	0.02	0.02	0.02	0.02
Dy	---	---	---	0.16	0.11	0.16	0.16
Ho	---	---	---	0.03	0.02	0.03	0.04
Er	---	---	---	0.08	0.07	0.09	0.12
Tm	---	---	---	0.02	0.01	0.01	0.02
Yb	---	---	---	0.11	0.11	0.10	0.12
Lu	---	---	---	0.01	0.02	0.02	0.02

Note: " = completely carbonatized meta-ultramafic rocks.
= meta-ultramafic rocks in the vicinity of the Baikie showings. nd = not detected.

3.3.1. Major Elements

Major oxides are plotted against Mg# as a fractionation index in a series of Harker variation diagrams in Figure 3.17. The metaperidotites south of Florence Lake show a fairly restricted range in Mg# (85-95) despite their intense alteration. Other major elements similarly show little variation, indicating that the ultramafic suite as a whole is compositionally homogeneous. Sample 87-135, which is the rock containing primary clinopyroxene, has less MgO (28.30 wt.%) and more CaO (9.26 wt.%) than the 'typical' metaperidotites (MgO=37.1-41.25 wt.%, CaO < 2 wt%). The lack of other meta-ultramafic rocks with similar compositions indicates that clinopyroxene-bearing peridotites (e.g., lherzolite, wehrlite) comprised a relatively minor portion of the ultramafic suite, and dunites and harzburgites appear to have dominated.

Also plotted are two samples (87-264A, 87-271) of completely carbonatized ultramafic rocks from southeast of Florence Lake. Compared to the 'typical' serpentinized peridotites, these rocks have similar Mg#'s and comparable concentrations of other major oxides. However, sample 87-271 contains only 8.18 wt.% SiO_2. This can be attributed to a loss of SiO_2 during the formation of abundant pervasive quartz veins within these rocks (see Plate 2.36).

Sample 87-157A is a sheared chlorite-carbonate schist (see Plate 2.29), and differs from all the other meta-ultramafic samples in having much lower MgO (12.62 wt.%), and higher TiO_2, Al_2O_3 and CaO. The sample is classified as

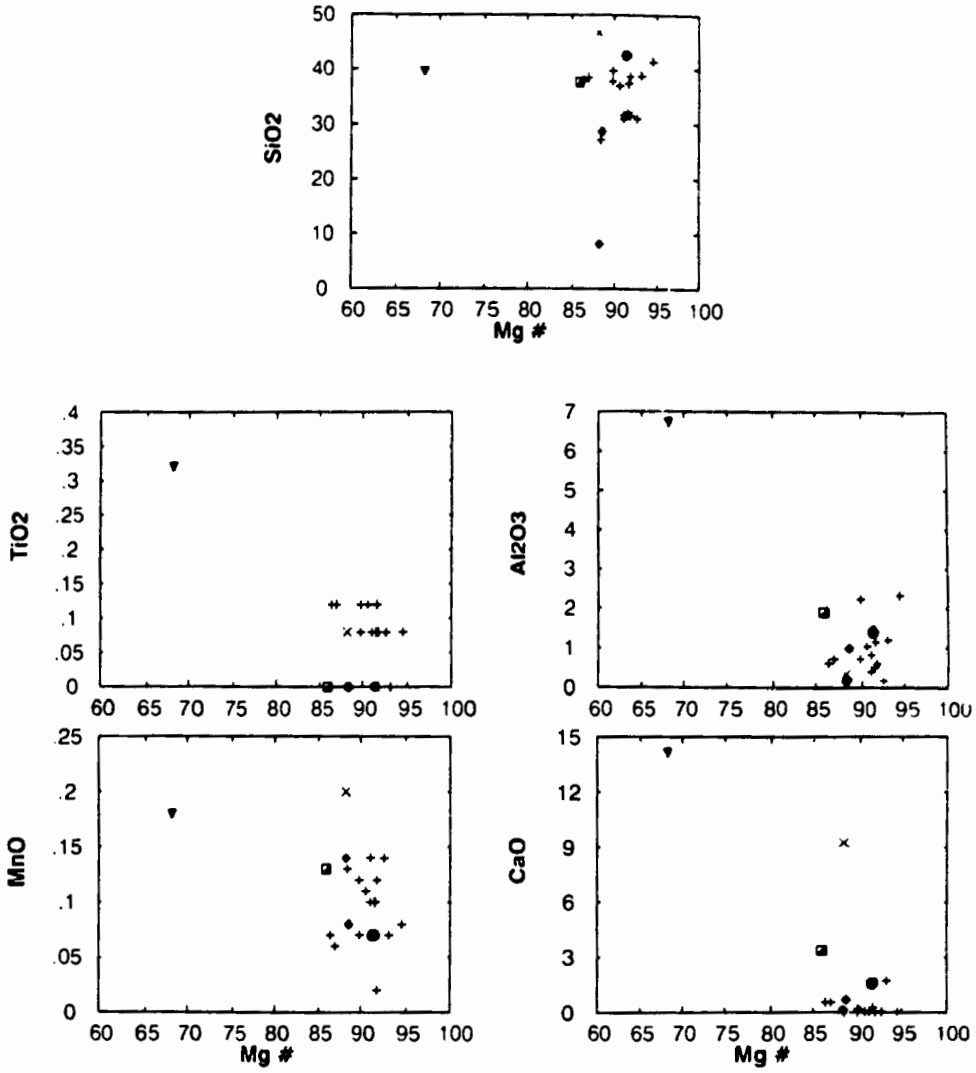

Figure 3.17. Major elements versus Mg# [(100*Mg)/(Mg+Fe^{+2})] for meta-ultramafic rocks, Florence Lake area. Symbols: crosses = metaperidotites south of Florence Lake; X = 87-135 (cpx-bearing metaperidotite); inverted solid triangle = 87-157A (sheared chlorite-carbonate schist); solid diamond = 87-264A and 87-271 (completely carbonatized ultramafic rocks); half-filled box = MBS-CTUM (talc-chlorite-carbonate schist at the Main Baikie showing); solid circle = 87-277 (moderately carbonatized serpentinite SW of Main Baikie showing).

ultramafic because of its high concentrations of Cr (1308 ppm) and Ni (2649 ppm).

Two meta-ultramafic samples (MBS-CTUM, 87-277) collected in the vicinity of the Baikie showings (see map - back pocket) are also plotted. Sample MBS-CTUM is a sample of the talc-carbonate schist hosting the Main Baikie showing, and it has lower MgO (28.60 wt.%) than most peridotites south of Florence Lake, but is generally comparable with respect to other major elements. Sample 87-277, a moderately carbonatized serpentinite located approximately 100 m southwest of the Main Baikie showing, contains similar concentrations of all major elements compared to metaperidotites south of Florence Lake.

3.3.2. Trace Elements

Cr and Ni are plotted against Mg# as a fractionation index in Figures 3.18A-B respectively. The metaperidotites south of Florence Lake contain high but variable Cr (1136-3065 ppm) and Ni (1983-3311 ppm) concentrations. Despite the relatively restricted range in Mg#, the samples display a broadly vertical distribution which may reflect accumulation of spinel and olivine. Compared to these peridotites, sample 87-135 has comparable Cr (2421 ppm) but much lower Ni (866 ppm), reflecting its lower modal olivine content. The two carbonatized samples have Ni concentrations (1832-1934 ppm) which are comparable to the minimum found in the typical peridotites; however, sample 87-271 contains the highest Cr (3931 ppm) of any ultramafic sample. Sample 87-157A has

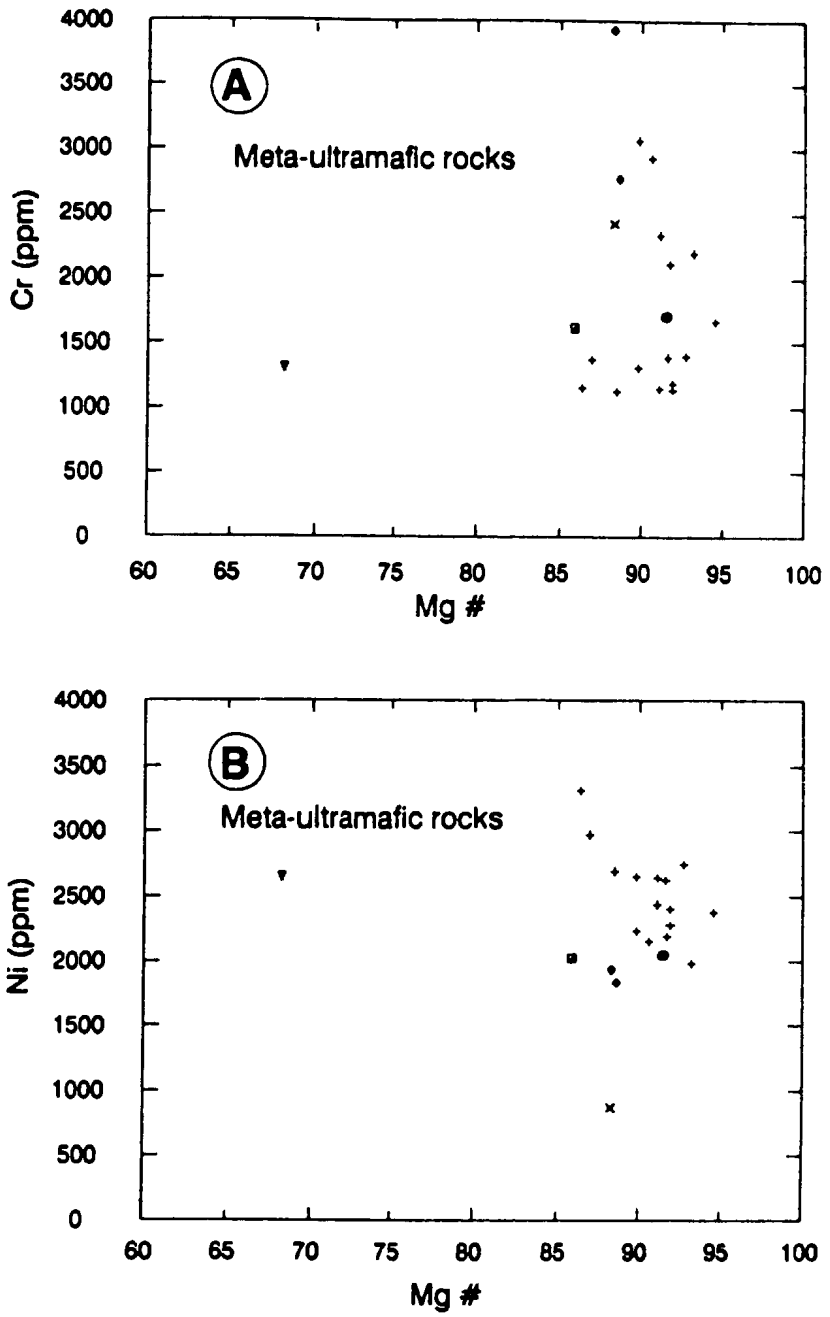

Figure 3.18. Harker variation diagrams for meta-ultramafic rocks, Florence Lake area. (A) Cr versus Mg#; (B) Ni versus Mg#. Symbols as for Figure 3.17.

comparable Cr and Ni contents to the typical metaperidotites.

The two Baikie meta-ultramafic samples also have Ni contents similar to the minimum of the metaperidotites south of Florence Lake, and comparable Cr contents.

3.3.3. Rare Earth Elements

Chondrite-normalized REE diagrams for four of the metaperidotites south of Florence Lake, and the two Baikie meta-ultramafic samples are plotted in Figures 3.19A and 3.19B respectively. The patterns for three Archean peridotitic komatiites are plotted in Figure 3.19C for comparison. Two samples (A2 and B) are from the Munro Township, Abitibi belt, Canada (Arth et al., 1977) and the third sample (KA2) is from Kambalda, Yilgarn block, Western Australia (Arndt and Jenner, 1986).

The REE patterns for Florence Lake metaperidotites are flat, with absolute REE concentrations generally variable and low ($\leq$ 1x chondrite). These low REE concentrations are a reflection of the high modal contents of cumulate olivine and orthopyroxene which have very low Kd's for REE.

In the metaperidotites south of Florence Lake (Figure 3.19A), the LREE and Eu display a greater overall variability between samples than do the HREE. Sample 87-185A has a pronounced negative Eu anomaly, 87-135 has a slight negative Eu anomaly, Eu is inexplicably not detected in 87-185B, and 87-181 has no Eu anomaly. These variations are most likely due to mobilization of Eu^{+2} during secondary processes. In

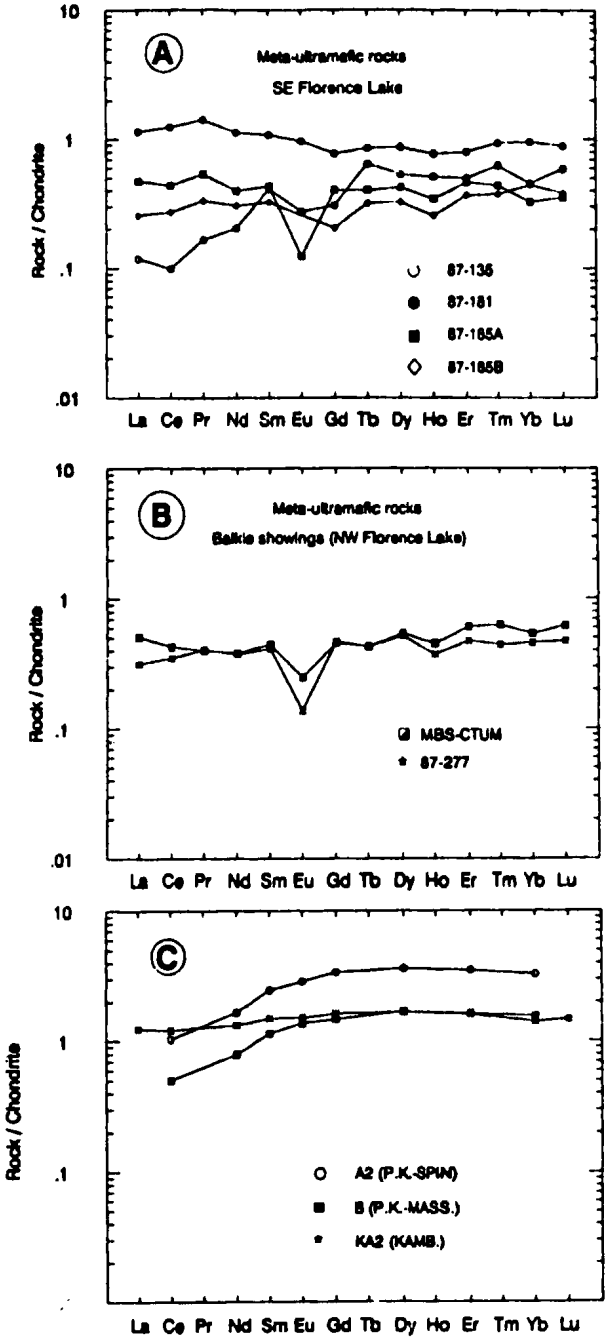

Figure 3.19. Chondrite-normalized REE diagrams for (A) meta-ultramafic rocks south of Florence Lake; (B) meta-ultramafic rocks at and near the Baikie showings, northwest of Florence Lake; and (C) peridotitic komatiites from other Archean greenstone belts. Samples A2 and B are spinifex-textured and massive komatiites respectively, Munro Township, Abitibi belt, Canada, and sample KA2 is a komatiitic olivine cumulate from Kambalda, Yilgarn block, Western Australia. See text for references. Chondrite normalizing values as for Figure 3.9 (from Wakita et al., 1971).

contrast to the flat patterns displayed by the other three samples, sample 87-135 is LREE-depleted. Since this sample is more fractionated (clinopyroxene-bearing) than the typical metaperidotites, the LREE-depletion is probably due to alteration.

The two Baikie samples both display similar flat REE patterns, pronounced negative Eu anomalies, and REE concentrations about 0.5x chondrite (Figure 3.19B). Both absolute REE concentrations and the shapes of these patterns are very similar to that displayed by sample 87-185A, indicating a common origin.

Compared to the Florence Lake and Baikie meta-ultramafic rocks (Figures 3.19A and 3.19B, respectively), typical Archean peridotitic komatiites generally have higher absolute REE concentrations, and their REE patterns are characteristically LREE-depleted (cf., Arth et al., 1977; Sun, 1984, 1987). Arndt and Jenner (1986) noted that sample KA2 (Figure 3.19C) has a relatively flat chondrite-normalized REE pattern and lacks the LREE-depleted character of most komatiites at Kambalda, Western Australia. They attributed these flat REE patterns to crustal contamination. By analogy, if the Florence Lake and Baikie meta-ultramafic rocks are komatiitic (see Section 5.2.1.1), their flat chondrite-normalized patterns may indicate that they are crustally-contaminated. More detailed investigations such as Sm-Nd isotopic determinations are required to test this possibility.

Archean komatiitic magmas are believed to be generated by

large degrees of partial melting of a pyrolite-type source, leaving a residue consisting of olivine ± orthopyroxene (e.g., Green, 1981). Under these conditions, incompatible trace elements (e.g., REE, Ti, Zr, Y, Nb, Ta, P) and major elements such as Al and Ca (which are not concentrated in olivine or orthopyroxene) will be concentrated in the melt, and should reflect the source character. Fractional crystallization of olivine and/or orthopyroxene at crustal depths will only affect absolute concentrations of incompatible elements, and element ratios in cumulate rocks should still reflect the source ratio. As noted previously, the petrography and geochemistry of meta-ultramafic rocks in the Florence Lake area indicate that the rocks originally consisted predominantly of peridotites comprising olivine ± orthopyroxene. Hence, their flat chondrite-normalized REE patterns indicate that the source area had similar characteristics, although the possibility of crustal contamination can not be overlooked.

3.3.4. Chrome Spinel Compositions

Microprobe analyses of chrome spinels in several meta-ultramafic samples are presented in Table 3.5. Analytical details are given in Appendix 2. A limited amount of microprobe work indicates that the chrome spinels are compositionally zoned. Table 3.5 shows that the core regions of spinels are variable in composition between samples, but are generally very Cr-rich (43-58 wt.% Cr_2O_3). The rim areas

Table 3.5. Microprobe analyses of chrome spinels from serpentinized peridotites, Florence Lake area.

SAMPLE #	87-009	87-009	87-009	87-009	87-009	87-138	87-138	87-138	87-138	87-138
Anal.	1	2	3	4	5	1	2	3	4	5
(Core/Rim)	Rim	Core	Core	Rim	Core	Core	Core	Core	Core	Core
Al2O3	10.49	11.89	11.93	10.28	12.34	15.70	15.06	14.48	14.90	15.55
Cr2O3	52.52	57.75	57.26	52.67	57.29	43.17	44.90	46.80	43.05	43.93
Fe2O3	4.02	1.45	1.81	4.62	1.53	9.14	7.12	7.52	9.00	6.97
FeO	31.24	19.36	19.07	30.87	18.58	26.46	25.88	25.80	25.84	26.09
MgO	1.56	9.52	9.66	1.88	10.03	5.12	5.14	5.56	5.08	4.92
Total	99.83	99.97	99.73	100.32	99.77	99.59	98.09	100.16	97.87	97.46
Al	3.48	3.69	3.71	3.39	3.82	4.97	4.85	4.57	4.81	5.03
Cr	11.67	12.02	11.93	11.64	11.88	9.18	9.69	9.91	9.33	9.53
Fe+3	0.85	0.29	0.36	0.97	0.30	1.85	1.46	1.52	1.86	1.44
Fe+2	7.35	4.26	4.20	7.22	4.08	5.95	5.91	5.78	5.92	5.99
Mg	0.65	3.74	3.80	0.78	3.92	2.05	2.09	2.22	2.08	2.01
Mg#	8.13	46.75	47.50	9.75	49.00	25.62	26.13	27.75	26.00	25.12
Cr#	77.03	76.51	76.28	77.45	75.67	64.88	66.64	68.44	65.98	65.45

Table 3.5. (continued).

SAMPLE #	87-124	87-124	87-124	87-124	87-173	87-173	87-173	87-173
Anal.	1	2	3	4	1	2	3	4
(Core/Rim)	Core	Core	Core	Core	Core	Core	Core	Core
Al2O3	11.65	12.04	13.45	10.74	9.96	9.87	9.58	10.26
Cr2O3	48.02	48.82	44.41	43.31	52.81	52.38	52.24	52.45
Fe2O3	3.45	4.32	6.19	10.50	5.64	5.92	4.50	4.97
FeO	29.01	27.00	27.52	27.51	28.80	30.37	29.40	29.21
MgO	3.41	3.65	3.22	2.95	3.21	2.25	2.28	2.83
Total	95.54	95.82	94.79	95.01	100.41	100.78	98.00	99.72
Al	4.05	4.05	4.56	3.70	3.25	3.24	3.23	3.38
Cr	11.19	11.02	10.10	10.00	11.57	11.52	11.81	11.58
Fe+3	0.76	0.93	1.34	2.31	1.18	1.24	0.97	1.04
Fe+2	7.15	6.45	6.62	6.72	6.67	7.07	7.03	6.82
Mg	0.85	1.55	1.38	1.28	1.33	0.93	0.97	1.18
Mg#	10.63	19.38	17.25	16.00	16.63	11.63	12.13	14.75
Cr#	73.43	73.13	68.89	72.99	78.07	78.05	78.52	77.41

show a marked increase in iron and an associated depletion in Mg, and to a lesser extent Cr and Al. This compositional trend is common in chrome spinels from ultramafic rocks having undergone serpentinization and/or regional metamorphism, and is associated with the formation of ferrit-chromite rims around chromite grains. Bliss and MacLean (1975) suggested that ferrit-chromite is formed when magnetite rims react with chromite cores during regional metamorphism of serpentinites.

Magmatic chrome spinels within ultramafic rocks from various petrotectonic settings (e.g., ophiolites, komatiites, stratiform complexes) have distinct chemical compositions (e.g., Irvine, 1967). Unfortunately, the obvious secondary mobilization of Mg, Cr and Al within spinels of this study preclude their use as petrogenetic indicators.

3.4. CARBONATE ROCKS

As noted previously, carbonate is ubiquitous throughout the FLG and the meta-ultramafic rocks. Carbonate occurs in a variety of forms: (1) thin (mm's) cross-cutting veinlets; (2) thin (mm's-cm's) folia within mafic metavolcanic schists; (3) larger lenses (several metres thick) of carbonate-quartz rocks within mafic metavolcanic schists; and 4) extensive zones (up to 1.25 km long) of intense carbonatization within meta-ultramafic rocks.

3.4.1. Mineral Chemistry

Microprobe analyses of a number of carbonates have shown

that several species exist. The cross-cutting carbonate veinlets consist of calcite, whereas the thin carbonate folia within the mafic metavolcanic schists are predominantly ankerite, although minor ferroan dolomite and calcite have also been identified. The carbonate lenses within the mafic metavolcanic rocks are comprised of ankerite, whereas carbonate within the meta-ultramafic rocks is ferroan magnesite (Table 3.6).

Microprobe analyses of chlorites within carbonatized ultramafic rocks are presented in Table 3.7.1. The abnormally low totals (81-85 wt.%) of many chlorite analyses can be attributed to poor polishing of this phase. The Cr_2O_3 and NiO contents of the chlorites are variable but generally high. The highest Cr_2O_3 (1.64-2.84 wt.%) and NiO (0.46-1.40 wt.%) contents are in samples from the carbonatized ultramafic belt southeast of Florence Lake. Chlorite in sample 87-247A, collected from the same area, has slightly lower Cr_2O_3 (0.29-0.57 wt.%.) and comparable NiO (0.43-0.68 wt.%) contents relative to the other samples. By comparison, chlorite from the talc-carbonate schist hosting the Main Baikie showing (MBS-CTUM, MBS-DS) has significantly lower Cr_2O_3 (0.18-0.82 wt.%) and NiO (0.08-0.14 wt.%) contents. A comparison of chlorite compositions from this study with various published chlorite analyses (Table 3.7.2) indicates that these are best classified as Cr-clinochlore.

Table 3.6. Microprobe analyses of carbonate lenses (*) and carbonatized ultramafic rocks.

SAMPLE #	ANAL	MGO	CAO	MNO	FEO	SR2O3	TOTAL
87-062 *	1	18.31	28.71	0.27	7.36	0.00	54.65
87-063-2	1	39.05	0.14	0.16	15.22	0.00	54.57
	2	41.67	0.09	0.01	9.18	0.00	50.95
	AVG.	40.36	0.12	0.09	12.20	0.00	52.76
87-065	1	39.65	0.11	0.16	14.02	0.02	53.96
87-125A	1	38.43	0.05	0.26	12.81	0.02	51.57
	2	41.06	0.16	0.07	9.55	0.00	50.84
	3	41.24	0.07	0.11	8.19	0.12	49.73
	4	41.39	0.10	0.07	7.70	0.00	49.26
	5	40.91	0.10	0.07	8.25	0.00	49.33
	AVG.	40.61	0.10	0.12	9.30	0.03	50.15
87-138	1	43.79	0.10	0.29	2.83	0.00	47.01
	2	43.88	0.05	0.29	2.23	0.05	46.50
	AVG.	43.84	0.08	0.29	2.53	0.03	46.76
87-185C	1	41.95	0.03	0.16	7.31	0.00	49.45
87-195	1	43.03	0.76	0.26	4.10	0.00	48.15
87-247A	1	44.20	0.05	0.03	5.61	0.07	49.96
	2	43.70	0.07	0.16	8.38	0.00	52.31
	3	43.70	0.09	0.09	8.93	0.00	52.81
	AVG.	43.87	0.07	0.09	7.64	0.02	51.69
87-262	1	42.32	0.17	0.14	7.27	0.00	49.90
87-264A	1	41.18	0.10	0.09	8.66	0.05	50.08
MBS-DS	1	39.80	0.30	0.37	6.69	0.00	47.16
	2	39.88	0.13	0.25	8.40	0.00	48.66
	AVG.	39.84	0.22	0.31	7.55	0.00	47.91

Table 3.7.1. Microprobe analyses of chlorites in carbonatized ultramafic rocks, Florence Lake area.

SAMPLE	ANAL	SIO2	TIO2	AL2O3	FEO(t)	MNO	MGO	CAO	NA2O	K2O	CR2O3	NIO	TOTAL
87-063-2	1	28.25	0.03	18.23	8.11	0.01	25.16	0.02	0.03	0.00	2.84	0.57	83.25
	2	30.18	0.02	17.09	7.99	0.03	26.17	0.02	0.00	0.00	1.96	0.46	83.92
	AVG.	29.22	0.03	17.66	8.05	0.02	25.67	0.02	0.02	0.00	2.40	0.52	83.59
87-065	1	27.10	0.02	21.00	7.78	0.00	24.59	0.02	0.00	0.04	2.16	0.70	83.41
	2	28.11	0.06	21.08	7.91	0.03	24.44	0.02	0.02	0.01	1.64	0.70	84.02
	AVG.	27.61	0.04	21.04	7.85	0.02	24.52	0.02	0.01	0.03	1.90	0.70	83.72
87-247A	1	32.76	0.04	14.78	5.15	0.01	27.64	0.04	0.01	0.01	0.57	0.68	81.69
	2	29.96	0.06	16.62	5.34	0.00	28.65	0.02	0.01	0.01	0.29	0.43	81.39
	AVG.	31.36	0.05	15.70	5.25	0.01	28.15	0.03	0.01	0.01	0.43	0.56	81.54
87-262	1	28.57	0.03	18.73	6.01	0.03	23.22	0.02	0.00	0.00	2.13	1.40	80.14
	2	29.22	0.02	17.61	6.11	0.03	25.30	0.00	0.00	0.02	2.11	0.94	81.36
	AVG.	28.90	0.03	18.17	6.06	0.03	24.26	0.01	0.00	0.01	2.12	1.17	80.75
MBS-CTUM	1	29.74	0.10	18.59	11.50	0.03	27.16	0.02	0.00	0.01	0.18	0.11	87.44
	2	30.25	0.13	17.43	10.65	0.04	27.67	0.01	0.00	0.00	0.31	0.12	86.61
	3	29.25	0.06	17.85	10.84	0.04	26.21	0.07	0.02	0.01	0.40	0.11	84.86
	4	29.04	0.09	17.80	9.82	0.03	27.09	0.02	0.01	0.01	0.80	0.14	84.85
	AVG.	29.57	0.10	17.92	10.70	0.04	27.03	0.03	0.01	0.01	0.42	0.12	85.94
MBS-DS	1	30.20	0.03	18.20	9.84	0.04	28.43	0.00	0.01	0.00	0.71	0.08	87.54
	2	31.43	0.05	16.47	9.45	0.00	28.93	0.04	0.04	0.01	0.82	0.13	87.37
	AVG.	30.82	0.04	17.34	9.65	0.02	28.68	0.02	0.03	0.01	0.77	0.11	87.46

Table 3.7.2. Analyses of selected chlorites (from Deer, Howie & Zussman, 1963).

Chlorite Name	SIO2	TIO2	AL2O3	FEO(t)	MNO	MGO	CAO	NA2O	K2O	CR2O3	NIO	TOTAL
Klementite	27.56	---	24.47	14.36	1.80	20.86	---	---	---	---	---	89.05
Thuringite	20.82	---	17.64	46.66	---	4.15	---	---	---	---	---	89.27
Chamosite	26.40	---	18.23	31.57	0.04	11.35	0.42	0.17	0.17	---	---	88.35
Corundophilite	23.20	---	24.42	16.88	---	22.76	1.04	---	---	---	---	88.30
Sheridanite	27.64	0.22	22.48	12.12	0.02	24.32	0.00	0.17	0.06	---	tr	87.03
Ripidolite	25.62	0.88	21.19	25.43	0.35	15.28	0.16	0.00	0.00	---	---	88.91
Clinochlore	28.73	0.41	19.16	12.96	0.15	26.37	0.06	0.01	0.03	---	---	87.88
Cr-clinochlore	31.87	0.17	14.51	5.43	tr	32.76	---	0.04	0.02	1.10	0.28	86.18
Brunsvigite	27.11	0.35	17.42	33.89	---	9.75	0.21	---	---	---	---	88.73
Penninite	33.83	---	12.95	5.27	---	34.94	---	---	---	---	---	86.99
Diabantite	33.46	---	10.96	27.28	0.40	16.52	0.92	0.29	---	---	---	89.83
Kammererite	32.12	---	9.50	1.98	---	35.36	1.24	---	---	7.88	---	88.08

3.4.2. Major and Trace Elements

Pearton (1981) demonstrated that despite intense alteration, talc-carbonate and quartz-carbonate rocks within the Murchinson greenstone belt, South Africa, are chemically (major elements, transition elements and REE) similar to komatiitic rocks from the same area. Similarly, the geochemistry of carbonate-rich rocks within the Florence Lake area clearly demonstrate their ultramafic and non-sedimentary character.

The whole-rock chemistry of two carbonatized ultramafic rocks (see Plates 2.36 to 2.39), and two samples from the carbonate lenses within the mafic metavolcanic schists (see Plate 2.6) are compared to the average 'typical' serpentinized peridotites from south of Florence Lake in Table 3.8. It should be noted that two samples from south of Florence Lake with 'atypical' whole rock chemistry, and two samples collected from northwest of Florence Lake (87-277, MBS-CTUM) have been excluded from the average.

The CaO versus MgO diagram (Figure 3.20A) clearly shows the similarity between the carbonatized ultramafic rocks and the serpentinized peridotites, both having high MgO contents and negligible CaO. In contrast, the carbonate lenses within the mafic metavolcanics contain significantly lower MgO and much higher CaO. This difference is a reflection of the carbonate phase in each lithology, which is ferroan magnesite in the carbonatized ultramafic rocks and ankerite in the carbonate lenses (see Table 3.6). In Figure 3.20B-C, Cr and Ni

Table 3.8. Chemical analyses of carbonate lenses, carbonatized ultramafic rocks and average serpentinized peridotites, Florence Lake area.

	CARBONATE LENSES		CARBONATIZED ULTRAMAFICS		
	TB-87-061	87-062	87-264A	87-271	AVG. U/M (15)
SiO2 (wt. %)	3.75	21.00	28.80	8.18	35.55
TiO2	0.00	0.00	0.00	0.00	0.08
Al2O3	0.32	0.48	0.99	0.15	0.89
Fe2O3*	7.90	6.70	6.53	9.60	7.94
MnO	0.24	0.24	0.08	0.14	0.10
MgO	15.10	12.35	25.56	36.45	39.28
CaO	27.90	23.20	0.70	0.16	0.34
Na2O	0.02	0.02	0.28	0.01	0.00
K2O	0.01	0.09	0.04	0.00	0.00
P2O5	0.01	0.01	0.29	0.02	0.01
LOI	42.32	34.27	32.92	43.60	15.96
Total	97.57	98.36	96.19	98.31	100.15
Cr (ppm)	nd	nd	2768	3931	1751
Ni	17	nd	1832	1934	2418
Sc	---	2.72	3.45	4.67	---
V	244	17	23	29	40
Cu	nd	nd	nd	nd	3
Zn	16	13	26	244	23
Rb	nd	2.38	1.58	0.19	nd
Ba	nd	nd	158	nd	nd
Sr	56	81.53	9.50	5.50	8
Ga	nd	nd	4	nd	2
Nb	1	0.03	0.02	0.01	2
Zr	3	4	5	3	7
Y	5	4.27	0.72	0.47	2
Ta	---	0.28	0.07	0.05	---
Hf	---	0.03	0.10	0.05	---
Pb	---	1.06	2.48	2.75	---
Th	---	0.03	0.09	0.07	---
U	---	0.00	0.19	0.08	AVG. U/M (3)
La (ppm)	---	0.83	0.46	0.52	0.21
Ce	---	1.90	1.07	1.16	0.59
Pr	---	0.29	0.14	0.15	0.09
Nd	---	1.52	0.52	0.61	0.39
Sm	---	0.56	0.16	0.12	0.12
Eu	---	0.44	0.04	0.03	0.02
Gd	---	0.73	0.14	0.11	0.12
Tb	---	0.12	0.02	0.02	0.02
Dy	---	0.69	0.16	0.11	0.16
Ho	---	0.14	0.03	0.02	0.03
Er	---	0.36	0.08	0.07	0.11
Tm	---	0.05	0.02	0.01	0.02
Yb	---	0.30	0.11	0.11	0.13
Lu	---	0.04	0.01	0.02	0.02

Note: nd = not detected.

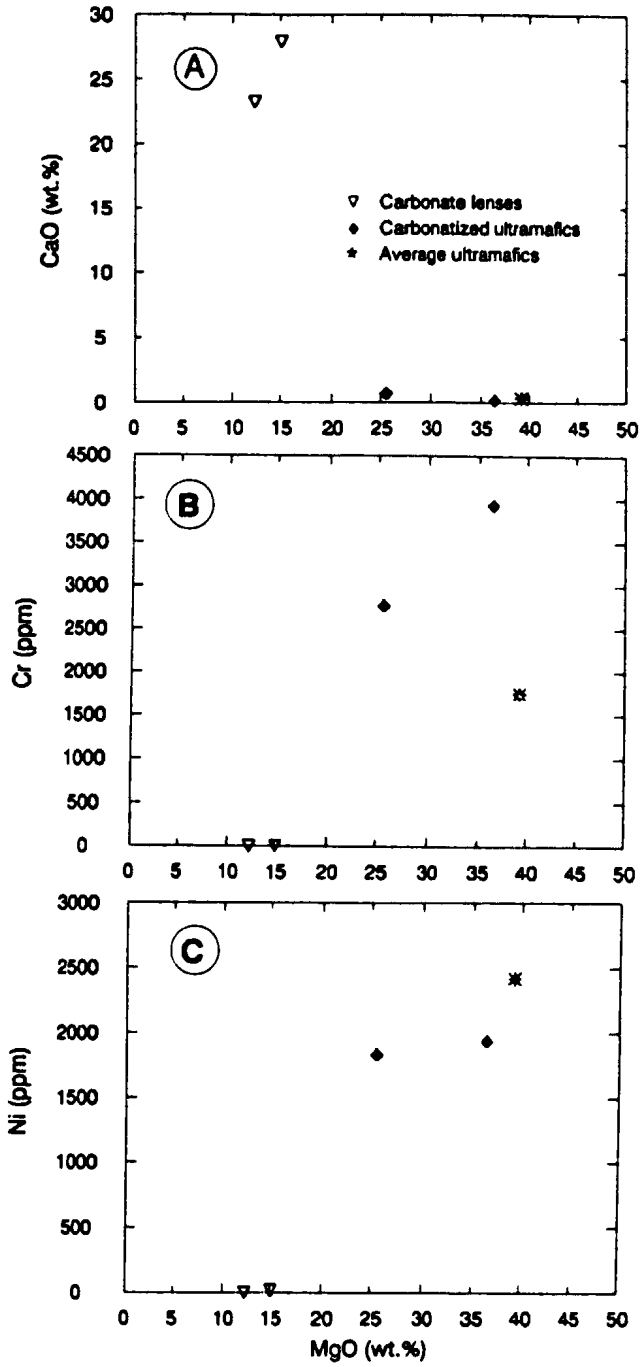

Figure 3.20. Harker variation diagrams for carbonate lenses within mafic metavolcanic rocks, carbonatized ultramafic rocks, and the average 'typical' meta-ultramafic rocks south of Florence Lake. (A) CaO versus MgO; (B) Cr versus MgO; and (C) Ni versus MgO.

are plotted against MgO to further differentiate the carbonate rocks. The carbonate lenses contain essentially no Cr or Ni, whereas the carbonatized ultramafic rocks contain very high Cr (2768-3931 ppm) and Ni (1832-1934 ppm) concentrations.

3.4.3. Rare Earth Elements

In Figure 3.21, chondrite-normalized REE patterns for the two carbonatized ultramafic samples and the carbonate lens sample are plotted with the range and average of the 'typical' metaperidotites from south of Florence Lake.

The patterns for the two carbonatized samples (87-264A, 87-271) are both slightly fractionated (La_n/Lu_n=3.4-3.8), with low absolute REE concentrations. The pattern for the carbonate lens sample is also slightly fractionated (La_n/Lu_n=1.9). The carbonatized ultramafic samples fall within the range displayed by the three peridotites, although the patterns for the latter are significantly flatter (La_n/Lu_n=0.3-1.2). This may indicate that the ultramafic rocks were slightly enriched in LREE during intense carbonatization. The presence of minor albite and trace fuchsite demonstrate that the rocks locally underwent Na- and K-metasomatism (see Section 2.8.3). In contrast, the carbonate lens sample falls completely outside the range of the metaperidotites, with higher REE concentrations and a pronounced positive Eu anomaly.

3.5. KANAIRIKTOK INTRUSIVE SUITE

Ermanovics and Raudsepp (1979a) described the Kanairiktok

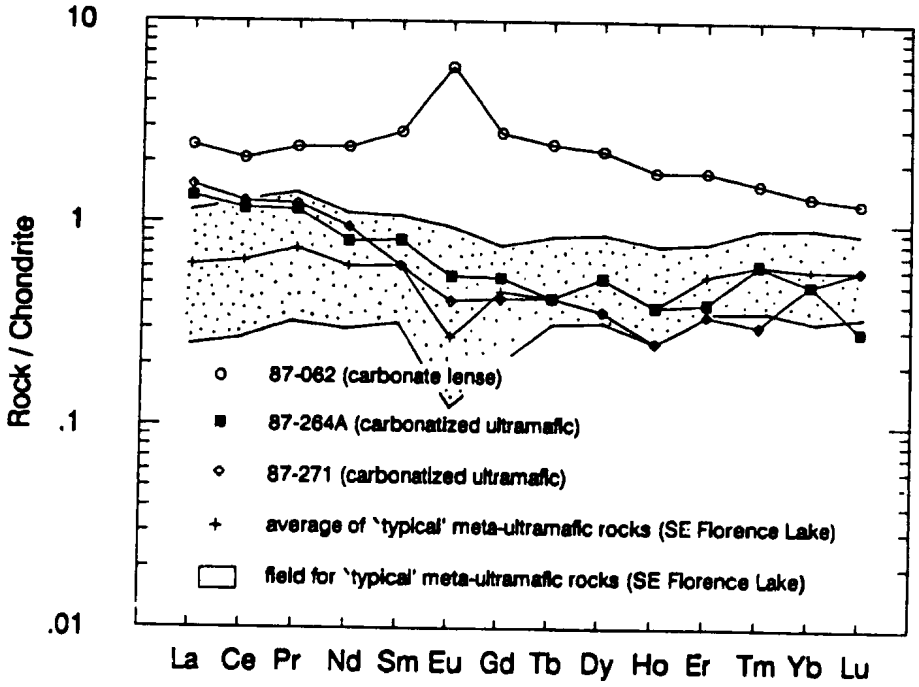

Figure 3.21. Chondrite-normalized REE diagram for carbonate lenses within mafic metavolcanic rocks, carbonatized ultramafic rocks, and the average and range of 'typical' meta-ultramafic rocks south of Florence Lake. Chondrite normalizing values as for Figure 3.9 (from Wakita et al., 1971).

Intrusive Suite as a variety of gneissic rocks of predominantly granodioritic to tonalitic composition.

Chemical analyses of six samples of the Kanairiktok Intrusive Suite from this study are presented in Table 3.9. In the following diagrams, nineteen samples of the Kanairiktok Intrusive Suite collected from the Makkovik Province to the southeast of the present study area (Wilton, in press), have also been included for comparison.

3.5.1. Major Elements

The major element data show that the Kanairiktok granitoids conform well to Barker's (1979) definition of trondhjemite (Table 3.10). In the normative feldspar plot (Figure 3.22), all the samples of this study plot in the trondhjemite field; the majority of Wilton's samples also plot in the trondhjemite field, however several plot in the tonalite field. There appear to be two groups of samples, one which plots well within the trondhjemite field, and another which plots in the tonalite field or straddles the boundary between the trondhjemite-tonalite fields. This grouping is also apparent on the Na_2O-K_2O-CaO plot (see Figure 3.24). On the AFM diagram (Figure 3.23), the samples fall along the trondhjemitic trend of Barker and Arth (1976). Barker and Arth (1976) also recognized a common calc-alkaline and trondhjemitic trend on the ternary Na_2O-K_2O-CaO (Figure 3.24); however, the Kanairiktok samples do not display any clear trend.

Table 3.9. Chemical analyses of trondhjemites, Kanairiktok Intrusive Suite.

	TB-87-038	87-039B	87-140	87-191	87-192	87-239
SiO2 (wt. %)	68.60	73.90	73.70	69.90	73.30	70.30
TiO2	0.32	0.16	0.20	0.40	0.24	0.24
Al2O3	15.30	14.30	13.80	15.30	14.30	15.50
Fe2O3*	2.50	1.04	1.48	2.43	1.40	2.12
MnO	0.04	0.01	0.03	0.04	0.04	0.05
MgO	1.45	0.60	0.46	0.86	0.47	0.75
CaO	1.30	1.38	2.50	2.74	1.52	1.88
Na2O	6.25	5.55	4.41	4.92	5.14	4.40
K2O	1.04	1.65	1.42	1.49	2.38	3.43
P2O5	0.09	0.02	0.06	0.07	0.03	0.06
LOI	1.59	0.80	0.83	1.45	1.01	1.25
Total	98.48	99.41	98.89	99.60	99.83	99.98
Cr (ppm)	nd	nd	nd	nd	nd	nd
Ni	nd	nd	nd	nd	nd	nd
Sc	---	---	3.11	5.31	---	4.23
V	41	9	11	32	13	25
Cu	nd	nd	nd	nd	nd	11
Zn	14	1	nd	36	7	23
Rb	29	41	29.83	38.28	62	63.37
Ba	235	460	474	482	493	580
Sr	240	215	195.80	329.08	164	161.74
Ga	19	14	15	20	21	18
Nb	3	2	3.81	1.83	3.00	7.82
Zr	130	73	102	129	75	106
Y	5	4	6.28	3.29	10	6.44
Ta	---	---	1.79	1.22	---	1.74
Hf	---	---	2.55	0.94	---	2.54
Pb	---	---	4.60	4.35	---	6.47
Th	---	---	2.93	1.94	---	1.94
U	---	---	0.61	0.33	---	0.74
La	---	---	14.33	14.81	---	10.39
Ce	---	---	27.54	25.23	---	19.70
Pr	---	---	3.12	2.93	---	2.29
Nd	---	---	9.97	9.99	---	7.90
Sm	---	---	1.80	1.81	---	1.67
Eu	---	---	0.33	0.41	---	0.31
Gd	---	---	1.42	1.35	---	1.51
Tb	---	---	0.21	0.16	---	0.22
Dy	---	---	1.23	0.75	---	1.22
Ho	---	---	0.23	0.13	---	0.25
Er	---	---	0.64	0.32	---	0.72
Tm	---	---	0.09	0.04	---	0.11
Yb	---	---	0.62	0.24	---	0.73
Lu	---	---	0.11	0.03	---	0.12

Note: nd = not detected.

Table 3.10. Major element contents of trondhjemites (after Barker, 1979) compared to granitoids of the Kanairiktok Intrusive Suite.

BARKER'S CRITERIA	SAMPLE #	87-038	87-039B	87-140	87-191	87-192	87-239
1. SiO2 > 68% and usually < 75%	SiO2	68.60	73.90	73.70	69.90	73.40	70.30
2. Al2O3 typically > 15% @ 70% SiO2 and < 14% @ 75% SiO2	Al2O3	15.30	14.30	13.80	15.30	14.30	15.50
3. (FeO* + MgO) < 3.4	FeO* + MgO	3.70	1.54	1.79	3.05	1.73	2.66
FeO*/MgO commonly is 2-3	FeO*/MgO	1.55	1.56	2.90	2.54	2.68	2.54
4. CaO ranges from 4.4-4.5% in Ca-trondhjemite to typical values of 1.5-3.0%.	CaO	1.30	1.38	2.50	2.74	1.52	1.88
5. Na2O typically is 4.0-5.5%	Na2O	6.25	5.55	4.41	4.92	5.14	4.40
6. K2O < ca. 2.5%, and typically < 2%	K2O	1.04	1.65	1.42	1.49	2.38	3.43

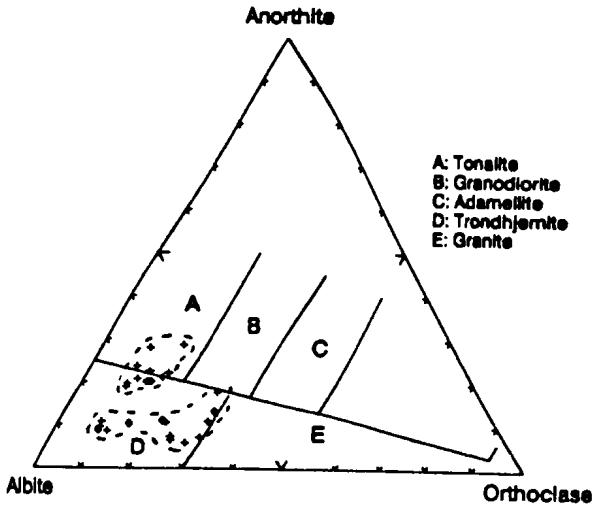

Figure 3.22. CIPW normative feldspar plot (after O'Connor, 1965) for the Kanairiktok Intrusive Suite. Symbols: solid diamonds = Florence Lake area, Nain Province; crosses = Moran Lake area, Makkovik Province. Dashed lines indicate two groups of trondhjemite-tonalite.

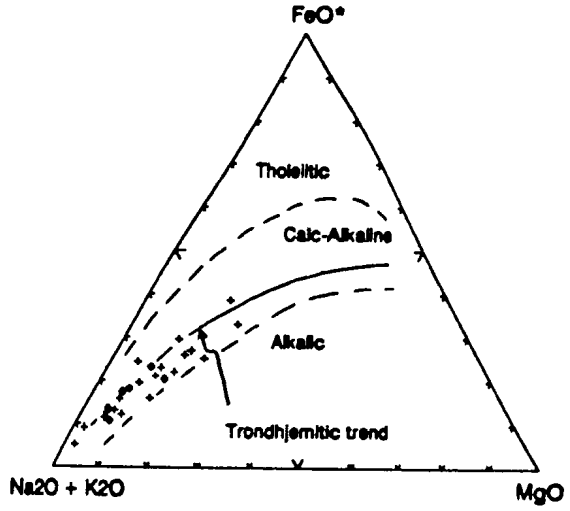

Figure 3.23. AFM diagram for Kanairiktok Intrusive Suite. Defined trends are after Barker and Arth (1976). Symbols as for Figure 3.22.

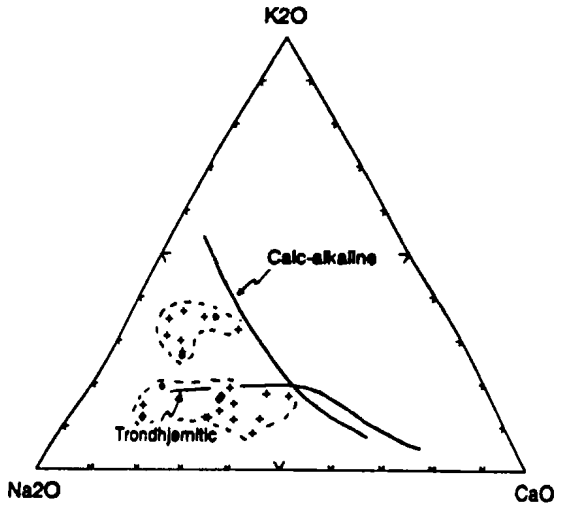

Figure 3.24. Na_2O-K_2O-CaO ternary plot for Kanairiktok Intrusive Suite. Defined trends are after Barker and Arth (1976). Dashed lines indicate two groups of trondhjemite-tonalite. Symbols as for Figure 3.22.

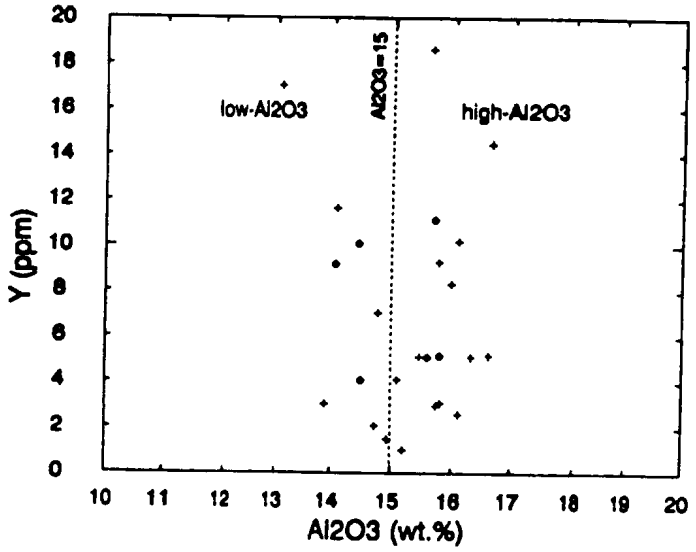

Figure 3.25. Y versus Al_2O_3 diagram for the Kanairiktok Intrusive Suite. The dividing line at Al_2O_3 = 15% separates low- and high-Al_2O_3 type trondhjemite (after Barker, 1979). The large range in Y values reflect variations in the degree of HREE-depletion. Symbols as for Figure 3.22.

A plot of Y versus Al_2O_3 (Figure 3.25) shows that the Kanairiktok trondhjemite-tonalite suite straddles the boundary between the low- and high-Al_2O_3 type (15 wt.%) trondhjemite of Barker (1979). The samples have quite variable Y contents (1-19 ppm), implying that HREE concentrations are similarly variable (see Section 3.5.2).

In the K_2O versus SiO_2 diagram (Figure 3.26), the Kanairiktok trondhjemites plot in and around the continental trondhjemite field (Coleman and Peterman, 1975).

3.5.2. Rare Earth Elements

Chondrite-normalized REE patterns for the Kanairiktok trondhjemites from this study and those of Wilton (in press) are shown in Figures 3.27A and 3.27B respectively. The REE range of FLG felsic supracrustals is shown in Figure 3.27A for comparison. It is apparent that all the Kanairiktok trondhjemites have similar fractionated REE patterns. The three samples of this study have very similar LREE concentrations, but HREE are more depleted in sample 87-191 (La_n/Lu_n=47.8) than the other two samples (La_n/Lu_n=8.6-13.5). This difference is also reflected in Y concentrations (see Table 3.10). Two of the samples show very slight negative Eu anomalies, which may be due to plagioclase fractionation. The REE patterns of Wilton's samples are similar to sample 87-191, with La_n/Lu_n=28.9-58.19.

The chondrite-normalized patterns for all the Kanairiktok trondhjemite samples fall completely within the range

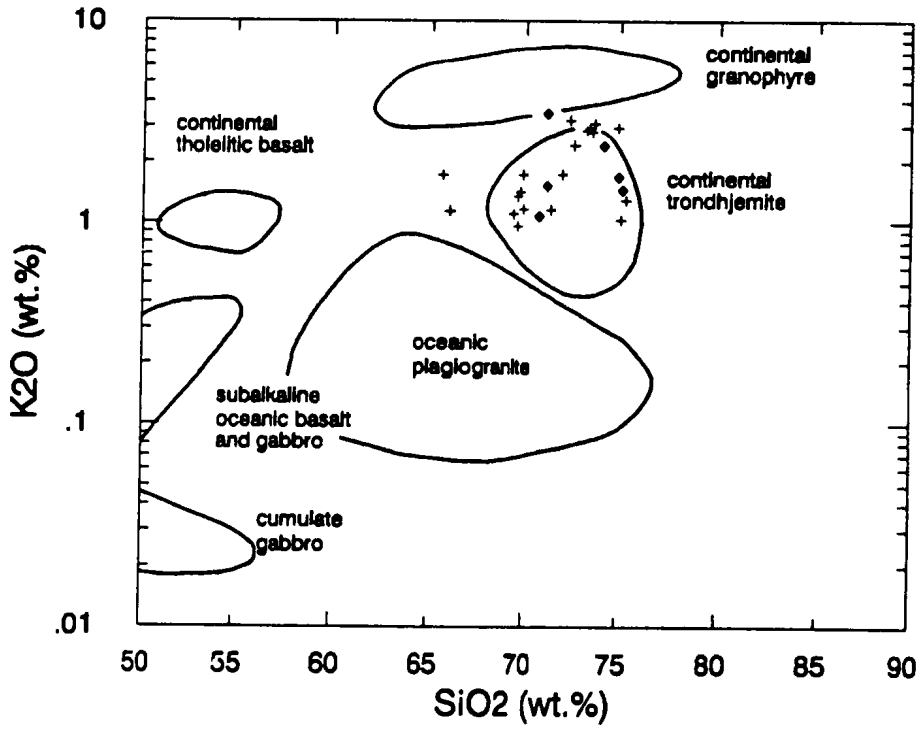

Figure 3.26. K_2O versus SiO_2 diagram for the Kanairiktok Intrusive Suite. Fields are after Coleman and Peterman (1975). Symbols as for Figure 3.22.

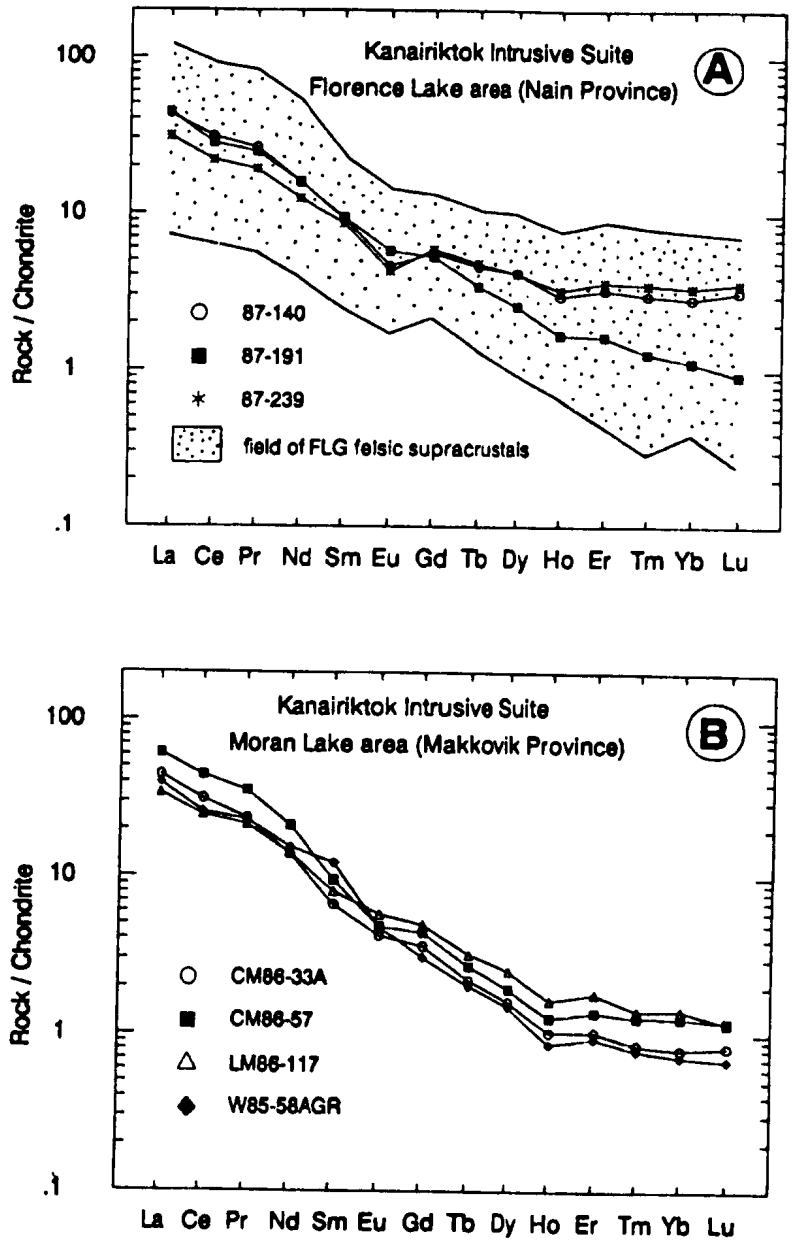

Figure 3.27. Chondrite-normalized REE diagrams for the Kanairiktok Intrusive Suite from (A) the Florence Lake area, Nain Province, and (B) the Moran Lake area, Makkovik Province. The range of REE for the Florence Lake Group felsic supracrustal rocks is plotted in (A) for comparison. Chondrite normalizing values as for Figure 3.9 (from Wakita et al., 1971).

displayed by the FLG felsic supracrustals (Figure 3.27A). Compared to the 'typical' FLG REE patterns (see Figure 3.10A), the patterns of samples 87-140 and 87-239 have identical shapes but slightly lower REE concentrations. The pattern of sample 87-191 and those of Wilton also have similar REE patterns, but are slightly more HREE-depleted.

3.5.3. Tectonic Discrimination - Spider Diagrams

On the tectonic discrimination diagrams of Pearce et al. (1984), the Kanairiktok trondhjemites plot in the volcanic arc granite field (Figure 3.28A-B). MORB-normalized spider diagrams for Kanairiktok trondhjemites are displayed in Figure 3.29A-B. All the samples display classic arc (or continental crust) signatures, with pronounced depletion in Nb relative to La and Th.

3.6. TECTONIC SETTING(S) OF ARCHEAN GRANITE-GREENSTONE TERRANES

The nature of Archean tectonism is the subject of considerable debate and goes well beyond the scope of this thesis, however, a brief discussion is warranted.

The most fundamental question facing geologists working in Archean terranes is whether plate tectonic processes similar to those operating today, also operated during the Archean. Thermal models based on the estimated eruption temperatures of peridotitic komatiites (1650°C, Green et al., 1975) indicate that heat production (and corresponding heat

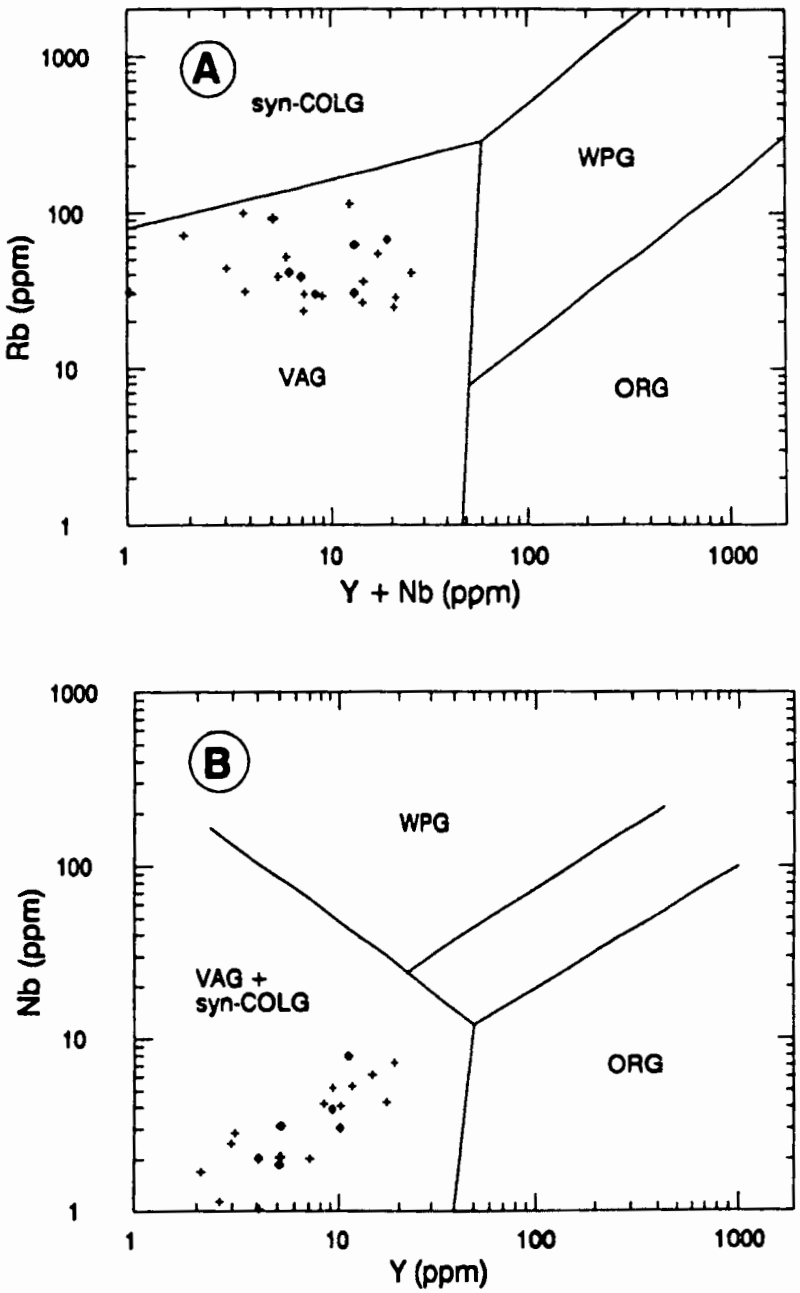

Figure 3.28. Tectonic discrimination diagrams for the Kanairiktok Intrusive Suite (after Pearce et al., 1984). (A) Rb versus Y + Nb; and (B) Nb versus Y. Fields: syn-COLG = syn-collision granites; ORG = ocean ridge granites; VAG = volcanic arc granites; WPG within-plate granites. Symbols as for Figure 3.22.

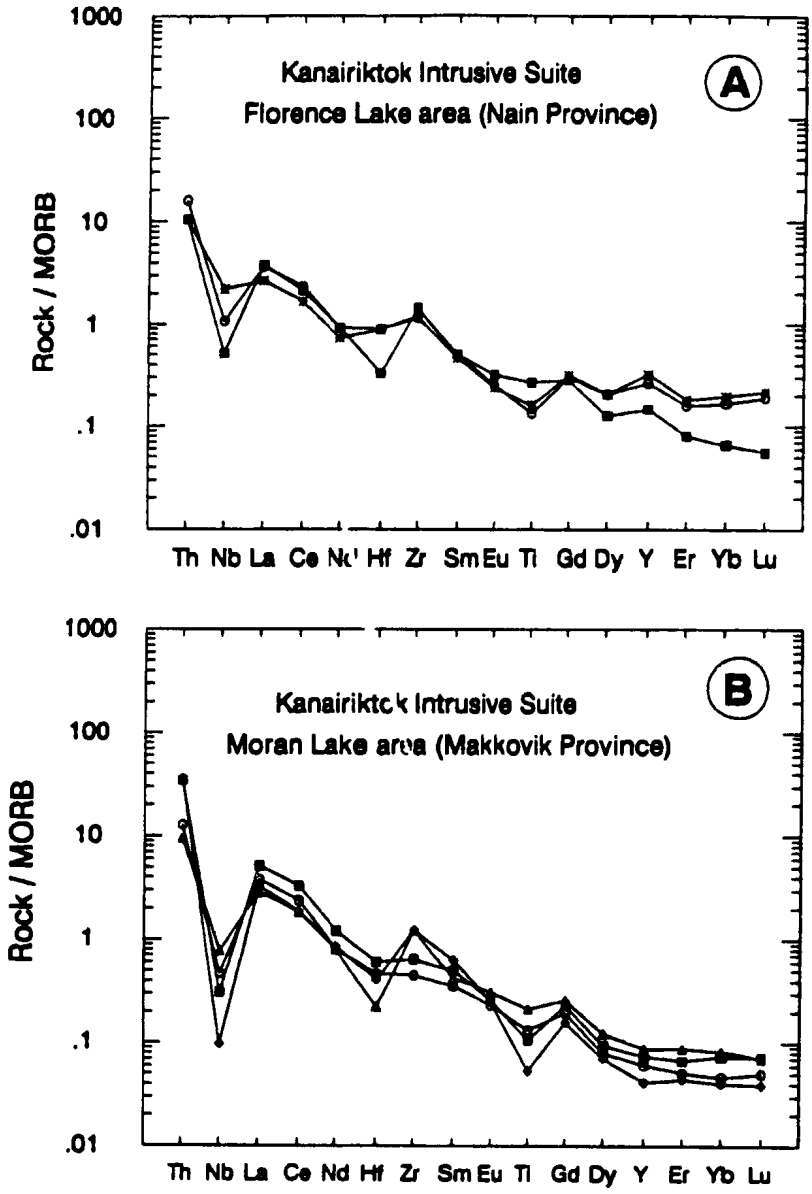

Figure 3.29. MORB-normalized spider diagrams for the Kanairiktok Intrusive Suite from (A) the Florence Lake area, Nain Province, and (B) the Moran Lake area, Makkovik Province. Symbols as for Figure 3.27. MORB normalizing values as for Figure 3.15 (from NEWPET, 1990).

loss) during the Archean was probably 2-3x greater than at present (e.g., Bickle, 1978). However, metamorphic temperature and pressure estimates for Archean high-grade terranes indicate that continental lithospheric gradients were similar to those of the present-day (Bickle, 1978). Consequently, many recent theoretical plate tectonic models for the Archean have largely concentrated on ways of dissipating these high heat flows through areas analogous to modern oceans: (1) oceanic crust with similar thicknesses to modern oceanic crust, but more ultramafic in composition (Arndt, 1983); (2) thicker oceanic crust (Sleep and Windley, 1982); (3) thinner, more ultramafic oceanic crust (Nisbet and Fowler, 1983); (4) faster spreading rates, and consequently faster subduction, with smaller lithospheric plates (Bickle, 1978; Abbott and Hoffman, 1984); and (5) greater spreading ridge length, and slower, rather than faster spreading (Hargraves, 1986).

Some authors (e.g., Baer, 1981) have argued that high heat flows during the Archean precluded subduction, and others (e.g., Ayres and Thurston, 1985) have cautioned against using modern plate tectonic analogues for Archean greenstone belts. Nevertheless, currently there appears to be a consensus among workers that uniquely Archean tectonic models should be avoided when modern analogues can adequately explain the tectonic evolution of granite-greenstone terranes (cf., Ludden and Hubert, 1986; Hoffman, 1988; Barley and Groves, 1990a; Thurston and Chivers, 1990).

A plethora of tectonic models has been proposed to

explain the origin and evolution of Archean granite-greenstone terranes (cf., Condie, 1981; Ayres et al., 1985). Individual greenstone belts have commonly been interpreted to have formed in a variety of tectonic settings: (1) intracontinental rifts (e.g., Henderson, 1981); (2) island arcs (e.g., Condie, 1985, 1989); and (3) back arc basins (e.g., Tarney et al., 1976; Helmstaedt et al., 1986). Based on studies in the Western Australian Shield, Groves and Batt (1984) defined two end-member types of greenstone belts, inferred to have formed in intracontinental rift settings: (1) relatively shallow-water 'platform-phase' greenstones formed under conditions of low extension; and (2) deep water 'rift-phase' greenstones formed in a more active extensional environment. More recently, Thurston and Chivers (1990) have proposed four lithostratigraphic associations within greenstone belts of the Superior Province, Canada, each with a modern plate tectonic analogue: (1) quartz arenite and carbonate-bearing sequences (shallow-water platform sequences); (2) mafic and ultramafic volcanic sequences (marginal basins); (3) cyclical, bimodal mafic and felsic volcanic sequences (volcanic arcs); and (4) 'Timiskaming'-type sequences (pull-apart basins). Hence, it appears that Archean greenstone belts are no less diverse in their tectonic settings than younger terranes, and no single model can be expected to adequately explain the tectonic evolution of all granite-greenstone terranes.

3.6.1. Paleotectonic Setting of the Florence Lake Granite-Greenstone Terrane

Paleotectonic interpretations of the FLG are made difficult by a paucity of preserved primary volcanosedimentary textures and structures, and a complete lack of detailed stratigraphic and structural studies. In addition, no geochronological work has ever been carried out on the Florence Lake Group.

Tarney et al. (1976) used the Late Mesozoic Rocas Verdes ophiolites in southern Chile, which are preserved more or less in situ in an ensialic back arc basin setting, as a modern analogue for Archean greenstone belts. These ophiolites have no ultramafic base, and grade upwards from gabbros with multiple and sheeted dykes, into a sequence of pillowed tholeiitic flows. The mafic sequence is intruded by calc-alkaline batholiths which are considered to represent the roots of a nearby volcanic arc, which shed felsic to intermediate detritus into the basin.

The gross lithological characteristics of the Florence Lake Group are similarly consistent with (although not restricted to) deposition in a back arc basin, wherein relatively voluminous tholeiitic basalts are intercalated with lesser felsic volcanic and siliceous sedimentary rocks which were derived from an adjacent volcanic arc and/or continental margin (Figure 3.30). Very fine-grained siliceous sedimentary rocks with local syngenetic pyrite horizons, and ankeritic carbonate lenses are interpreted to represent chert and marble

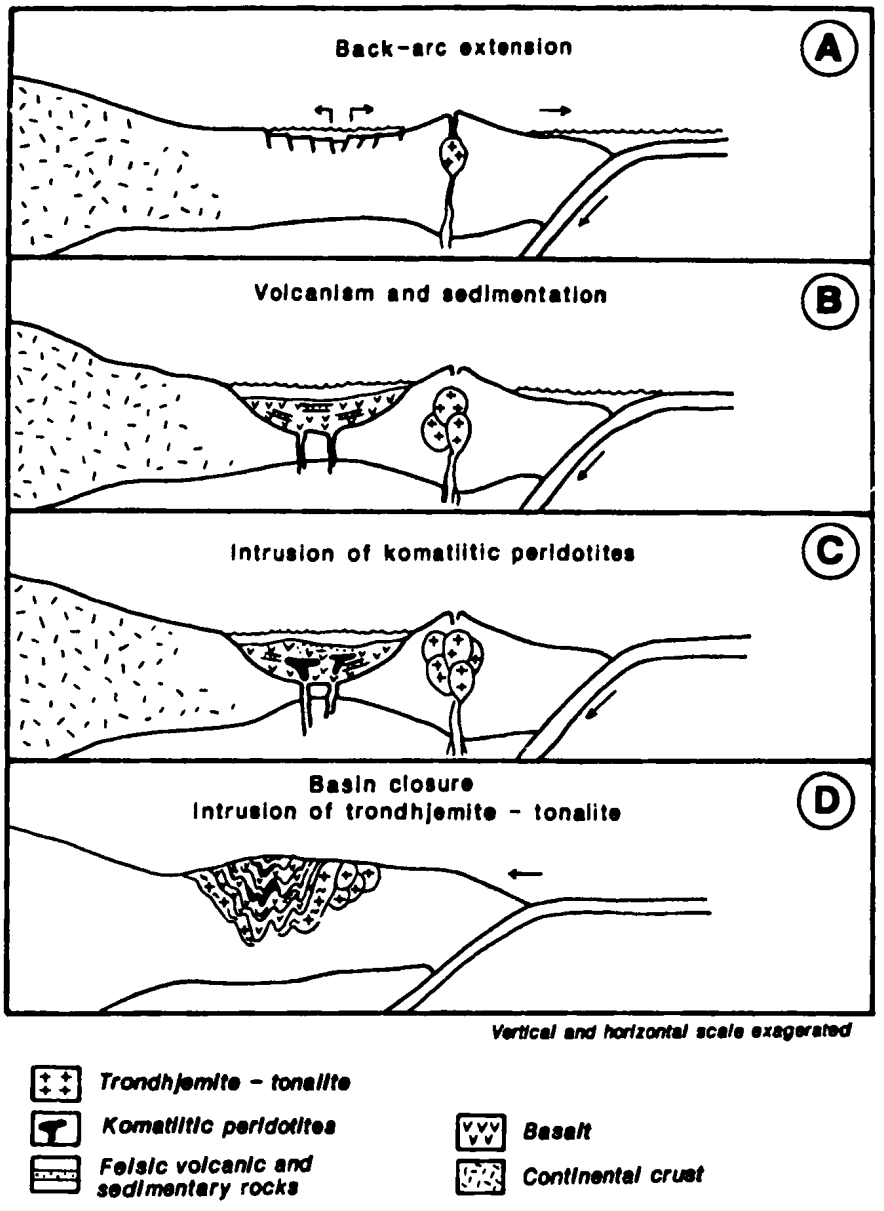

Figure 3.30. Schematic model for the development of the Florence Lake Group - Kanairiktok Intrusive Suite (modified after Tarney et al., 1976). A. Initial back-arc extension produces crustal thinning; B. Eruption of N-MORB basalts (Unit 1) with intercalations of felsic volcanogenic tuffs and cherty sediments (Unit 2); C. Intrusion of komatiitic peridotites (Unit 3) as dykes and/or sills (?); D. Movement of the arc towards the continent produces deformation of the greenstone sequence with intrusion of syn- to post-tectonic trondhjemite-tonalite (Unit 4).

respectively. The presence of these chemical sediments along with pillowed basalts demonstrates that the Florence Lake Group was at least in part deposited subaqueously. Unfortunately, volcanosedimentary features which might indicate water depths such as cross-bedding in clastic sedimentary rocks and hyalotuff, hyaloclastite and vesicles in volcanic rocks (i.e., shallow water) were not observed. Serpentinized peridotites intruded the volcanosedimentary sequence as sills and/or dykes, and the entire sequence was subsequently enveloped and intruded by trondhjemite and tonalite of the Kanairiktok Intrusive Suite.

Tectonic discrimination diagrams (Section 3.2.4) show that the FLG basalts have geochemical characteristics which are common to both MORB and IAB. However, based on La/Nb ratios, the FLG basalts are clearly dissimilar to IAB. Spider diagrams (Figures 3.15A-B) provide the most unequivocal evidence that the FLG basalts are 'MORB-like' and distinctly 'non-arc'. In Figure 3.31 the average primitive mantle-normalized spidergrams for Group 1 and 2 basalts are compared with typical patterns of N-MORB (after Hofmann, 1988), E-MORB and LKT (after Holm, 1985). Although the absolute element concentrations of FLG basalts are slightly lower than typical N-MORB (i.e., less fractionated) the overall shapes of the patterns are essentially identical. The FLG basalts are clearly enriched in Th relative to N-MORB, and they lack the pronounced Nb-depletion relative to La and Th displayed by basalts derived from arc magmatism (Figure 3.31).

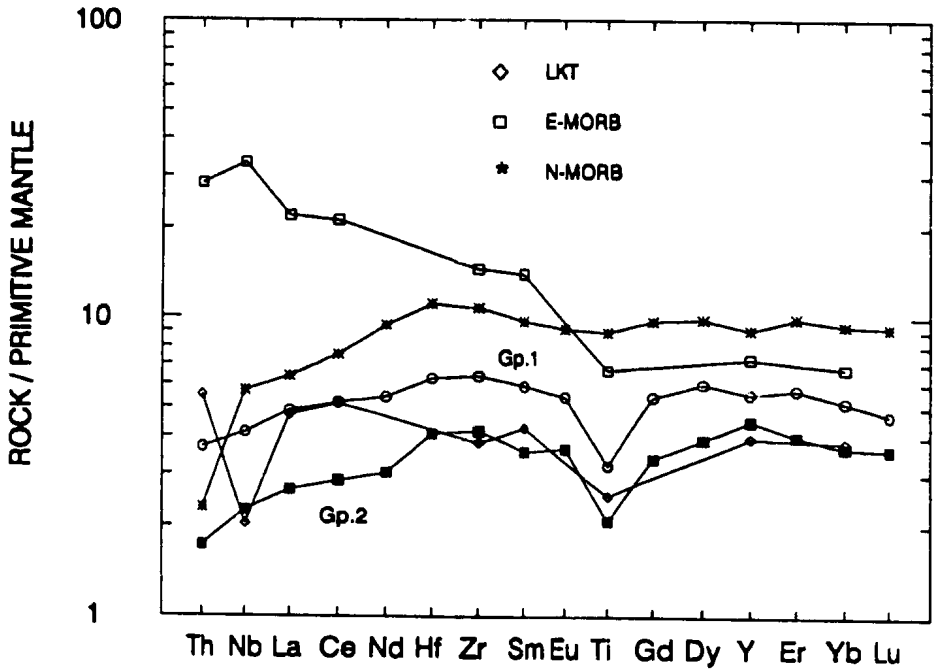

Figure 3.31. Primitive mantle-normalized spider diagrams for average FLG Group 1 and 2 basalts compared to N-MORB (after Hofmann, 1988), E-MORB and low-K tholeiites (after Holm, 1985). Primitive mantle normalizing values are from Hofmann (1988): Th (0.0813), Nb (0.6175), La (0.6139), Ce (1.6011), Nd (1.1892), Hf (0.2676), Zr (9.714), Sm (0.3865), Eu (0.1456), Ti (1810), Gd (0.5128), Dy (0.6378), Y (3.940), Er (0.4167), Yb (0.4144), Lu (0.0637).

In contrast to the basalts, the FLG felsic supracrustals and Kanairiktok trondhjemites display classic arc (or continental crust) signatures, with pronounced Nb-depletion relative to La and Th (Figures 3.16 and 3.29).

Hence, both lithological and geochemical characteristics are consistent with the Florence Lake Group having been deposited subaqueously in a back arc basin, which lay proximal to a volcanic arc and/or continental margin, shedding intermittent detritus into the basin.

3.6.2. Comparison of Florence Lake Group Basalts with Precambrian Greenstone Basalts

Several workers have noted geochemical changes across the Archean-Proterozoic boundary (2.5 Ga), and these are generally interpreted to reflect changes in mantle or crustal compositions (e.g., Condie, 1985; Taylor and McLennan, 1985).

Condie (1989) has reviewed the geochemical characteristics of Precambrian greenstones and the geochemical changes between the Archean-Proterozoic eons. In his review, Condie excluded volcanic rocks associated with arkose and conglomerate (i.e., rift associations) and quartzite, shale and carbonate (i.e., craton associations).

Condie (1989) divided Precambrian greenstones into those formed in four age groups: (1) Early Archean ($\geq$ 3500 Ma); (2) Late Archean (2500-3500 Ma); (3) Early Proterozoic (1500-2500 Ma); and (4) Late Proterozoic (500-1500 Ma). He noted a paucity of basalts with N-MORB chemical characteristics in

both Archean and Proterozoic greenstone belts, and the complete lack of basalts with within-plate (WPB, T-, and E-MORB) characteristics in all Precambrian basalts except in the early Proterozoic where they are very minor (Table 3.11). Condie cites three possible reasons why MORB-like basalts are so rare in Precambrian greenstone belts: (1) insufficient sampling of rocks with MORB compositions; (2) alteration or crustal contamination of MORB resulting in rocks with arc signatures; (3) selective preservation of arc sequences. According to Condie, most Precambrian greenstone belts, and the Archean sequences in particular, owe their preservation to underplating by tonalite-granodiorite intrusions, which are an expected product in arc systems. Condie (1989, p. 2, 16) notes "The greenstone assemblage is similar to modern arc-related assemblages deposited in various forearc, intra-arc, and back-arc basins" and "It is difficult to escape the conclusion that Archean greenstone basalts are dominantly tholeiites with IAB geochemical characteristics derived from relatively depleted mantle sources".

Chondrite-normalized REE patterns of average FLG Group 1 and 2 basalts are compared with those of average Archean and Proterozoic greenstone basalts (after Condie, 1989) in Figure 3.32. As noted previously, the FLG basalts have chondrite-normalized REE patterns which vary from flat (Group 1) to slightly LREE-depleted (Group 2). These patterns contrast with Condie's average Early and Late Archean basalts which are slightly LREE-enriched. Average Proterozoic greenstone basalts

Table 3.11

Classification of basalts from Precambrian greenstone successions (after Condie, 1989).

	≥ 3500 Ma		2500-3500 Ma		1500-2500 Ma		500-1500 Ma	
	n	(%)	n	(%)	n	(%)	n	(%)
IAB	15	29	104	67	49	18	9	20
CABI	21	40	26	17	120	44	25	54
CABC	13	25	15	10	96	35	10	22
N-MORB	3	6	10	6	5	2	2	4
T-MORB, E-MORB, WPB	--	--	--	--	3	1	--	--
Total	52*		155*		273		46	

IAB = island arc basalt
CABI = calc-alkaline basalt from island arcs
CABC = calc-alkaline basalt from continental-margin arcs
NMORB = normal mid-ocean ridge basalt
TMORB = transitional mid-ocean ridge basalt
EMORB = enriched mid-ocean ridge basalt
WPB = oceanic within-plate basalt

n = number of samples; % = percentage of total.

* Excluding 223 analyses from the Pilbara province in Western Australia (Glickson and Hickman, 1981; Glikson et al., 1986) for which critical trace-element data are not available.

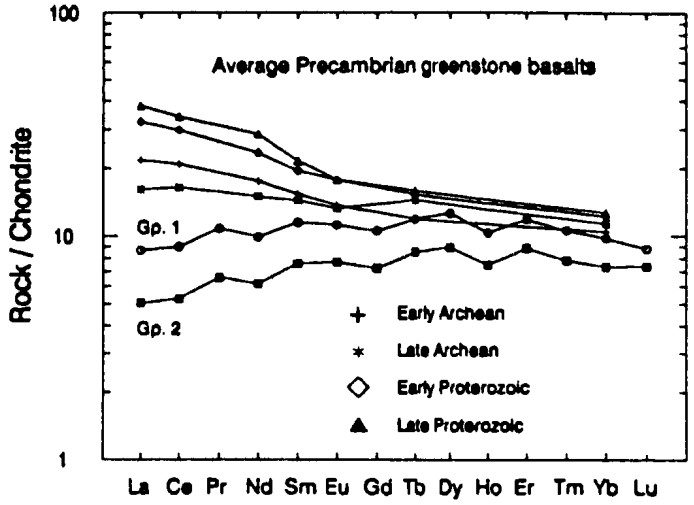

Figure 3.32. Chondrite-normalized REE diagram for average FLG Group 1 and 2 basalts compared to average Precambrian greenstone basalts (after Condie, 1989). Chondrite normalizing values as for Figure 3.9 (from Wakita et al., 1971).

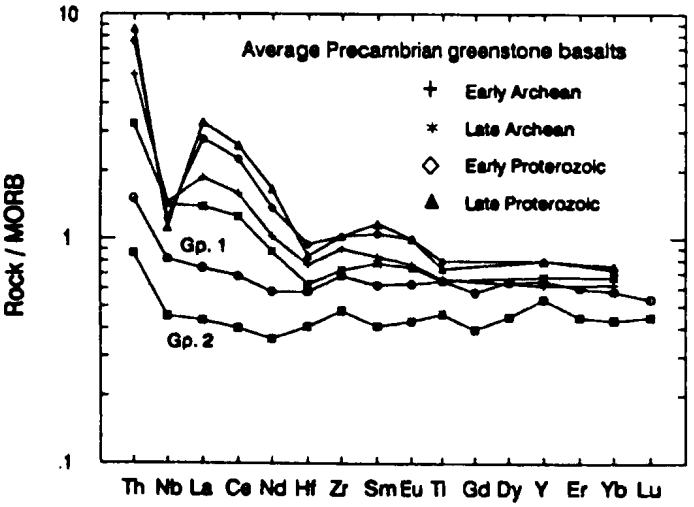

Figure 3.33. MORB-normalized spider diagram for average FLG Group 1 and 2 basalts compared to average Precambrian greenstone basalts (after Condie, 1989). MORB normalizing values as for Figure 3.15 (from NEWPET, 1990).

are more fractionated that those of the Archean.

MORB-normalized spider diagrams of average FLG basalts are compared with Archean and Proterozoic greenstone basalts (after Condie, 1989) in Figure 3.33. The average Proterozoic, and to a lesser extent the Early Archean basalts, show pronounced negative Nb anomalies relative to La and Th. In contrast, the average Late Archean basalts do not show a depletion in Nb, and the curves from Ce to Th are identical to those of the FLG basalts. Condie (1989) did note a slight negative Nb anomaly for the Late Archean basalts using the N-MORB normalizing values of Pearce (1983), and he suggested that since analytical errors generally result in higher concentrations of Nb (and Ta), the size of the Nb-Ta anomalies should be considered minimal. However, it appears that the relative Nb-depletions of average Late Archean basalts noted by Condie are an artifact of Pearce's (1983) N-MORB normalizing values, as the negative Nb anomalies disappear when they are normalized to primitive mantle (Hofmann, 1988) and other N-MORB values (e.g., Hofmann, 1988).

3.7. PROTEROZOIC DIABASE AND GABBRO DYKES

Widespread and voluminous mafic dyke swarms in many Precambrian cratons indicate considerable extension of the continental crust (Tarney and Weaver, 1987). Recently, Gower et al. (in press) have reviewed the geology, petrography and geochemistry of six middle Proterozoic (ca. 1300-1400 Ma) mafic suites in Labrador: (1) the Mealy dykes; (2) Michael

gabbro; (3) Shabogamo Intrusive Suite; (4) Seal Lake Group; (5) Harp dykes; and (6) Nain dykes (Figure 3.34). Gower et al. refer to the large area affected by this magmatism as the Middle Proterozoic Mafic Magmatic Belt (MPMMB). All suites reportedly contain the essential mineralogy olivine, clinopyroxene, and plagioclase, and chemically they are classified as tholeiitic, subalkaline transitional to alkaline basalts.

As noted previously, diabase dykes of at least two ages cut all other lithologies in the Florence Lake area. The large north-south to northeast-southwest-trending gabbro dykes appear to be older than the smaller east-west-trending diabase dykes. The dykes are informally referred to here as: (1) the Florence Lake gabbro (N-S to NE-SW) dykes; and (2) the Florence Lake diabase (E-W) dykes.

3.7.1. Clinopyroxene Chemistry

Microprobe analytical data for clinopyroxene in Florence Lake (FL) gabbro and diabase dykes are presented in Table 3.12.

Following the nomenclature of Yagi and Onuma (1967), augites containing 1-2% wt.% TiO_2 are termed titaniferous augites, whereas those containing greater than 2 wt.% are termed titanaugites. Table 3.12 shows that titanaugite is restricted to the fine-grained FL diabase dykes, whereas the medium- and coarse-grained FL gabbro dykes contain titaniferous augite.

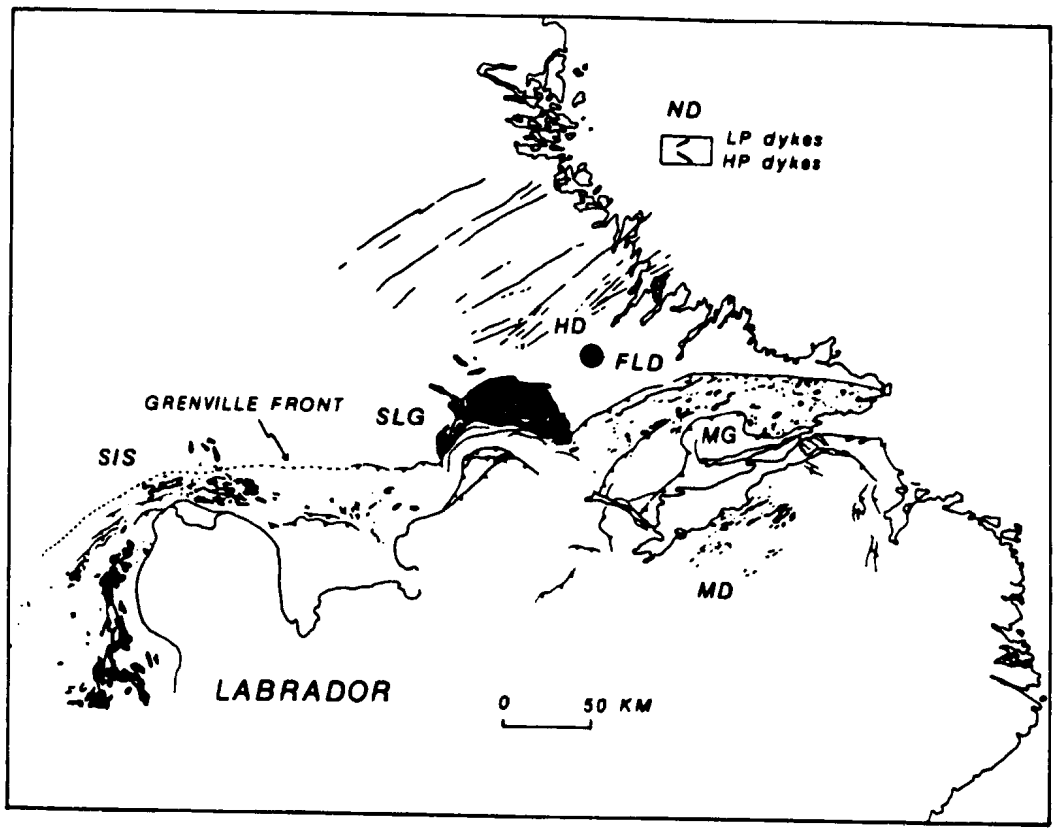

Figure 3.34. Location of the Florence Lake dykes (FLD) with respect to the ca. 1300-1400 Ma Middle Proterozoic mafic suites in Labrador (modified after Gower et al., in press). Abbreviations: SIS = Shabogamo Intrusive Suite; SLG = Seal Lake Group; MG = Michael Gabbro; MD = Mealy Dykes; HP = Harp Dykes; and ND = Nain Dykes.

Table 3.12. Microprobe analyses of clinopyroxene in Proterozoic diabase and gabbro dykes, Florence Lake area.

SAMPLE # (GRAIN SIZE)	ANAL	SIO2	TIO2	AL2O3	FEO	MNO	MGO	CAO	NA2O	K2O	CR2O3	NIO	TOTAL
87-015B	1	46.55	3.40	4.27	13.49	0.20	10.90	21.11	0.62	0.00	0.03	0.02	100.59
(F.G.)	2	46.72	3.59	4.14	13.51	0.26	10.29	20.26	0.56	0.00	0.03	0.07	99.43
	3	46.47	3.11	4.02	13.11	0.25	11.34	20.15	0.57	0.00	0.00	0.02	99.04
	4	47.28	2.92	4.38	13.36	0.29	11.11	19.99	0.56	0.01	0.03	0.01	99.94
	AVG	46.76	3.26	4.20	13.37	0.25	10.91	20.38	0.58	0.00	0.02	0.03	99.75
87-031B	1	49.09	2.26	3.30	12.63	0.37	12.23	19.75	0.46	0.00	0.05	0.00	100.14
(F.G.)	2	49.14	2.08	3.28	13.38	0.27	12.35	19.28	0.50	0.01	0.01	0.00	100.30
	3	48.05	2.83	4.12	12.68	0.25	11.91	19.50	0.53	0.01	0.02	0.04	99.94
	4	47.75	2.79	3.95	12.23	0.25	11.78	20.64	0.40	0.01	0.02	0.04	99.86
	AVG	48.51	2.49	3.66	12.73	0.29	12.07	19.79	0.47	0.01	0.03	0.02	100.06
87-056	1	47.14	3.30	4.32	12.80	0.23	10.84	20.14	0.50	0.00	0.00	0.02	99.29
(F.G.)	2	46.40	3.03	4.56	12.95	0.14	11.11	20.46	0.48	0.01	0.01	0.05	99.20
	3	47.76	3.00	4.13	12.99	0.25	11.29	19.51	0.51	0.00	0.01	0.00	99.45
	4	47.49	2.66	3.92	13.74	0.19	11.13	19.89	0.39	0.00	0.02	0.05	99.48
	AVG	47.20	3.00	4.23	13.12	0.20	11.09	20.00	0.47	0.00	0.01	0.03	99.36
87-101	1	51.63	0.81	2.40	12.77	0.44	11.98	20.28	0.33	0.00	0.00	0.02	100.66
(M.G.-C.G.)	2	51.35	0.77	2.29	12.01	0.39	11.86	20.71	0.29	0.00	0.00	0.05	99.72
	3	51.38	1.01	2.16	12.36	0.23	13.80	19.19	0.32	0.02	0.02	0.03	100.52
	4	50.71	1.25	2.79	12.05	0.24	13.33	19.36	0.40	0.00	0.02	0.08	100.23
	AVG	51.27	0.96	2.41	12.30	0.33	12.74	19.89	0.34	0.01	0.01	0.05	100.28
TB-87-110	1	48.58	1.41	3.93	11.79	0.14	12.90	19.75	0.44	0.00	0.19	0.01	99.14
(M.G.-C.G.)	2	48.60	1.38	4.38	12.05	0.15	12.96	20.15	0.48	0.00	0.27	0.00	100.42
	3	49.62	1.38	4.09	11.89	0.21	13.32	19.47	0.47	0.00	0.21	0.00	100.66
	4	49.46	1.31	3.70	12.37	0.18	12.53	19.45	0.44	0.01	0.11	0.01	99.57
	AVG	49.07	1.37	4.03	12.03	0.17	12.93	19.71	0.46	0.00	0.20	0.01	99.95
TB-87-112	1	50.28	1.38	3.23	11.55	0.29	12.82	19.07	0.49	0.02	0.04	0.05	99.22
(M.G.-C.G.)	2	51.54	1.11	2.14	11.70	0.30	13.55	19.26	0.29	0.00	0.01	0.05	99.95
	3	50.25	1.28	3.63	11.57	0.29	13.83	18.71	0.42	0.00	0.27	0.04	100.29
	4	51.40	0.97	1.88	12.50	0.32	13.75	17.98	0.35	0.00	0.01	0.04	99.20
	AVG	50.87	1.19	2.72	11.83	0.30	13.49	18.76	0.39	0.01	0.08	0.05	99.67
TB-87-246	1	51.19	0.95	1.82	10.93	0.28	14.13	19.23	0.34	0.00	0.01	0.01	98.89
(M.G.)	2	51.53	1.08	1.45	11.75	0.30	14.49	19.84	0.39	0.00	0.04	0.00	100.87
	3	51.59	1.01	1.80	11.84	0.27	14.61	19.35	0.44	0.02	0.02	0.00	100.95
	4	50.16	1.19	2.20	11.67	0.27	14.00	19.64	0.29	0.00	0.02	0.00	99.44
	AVG	51.12	1.06	1.82	11.55	0.28	14.31	19.52	0.37	0.01	0.02	0.00	100.04

In Figure 3.35, Al and Ti in augites of FL dykes are compared with those of the Harp (Meyers and Emslie, 1977), Mealy (Emslie et al., 1984) and Nain (Wiebe, 1985) dykes. Clearly, the augites in FL diabase dykes are most similar to those contained within the Nain HP (high P_2O_5) dykes of Wiebe (1985), and are the most Ti- and Al-rich of any of the dyke suites. Augites from FL gabbro dykes show a very large range in Al contents, and have Ti concentrations generally comparable to the other MPMMB suites.

3.7.2. Whole-Rock Geochemistry

Five FL diabase dykes and one gabbro dyke were analyzed for major and trace elements, and three of these were also analyzed for REE (Table 3.13).

3.7.2.1. Major and Trace Elements

Major and trace elements for the FL dykes are plotted on a series of Harker variation diagrams in Figures 3.36 and 3.37 using Mg# as a fractionation index. The average compositions of the six MPMMB suites (from Gower et al., in press) noted above are also plotted for comparison. It is apparent that although the FL dykes have many similarities with the other suites, there are also notable differences which clearly demonstrate that the FL diabase dykes are more evolved than the other suites, and are most similar to the Nain HP dykes (Wiebe, 1985). With respect to major elements, the FL diabase dykes have relatively lower SiO_2, MgO, and Al_2O_3, higher TiO_2,

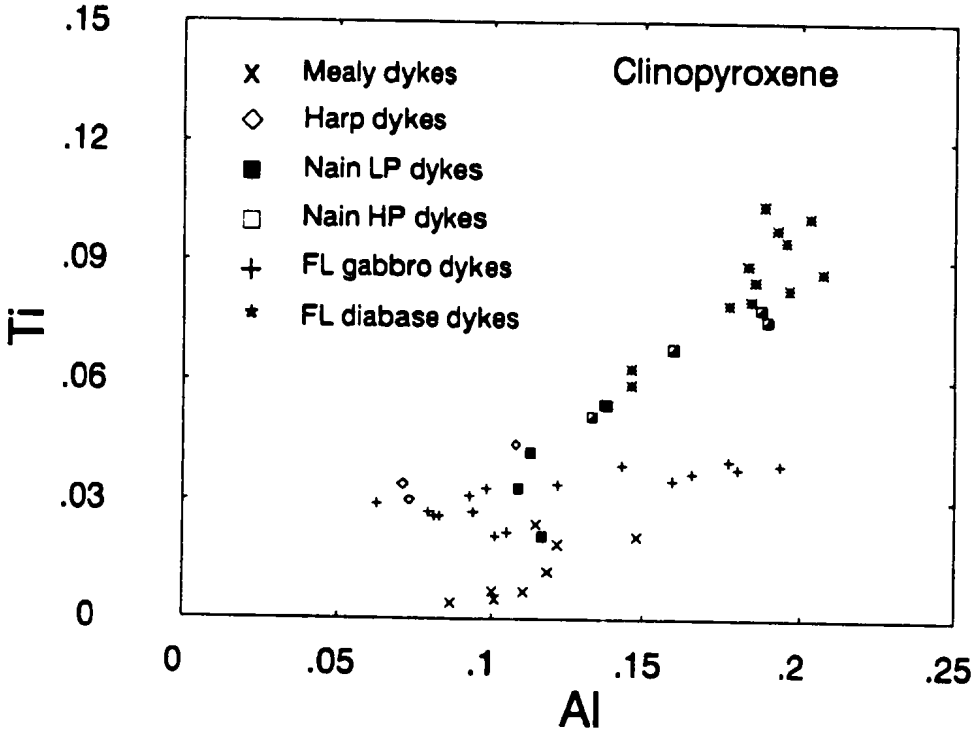

Figure 3.35. Number of atoms of Ti and Al on the basis of six oxygens in clinopyroxene in the Florence Lake (this study), Nain (Wiebe, 1985), Mealy (Emslie et al., 1984) and Harp (Myers and Emslie, 1977) dykes.

Table 3.13. Chemical analyses of Proterozoic diabase and gabbro dykes, Florence Lake area.

	TB-87-047B	87-056	87-087B	87-101	87-229A	87-229B
SiO2 (wt. %)	41.70	45.20	44.90	45.50	42.10	42.10
TiO2	4.40	3.64	3.72	1.00	3.96	3.80
Al2O3	13.10	12.00	12.50	19.40	12.60	12.10
Fe2O3*	20.56	19.07	19.17	10.21	19.31	19.26
MnO	0.24	0.23	0.25	0.15	0.20	0.61
MgO	4.97	5.07	5.04	5.73	5.19	6.47
CaO	7.60	8.36	9.46	11.18	7.74	7.82
Na2O	2.17	2.11	2.65	2.42	3.07	2.14
K2O	0.96	0.77	0.36	0.60	1.12	1.89
P2O5	1.18	1.21	1.26	0.10	1.46	1.46
LOI	2.23	2.42	1.43	2.25	1.73	0.91
Total	99.11	100.08	100.74	98.54	98.48	98.56
Cr (ppm)	nd	nd	nd	84	nd	27
Ni	16	7	8	75	11	28
Sc	39.56	---	---	29.01	---	37.84
V	308	306	326	143	240	267
Cu	nd	nd	nd	32	nd	122
Zn	179	140	115	52	98	126
Rb	22.58	21	5	17.27	24	51.73
Ba	514	462	381	115	641	738
Sr	198.40	204	226	279.25	304	250.48
Ga	21	20	22	20	25	22
Nb	19.86	18	18	4.59	19	18.43
Zr	380	345	337	60	366	362
Y	63.99	71	67	17.18	69	64.56
Ta	1.40	---	---	0.66	---	1.43
Hf	9.51	---	---	1.75	---	8.86
Pb	4.21	---	---	1.81	---	4.00
Th	2.04	---	---	0.41	---	1.70
U	0.69	---	---	0.12	---	0.56
La (ppm)	44.33	---	---	4.74	---	41.63
Ce	102.69	---	---	11.81	---	98.65
Pr	13.94	---	---	1.67	---	13.11
Nd	56.48	---	---	7.68	---	54.61
Sm	13.39	---	---	2.31	---	12.88
Eu	3.69	---	---	0.89	---	3.24
Gd	12.57	---	---	2.58	---	12.59
Tb	2.10	---	---	0.48	---	2.00
Dy	12.85	---	---	3.06	---	11.91
Ho	2.59	---	---	0.68	---	2.43
Er	7.43	---	---	2.03	---	7.07
Tm	1.01	---	---	0.29	---	1.00
Yb	6.14	---	---	1.80	---	6.24
Lu	0.95	---	---	0.30	---	0.97

Note: nd = not detected.

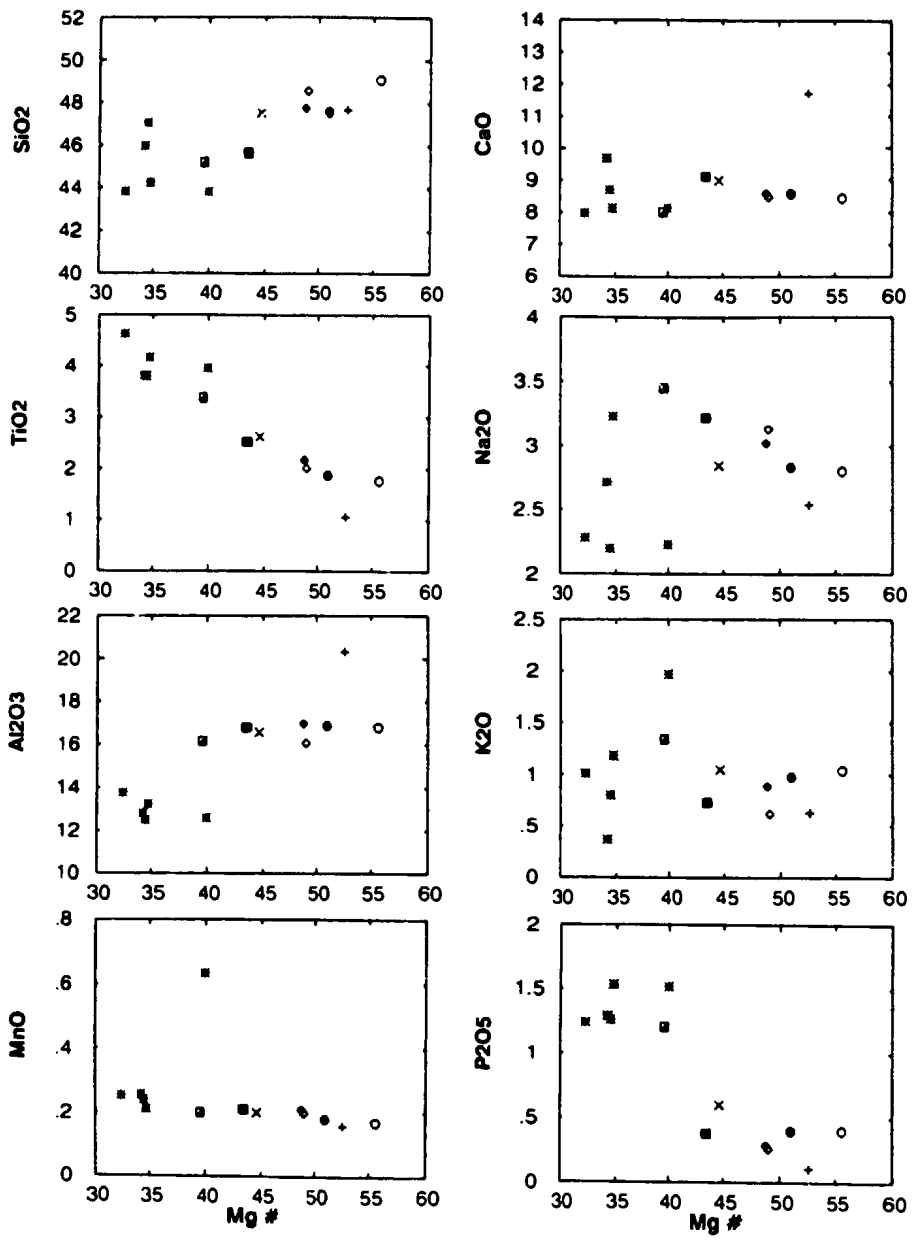

Figure 3.36. Major elements versus Mg# for Florence Lake dykes and the averages of the Middle Proterozoic mafic suites in Labrador (after Gower et al., in press). Symbols: asterisks = FL diabase dykes; cross = FL gabbro dyke; half-filled square = Nain HP dykes; solid square = Nain LP dykes; open diamond = Harp dykes; solid diamond = Seal Lake group; X = Mealy dykes; open circle = Shabogamo Intrusive Suite; solid circle = Michael gabbro.

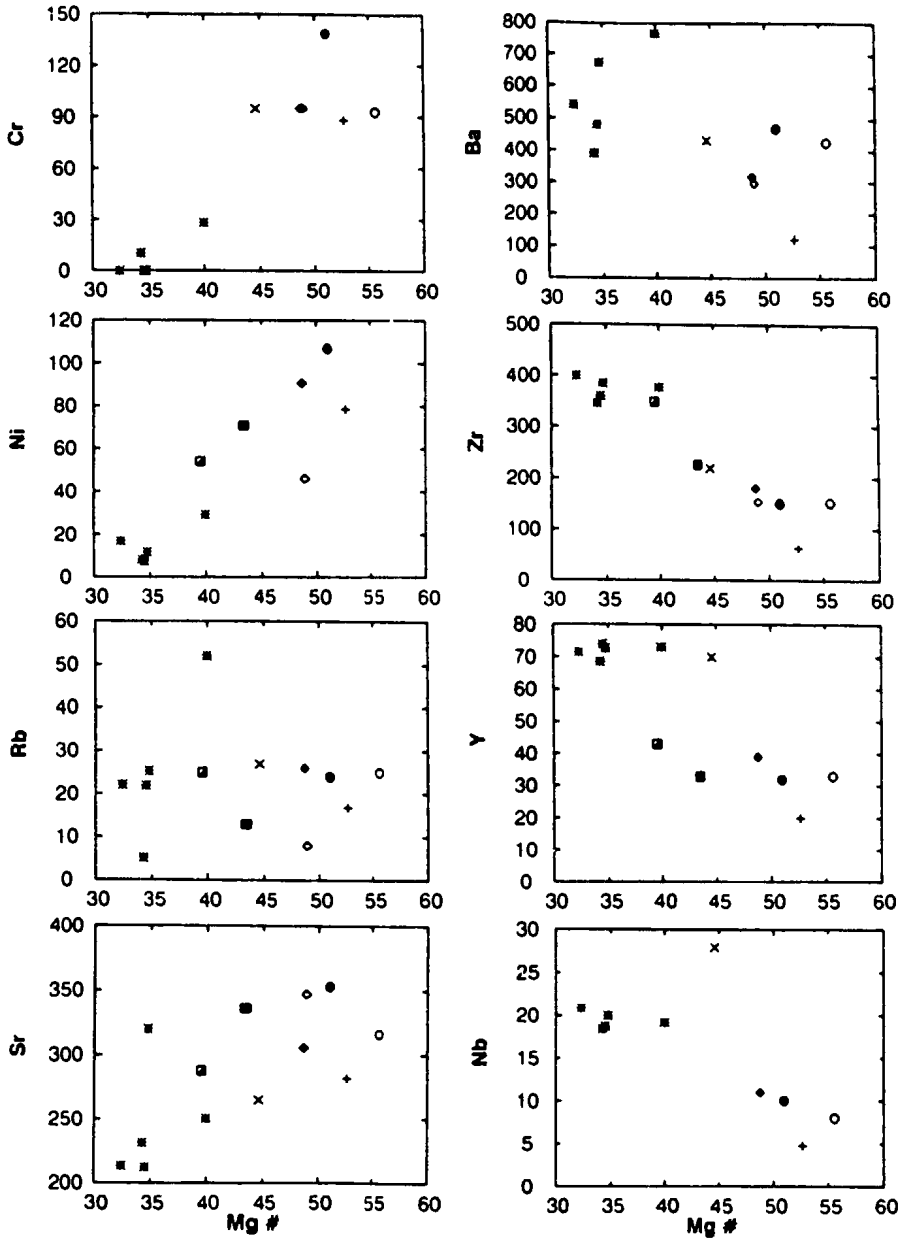

Figure 3.37. Trace elements versus Mg# for the Florence Lake dykes and the averages of the Middle Proterozoic mafic suites in Labrador (after Gower et al., in press). Symbols as for Figure 3.36.

Fe_2O_3* and P_2O_5, and comparable CaO, MnO, Na_2O and K_2O (Figure 3.36). These differences are also reflected in trace elements, with the FL diabase dykes having relatively higher concentrations of Zr, Y, Nb (HFSE) and lower Cr, Ni, and Sr (Figure 3.37). The single FL gabbro dyke (87-101) is similar to the other mafic suites, but is clearly more fractionated.

On the total alkalies versus SiO_2 diagram, the FL dykes appear to be transitional from subalkaline to alkaline (Figure 3.38). On the AFM diagram (Figures 3.39) the FL dykes plot in the tholeiitic field.

3.7.2.2. Rare Earth Elements

Chondrite-normalized REE patterns for the FL dykes and the average patterns for each of the Proterozoic mafic suites (after Gower et al., in press) are displayed in Figures 3.40A-B respectively. The FL diabase dykes have fractionated (La_n/Lu_n=4.3-4.7) REE patterns essentially identical to the Nain HP dykes, and both are significantly more LREE-enriched than all other suites. Sample 87-229B displays a slight negative Eu anomaly, indicating plagioclase fractionation. The FL gabbro dyke has the lowest REE concentrations and has a relatively flat (La_n/Lu_n=1.6) pattern compared to the FL diabase dykes and the other MPMMB suites.

3.7.2.3. Tectonic Discrimination Diagrams

Nisbet and Pearce (1977) developed a tectonic discrimination diagram for basalts based on clinopyroxene

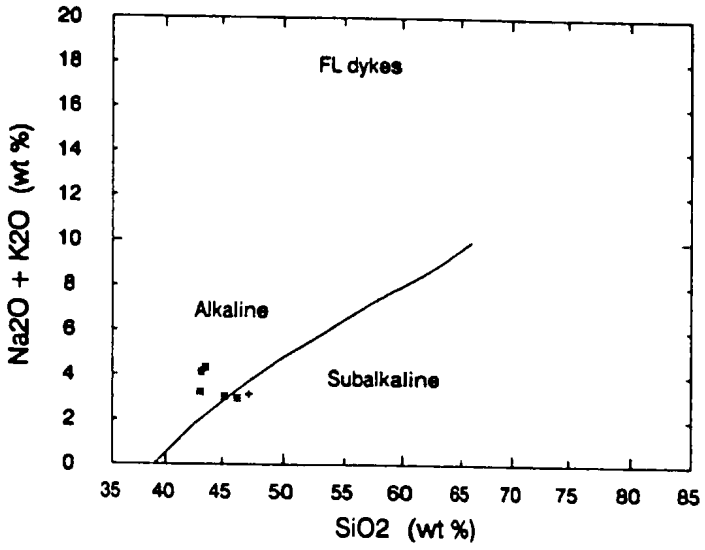

Figure 3.38. Total alkalis versus SiO_2 diagram for the Florence Lake dykes. Dividing line between alkaline and subalkaline fields (after Irvine and Baragar, 1971). Symbols as for Figure 3.36.

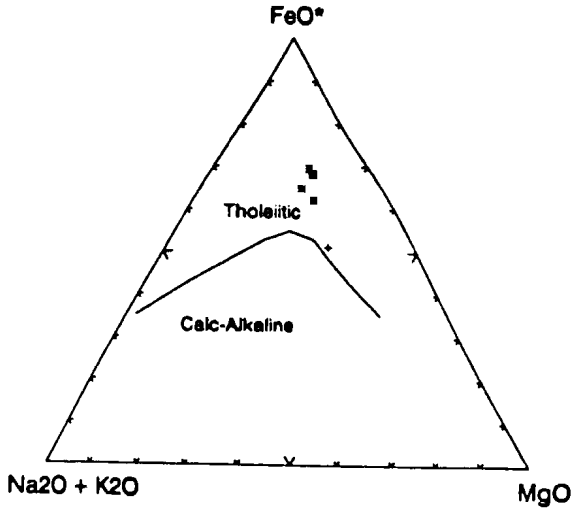

Figure 3.39. AFM diagram for the Florence Lake dykes. Dividing line between tholeiitic and calc-alkaline fields (after Irvine and Baragar, 1971). Symbols as for Figure 3.36.

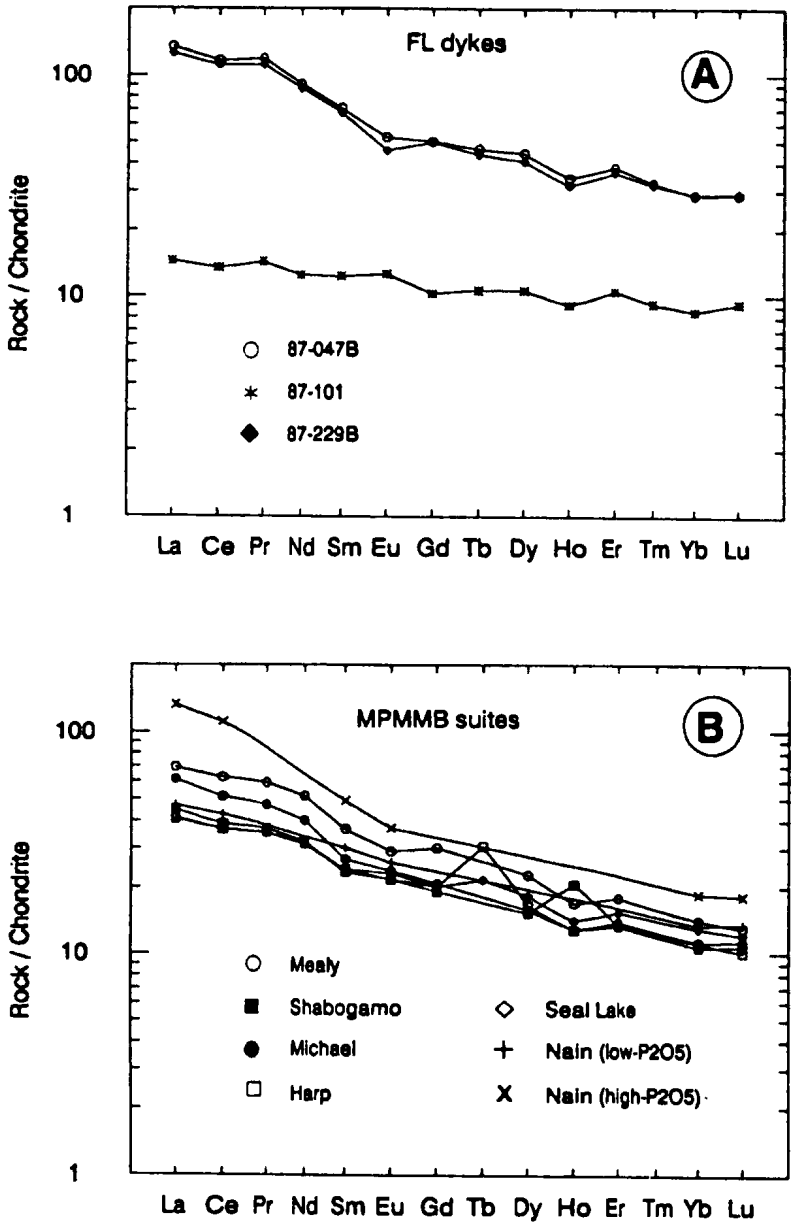

Figure 3.40. Chondrite-normalized REE diagrams for (A) Florence Lake dykes, and (B) averages of the Middle Proterozoic mafic suites in Labrador (after Gower et al., in press). Chondrite normalizing values as for Figure 3.9 (from Wakita et al., 1971).

compositions (Figure 3.41). On the $MnO-TiO_2-Na_2O$ diagram, the FL diabase dykes plot in the within-plate alkali basalt field, whereas the FL gabbro dykes plot in the field of overlap between all tectonic settings.

On the $K_2O-TiO_2-P_2O_5$ discrimination diagram (Pearce et al., 1975) all the FL dykes plot in the continental basalt field (Figure 3.42). On the Zr-Nb-Y discrimination diagram (Meschede, 1986) the FL diabase dykes plot in the field of overlap between within-plate tholeiites and volcanic arc basalts whereas the FL gabbro dyke plots in the field of overlap between N-MORB and volcanic arc basalts (Figure 3.43).

Compared with 'typical' continental tholeiites, the FL diabase dykes generally have low Mg#'s, much higher P_2O_5 (> 1% wt.%) (Figure 3.44A) and generally higher TiO_2 contents (Figure 3.44B). In contrast, the FL gabbro dyke has slightly lower P_2O_5 and TiO_2 contents compared to typical continental tholeiites.

3.7.2.4. Spider Diagrams

Primitive mantle-normalized spider diagrams for the FL dykes and the averages of the MPMMB suites (after Gower et al., in press) are presented in Figures 3.45A-B respectively. The FL diabase dykes have very pronounced negative Sr and Nb anomalies, whereas the FL gabbro dyke has a positive Sr anomaly and a very slight negative Nb anomaly (Figure 3.45A). Compared to the MPMMB suites (Figure 3.45B), the FL diabase dykes are very similar to the Nain HP dykes which have

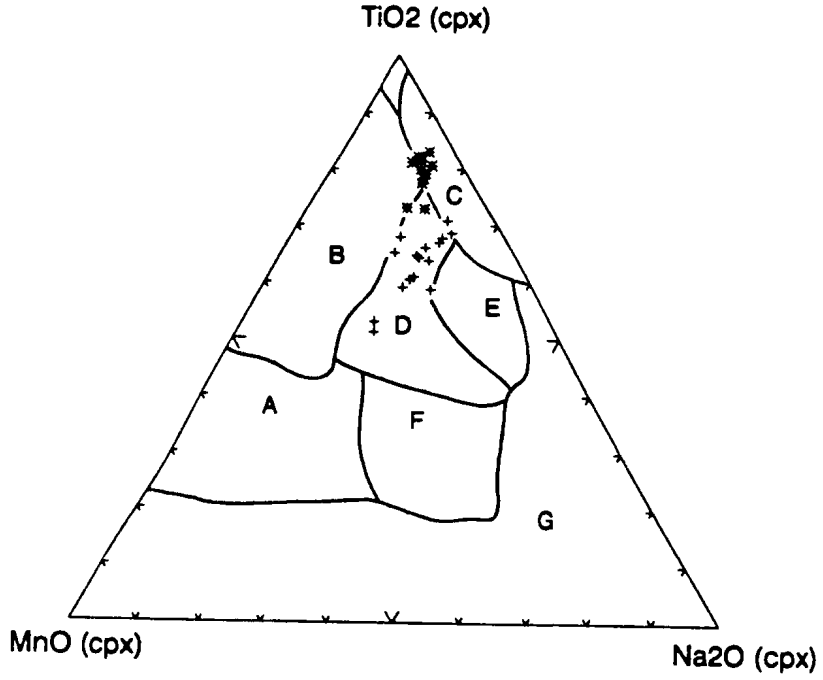

Figure 3.41. MnO-TiO_2-Na_2O in clinopyroxenes as a petrotectonic indicator (after Nisbet and Pearce, 1977). Fields: A: volcanic arc basalts (VAB); B = ocean-floor basalts (OFB); C = within-plate alkali basalts (WPA); D = all settings; E = within-plate tholeiites (WPT) + WPA + VAB; F = VAB + WPA; and G = WPA. Symbols as for Figure 3.36.

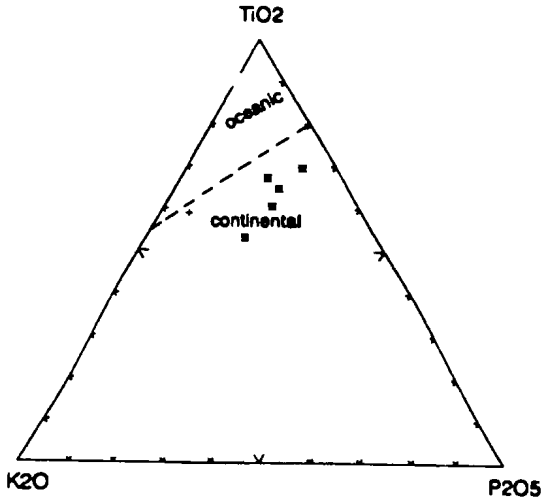

Figure 3.42. K_2O-TiO_2-P_2O_5 tectonic discrimination diagram (after Pearce et al., 1975) for Florence Lake dykes. Symbols as for Figure 3.36.

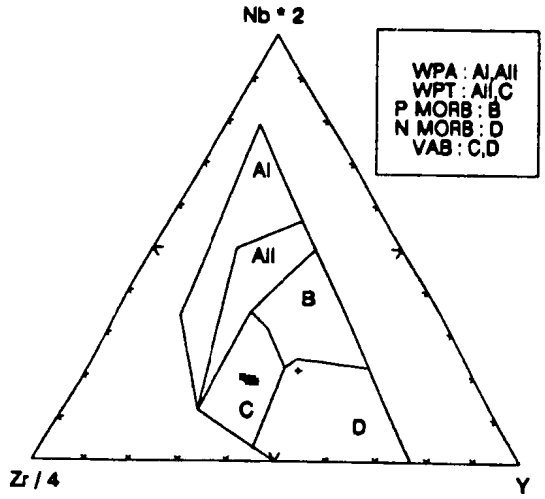

Figure 3.43. Zr/4-Nb*2-Y tectonic discrimination diagram (after Meschede, 1986) for the Florence Lake dykes. Symbols as for Figure 3.36.

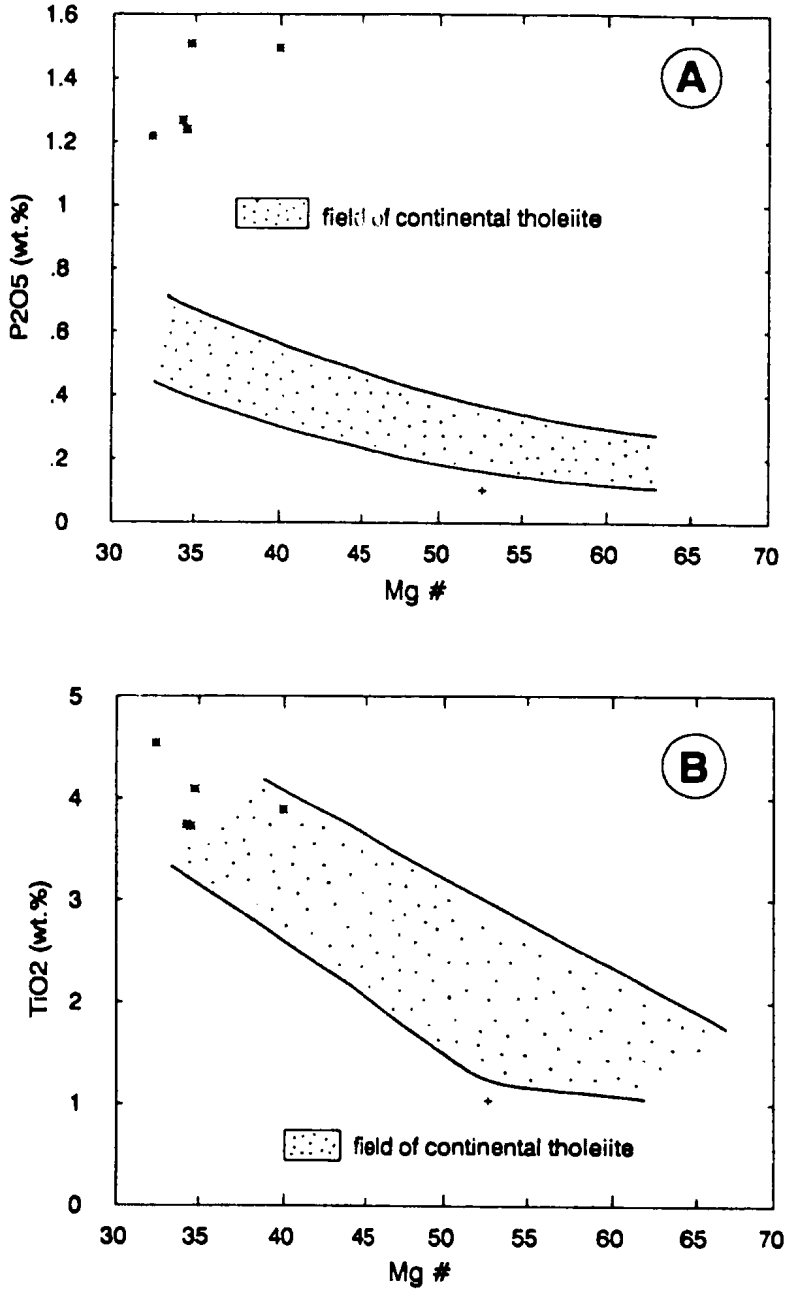

Figure 3.44. Comparison of the Florence Lake dykes to "typical" continental tholeiites (after Dupuy and Dostal, 1984). (A) P_2O_5 versus Mg#; and (B) TiO_2 versus Mg#. Symbols as for Figure 3.36.

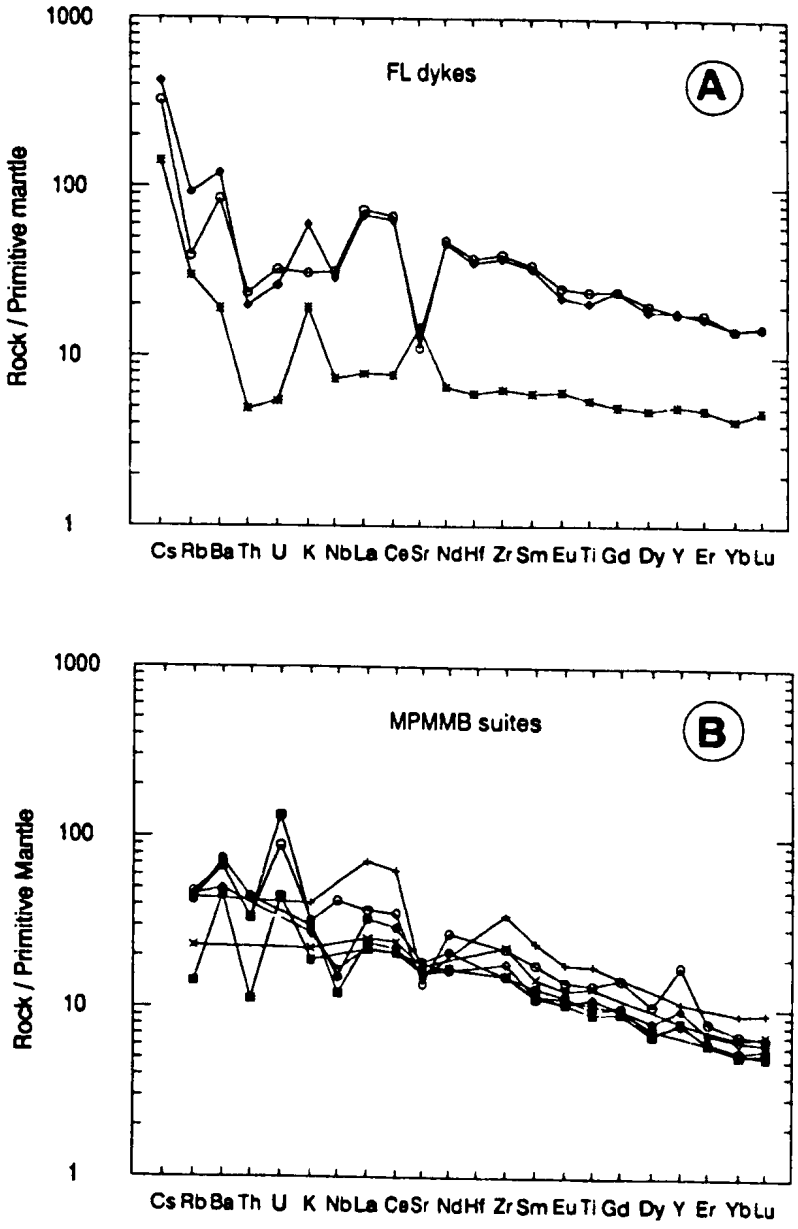

Figure 3.45. Primitive mantle-normalized spider diagrams for (A) Florence Lake dykes, and (B) averages of the Middle Proterozoic mafic suites in Labrador (after Gower et al., in press). Primitive mantle normalizing values are from NEWPET (1990): Cs (0.007); Rb (0.555); Ba (6.27); Th (0.088); U (.022); K (267); Nb (0.65); La (0.63); Ce (1.59); Sr (18.9); Nd (1.21); Hf (0.28); Zr (9.8); Sm (0.399); Eu (0.15); Ti (1134); Gd (0.533); Dy (0.661); Y (3.9); Er (0.432); Yb (0.442); and Lu (0.066). Symbols as for Figure 3.40.

identical Nb and La concentrations, and also have the same pronounced negative Sr anomaly which characterizes the FL diabase dykes. Although there are no pronounced Eu anomalies in the FL diabase dykes, a slight negative Eu anomaly in sample 87-229B indicates plagioclase fractionation. It might be argued that the Sr-depletion is due to alteration, however, the degree of Sr-depletion in the two FL diabase dykes and the Nain HP dykes is essentially identical, and it seems rather unlikely that this could be duplicated by alteration. Dupuy and Dostal (1984) have noted that the fractionation trend of continental tholeiites (CT) is characterized by an increase in Cr and Ni and a decrease in LFSE with increasing Mg#; however, Sr remains relatively constant. This trend is apparent in Figures 3.45A-B, wherein the FL diabase and Nain HP dykes contain comparable Sr concentrations to the other less evolved mafic dyke suites.

Proterozoic dyke swarms are similar to Phanerozoic continental flood basalts (CFB) in that they erupt large volumes of predominantly Fe-rich quartz tholeiites (Tarney and Weaver, 1987). In Figure 3.46A-C, spidergrams for the FL diabase dykes are compared to 'typical' continental basic rocks (after Thompson et al., 1983, 1984). Continental alkalic basic rocks (Figure 3.46A) and those CFB which resemble ocean island basalts (OIB) (Figure 3.46B) are characterized by positive Nb anomalies relative to La. In contrast, CFB which are characterized by Nb-depletion relative to La (Figure 3.46C) are considered to represent crustally contaminated (Nb-

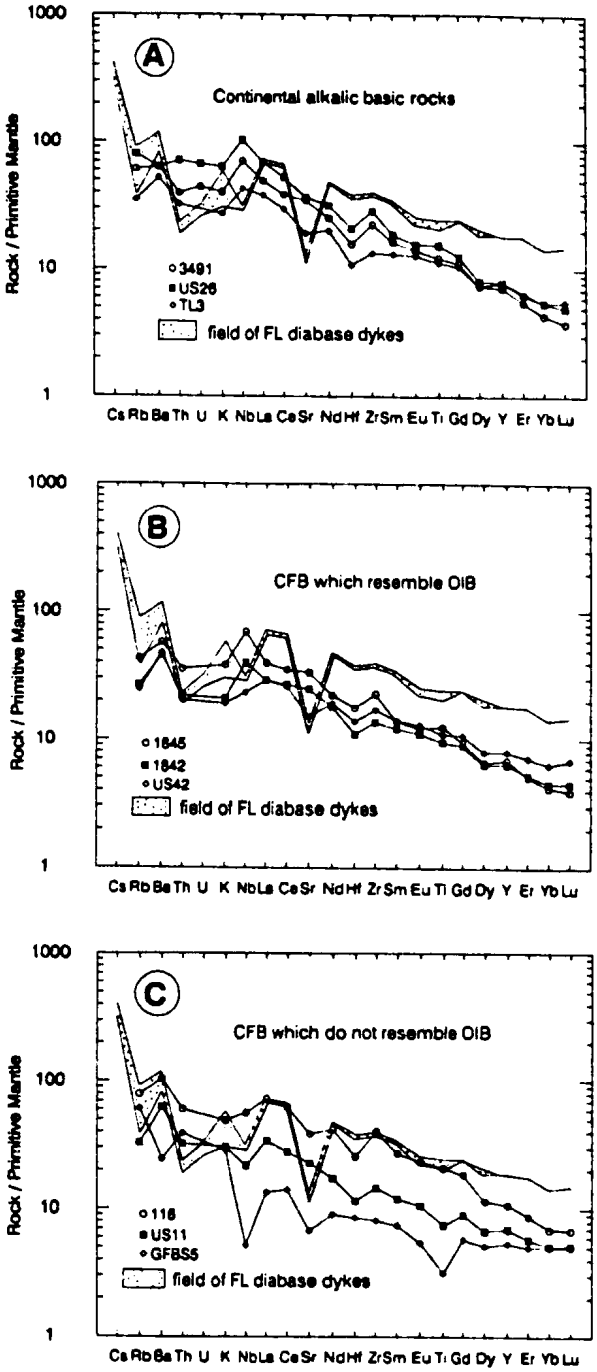

Figure 3.46. Primitive mantle-normalized spider diagrams comparing Florence Lake dykes with (A) continental alkalic basic rocks, (B) continental flood basalts (CFB) which resemble ocean island basalts (OIB), and (C) CFB which do not resemble OIB (after Thompson et al., 1983, 1984). Primitive mantle normalizing values as for Figure 3.45.

depletion, high LFSE) equivalents of OIB (Thompson et al., 1983, 1984). The FL diabase dykes are most similar to these Nb-depleted, LFSE-enriched CFB (Figure 3.46C).

3.7.2.5. Discussion

The east-west-trending FL diabase dykes are both mineralogically and chemically distinct from the Harp dykes with which they have been informally compared (e.g., Ermanovics and Raudsepp, 1979a; Ryan, 1984). Olivine has not been identified in any of the FL dykes, and augites from FL diabase dykes contain significantly higher TiO_2 contents compared with those of the Harp dykes (see Figure 3.35). The whole rock chemistry of FL diabase dykes also distinguishes these from the Harp dykes and the other MPMMB suites within Labrador. Geochemically, the FL diabase dykes are very similar to the Nain HP dykes (Wiebe, 1985).

Wiebe (1985) noted the compositional differences between the Nain HP and LP dykes, but he did not discuss its significance. Gower et al. (in press) note that the Nain LP dykes could have been derived by fractionation of magmas which generated the Seal Lake Group and Harp dykes, but suggested that because of their contrasting trend and compositions, the Nain HP dykes "record a mafic event distinct from that represented by the other suites." The relative ages of the Nain HP and LP dykes is not known because no cross-cutting relationships have been observed (Wiebe, 1985).

Spatially the FL dykes are located nearest to the Harp

dykes (Figure 3.34). According to Meyers and Emslie (1977), the main Harp dyke swarm trends northeast; however, smaller dykes conjugate to the main swarm are present locally. The Nain LP dykes strike between east-west and northeast-southwest which is similar to the Harp dykes. The Nain HP dykes display an arcuate trend from northwest-southeast in the south to northeast-southwest in the north (Wiebe, 1985). Wiebe has suggested that these Nain HP dykes may be similar to the small conjugate Harp dykes described by Meyers and Emslie (1977). The similarity in composition between the FL diabase dykes and the Nain HP dykes may have important implications concerning the evolution of other Middle Proterozoic mafic dyke swarms in Labrador. The relationship appears to be one where a relatively small and apparently younger (?) set of more evolved diabase dykes are conjugate to the main dyke swarm. More detailed geological mapping, geochemical sampling and chronological work would help to substantiate or refute this suggestion.

CHAPTER 4. MINERALIZATION

4.1. INTRODUCTION

Granite-greenstone terranes form an integral part of many Archean cratons around the world. The greenstone belts host a wide variety of mineral deposits: (1) banded iron formations (BIF); (2) volcanogenic massive sulphide (VMS) Fe-Cu-Zn deposits; (3) mafic to ultramafic Fe-Ni-Cu (+ minor platinum-group elements) sulphide deposits; and (4) epigenetic lode Au deposits.

Airborne geophysical surveys by BRINEX (Wilson, 1959) and BP Minerals Ltd. (Jagodits, 1983) have formed the basis for sporadic mineral exploration throughout the Florence Lake Group over the past thirty years. Mineral occurrences within the Florence Lake area can generally be discussed in terms of (1) asbestos and (2) base-metals. Base-metals can be divided into Fe-Cu-Zn sulphides associated with volcanosedimentary rocks and Fe-Ni-Cu sulphides associated with ultramafic rocks.

Analytical results for precious metals (platinum-group elements and gold) associated with base-metal occurrences are discussed separately.

4.2. ASBESTOS

The meta-ultramafic rocks south of Florence Lake host several small asbestos occurrences. A ground magnetometer survey over the ultramafic rocks in 1959 (Roderick, 1959b) showed that the highest readings were over the Robin Lake

asbestos showing (Piloski, 1960), which had been discovered the previous year. Piloski (1960) described the asbestos as slip-fibre associated with abundant magnetite in seams of apparently random orientation. Trenching across the showing revealed the presence of a number of very thin (up to 0.3 cm) fractures with good cross fibres (Plate 4.1). The economic potential of the asbestos showings is limited by their small size and overall poor fibre quality.

4.3. BASE-METALS

4.3.1. Fe-Cu-Zn Sulphides

Thin (≤ 1 m thick) conformable pyritic horizons are locally abundant within the volcanosedimentary rocks (Piloski, 1963; Stewart, 1983); however, these are invariably either barren or contain low base-metal contents (Stewart, 1983).

Approximately 1.25 km southeast of Florence Lake, gossanous pyrite horizons occur within fine-grained siliceous metasedimentary rocks (see Plate 2.15) near the carbonatized meta-ultramafic contact. Petrographic examination of two samples shows that the host rocks are fine-grained quartz-sericite schists, and pyrite is the only sulphide present. In one sample, pyrite forms anhedral to euhedral grains, which along with quartz, are concentrated as thin (1-2 mm) bands. The quartz in these bands is coarser grained than the fine-grained quartz throughout the remainder of the schist, and it is highly strained with sutured grain boundaries. In the other

Plate 4.1. Asbestos fibres in a dark blue serpentinized peridotite located approximately 4 km south of Florence Lake (see map - back pocket).

sample, pyrite is far more abundant (50 vol.%) and is pervasive, with no apparent association with coarser grained quartz.

Stewart (1983) considered the pyritic horizons to be metamorphosed chert-pyrite chemical sediment or exhalite. This seems to be a reasonable interpretation considering the very fine grain size and siliceous nature of the rocks; however, one of the samples examined in this study contains a single quartz grain approximately 2 mm in diameter, indicating that the rocks are at least in part detrital.

Two small showings south of Florence Lake contain minor base-metal sulphides in addition to pyrite (see map - back pocket). An Fe-Cu-Zn sulphide showing located approximately 2.75 km south of Florence Lake comprises pyrite, pyrrhotite, chalcopyrite and sphalerite within a strongly sheared fine-grained metasedimentary (?) or metavolcanic (?) rock with quartz fragments up to 3-4 mm in diameter (Plate 4.2). The rocks are fractured and contain minor thin ($\leq$ 1 mm wide) cross-cutting quartz-epidote veinlets. Pyrite is by far the most abundant sulphide and forms segregations up to 5 mm in diameter. Pyrrhotite and pyrite are locally intergrown, and each mineral has been seen to rim the other. Very minor sphalerite and chalcopyrite are present as fine disseminations and occur along small fractures (Plate 4.3).

A small Fe-Cu sulphide occurrence (Sunfish Lake showing) located approximately 5.5 km south of Florence Lake, consists of pyrrhotite, pyrite and chalcopyrite within a fine-grained

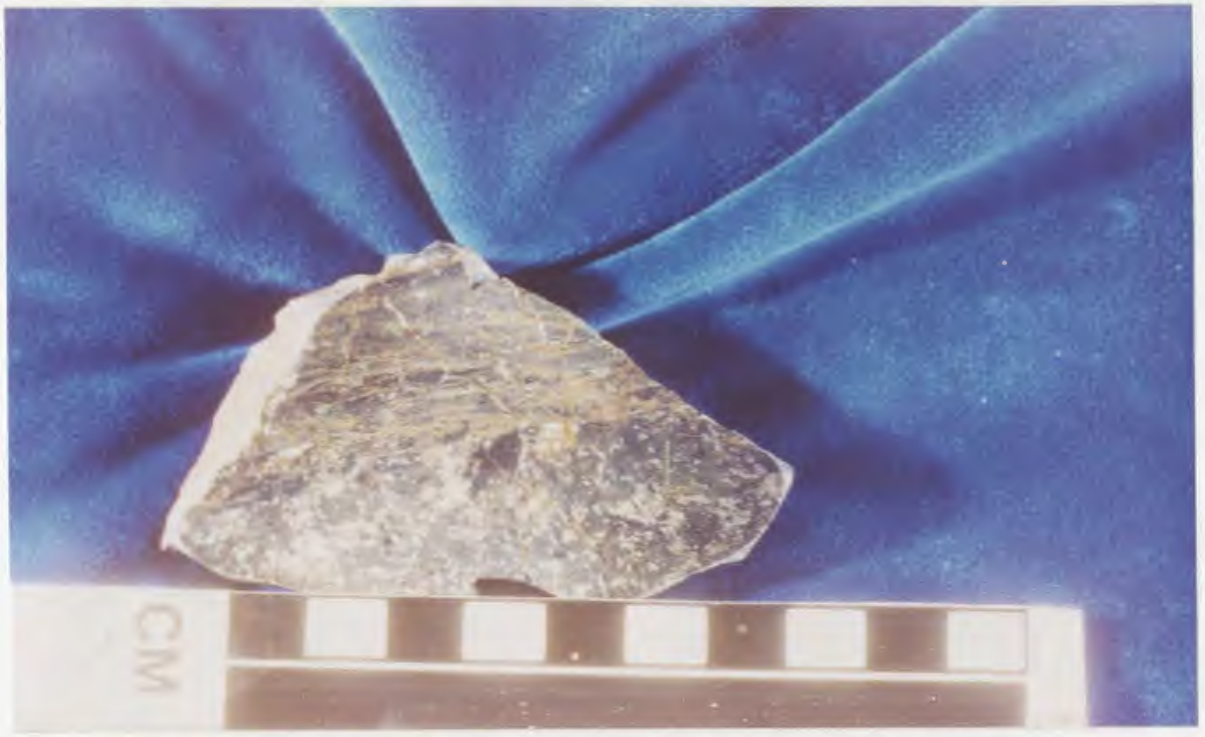

Plate 4.2. A small base-metal sulphide occurrence located approximately 2.75 km south of Florence Lake, consists dominantly of pyrite and pyrrhotite segregations up to 3-4 mm in diameter (photo), and minor chalcopyrite and sphalerite in a dark siliceous metavolcanic/metasedimentary (?) rock.

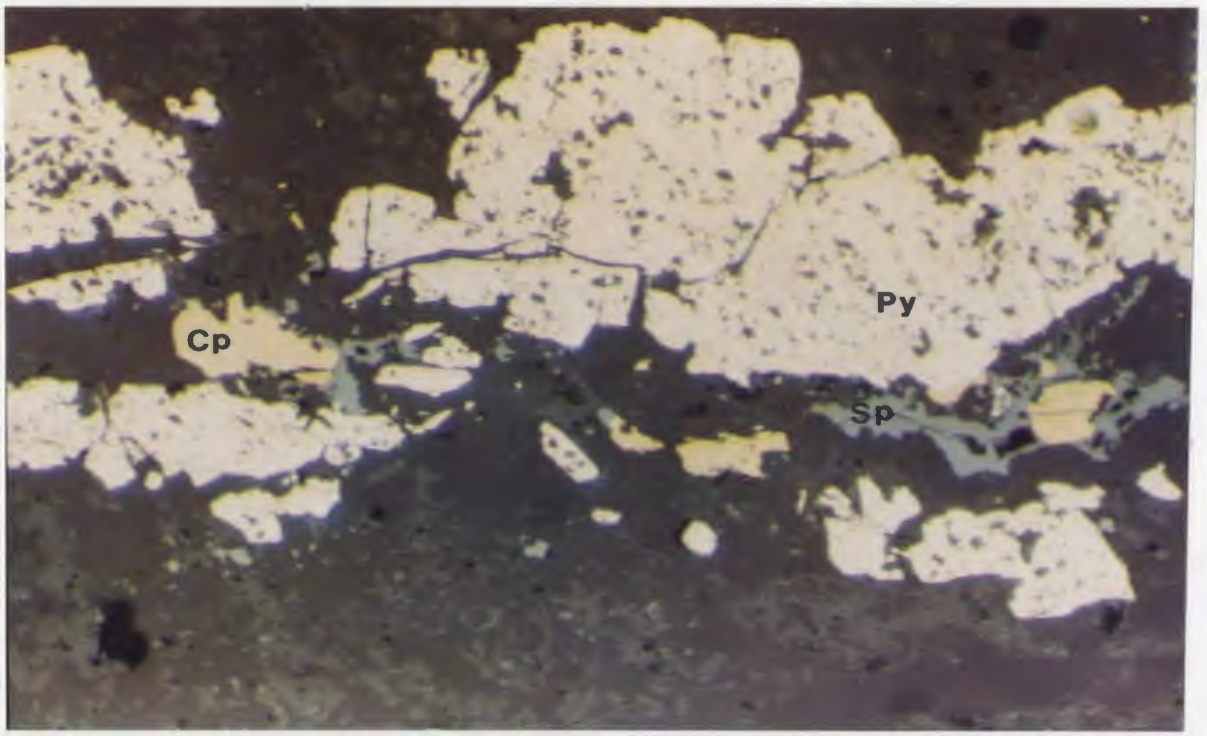

Plate 4.3. Pyrite (py) and pyrrhotite form segregations up to 3-4 mm in diameter, and minor chalcopyrite (cp) and sphalerite (sp) are both disseminated and concentrated along small fractures [87-021, 150x, RL].

schist near the carbonatized meta-ultramafic contact. A small ankeritic carbonate lens, which may represent chemical sediment or exhalite, lies adjacent to the mineralization, indicating that the mineralization itself was probably formed by volcanogenic exhalative activity. The sulphides are both disseminated and massive (Plate 4.4), and locally are concentrated along small fractures. Massive sulphides consist of pyrrhotite rimmed and replaced by pyrite, and overprinted by pyrite cubes intergrown with chalcopyrite (Plates 4.5 and 4.6). Numerous fragments up to 7 mm in diameter consisting of quartz, chlorite, and the host lithology are contained within the massive sulphide (see Plate 4.4).

Small quartz veinlets (mm's wide) carrying minor pyrite and chalcopyrite are also present throughout the Florence Lake Group. However, besides being very small, these are also sparse, with no significant concentration of veinlets or sulphides being recognized.

Piloski (1960) noted the presence of several small Fe-Cu sulphide showings comprising disseminated pyrite and pyrrhotite, and minor chalcopyrite, in intermediate to basic gneisses in an area southwest of Knee Lake. Although the author has not examined these showings, one grab sample collected southeast of Knee Lake contains disseminated pyrite and chalcopyrite in a breccia containing numerous fragments (up to several cm's) of very fine-grained quartz-sericite schist. The matrix surrounding the fragments is highly chloritized and locally contains quartz and carbonate. The

Plate 4.4. Massive sulphide from a small base-metal sulphide occurrence (Sunfish Lake showing) located approximately 5.5 km south of Florence Lake. Note the various fragments (up to 7 mm in diameter), including vein-quartz and what appears to be the host lithology (schist), within the massive sulphide.

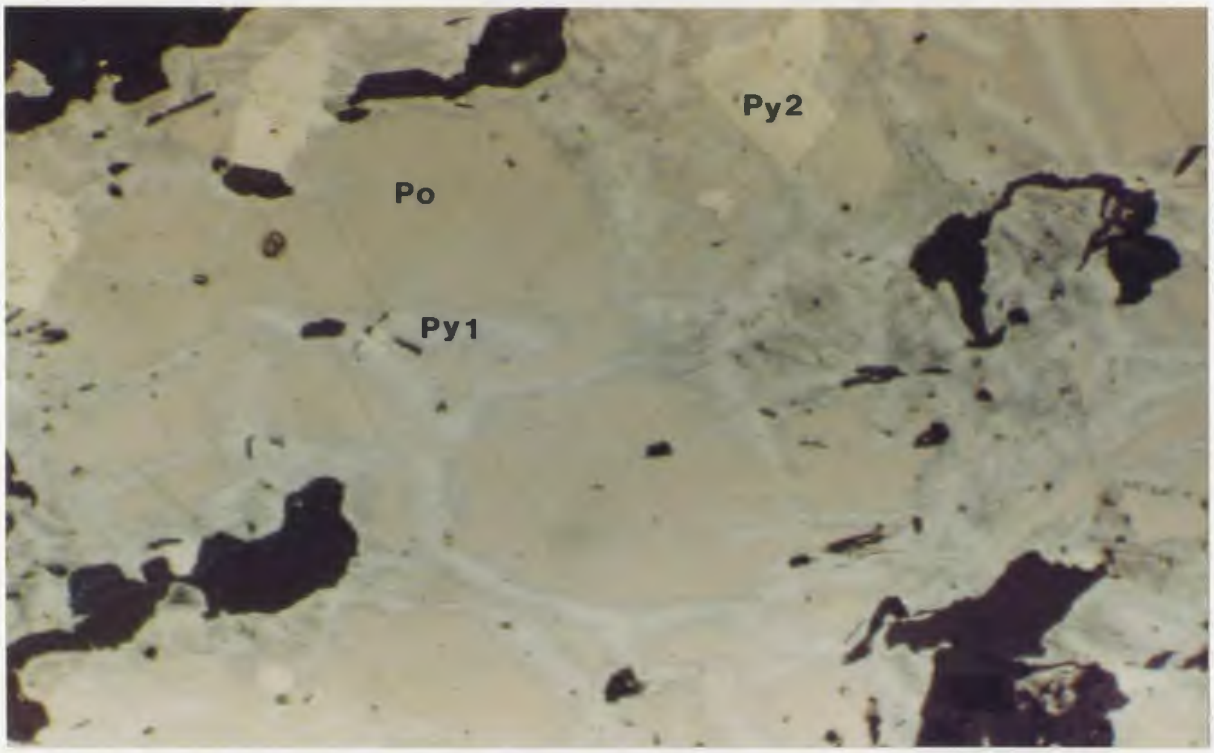

Plate 4.5. Massive sulphide from the Sunfish Lake showing consists of 'early' pyrrhotite (po) rimmed and replaced by pyrite (py1), and overprinted by 'later' pyrite (py2)cubes [87-123A, 150x, RL].

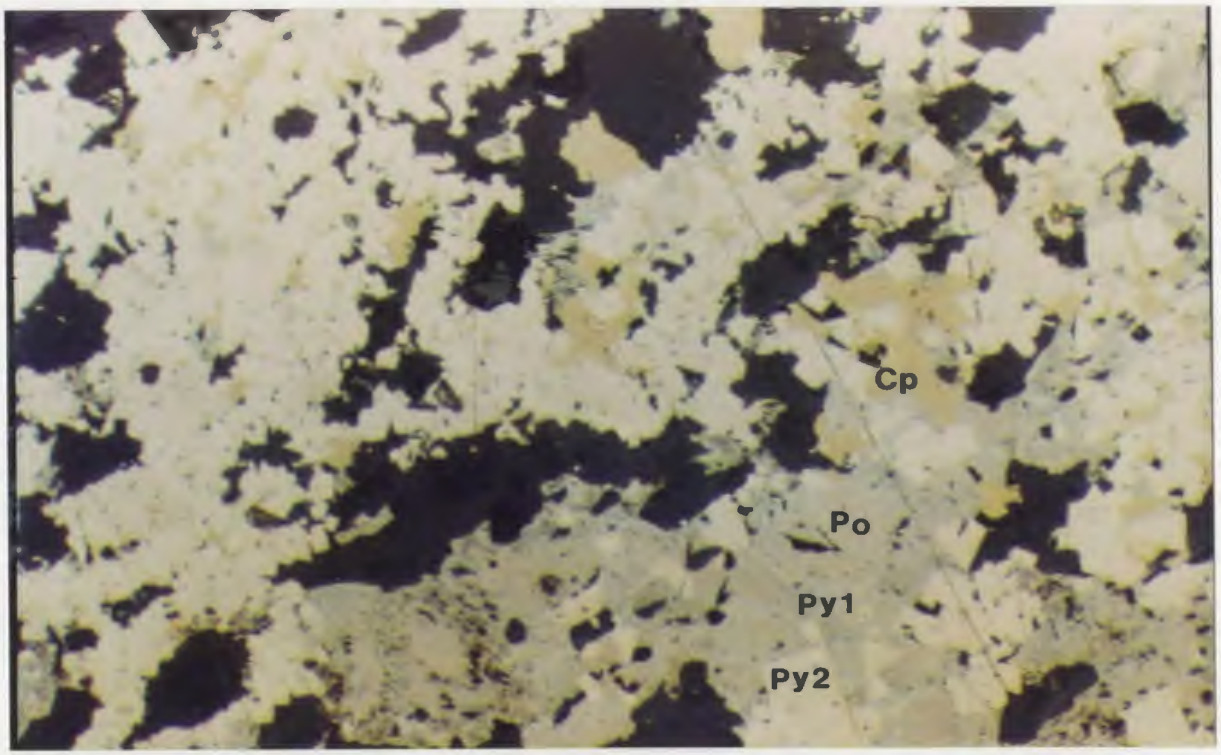

Plate 4.6. Massive sulphide from the Sunfish Lake showing with 'early' pyrrhotite (po) rimmed and replaced by pyrite (py1), and overprinted by 'later' pyrite (py2) cubes intergrown with chalcopyrite (cp) [87-123A, 150x, RL].

sulphides are generally found in these matrix areas and in fractures within the breccia fragments, although locally the sulphides simply appear to overprint the lithic fragments.

4.3.2. Fe-Ni-Cu Sulphides

4.3.2.1. Baikie Showings

4.3.2.1.1. General Geology

The Baikie showings (see map - back pocket) comprise three separate occurrences (viz., Main Baikie, North Baikie and South Baikie) of Fe-Ni-Cu (+ minor PGE) sulphides (Figure 4.1). The mineralization is hosted by xenoliths of meta-ultramafic talc-carbonate schists within trondhjemite of the Kanairiktok Intrusive Suite. These xenoliths crop out intermittently over a strike length of 150 m in a weak, northeast-trending linear defined by a low-lying boggy area where the showings are located, and a small northeast-trending rise (2-3 m in relief) to the east (Figure 4.1).

According to Piloski (1962), most of the Baikie area is underlain by chlorite schists (greenstones), with lesser amounts of amphibolitic greenstone and minor granite. Piloski noted an intrusive contact between the greenstones and a gneissic hornblende-biotite granite, with small bodies and dykes of granite and hornblende gneiss intruding the chlorite schists. Based on magnetic patterns, he speculated that the mineralized schists do not constitute a continuous unit, but instead appear to consist of a number of isolated lenses or pods.

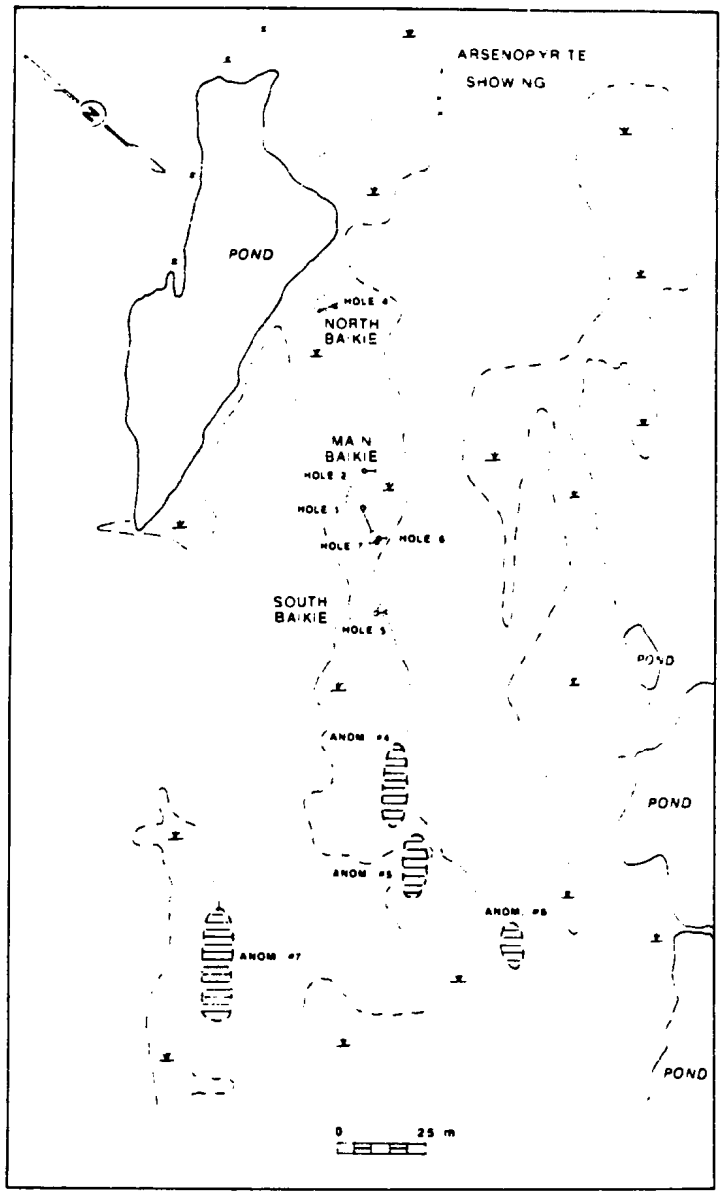

Figure 4.1. Sketch map showing the locations of mineral showings, ground magnetic anomalies, and BRINEX packsack drill holes in the Baikie area, northwest of Florence Lake (modified after Piloski, 1962).

Sutton (1970) remapped the area northwest of Florence Lake at a scale of 1:24000, primarily to determine the relationship of the granite-greenstone contact in the context of the Baikie showings. Sutton described the Baikie showings as occurring within a 500 m wide contact zone of mixing between greenstone and granodiorite gneiss. He suggested that the rocks are intensely modified by syn-foliation deformation and shearing, with the greenstones being altered to talc and actinolite schists, and the granodiorites to fine-grained quartz-feldspar phyllonites. Sutton suggested that this zone marks the site of an 'early' tectonic granite-greenstone contact, and he speculated that the structure was deep-seated because of the presence of a lens of foliated serpentinite near the southern end of the contact zone.

Re-examination of the area in the vicinity of the Baikie showings (Brace and Wilton, 1989) indicates that the granite-greenstone contact is intrusive in nature as originally suggested by Piloski (1962). In this area, the Kanairiktok trondhjemite is relatively massive, and small angular xenoliths of mafic schists (chlorite- and amphibolite-schists) are so numerous that the rocks are more properly termed agmatites (Plate 4.7).

The host rocks to the Baikie mineralization were originally described as talc-chlorite (Piloski, 1962) and talc schists (Sutton, 1970). Apparently, these early workers did not recognize the presence of abundant carbonate within the rocks. Stewart (1983) first suggested that these highly

Plate 4.7. Small angular xenoliths of amphibolite within trondhjemite are locally so abundant near the Baikie showings that the rocks are more properly termed agmatites.

Plate 4.8. Several outcrops south of the Main Baikie showing provide evidence of several periods of intrusion. Massive trondhjemite with few mafic minerals (left) cross-cuts alternating trondhjemite and amphibolite bands (lower right) and the layering in a small amphibolite xenolith (center).

altered xenoliths represent carbonatized ultramafic rocks, which appear to be confined to the area outlined by the northeast-trending linear. A number of outcrops at the edge of the linear south of the Main Baikie showing, provide evidence of remobilization and several periods of intrusion of the trondhjemite as veins and dykes (Plate 4.8). A number of different phases, each with varying proportions of mafic minerals, is present. One small outcrop contains a xenolith of garnet (almandine) amphibolite.

4.3.2.1.2. Mineralization

Figure 4.1 shows the location of six pack-sack drill holes and ground magnetic anomalies with respect to the Baikie showings (after Piloski, 1962). Anomalies #'s 1, 2 and 3 correspond to the Main, North and South Baikie showings respectively. Piloski (1960) described the mineralization at the Baikie showings as disseminated and locally massive (Main Baikie showing) pyrrhotite and pyrite in talc-chlorite schists. Apparently all the drill holes intersected the mineralized schist unit; however, massive sulphides were not intersected in any of the drill holes, including Hole # 1 which was drilled directly under the Main Baikie showing (Piloski, 1962). Cross sections for the six drill holes are presented in Figure 4.2 along with assay results for Ni in chip and drill core samples (Piloski, 1962). A summary of assay results for Ni and Cu is presented in Table 4.1. The results clearly show that the only mineralization of note is

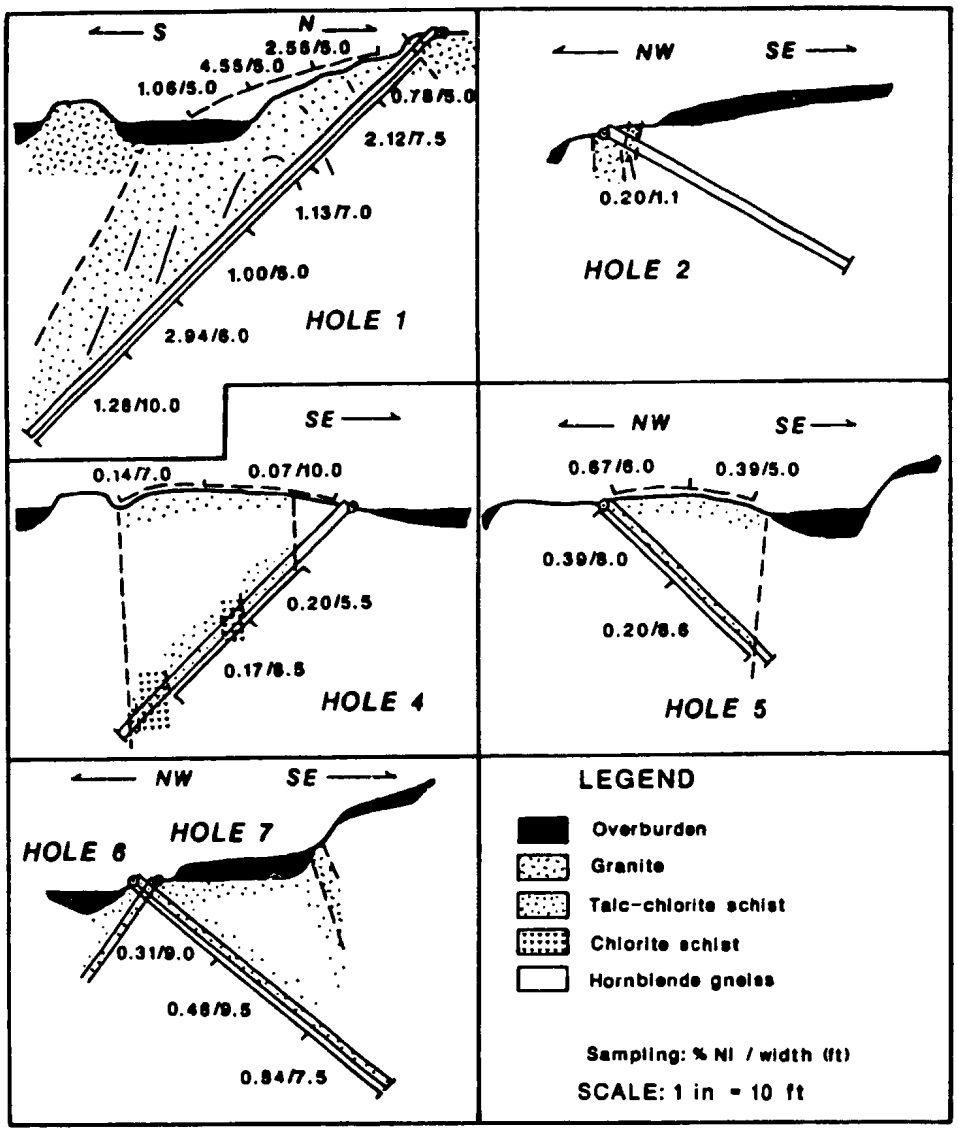

Figure 4.2. BRINEX packsack drill sections showing geology and assay results for Ni (% Ni / width ft.) (modified after Piloski, 1962).

that at the Main Baikie showing, and it is apparent that Ni concentrations for many samples (1000-2900 ppm) are not unlike those of unmineralized meta-ultramafic rocks south and southeast of Florence Lake (2000-3000 ppm Ni). These low Ni concentrations support the field observations, which indicate that the North and South Baikie showings contain very low sulphide contents.

TABLE 4.1. Assay results for channel and drill samples at the Baikie showings (after Piloski, 1962).

	Channel Samples		Drill Samples
Location	% Ni / ft	% Cu / ft	% Ni / ft
Main Baikie	2.65 / 15.0	0.07 / 15.0	
Hole # 1			1.44 / 43.5
North Baikie	0.10 / 17.0	0.005 / 17.0	
Hole # 4			0.18 / 14.0
South Baikie	0.54 / 11.0	0.01 / 11.0	
Hole # 5			0.29 / 16.6
Hole # 2			0.20 / 1.10
Hole # 6			0.52 / 26.0

Westoll (1971) noted that "It appears that the best mineralized zone is restricted to the nose of a strongly plunging minor fold...". However, nowhere in the BRINEX reports (Piloski, 1960, 1962; Sutton, 1970) is there mention of a fold at the Main Baikie showing, and the only reference

to a fold that can be found is on the drill section of Piloski (1962), wherein a fold is vaguely suggested (Figure 4.2). Certainly, there is no evidence for a fold at surface, although admittedly the outcrop is extensively blasted.

A sketch map of the Main Baikie showing is presented in Figure 4.3. The Fe-Ni-Cu sulphides are contained within a 4 x 6 m meta-ultramafic xenolith within trondhjemite of the Kanairiktok Intrusive Suite (Plate 4.9). The host rock has been completely replaced by an assemblage of talc + carbonate (ferroan magnesite) + chlorite. Opaque oxides consist of relict chromite cores rimmed by magnetite, and discrete anhedral magnetite grains generally less than 0.5 mm in diameter. Primary igneous silicate phases have been totally obliterated.

Examination of polished thin sections during this study reveals that pentlandite and chalcopyrite are present in addition to pyrrhotite and pyrite (Piloski, 1960). Pentlandite, pyrrhotite, pyrite and very minor chalcopyrite are disseminated and locally form massive sulphide (with magnetite) patches up to 50 cm in diameter (Plate 4.10). Disseminated sulphides occur as individual grains (< 0.1 mm) and sulphide intergrowths up to 2 mm in diameter (Plates 4.11 and 4.12). Massive sulphide consists of pyrrhotite- and pentlandite-rich segregations with intergrown pyrite and minor chalcopyrite (Plates 4.13 and 4.14). Pentlandite occurs as irregular blocky segregations with a pronounced octahedral cleavage, and pyrrhotite, as anhedral granular segregations.

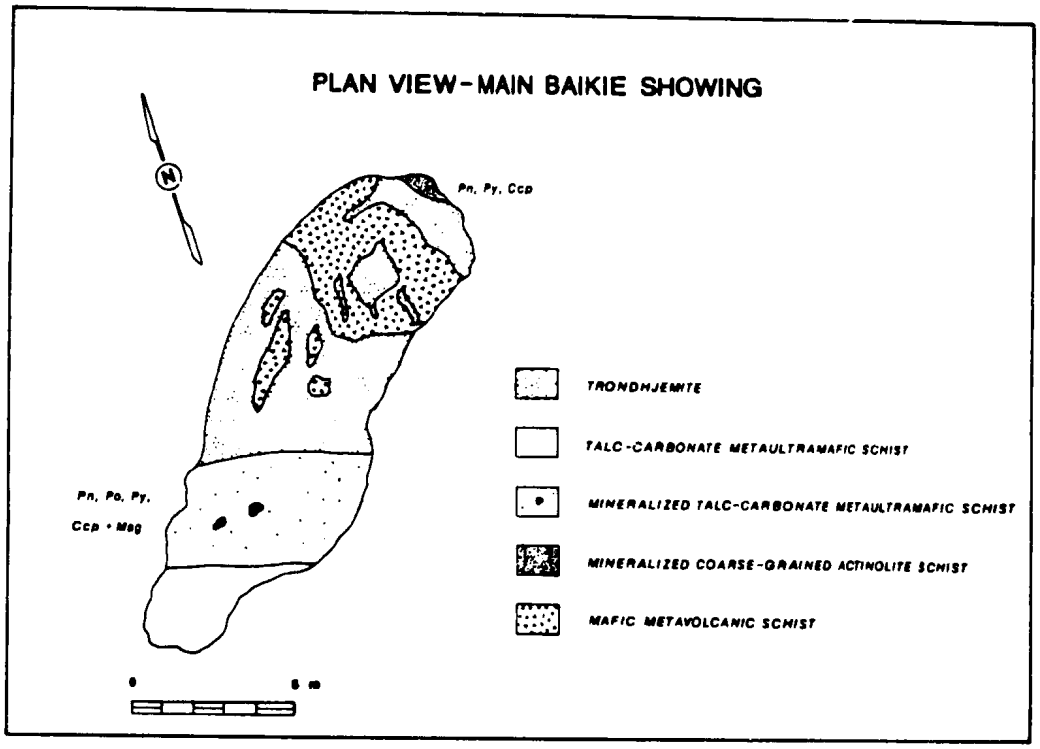

Figure 4.3. Plan view of the Main Baikie showing, which consists of disseminated and locally massive sulphide patches within a talc-carbonate meta-ultramafic xenolith in trondhjemite of the Kanairiktok Intrusive Suite. Sulphides comprise pentlandite, pyrrhotite, pyrite and minor chalcopyrite. Magnetite and chromite rimmed by magnetite are also present.

Plate 4.9. The Main Baikie Fe-Ni-Cu sulphide showing, located approximately 2.8 km northwest of Florence Lake, is hosted by a talc-carbonate meta-ultramafic xenolith (right) within Kanairiktok trondhjemite (left).

Plate 4.10. Massive sulphide from the Main Baikie showing consists of pentlandite, pyrrhotite, pyrite and minor chalcopyrite, and magnetite.

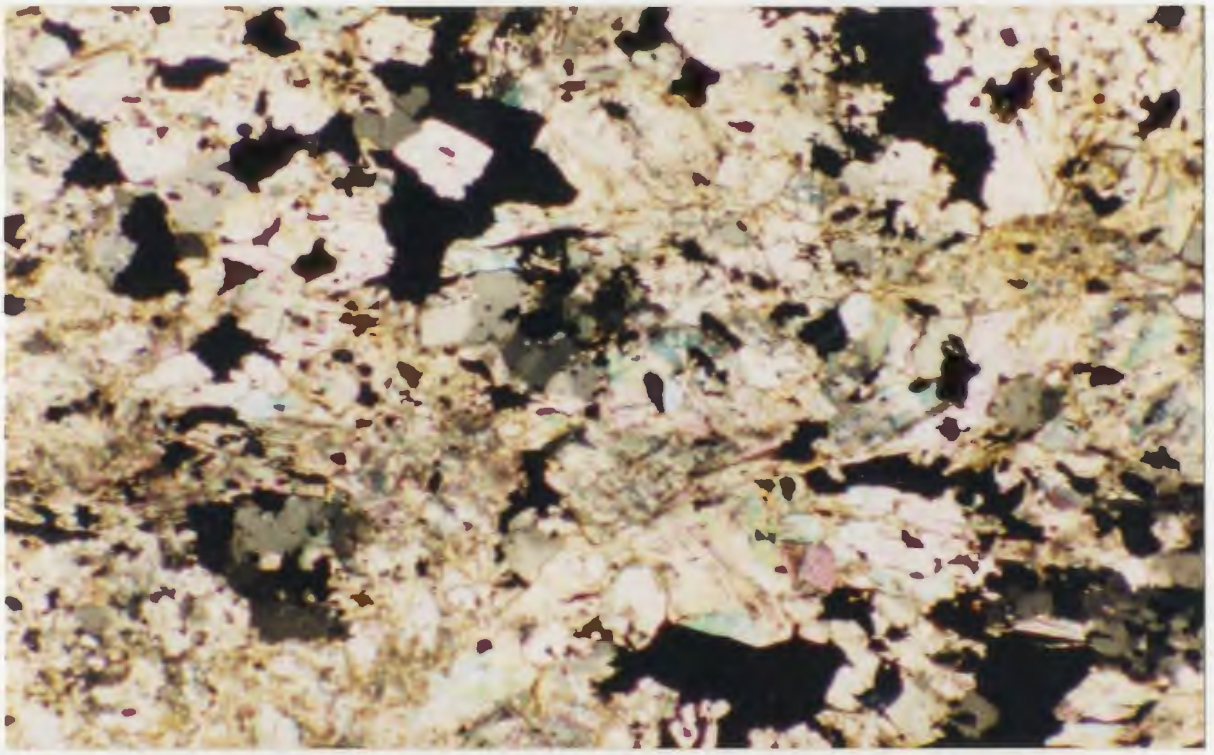

Plate 4.11. Disseminated Fe-Ni-Cu sulphides (opaque) in talc-carbonate meta-ultramafic schist, Main Baikie showing [MBS-DS, 45x, XN].

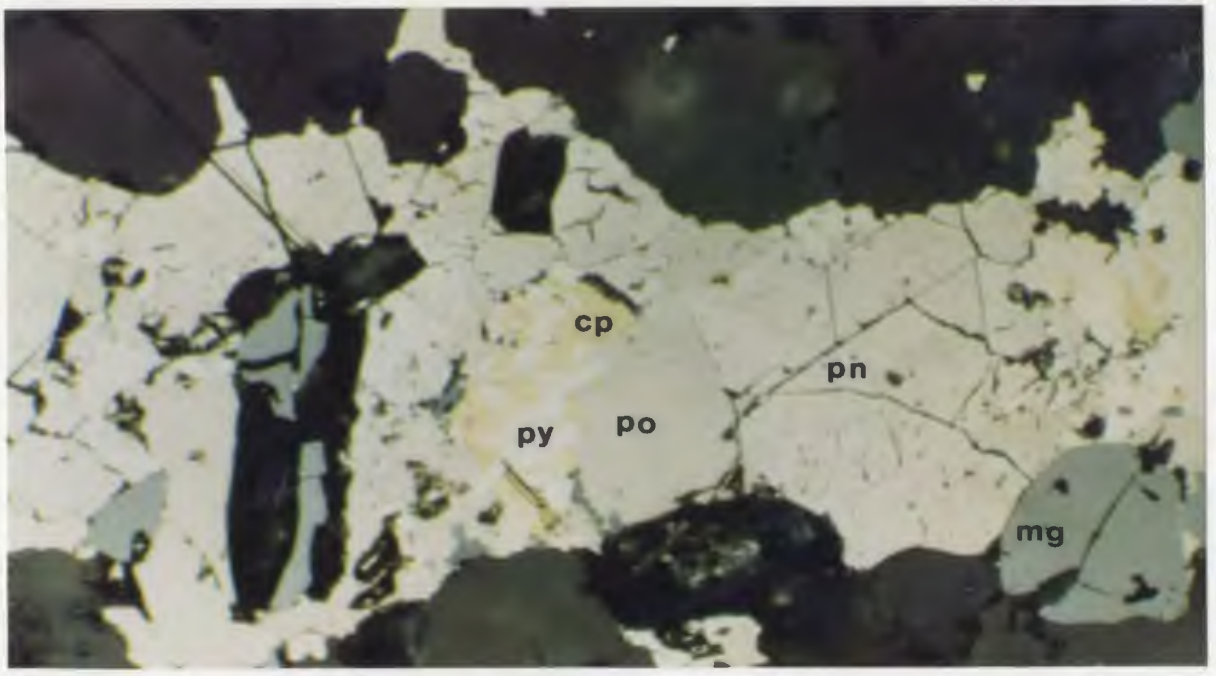

Plate 4.12. Fe-Ni-Cu sulphides are disseminated and form sulphide intergrowths in the talc-carbonate meta-ultramafic schist, Main Baikie showing. Sulphides comprise pentlandite (pn), pyrrhotite (po) and minor chalcopyrite (cp) intergrown with pyrite (py). The medium grey anhedral grains are magnetite (mg) [MBS-DS, 300x, RL].

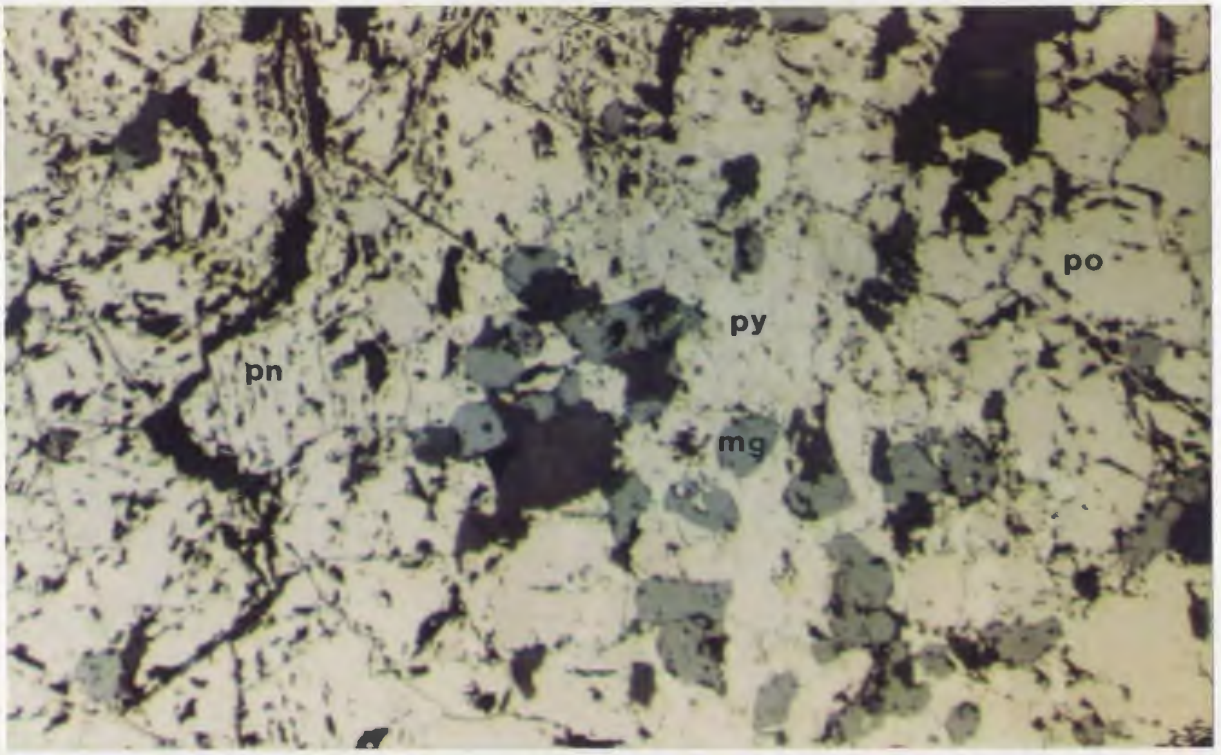

Plate 4.13. Massive sulphides from the Main Baikie showing with a pyrite (py) band, and pentlandite (pn) and pyrrhotite (po). The medium-grey anhedral grains are magnetite (mg) [MBS-MS, 50x, RL].

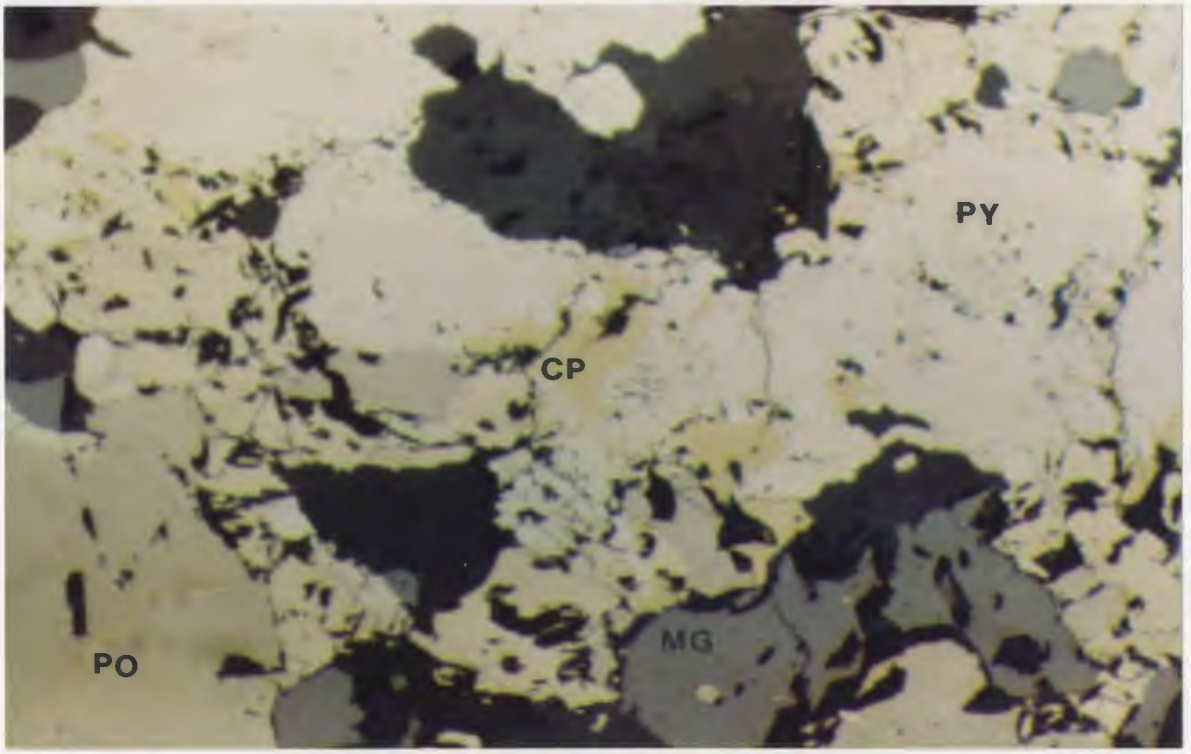

Plate 4.14. Massive sulphides at the Main Baikie showing consist of minor chalcopyrite (cp) intergrown with pyrite (py), pyrrhotite (po) and pentlandite (pn). Magnetite (mg) is abundant and forms small anhedral grains up to 0.5 mm in diameter [MBS-MS, 150x, RL].

Pyrite, in places, forms bands within the pyrrhotite and pentlandite (Plate 4.13). Magnetite constitutes approximately 5 vol.% of the massive sulphide and forms anhedral grains up to 0.5 mm in diameter.

A small xenolith (approximately 0.5 m in diameter) of actinolite schist located on the northeast side of the same outcrop hosting the Main Baikie showing (see Figure 4.3), also contains Fe-Ni-Cu sulphides and minor chromite, but in contrast to the main showing, does not contain pyrrhotite or magnetite. Pyrite is by far the most abundant sulphide phase, and occurs as intergrowths with pentlandite and as segregations along grain boundaries between actinolite crystals (Plates 4.15 and 4.16). Minor chalcopyrite is invariably intergrown with pyrite.

Semi-quantitative analyses of Fe-Ni sulphides in the talc-carbonate (Main Baikie) and actinolite schist xenoliths indicate that pentlandite in the latter (87-276) is slightly more Ni-rich and Fe-poor (Table 4.2).

Table 4.2. Semi-quantitative SEM analyses of Fe-Ni sulphides at the Main Baikie showing and trace Fe-Ni sulphides in metaperidotites south of Florence Lake.

	BAIKIE SHOWING			SOUTH OF FLORENCE LAKE		
Sample #	MBS-MS	MBS-MS	MBS-MS	87-276	87-184B	87-174
Phase	Pyrite	Pyrrhotite	Pentlandite	Pentlandite	Pentlandite	Millerite
S	52.24	38.37	32.74	32.04	33.24	35.47
Fe	46.79	61.27	31.87	27.71	24.15	0.03
Ni	0.97	0.36	35.39	40.25	42.61	64.50

Plate 4.15. Fe-Ni-Cu sulphides (opaque) occur along grain boundaries in the actinolite schist xenolith, Main Baikie showing [87-276, 15x, XN].

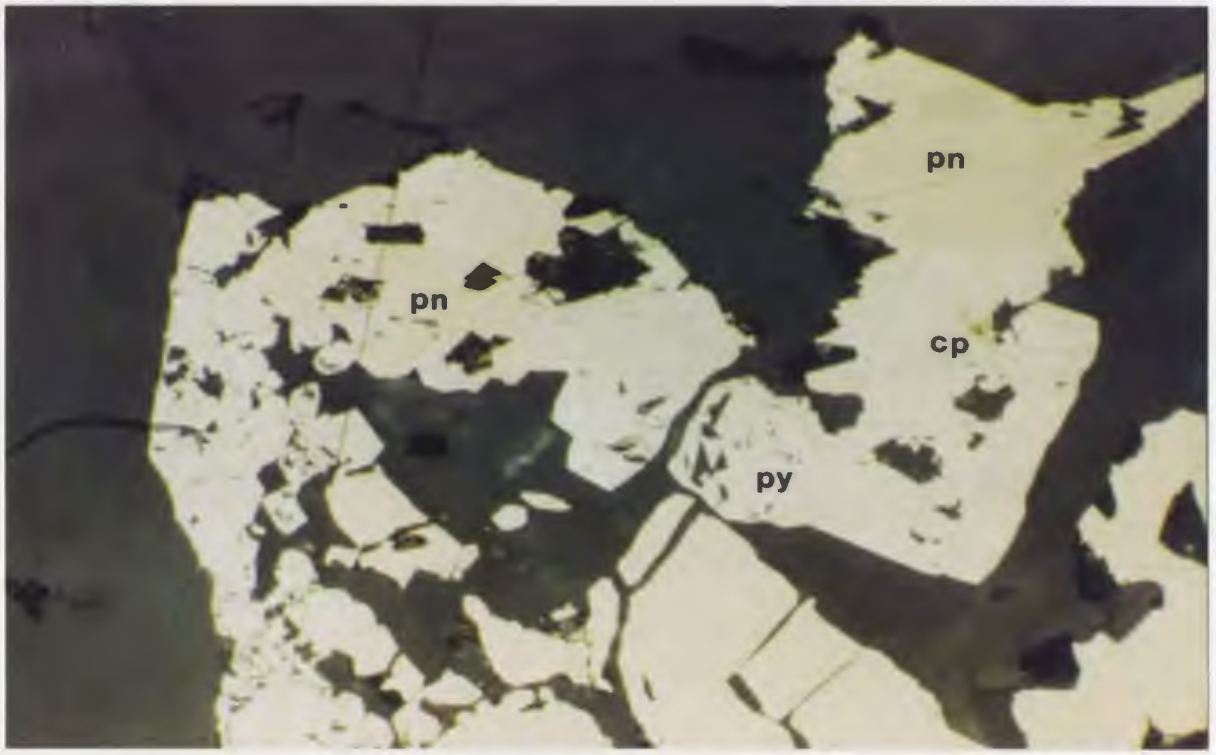

Plate 4.16. Fe-Ni-Cu sulphides in the actinolite schist consist of minor chalcopyrite (cp) intergrown with pyrite (py) and pentlandite (pn); however, pyrrhotite and magnetite are absent [87-276, 300x, RL].

An arsenopyrite showing is located approximately 165 m northeast of the Main Baikie showing along the same linear (Figure 4.1). Sutton (1970) described the showing as "a 50cm. wide band of phyllonite, containing 5-25% of a prismatic mineral identical to pyrite except for its crystal form...". Inexplicably, Sutton presented assay results for the mineralized samples, but arsenic was not detected. Stewart (1983) correctly identified the sulphide as arsenopyrite, and suggested that it is hosted in a minor ultramafic intrusion which has undergone extensive carbonate-quartz alteration. Petrographic examination of the host rock during this study shows that the mineralization is hosted within a very fine-grained carbonate-rich quartz-sericite schist, which is in sharp contact with an overlying mafic schist (Plate 4.17). Euhedral prismatic arsenopyrite crystals up to 4-5 mm in length are pervasive throughout the rock (Plate 4.18), which is cut by 'late stage' clear quartz and calcite veins. However, these veins do not control the mineralization. Examination of polished thin sections shows that some arsenopyrite crystals contain small (< 0.1 mm) inclusions of chalcopyrite. Pyrite locally forms small crystals up to 0.5 mm in diameter that also contain small inclusions of chalcopyrite, and pyrite also occurs along small fractures within the arsenopyrite crystals.

4.3.2.2. Meta-Ultramafic Rocks South of Florence Lake

No significant sulphide mineralization has been observed

Plate 4.17. An arsenopyrite showing located approximately 125 m northeast of the Main Baikie showing along the same linear, is hosted by a fine-grained carbonatized quartz-sericite schist (bottom) in sharp contact with an overlying fine-grained mafic schist (top).

Plate 4.18. Euhedral arsenopyrite crystals in a fine-grained carbonatized quartz-sericite schist. Some arsenopyrite crystals contain small (< 0.1 mm) inclusions of chalcopyrite, and pyrite locally forms small crystals (up to 0.5 mm) which also contain small chalcopyrite inclusions.

within meta-ultramafic rocks south and southeast of Florence Lake. However, trace (« 1%) amounts of pentlandite and millerite (Table 4.1) have been identified in several samples on a microscopic scale (Plates 4.19 and 4.20). The sulphides are generally very small (0.15 mm), monomineralic grains, and it is unclear whether they are primary or metamorphic in origin. During serpentinization, iron in olivine may redistribute and enter the structure of serpentine or brucite, or form discrete opaque phases including magnetite, awarite, pentlandite, ferrit-chromite, etc. (Ashley, 1975). Semi-quantitative analyses of pentlandite in a serpentinite sample (87-184B) indicates that it is slightly more Ni-rich and Fe-poor compared to pentlandite at the Main Baikie showing (see Table 4.2).

4.4. PRECIOUS METALS (PGE AND AU) ASSOCIATED WITH BASE-METALS

4.4.1. Introduction

Exploration programs by BRINEX (e.g., Piloski, 1962) and BP Minerals Ltd. (Guthrie, 1983; Stewart, 1983) concentrated primarily on evaluating the potential for base-metal and gold deposits in the Florence Lake Group. Stewart (1983) reported negligible Au concentrations in both the small base-metal occurrences and the intensely carbonatized rocks. Interestingly, BP Minerals Limited did not analyze samples for platinum-group elements (PGE), and it was not until the Baikie showing was sampled in 1987 by International Platinum Corporation of Canada (Reusch, 1987) that it was recognized

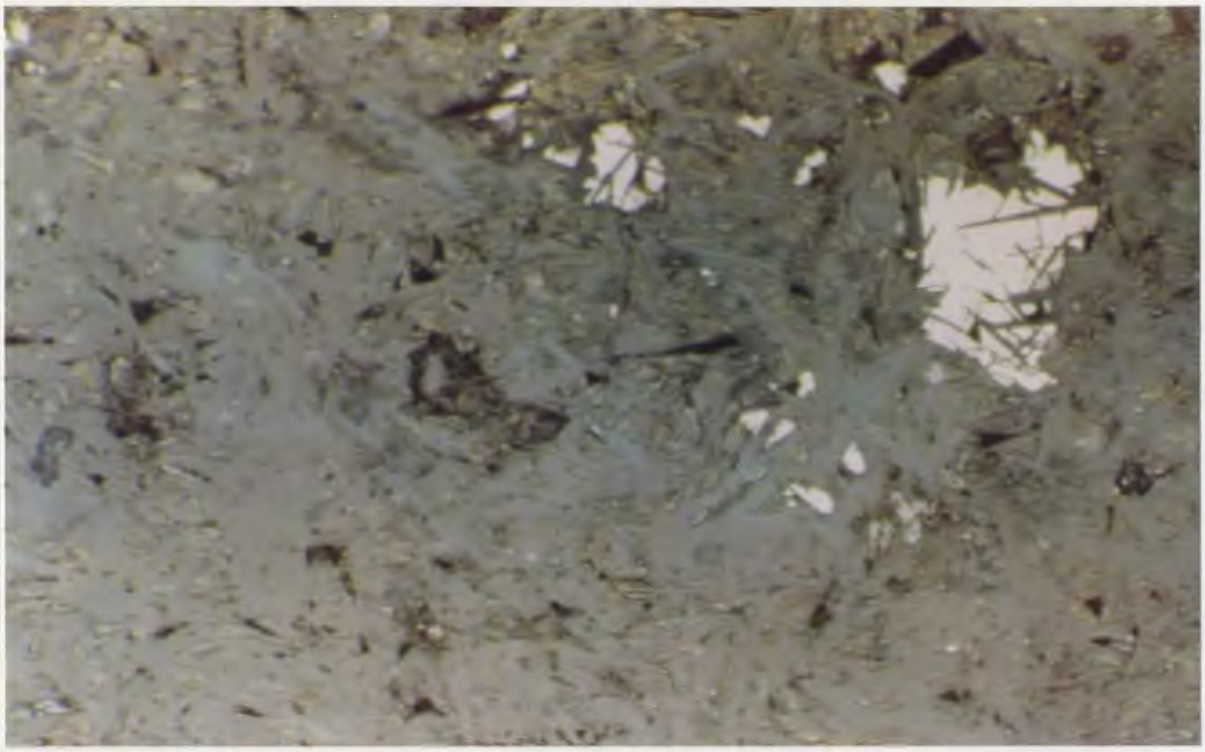

Plate 4.19. Trace (« 1%) pentlandite in a clinopyroxene-bearing serpentinized peridotite located south of Florence Lake [87-135, 300x, RL].

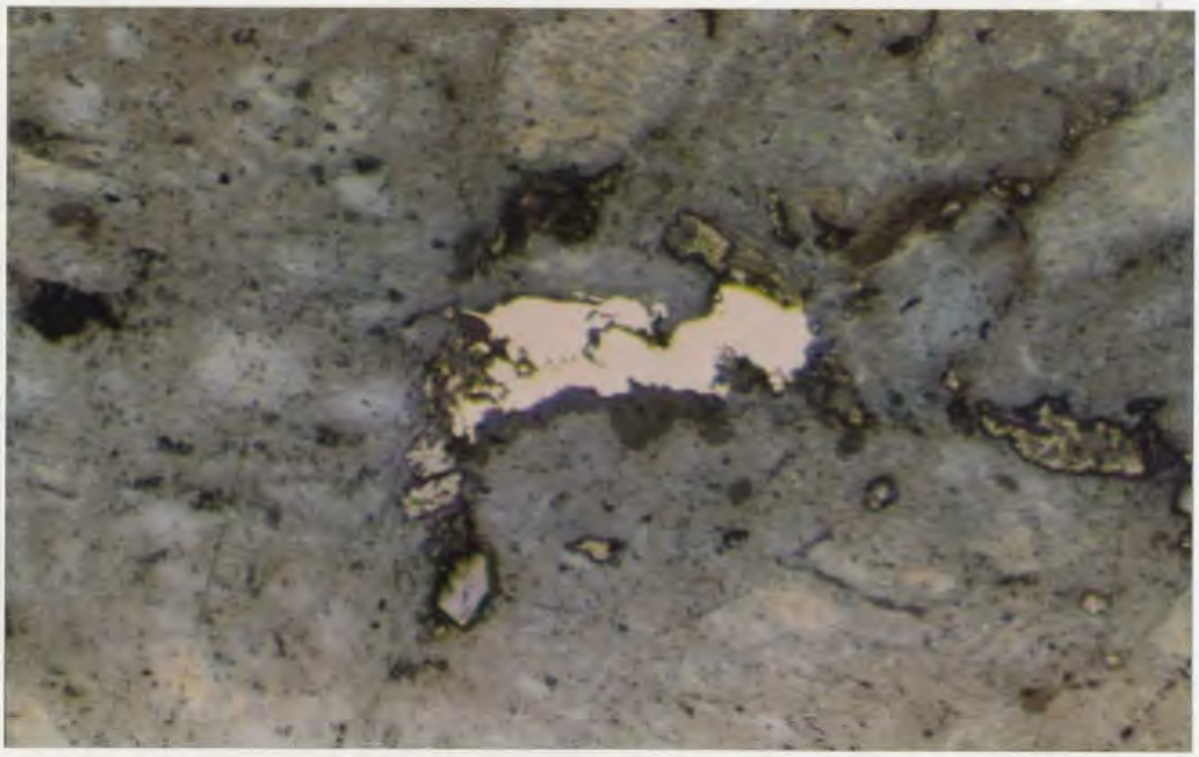

Plate 4.20. Trace (« 1%) millerite in a totally serpentinized peridotite located south of Florence Lake [87-174, 50x, RL].

that the showing contained elevated PGE concentrations.

4.4.2. Analytical Results

Analytical techniques for the determination of PGE, Au, Ni, Cu, and S are described in Appendix I. PGE and Au concentrations in mineralized samples were recalculated to values expected in 100% sulphide and normalized to average C1-chondrite (values from Naldrett & Duke 1980). The recalculation procedure used here follows that of Wilson (1988), where the modal proportion of pyrrhotite to pyrite in the massive (MBS-MS) and disseminated (MBS-DS) sulphide samples at the Baikie showing was estimated to be 9:1 from examination of polished thin sections. The mineralized actinolite schist sample contains pyrite, but no pyrrhotite. All other samples contain negligible sulphide contents, hence only whole-rock PGE and Au concentrations are presented.

4.4.2.1. Baikie Showings

Analytical results for three mineralized grab samples from the Main Baikie showing are presented in Table 4.3. In evaluating the whole-rock data, the massive sulphide (MBS-MS) contains the highest concentrations of total PGE. The actinolite schist (87-276), however, has the highest concentration of Pt (93 ppb), whereas the massive sulphide has only slightly higher Pt (36 ppb) compared to the disseminated sulphide (MBS-DS) (25 ppb). The Pd concentration in the massive sulphide (1209 ppb) is considerably higher than for

Table 4.3. Ni, Cu, S, PGE and Au concentrations in samples.

Sample #	Ni (ppm)	Cu (ppm)	S (ppm)	Pt (ppb)	Pd (ppb)	Rh (ppb)	Ru (ppb)	Ir (ppb)	Os (ppb)	Au (ppb)	Cu/ (Cu+Ni)	Pt/ (Pt+Pd)	(Pt+Pd)/ (Ru+Ir+Os)
MINERALIZED SAMPLES, BAIKIE SHOWING													
MBS-MS	140634	314	365548	36.3	1208.5	110.7	315.5	126.8	64.1	28.7	0.002	0.029	2.458
				*37.4	*1244.8	*114	*324.9	*130.6	*66.0	*29.6			
MBS-DS	11359	356	34684	24.6	181.2	15.3	61.4	24.8	19.5	6.6	0.030	0.120	1.947
				*270.6	*1992.8	*168.1	*675.0	*273.1	*214.4	*72.7			
TB-87-276	8408	374	32367	93.0	180.1	40.8	151.1	53.2	59.8	3.6	0.043	0.341	1.034
				*1328.0	*2571.8	*582.6	*2157.7	*759.7	*853.9	*51.4			
UNMINERALIZED METAULTRAMAFIC ROCKS AT AND NEAR BAIKIE SHOWING													
MBS-CTUM	2020	26	2507	5.1	11.8	1.2	5.0	2.3	2.1	0.9	0.013	0.301	1.802
TB-87-256D	2027	nd	415	8.8	11.0	1.8	8.5	2.9	4.1	167.9		0.444	1.274
TB-87-277	2052	nd	566	2.3	3.0	0.6	4.9	4.2	4.1	2.9		0.438	0.405
ULTRAMAFIC ROCKS FROM SOUTH OF FLORENCE LAKE WITH SLIGHTLY ELEVATED Pt AND Pd													
TB-87-135	866	63	581	26.9	55.8	2.7	4.5	0.7	0.4	4.0	0.068	0.326	14.960
TB-87-157A	919	63	240	7.0	10.4	0.9	3.8	1.3	1.2	1.7	0.064	0.402	2.748
'TYPICAL' ULTRAMAFIC ROCKS FROM SOUTH OF FLORENCE LAKE													
TB-87-180C	3311	nd	295	1.0	2.0	0.3	2.5	3.4	2.1	2.0		0.338	0.385
TB-87-181	2649	nd	737	0.8	1.1	0.2	3.4	2.2	2.7	0.7		0.444	0.226
TB-87-184A	2148	nd	637	1.6	1.7	0.5	4.6	0.9	0.4	4.8		0.497	0.557
TB-87-185A	2276	nd	279	0.6	0.6	0.3	4.2	1.8	2.1	1.9		0.496	0.153
TB-87-185B	2397	nd	159	0.8	1.0	0.4	5.2	2.4	2.9	2.0		0.451	0.174
TB-87-185C	2767	nd	321	0.6	0.6	0.3	4.6	2.0	2.4	0.6		0.491	0.126
TB-87-271	1934	nd	451	1.5	1.3	0.5	6.8	1.0	1.4	1.9		0.510	0.332
BASE-METALS IN METASEDIMENTARY/METAVOLCANIC ROCKS													
TB-87-021	1035	611	84966	2.7	5.8	0.2	2.5	0.3	0.4	89.9	0.371	0.315	2.684
TB-87-123A	140	1580	42459	0.6	1.5	nd	13.6	0.1	nd	11.7	0.919	0.282	0.148
TB-87-270	34	22	31490	0.2	0.4	0.1	5.4	nd	nd	8.6	0.393	0.267	0.111
MEAN MEASURED DETECTION LIMITS													
				0.20	0.34	0.10	0.17	0.05	0.52	1.92			

* PGE concentrations recalculated to values expected in 100% sulfide.

nd = not detected

the other two samples, which are essentially identical (181 ppb in the disseminated sulphide and 180 ppb in the actinolite schist).

The chondrite-normalized (values after Naldrett and Duke, 1980) PGE patterns for 100% sulphide from the Main Baikie showing are plotted in Figure 4.4. The low (Pt+Pd)/(Ru+Ir+Os) ratios of the three Baikie samples (Table 4.3) are reflected in the relatively flat PGE patterns, which maintain an overall gentle positive slope from Os to Pd, but with pronounced negative Pt and Au anomalies (Figure 4.4). The PGE and Au concentrations range between 0.1-5x C1-chondrite, except for Pt in the massive sulphide, which shows an extreme depletion relative to Rh and Pd. Examination of Ni and Cu contents in Table 4.3 reveals that the samples have very low concentrations of Cu. The massive sulphide contains approximately the same amount of Cu, yet much more Ni than the disseminated sulphide, reflecting the much higher modal percentage of pentlandite in the former. The actinolite schist has the highest Cu and lowest Ni contents of the mineralized Baikie samples.

The arsenopyrite mineralization located northeast of the Main Baikie showing was not assayed in this study; however, a sample collected by Stewart (1983) returned only 13 ppb Au, and a quartz vein from the same showing returned 3 ppb Au. Wilton (1987) also reported negligible PGE and/or Au concentrations for mineralized samples from this showing.

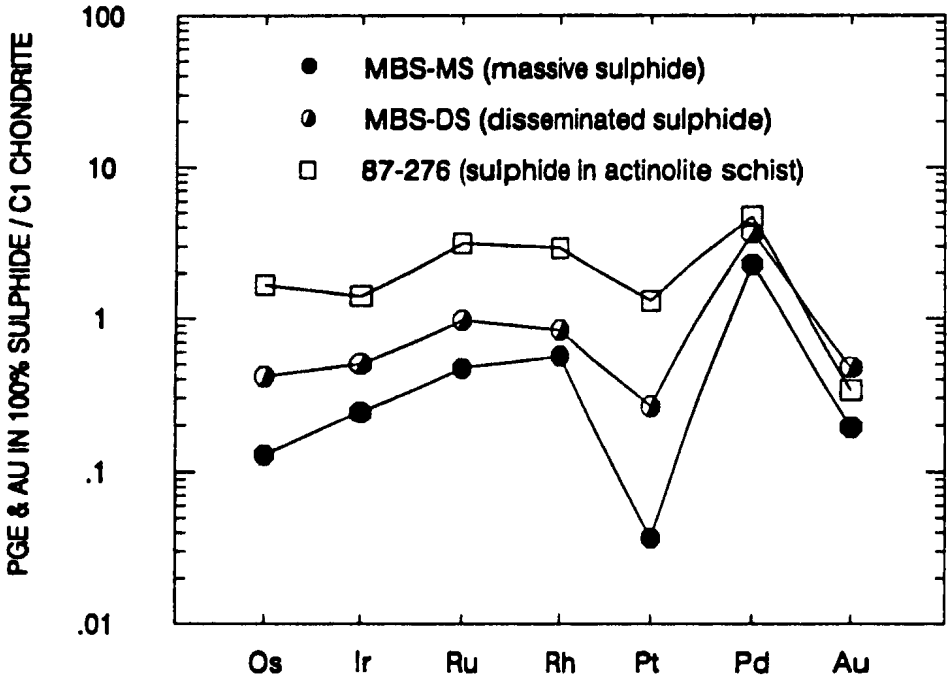

Figure 4.4. Chondrite-normalized plots of PGE and Au for sulphides from the Main Baikie showing. Average C1 chondrite normalizing values are from Naldrett and Duke (1980): Os (514), Ir (540), Ru (690), Rh (200), Pt (1,020), Pd (545), Au (152).

4.4.2.2. Unmineralised Ultramafic Rocks at the Baikie Showings

Data for unmineralized ultramafic rocks in the vicinity of the Baikie showing are plotted in Figure 4.5. MBS-CTUM, a sample of the talc-carbonate-chlorite schist xenolith hosting the Main Baikie showing, contains only trace (« 1%) amounts of sulphide. 87-256D is a grab sample of talc-carbonate schist from the North Baikie showing, and 87-277 is a serpentinized ultramafic rock (minor carbonate) containing trace (« 1%) sulphides. The PGE concentrations are low, and the profiles, quite flat. Sample MBS-CTUM shows a depletion in Au relative to Pd, in contrast to the other unmineralized ultramafic rocks, and sample 87-256D shows an elevated Au content (168 ppb). A 1.5 m-long chip sample across the same outcrop, however, returned <2 ppb Au (Wilton, 1987).

4.4.2.3. Ultramafic Rocks South of Florence Lake

The PGE and Au concentrations of ultramafic rocks south of Florence Lake are shown in Figure 4.6. The concentrations of the 'typical' ultramafic rocks are quite low, with (Pt+Pd)/(Ru+Ir+Os) ratios < 1. These flat PGE patterns may reflect the presence of cumulate olivine and chromite in the peridotites.

Two samples (87-135, 87-157A) show slightly elevated Rh, Pt, and Pd relative to the typical ultramafic rocks, and have a slight Au depletion relative to Pd which is characteristic of the mineralized samples at the Baikie showing. Sample 87-135 is the only ultramafic rock collected south of Florence

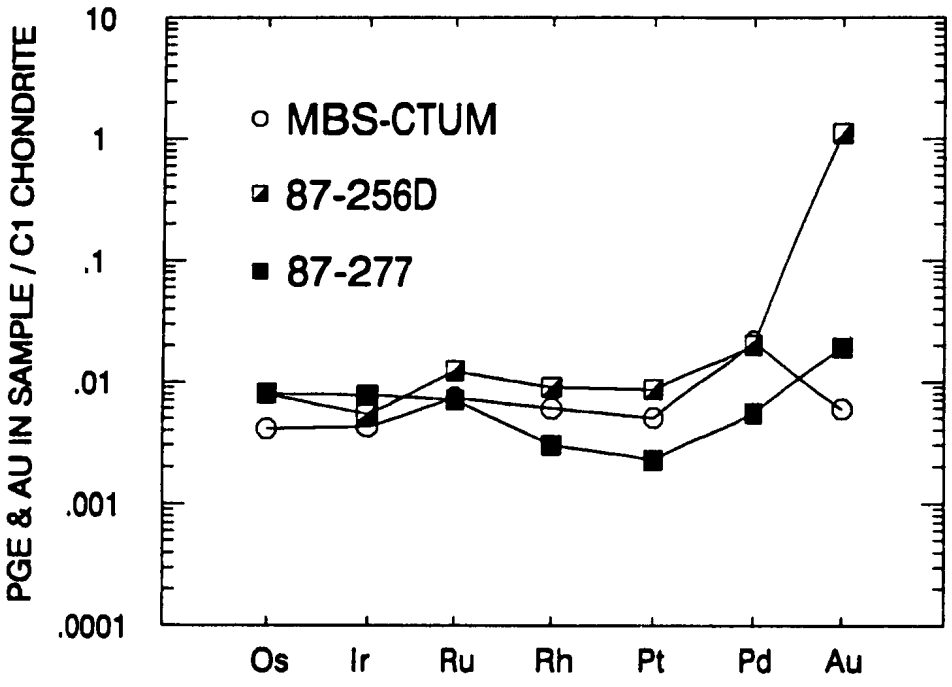

Figure 4.5. Chondrite-normalized plots of PGE and Au for unmineralized meta-ultramafic rocks at and near the Baikie showings. C1 chondrite normalizing values as for Figure 4.4 (from Naldrett and Duke, 1980).

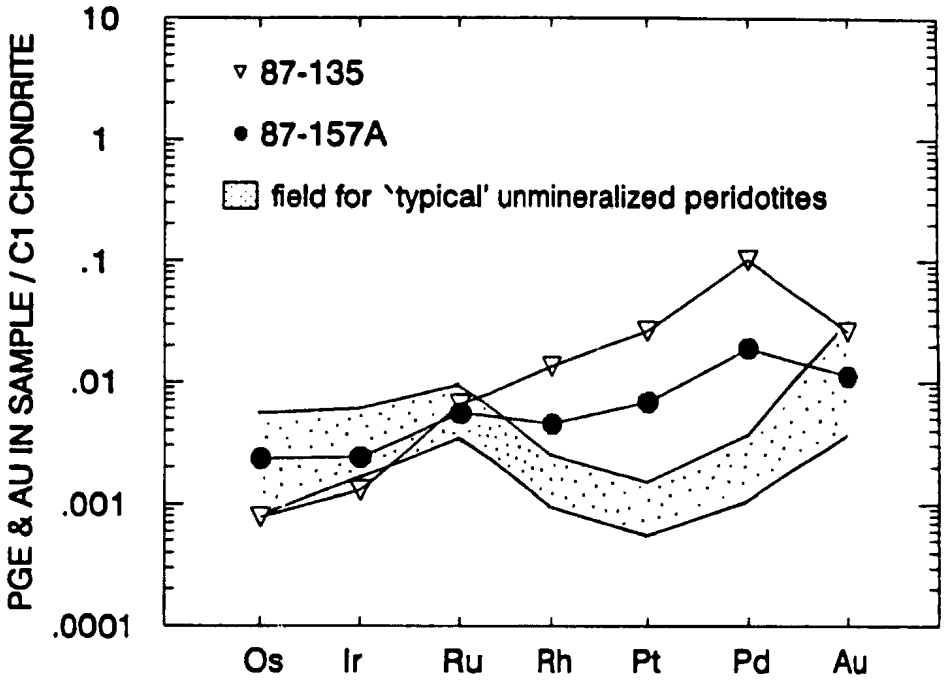

Figure 4.6. Chondrite-normalized plots of PGE and Au for 'typical' unmineralized serpentinized peridotites located south of Florence Lake (dotted field), and two samples with slightly elevated Rh, Pt and Pd. C1 chondrite normalizing values as for Figure 4.4 (from Naldrett and Duke, 1980).

Lake which contains a primary igneous silicate phase, that being clinopyroxene. This sample also contains traces (« 1%) of pentlandite (see Plate 4.19). The very low concentrations of Os and Ir, and slightly elevated Rh, Pt and Pd contents, result in a relatively high (Pt+Pd)/(Ru+Ir+Os) value (14.96). Sample 87-157A is a sheared carbonate-chlorite schist with secondary euhedral chromite and magnetite and trace (« 1%) sulphides. It too has slightly elevated Pt, Pd, and Rh relative to the typical unmineralized ultramafic rocks. Only these two samples contain detectable Cu concentrations among the ultramafic rocks analyzed from south of Florence Lake (Table 4.2). As this may indicate a positive correlation between elevated Pt and Pd concentrations and trace sulphides, Cu is potentially a useful pathfinder trace element in the exploration for PGE deposits within these ultramafic rocks. Ni has limited potential because of the naturally high and variable background concentrations in ultramafic rocks.

4.4.2.4. Base-Metals in Metasedimentary/Metavolcanic Rocks

PGE and Au concentrations in fine-grained metasedimentary and metavolcanic rocks containing pyrite and base-metal sulphides are presented in Figure 4.7. The concentrations are extremely low, and only sample 87-021 (see Plates 4.2 and 4.3) from a pyrite-pyrrhotite-sphalerite-chalcopyrite occurrence (see map - back pocket) has an elevated Au content (94 ppb).

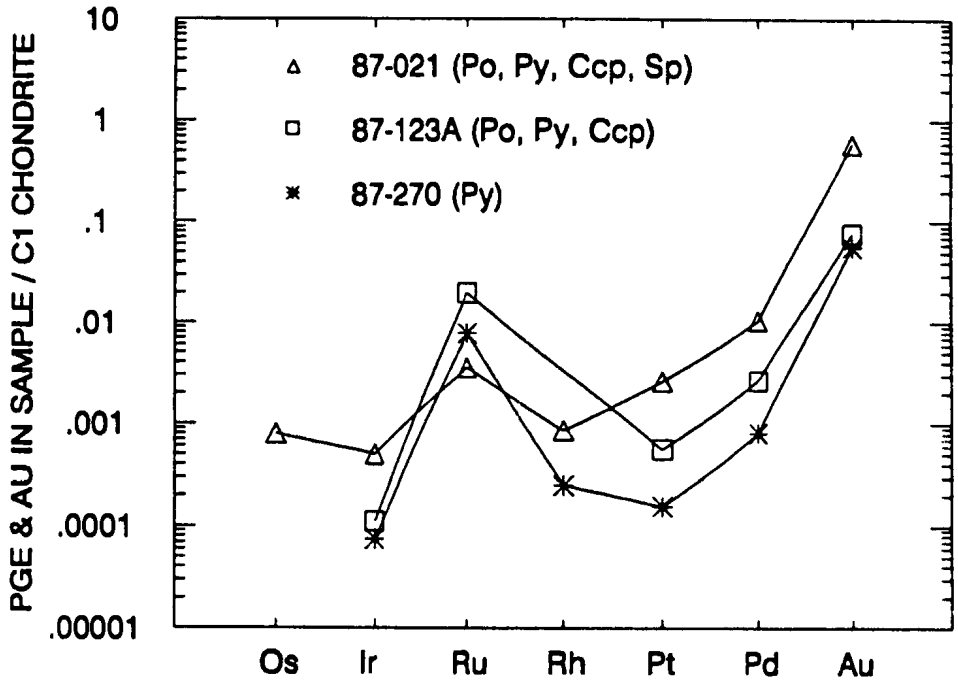

Figure 4.7. Chondrite-normalized plots of PGE and Au for two samples containing minor base-metal sulphides (87-021, -123A) and a barren pyrite horizon (87-270). C1 chondrite normalizing values as for Figure 4.4 (after Naldrett and Duke, 1980).

CHAPTER 5. METALLOGENY

5.1. INTRODUCTION

The metallogeny of Archean greenstone belts has been reviewed by various authors (e.g., Anhaeusser, 1976; Hutchinson, 1984; Groves and Batt, 1984; Thurston and Chivers, 1990).

The distribution of mineral deposits and the intensity of mineralization is heterogeneous both spatially and temporally within Archean greenstone belts around the world (cf., Groves and Batt, 1984; Barley and Groves, 1990a). Various authors (e.g., Groves and Batt, 1984; Thurston and Chivers, 1990) have attributed these differences to contrasting paleotectonic settings.

Groves and Batt (1984) recognized two end-member types of greenstone belts in Western Australia, viz., platform- and rift-phase greenstone belts. They suggested that the degree of basinal extension controls the intensity of faulting, rapidity of burial, water depth, and extent of eruption of komatiitic and felsic magma, which in turn controls the nature and intensity of mineralization. Groves and Batt (1984) suggested that rift-phase greenstones (e.g., Norseman-Wiluna belt, Yilgarn Block, Western Australia; Abitibi belt, Superior Province, Canada), which appear to be temporally restricted to the Late Archean (ca. 2.7-2.65 Ga), are the most intensely mineralized.

More recently, Thurston and Chivers (1990) proposed four

lithostratigraphic associations within Archean greenstone belts in the Superior Province, Canada (see Section 3.6). Each has analogous modern plate tectonic settings and distinct metallogenic associations (Table 5.1). Thurston and Chivers (1990) suggest that some of the sequences termed 'rift' greenstones by Groves and Batt (1984) are actually volcanic arc sequences. Nisbet (1987) emphasized that great caution is required in using such generalized models because of differences in interpretation concerning the tectonic setting of Archean greenstone belts.

5.2. METALLOGENY OF THE FLORENCE LAKE GROUP

The Florence Lake Group constitutes a relatively small (65 km long x maximum 5 km wide) greenstone belt, and although no economic mineral deposits have been discovered to date, several small mineral occurrences provide important metallogenic information.

5.2.1. Archean Fe-Ni-Cu (+ minor PGE) Sulphide Deposits

Magmatic Fe-Ni-Cu (+ minor PGE) sulphide deposits within mafic and ultramafic rocks can be classified in terms of their petrotectonic setting (Naldrett and Macdonald, 1980; Naldrett and Duke, 1980). Deposits within Archean greenstone belts (Setting III - Naldrett and Duke, 1980) are ubiquitously associated with komatiitic lavas and intrusions, and tholeiitic intrusions. Characteristic textures in most ores clearly show that the sulphides are magmatic in origin,

Table 5.1. Lithostratigraphic and metallogenic associations in Archean greenstone belts (summarized from Thurston and Chivers, 1990).

Lithostratigraphic Association	Characteristic Lithologies	Metallogenic Associations
1). Shallow water platform sequences	Quartz arenites Carbonate sediments	Detrital Au and U Oxide facies BIF Pb- and sulphate-rich VMS deposits Stratibound and vein-type barite and scheelite Stratibound tourmaline
2). Deep water ultramafic-mafic volcanic (marginal basin) sequences	Abundant komatiites and tholeiitic basalts, and associated intrusions	Ni-Cu (PGE) sulphides
3). Cyclic, bimodal volcanic (volcanic arc) sequences	Proximal to distal deep-water subaqueous basalts and andesites, proximal shallow-water to subaereal felsic volcanics and pyroclastics	VMS Cu-Zn Porphyry-style Cu-Mo BIF
4). 'Timiskaming'-type (pull-apart basin) sequences	Alkalic to calc-alkalic volcanics and fluviatile sediments (e.g., polymictic conglomerates)	Epigenetic lode Au BIF

although post-magmatic processes such as metamorphism, deformation and alteration have remobilized and redistributed metals in some deposits (e.g., Groves et al., 1974; Groves and Keays, 1979; Lesher and Keays, 1984).

Naldrett (1981) recognized three types of komatiite-related Fe-Ni-Cu (+ minor PGE) sulphide deposits: (1) small (1-5 million tonnes) high-grade (1.5-3.5% Ni) orebodies at the base of komatiite flows (e.g., Kambalda, Western Australia; Langmuir, Abitibi belt, Canada); (2) medium-sized (10-40 million tonnes), fairly high-grade (1.5-2.5% Ni) deposits at the base of intrusive ultramafic bodies, which are generally thought to have been associated with komatiitic volcanism, and perhaps represent feeders (e.g., Proterozoic Cape Smith - Wakeham Bay belt, Ungava, Canada); and (3) very large (100-250 million tonnes), low-grade (0.6% Ni) deposits in dunitic lenses which are interpreted as intrusive, sill-like bodies feeding komatiitic volcanism (e.g., Mt. Keith, Western Australia; Dumont, Abitibi belt, Canada). Sulphides vary from massive, net-textured (matrix) and disseminated in deposit types 1 and 2, to finely disseminated in deposit type 3. The dominant ore mineralogy of the deposits generally consists of pyrrhotite, pentlandite, pyrite and magnetite, and minor chalcopyrite.

..enetic models for komatiite-related magmatic Fe-Ni-Cu (+ minor PGE) sulphide deposits require: (1) the presence of a sulphur-saturated komatiitic magma; and (2) precipitation of an immiscible sulphide phase, which scavenges metals, either

at shallow depth (komatiitic dunite intrusion) or during extrusion (komatiite flow, senso stricto). The precipitation of an immiscible sulphide phase can result from a number of processes: (1) mixing of two chemically distinct magmas (e.g., Irvine, 1977; Campbell et al., 1983); (2) contamination by sulphur (e.g., Lesher and Groves, 1986); and (3) contamination by silica (e.g., Irvine, 1975; Naldrett and Macdonald, 1980). The source of sulphur in komatiite-related sulphide deposits is probably the most controversial issue concerning ore genesis. Some genetic models consider the sulphur to be mantle-derived (e.g., Naldrett, 1973); however, there are theoretical problems involved in transporting dense sulphides in low viscosity komatiitic magmas, and there is also a large volume of sulphide relative to the volume of the host ultramafic units (Gresham, 1986). Huppert et al. (1984) calculated that extremely hot (1400-1700°C), low viscosity komatiitic magmas flow turbulently, and as a result, will assimilate conduit wall rocks and floor rocks during magma ascent and eruption. Assimilation of sulphur-rich rocks either during magma ascent or eruption will contribute sulphur to the magma (Figure 5.1). During eruption, melting of underlying sulphidic and/or siliceous floor rocks will induce precipitation of sulphides, which then accumulate in thermal erosion channels to form the orebodies (Figure 5.2). Several workers (e.g., Lesher et al., 1984; Lesher and Groves, 1986) have noted a close spatial association between komatiite-associated Fe-Ni-Cu (+ minor PGE) sulphide deposits and

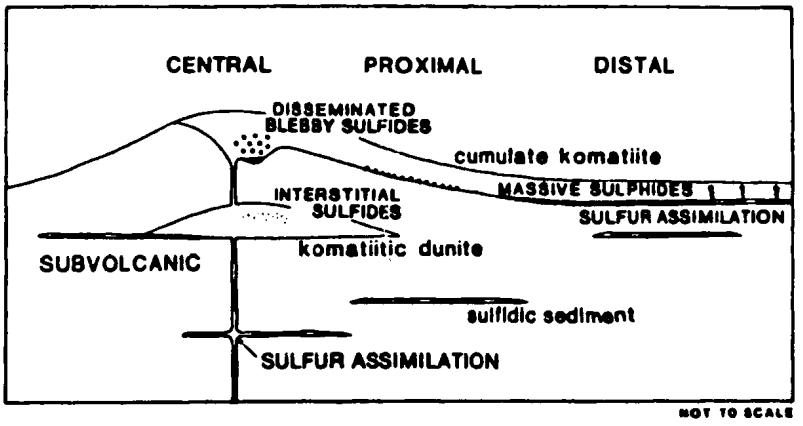

Figure 5.1. Generalized model for the formation of komatiite-associated nickel sulphide deposits by assimilation of crustal sulphur. Sulphides are shown in black: solid for sulphide ores (dotted = disseminated; spotted = blebby; filled = massive), striped for sulphidic sediments (after Lesher and Groves, 1986).

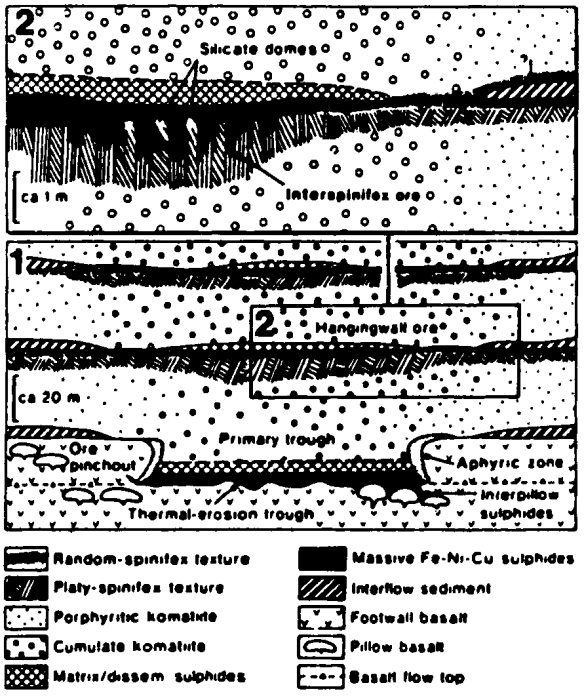

Figure 5.2. Schematic representation, not to scale, of (1) relationships in the lower part of the Kambalda komatiite pile emphasizing embayments (trough) structures and showing hanging wall ores; and (2) relationships between massive ores, interspinifex ores and komatiite flow-tops at Lunnon Shoot (after Groves et al., 1986).

sulphidic sediments at Kambalda, Western Australia, thus lending support to the assimilation model. Groves et al. (1986) have cautioned against the general use of the thermal erosion model, and have suggested that thermal erosion occurs only where basal concentrations of high thermally conductive sulphide liquid already exist. Arndt and Jenner (1986, p. 250-251) have questioned this latter argument, pointing to its "very shakey fluid dynamic basis". Gresham (1986) has argued that detailed field relationships at Kambalda are inconsistent with sediment assimilation (e.g., Lesher and Groves, 1986) and thermal erosion (Huppert et al., 1984) models, and the deposits display many enigmatic and variable geological features which are difficult to explain by any generalized genetic model. Duke (1986) has presented evidence which indicates that magma mixing was the cause of sulphide precipitation in the komatiitic Dumont sill, Abitibi Belt, Quebec. Hence, it appears that sulphide precipitation may ultimately be caused by number of processes in various deposits.

5.2.1.1. Fe-Ni-Cu (+ minor PGE) Sulphides in the Florence Lake Group

Any genetic model that could explain the origin of sulphides at the Baikie showings is complicated for two reasons: (1) primary textures have been totally obliterated; and (2) the host rocks are present only as xenoliths, so that original stratigraphic and structural relationships with other

supracrustal rocks are unknown. However, concentrations of Ni, Cu, PGE and Au associated with the sulphides provide important information concerning the nature of the host rocks.

Naldrett and Duke (1980) noted that (Pt+Pd)/(Ru+Ir+Os) ratios of magmatic sulphides, reflected by the slopes of their chondrite-normalized PGE patterns, are systematically related to the composition of their igneous host rock. (Pt+Pd)/(Ru+Ir+Os) ratios are lowest (flat PGE patterns) in sulphides associated with rocks which have crystallized from the most ultramafic magmas, and increase (steep positive slope) in sulphides associated with gabbroic magmas. For example, sulphides associated with Archean peridotitic komatiite magmas have (Pt+Pd)/(Ru+Ir+Os) ratios ≤ 2, whereas magmatic sulphide deposits related to gabbroic magmas generally have (Pt+Pd)/(Ru+Ir+Os) ratios ≥ 13 (Naldrett and Duke, 1980; Naldrett, 1981).

Chondrite-normalized PGE patterns for the Baikie showing sulphides are plotted and compared with those of several types of magmatic sulphide deposits (Naldrett and Duke, 1980; Naldrett, 1981) on Figure 5.3. The low (Pt+Pd)/(Ru+Ir+Os) ratios of the Baikie samples (1.034-2.458) are reflected in their relatively flat PGE patterns, which are most similar to Archean komatiite-related deposits. These patterns contrast markedly from the steep positive slopes characterizing deposits associated with Archean differentiated tholeiitic intrusions such as the Montcalm and Kanichee deposits in the Abitibi belt of Ontario, which have (Pt+Pd)/(Ru+Ir+Os) ratios

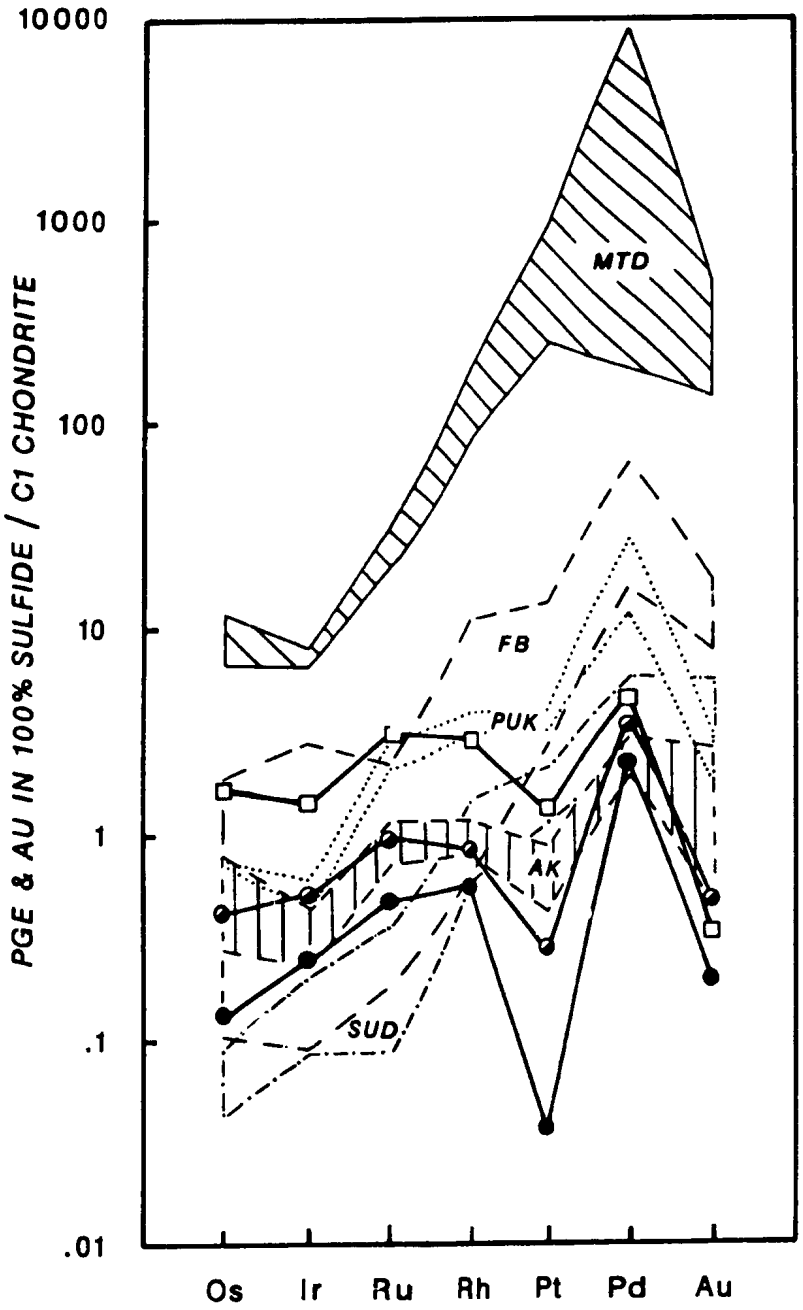

Figure 5.3. Chondrite-normalized patterns of PGE and Au for sulphides from the Main Baikie showing (symbols as for Figure 4.4) compared to patterns for several types of magmatic sulphide deposits (after Naldrett and Duke, 1980; Naldrett, 1981). Fields: Merensky-type deposits (MTD); flood basalt-related deposits (FB); Sudbury deposits (SUD); Proterozoic Ungava komatiite-related deposits (PUK); Archean komatiite-related deposits (AK). C1 chondrite normalizing values as for Figure 4.4 (from Naldrett and Duke, 1980).

of > 12.7 and 12.6 respectively (Naldrett, 1981).

Naldrett and Cabri (1976) suggested that sulphides associated with tholeiitic magmas display a negative linear relationship between Cu/(Cu+Ni) and Pt/(Pt+Pd) ratios, whereas komatiite-related deposits are characterized by both low Cu/(Cu+Ni) and Pt/(Pt+Pd) ratios. The similarity of the Baikie mineralization to komatiite-associated occurrences is further supported by Figure 5.4 (after Naldrett, 1981), wherein the talc-carbonate host rock and the mineralized actinolite schist plot in the Archean komatiite field. The massive and disseminated sulphide samples from the Main Baikie showing, however, plot well below the komatiite field, owing to their strong depletion in Pt. These samples may have suffered Pt loss during secondary metamorphism and alteration, as indicated by the large negative Pt anomalies on the chondrite-normalized plot (Figure 5.3). The Cu/(Cu+Ni) values are also generally komatiitic, although the massive sulphide has anomalously low Cu and may also have suffered Cu loss. The two ultramafic samples with detectable Cu concentrations from south of Florence Lake are similarly classified as having an Archean 'komatiitic' affinity (Figure 5.4).

Similarly, Figures 5.5A and 5.5B (after Barnes, 1987) demonstrate that the Florence Lake and Baikie samples are generally komatiitic, although the extremely high Ni/Cu ratio in the massive sulphide is evident in Figure 5.5A.

Evidence for hydrothermal mobilization of the PGE would be fractionation of Pd and Pt from Os, Ir, Ru and Rh (e.g.,

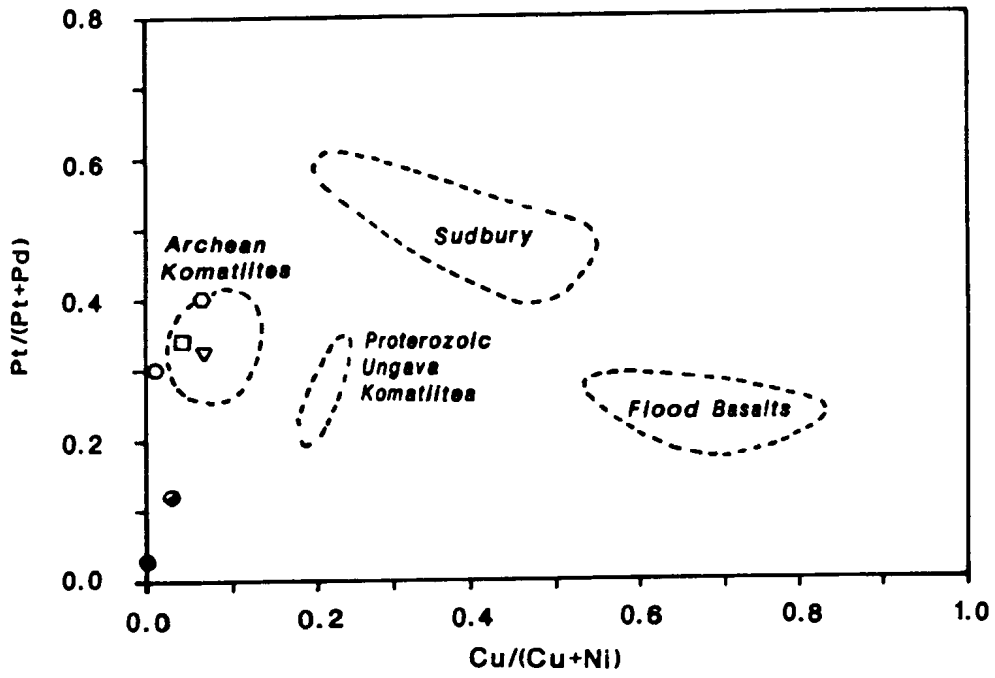

Figure 5.4. Pt/(Pt+Pd) vs. Cu/(Cu+Ni) diagram for Baikie showing samples (MBS-MS, MBS-DS, 87-276), the unmineralized talc-carbonate host rock (MBS-CTUM) and two meta-ultramafic samples from south of Florence Lake (87-135, 87-157A). Symbols as for Figures 4.4, 4.5 and 4.6. Fields are from Naldrett (1981).

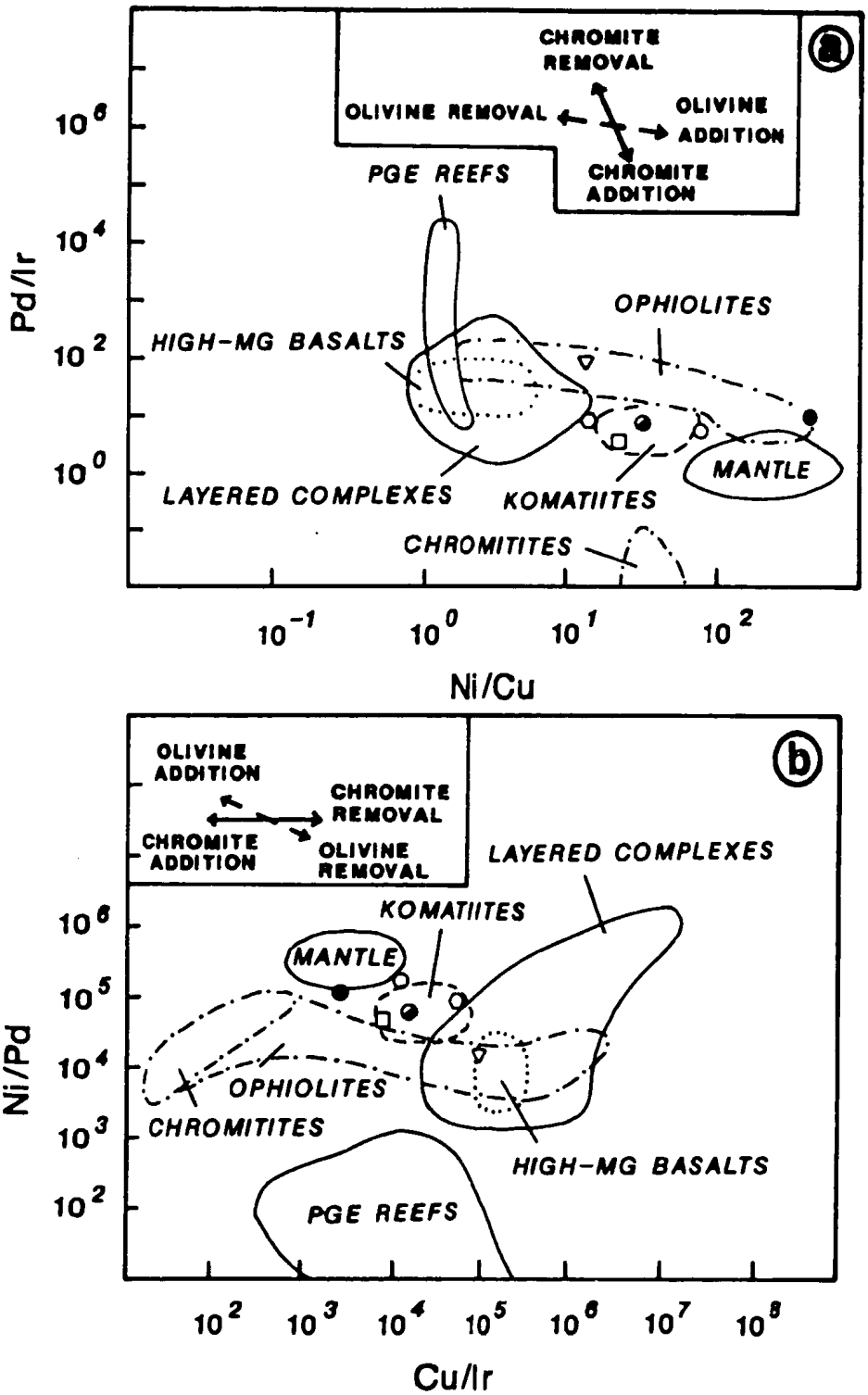

Figure 5.5. (a) Log (Pd/Ir) vs log (Ni/Cu) diagram; and (b) log (Ni/Pd) vs log (Cu/Ir) diagram (after Barnes, 1987) for the Baikie showing samples, the unmineralized talc-carbonate host rock, and two meta-ultramafic samples from south of Florence Lake. Symbols as for Figures 4.4, 4.5 and 4.6.

McCallum et al., 1976; Rowell and Edgar, 1986; Mountain and Wood, 1988). The unfractionated chondrite-normalized PGE patterns and the similar Pd concentrations among the sulphide samples (Figure 5.3) indicate the PGE have not been significantly remobilized by hydrothermal processes. One striking feature, however, is the very Pt-depleted nature of the massive sulphide and, to a lesser extent, the disseminated sulphide (Figure 5.3), which is reflected in their extremely low Pt/(Pt+Pd) values of 0.029 and 0.120, respectively. Barnes et al. (1985) have pointed out that Pt and Au appear to be mobilized and significantly depleted in komatiites that have undergone talc-carbonate alteration. The elevated Au content (93 ppb) in sample 87-256D from the North Baikie showing, and the strong Pt and Au depletion of the sulphides from the main showing, indicate that Pt and Au have been remobilized during secondary processes. The extremely low Cu content of the massive sulphide indicates that Cu may also have been mobilized and lost.

Therefore, sulphides at the Baikie showing and within meta-ultramafic rocks south of Florence Lake, are chemically similar to Archean komatiites with respect to their PGE and Cu-Ni concentrations, and their geological features are consistent with a komatiitic affinity. The meta-ultramafic rocks south of Florence Lake appear to be intrusive into volcanosedimentary rocks of the Florence Lake Group (Ermanovics and Raudsepp, 1979a;b; Brace and Wilton, 1989), and textural and geochemical characteristics indicate that

they consist predominately of serpentinized dunites, commonly with a relict cumulate texture. These rocks may represent komatiitic dunite intrusions, which most workers interpret to represent feeders to komatiite flows (e.g., Naldrett, 1981). The nature of meta-ultramafic rocks in the vicinity of the Baikie showings is more equivocal; however, absolute REE concentrations are comparable to those of meta-peridotites south of Florence Lake (see Figure 3.23), indicating that they are also probably cumulates.

The recognition of ultramafic rocks with komatiitic affinities within the Florence Lake Group has regional significance, as it represents the first suggestion of komatiitic magmatism in the Archean Nain Structural Province, and thus raises the possibility of more metallogenic models than previously presented. Collerson et al. (1976) reported high-Mg mafic rocks with bladed olivine crystals (not spinifex) that intruded into the Hunt River Greenstone Belt, 50 km north of Florence Lake; however, these authors did not definitively identify those rocks as komatiitic, and in fact suggested that they were chemically distinct from the typical Barberton Mountainland and Munro Township komatiitic rocks.

5.2.2. Archean Volcanogenic Massive Sulphide (VMS) Fe-Cu-Zn Deposits

A typical volcanogenic massive sulphide (VMS) deposit consists of a stratiform lens of massive sulphide, stratigraphically underlain by a discordant stockwork or

stringer zone of vein-type sulphide contained in a pipe of hydrothermally altered rock (Lydon, 1984). Post-depositional metamorphism and deformation can strongly change the textures and morphology of deposits.

It is widely accepted that VMS deposits of all ages form by precipitation of sulphides onto the sea-floor from hydrothermal, metalliferous fluids, which leached metals from the underlying rocks during convective circulation (cf., Hutchinson, 1984).

The nature and genesis of Archean volcanogenic massive sulphide (VMS) Fe-Cu-Zn deposits has been reviewed by various authors (e.g., Sangster and Scott, 1976; Franklin et al., 1981; Hutchinson, 1982). In contrast to post-Archean VMS deposits, Archean deposits are characteristically Pb-poor. Hutchinson (1984) noted that the transition from Cu-rich to Pb-rich VMS deposits is an intrinsic feature of the broad change from Archean to Proterozoic metallogeny.

The largest and most economically important Archean VMS Cu-Zn deposits are within the Late Archean greenstone belts of the Superior Province, Canada. Although small deposits occur in stratigraphically lower basaltic rocks (Hutchinson, 1984), the largest deposits are invariably associated with felsic volcanic and pyroclastic rocks of proximal felsic domes. Thurston and Chivers (1990) interpreted these sequences to have formed in a volcanic arc setting. In contrast to these arc-related VMS deposits, those deposits within Archean shallow-water platform greenstone sequences are Pb- and

sulphate-rich (Groves and Batt, 1984; Thurston and Chivers, 1990).

Lowe (1985) stressed the importance of depositional water depths in the formation and preservation of Archean VMS deposits. Under deep-water conditions, both proximal massive and distal ores would be preserved. In contrast, proximal massive ores deposited subaerially or in shallow water would likely be eroded following volcanism, whereas smaller distal deposits would more likely be preserved. Barley and Groves (1990a) suggest that the relative absence of VMS deposits in the Norseman-Wiluna belt, Western Australia, may reflect the partly subaerial nature of proximal calc-alkaline volcanics, or the scarcity of proximal silicic volcanic facies in deeper-water associations.

Dimroth et al. (1985) noted that the fact that many VMS deposits are draped over rhyolite domes or flows has probably been overemphasized, and they stressed the importance of synvolcanic faults in controlling the distribution of VMS deposits. These faults form by downfaulting of crustal blocks, and act as conduits for magma and hydrothermal fluids. According to Dimroth et al. (1985), the rhyolite domes and feeder dykes are favourable sites of ore deposition only because the associated subvolcanic felsic intrusions are a strong heat source, and are therefore more likely to drive a vigorous hydrothermal system than the smaller mafic feeder dykes.

In summary, three of the most important requirements for

the formation and preservation of Archean VMS deposits are: (1) a strong heat source to drive a vigorous hydrothermal system (e.g., subvolcanic felsic intrusions); (2) the presence of synvolcanic faults which act as conduits for magmas and hydrothermal fluids; and (3) sufficiently deep water conditions which prevents erosion of the deposit following ore deposition. Given these conditions, VMS deposits may occur within any volcanosedimentary unit.

5.2.2.1. Fe-Cu-Zn Sulphides in the Florence Lake Group

The numerous pyritic bands within siliceous supracrustal rocks of the Florence Lake Group are invariably barren of base-metals, and are herein interpreted to represent syngenetic pyrite.

Two small base-metal occurrences (see Section 4.3.1) were briefly examined in the Florence Lake area during this study. A small Fe-Cu-Zn sulphide occurrence located 2.75 km south of Florence Lake is somewhat enigmatic. The sulphides are hosted by what appears to be a strongly sheared felsic lithology, and consist predominantly of pyrite patches with minor pyrrhotite, and chalcopyrite and sphalerite as disseminations, and in small fractures. No massive sulphides are present, and it is unclear whether the sulphides are epigenetic or represent remobilized syngenetic sulphides.

In contrast, the Fe-Cu sulphide occurrence located about 5.5 km south of Florence Lake contains both disseminated and minor massive sulphides comprising pyrrhotite, pyrite, and

minor chalcopyrite, within a fine-grained schist. The mineralization lies adjacent to a small carbonate lens (ankerite), which may represent chemical sediment or exhalite, indicating that the mineralization itself may be related to volcanogenic exhalative activity.

The conditions which appear to favour and control large VMS deposits are either unknown or lacking in the Florence Lake Group. Water depths are essentially unknown, although the presence of pillow basalts and chemical sediments demonstrate that the sequence was at least in part subaqueous. Also, no well-developed felsic volcanic centers or synvolcanic faults have been recognized within the Florence Lake Group. However, it should be stressed that this does not preclude the presence of synvolcanic faults, since intense deformation within the sequence probably requires detailed stratigraphic and structural studies for their recognition.

5.2.3. Archean Lode Gold Deposits

The nature and genesis of Archean lode gold deposits is an extremely broad and controversial subject, and only a very brief account is given here. A tremendous amount of literature has been published concerning these deposits, however, there are several excellent review articles (e.g., Roberts, 1987; Colvine et al., 1988).

The distribution of Archean lode gold deposits is fundamentally controlled by crustal-scale, deep-seated, brittle-ductile faults and shear zones (e.g., Colvine, 1989;

Groves et al., 1989) which separate zones of contrasting lithostratigraphy and structural style. These major lineaments are believed to have acted as conduits for fluids and magmas derived from the upper mantle and lower crust, which resulted in regional-scale wallrock alteration (carbonatization, silicification, sulphidation and K-metasomatism) and a distinctive suite of late-kinematic felsic (granitic, syenitic, porphyritic and lamprophyritic) intrusions. Although the major structures control the distribution of gold mineralization, they themselves are rarely mineralized, and gold deposits are instead located along smaller subsidiary structures.

The major faults and shear zones are generally considered to have formed in response to compression as a result of collisional tectonics (e.g., Colvine, 1989; Barley and Groves, 1990b). Barley and Groves (1990b) conclude that tectonic controls on the distribution of Late Archean gold mineralization in the Norseman-Wiluna Belt, Yilgarn Craton, are similar to those which control the distribution of mesothermal gold mineralization in post-Archean terranes at obliquely convergent plate margins such as the North American Cordilerra. Colvine (1989) suggested that auriferous fluids are focused through pull-apart structures which form in response to transcurrent motion along the major regional shear zones. According to Colvine (1989), the formation of pull-apart structures in Archean greenstone belts is supported by the occurrence of specific lithostratigraphic units (e.g.,

Timiskaming-type fluvial-alluvial polymictic conglomerates, alkaline volcanic rocks and intermediate to felsic intrusions) within the deformation zones. Thurston and Chivers (1990) suggest that gold deposits within pull-apart basins (Table 5.1) are restricted to those basins which formed at tectonic domain or subprovince boundaries.

Because the gold deposits are epigenetic, they can be hosted by any lithology within the greenstone belts, including the late-stage fault-controlled felsic intrusions. The style and morphology of gold mineralization is highly variable, and depends on the nature of the dilational zones. These are controlled by ambient pressure and temperature, host-rock lithology, strain rate and fluid pressure (Colvine, 1989). Since most gold deposits formed during regional metamorphism, the style of mineralization is related to the metamorphic grade of the host lithology. In lowest greenschist facies rocks, gold mineralization is hosted by brittle structures such as veins and breccias, whereas in rocks of lower to middle amphibolite facies, foliation-parallel mineralization predominates with minor veining in ductile shear zones (Colvine, 1989). In the case of banded iron formation and other iron-rich sedimentary host rocks, the mineralization forms layered replacement deposits (Barley and Groves, 1990b). Free gold occurs in quartz veins in some deposits, but commonly gold is associated with pyrite, pyrrhotite and/or arsenopyrite in wallrock alteration zones (Barley and Groves, 1990b). Accessory opaque minerals associated with the

mineralization include molybdenite, stibnite, tellurides, scheelite, galena, sphalerite, chalcopyrite, and magnetite. Fluid inclusion and stable isotope studies (e.g., Colvine et al., 1988) indicate that the fluids were mesothermal (250-400°C), low salinity, CO_2-H_2O-bearing fluids.

Geological studies indicate that gold mineralization was contemporaneous with extensive magmatism, tectonism, and metamorphism related to cratonization of the crust. Many genetic models have been proposed for Archean lode gold deposits (cf., Roberts, 1987; Colvine et al., 1988). The source of the fluids remains one of the most contentious issues, and many sources have been proposed: (1) metamorphic fluids produced by mantle and crustal outgassing (e.g., Groves et al., 1989); (2) magmatic fluids derived from late-stage felsic intrusions (Burrows et al., 1986; Burrows and Spooner, 1989); and (3) fluids derived from granulitization of the lower crust (Colvine, 1989; Fyon et al., 1989). Stable isotope data are equivocal, and are consistent with a metamorphic and/or magmatic fluid, but preclude a significant contribution from meteoric or seawater (Colvine, 1989).

5.2.3.1. Gold Deposits in the Florence Lake Group

No gold occurrences have been discovered within the Florence Lake Group to date. Stewart (1983) noted two potential geological environments for gold mineralization within the Florence Lake Group: (1) small syngenetic quartz-pyrite horizons; and (2) intensely carbonatized zones

associated with major faults.

Stewart (1983) reported negligible gold concentrations associated with the small quartz-pyrite showings, and he noted that although the carbonatized zones within the Florence Lake area are significant in size, they are invariably devoid of sulphides. Stewart noted that the associated quartz veins are discontinuous and multi-directional, and he suggested that they appear to be "sweat-outs" from the original host.

Stewart (1983) noted only two occurrences of significant sulphide mineralization within carbonatized rocks. A grab sample from the arsenopyrite showing located northeast of the Main Baikie Showing (Plates 4.17 and 4.18) assayed only 13 ppb Au, and a quartz vein from the same location assayed 3 ppb Au. A carbonatized rock containing heavily disseminated pyrite (up to 20 vol.%), collected on the shore of Ugjoktok Bay, assayed 60 ppb Au and 4000 ppb Ag. Assay results for quartz veins collected from fourteen different locations (excluding the Baikie showing) were similarly disappointing; one sample returned 58 ppb Au, whereas the remainder assayed < 2 ppb Au.

The extensive zone of carbonatized ultramafic rocks southeast of Florence Lake extends for about 1.25 km along strike. The rocks have undergone intense deformation characterized by folding (Plate 2.37) and local boudinaging of more competent felsic porphyritic rocks (Plates 2.38 and 2.19). The rocks are commonly cut by numerous small quartz veins which characteristically infill tension gashes, and appear to have formed in situ as a result of the

carbonatization process.

Although the alteration system at Florence Lake displays some features similar to those associated with Archean lode gold deposits, there are also some very important differences. The intensely altered ultramafic rocks in the Florence Lake area have undergone intense carbonatization, and local Na- and K-metasomatism as indicated by the presence of albite porphyroblasts and traces of fuchsite (Section 2.6.2). However, more localized silicification (including shear-related quartz veins) and sulphidation which invariably accompany gold mineralization appear to be completely lacking in the Florence Lake carbonatized ultramafic rocks.

Although the potential for gold deposits within these carbonatized rocks is considered to be low, exploration efforts concentrated along faults or shear zones adjacent to, or linked to these alteration systems, may reveal the presence of epigenetic gold mineralization.

CHAPTER 6. CONCLUSIONS

This thesis constitutes a regional study of the geology, geochemistry and metallogeny of the Florence Lake Group and associated meta-ultramafic and trondhjemitic rocks. This chapter summarizes the more important conclusions:

1). The Florence Lake Group (FLG) contains a bimodal volcanic sequence consisting dominantly of mafic metavolcanic rocks comprising schists, flows, pillow lavas and minor synvolcanic sills. Felsic metavolcanic and siliceous metasedimentary rocks are also present, but are less extensive.

2). Fine-grained quartz-sericite schists of the FLG are considered to represent metapelitic and cherty metasedimentary rocks, whereas felsic rocks containing plagioclase and quartz fragments are interpreted to be volcanogenic tuffs and porphyries. This is evidenced by the retention of delicate volcanic features such as embayed quartz, and euhedral plagioclase and quartz phenocrysts. Transition elements (Cr and Ni) were not detected in any of the porphyritic samples, indicating that if the rocks are sedimentary in origin, they were derived from a source area essentially devoid of mafic and/or ultramafic lithologies.

3). Based on the relative depletion of LREE, the FLG basalts can be divided into two groups: (1) Group 1 basalts have flat chondrite-normalized patterns; (2) Group 2 basalts are slightly LREE-depleted. On tectonic discrimination and spider diagrams, the FLG basalts are chemically similar to N-MORB,

although several samples show compositions slightly transitional towards IAT. In contrast, the felsic supracrustal rocks display classic arc (or continental crust) signatures.

4). The presence of pillow lavas and minor chemical sediments (chert and marble) shows that the FLG was at least in part deposited subaqueously; however, volcanosedimentary features which might indicate water depths are absent.

5). Carbonate is ubiquitous throughout the Florence Lake Group and the meta-ultramafic rocks, and occurs in a variety of forms: (1) thin (mm's) cross-cutting veinlets (calcite); (2) thin (mm's-cm's) bands parallel to foliations (ankerite, ferroan dolomite and calcite); (3) lenses up to several metres thick within mafic metavolcanic schists (ankerite); and (4) extensive zones of intense carbonatization with complete replacement of ultramafic rocks (ferroan magnesite).

6). Meta-ultramafic rocks south of Florence Lake consist dominantly of serpentinized peridotites, which appear to have intruded the FLG as dykes and/or sills. Relict cumulate textures and whole rock chemistry indicate that the sequence originally consisted of dunite ± harzburgite; clinopyroxene-bearing phases (e.g., lherzolite, wehrlite) appear to have been volumetrically minor. The nature of meta-ultramafic rocks in the vicinity of the Baikie showings is more ambiguous because primary textures are totally obliterated and the rocks are present only as xenoliths within trondhjemite. However, REE concentrations are similar to the cumulate metaperidotites south of Florence Lake, thus indicating a common origin.

7). A sequence of carbonate-quartz rocks southeast of Florence Lake appears to form a northeastern extension of the main ultramafic body. Locally the rocks take on a sedimentary appearance; however, mineral and whole rock chemistry (major elements, transition elements and REE) clearly show that the rocks are ultramafic in origin. Metamorphic assemblages within the ultramafic rocks can be explained in terms of a series of metamorphic reactions at low to moderate values of X_{CO2}. Locally, the presence of albite porphyroblasts and traces of fuchsite indicate that saline, metasomatic fluids carrying Na^+ and K^+ were locally important within these intensely carbonatized ultramafic rocks.

8). The Kanairiktok Intrusive Suite consists of massive, gneissic and mylonitic trondhjemite-tonalite which show variable degrees of HREE-depletion, possibly related to varying depths of formation. The rocks are chemically classified as volcanic arc granitoids on tectonic discrimination diagrams, and on spider diagrams they display classic arc (or continental crust) signatures.

9). Lithological and geochemical characteristics are consistent with the FLG having been deposited subaqueously in a back-arc basin which lay proximal to a volcanic arc and/or continental margin.

10). Post-tectonic Proterozoic diabase and gabbro dykes in the Florence Lake area, informally called the Florence Lake (FL) dykes, appear to be of two ages: (1) an older (?) set of

north- to northeast-trending gabbro dykes, viz., the FL gabbro dykes; and (2) a younger (?) set of east-west-trending smaller diabase dykes, viz., the FL diabase dykes. In the past, these dykes have generally been compared to the Harp dykes further to the north. Although the FL gabbro dykes may be correlative to the Harp dykes, the smaller FL diabase dykes are both mineralogically and chemically distinct from the Harp dykes and other Middle Proterozoic mafic suites within Labrador. However, the similarity between the FL diabase dykes and the Nain HP dykes is striking, and may have important implications concerning the evolution of other Proterozoic mafic suites in Labrador. The relationship appears to be one where a relatively small and apparently younger (?) set of more evolved diabase dykes (FL diabase dykes) are conjugate to the main dyke swarm (FL gabbro dykes).

11). Fe-Ni-Cu sulphides at the Main Baikie showing consist of disseminated and locally massive pentlandite, pyrrhotite, pyrite and minor chalcopyrite, and magnetite and chromite within a talc-carbonate meta-ultramafic xenolith in trondhjemite. A small actinolite schist xenolith on the northeast side of the same outcrop is also mineralized, but in contrast to the main xenolith, does not contain pyrrhotite or magnetite. Whole rock analyses have returned elevated platinum-group element (PGE) concentrations of up to 1208 ppb Pd and 93 ppb Pt. SEM investigations did not reveal the presence of any platinum-group minerals (PGM), and the PGE appear to be in solid solution with the major sulphide phases.

12). No significant sulphide mineralization has been observed

within meta-ultramafic rocks south of Florence Lake; however, trace (« 1%) Fe-Ni sulphides including pentlandite and millerite have been observed in several samples on a microscopic scale. PGE concentrations in these rocks are very low; however, two samples with slightly elevated Rh, Pt and Pd concentrations were also the only two samples with detectable Cu. As this may indicate a positive correlation between elevated PGE and above background Cu concentrations, Cu is potentially a useful pathfinder trace element in the exploration for PGE deposits within these ultramafic rocks.

13). Concentrations of PGE, Ni and Cu indicate that the metaperidotites south of Florence Lake and the meta-ultramafic xenoliths at the Baikie showing are komatiitic. The recognition of ultramafic rocks with komatiitic affinities within the Florence Lake area represents the first evidence of komatiitic magmatism in the Archean Nain Structural Province.

14). Thin conformable pyrite horizons within fine-grained quartz-sericite schists are interpreted to be syngenetic pyrite. No significant base-metal sulphides are associated with these horizons.

15). The Sunfish Lake showing located south of Florence Lake consists of disseminated and minor massive pyrrhotite, pyrite and chalcopyrite. A small ankeritic carbonate lens adjacent to the mineralization may represent chemical sediment or exhalite, indicating that the mineralization may also be exhalative.

16). Evaluating the potential for VMS deposits within the FLG is difficult because of a lack of stratigraphic and structural control, and volcanosedimentary features which indicate water depths are also lacking. However, major felsic domes, with which many large deposits are associated with in the Superior Province, are absent within the FLG; instead, felsic volcanic rocks are thinly intercalated with the more voluminous mafic volcanic rocks.

17). Alteration assemblages within meta-ultramafic rocks in the Florence Lake area display some similarities to those associated with Archean lode gold deposits; however, there are also some important differences. Although the Florence Lake rocks have undergone intense carbonatization and local Na-and K-metasomatism, more localized silicification (including shear-related quartz veins) and sulphidation which invariably accompany gold mineralization appear to be completely lacking. Abundant quartz veins which infill tension gashes in the carbonatized rocks are interpreted to have formed in situ as a result of the carbonatization process.

BIBLIOGRAPHY

Abbott, D.H. and Hoffman, S.E., 1984. Archean plate tectonics revisited 1. Heat flow, spreading rate, and the age of subducting oceanic lithosphere and their effects on the origin and evolution of continents. Tectonics, v. 3, no. 4, pp. 429-448.

Anhaeusser, C.R., 1976. Archaean metallogeny in southern Africa. Economic Geology, v. 71, pp. 16-43.

Arengi, J.T., 1987. Summary report on the Baikie Property, central Labrador. Unpublished Platinum Exploration Canada Inc. Report, 9 pp.

Arndt, N.T., 1983. Role of a thin, komatiite-rich oceanic crust in the Archean plate-tectonic process. Geology, v. 11, pp. 372-375.

Arndt, N.T. and Jenner, G.A., 1986. Crustally contaminated komatiites and basalts from Kambalda, Western Australia. Chemical Geology, v. 56, pp. 229-255.

Arth, J.G., Arndt, N.T. and Naldrett, A.J., 1977. Genesis of Archean komatiites from Munro Township, Ontario: trace-element evidence. Geology, v. 5, pp. 590-594.

Arth, J.G. and Barker, F., 1976. Rare-earth partitioning between hornblende and dacitic liquid and implications for the genesis of trondhjemitic-tonalitic magmas. Geology, v. 4, pp. 534-536.

Arth, J.G. and Hanson, G.N., 1975. Geochemistry and origin of the early Precambrian crust of northeast Minnesota. Geochimica et Cosmochimica Acta, v. 39, pp. 325-362.

Ashley, P.M., 1975. Opaque mineral assemblage formed during serpentinization in the Coolac Ultramafic Belt, New South Wales. Journal of the Geological Society of Australia, v. 22, pp. 91-102.

Ayres, L.D. and Thurston, P.C., 1985. Archean supracrustal sequences in the Canadian Shield: an overview. In: Evolution of Archean Supracrustal Sequences, Ayres, L.D., Thurston, P.C., Card, K.D. and Weber, W. (eds.), Geological Association of Canada Special Paper 28, pp. 343-380.

Ayres, L.D., Thurston, P.C., Card, K.D. and Weber, W., 1985 (eds.). Evolution of Archean Supracrustal Sequences, Geological Association of Canada Special Paper 28.

Baer, A.J., 1981. Geotherms, evolution of the lithosphere and plate tectonics. Tectonophysics, v. 72, pp. 203-227.

Barker, F., 1979. Trondhjemite: definition, environment and hypothesis of origin. In: Trondhjemites, dacites, and related rocks, Barker, F. (ed.), Elsevier, Amsterdam, pp. 1-12.

Barker, F. and Arth, J.G., 1976. Generation of trondhjemitic-tonalitic liquids and Archean bimodal trondhjemite-basalt suites. Geology, v. 4, pp. 596-600.

Barley, M.E. and Groves, D.I., 1990a. Deciphering the tectonic evolution of Archean greenstone belts: the importance of contrasting histories to the distribution of mineralization in the Yilgarn Craton, Western Australia. Precambrian Research, v. 46, pp. 3-20.

Barley, M.E. and Groves, D.I., 1990b. Mesothermal gold mineralization in the Yilgarn Craton, Western Australia, the result of late Archean convergent tectonics? Chron. rech. min., No. 498, pp. 3-13.

Barnes, S.-J., 1987. Unusual nickel and copper to noble-metal ratios from the Råna Layered Intrusion, northern Norway. Norsk Geol. Tidsskr., v. 67, pp. 215-231.

Barnes, S.-J., Naldrett, A.J. and Gorton, M.P., 1985. The origin of the fractionation of platinum-group elements in terrestrial magmas. Chemical Geology, v. 53, 303-323.

Batterson, M., Simpson, A. and Scott, S., 1988. Quaternary mapping and drift exploration in the Central Mineral Belt (13 K/7 and 13 K/10), Labrador. In: Current Research, Newfoundland Department of Mines, Mineral Development Division, Report 88-1, pp. 331-341.

Bickle, M.J., 1978. Heat loss from the Earth: A constraint on Archean tectonics from the relation between geothermal gradients and the rate of plate production. Earth and Planetary Science Letters, v. 40, pp. 301-315.

Bliss, N.W. and MacLean, W.H., 1975. The paragenesis of zoned chromite from central Manitoba. Geochimica et Cosmochimica Acta, v. 39, pp. 973-990.

Bondar, W.F., 1963. Geochemical exploration, Ujutok area, Labrador, 1963. Unpublished BRINEX Report.

Brace, T.D. and Wilton, D.H.C., 1989. Preliminary lithological, petrological, and geochemical investigations of the Archean Florence Lake Group, central Labrador. In: Current Research, Part C, Geological Survey of Canada, Paper 89-1C, pp. 333-344.

Brace, T.D. and Wilton, D.H.C., 1990. Platinum-group elements in the Archean Florence Lake Group, Central Labrador. Canadian Mineralogist, v. 28, pp. 419-429.

Bridgwater, D., Watson, J. and Windley, B.F., 1973. The Archaean craton of the North Atlantic region. Philosophical Transactions of the Royal Society of London, ser. A., v. 273, pp. 493-512.

Brooks, C.K., 1976. The Fe_2O_3/FeO ratio of basaltic analyses: an appeal for a standardized procedure. Bulletin of the Geological Society of Denmark, v. 25, pp. 117-120.

Burrows, D.R. and Spooner, E.T.C., 1989. Relationships between Archean gold quartz vein-shear zone mineralization and igneous intrusions in the Val d'Or and Timmins areas, Abitibi subprovince, Canada. In: The Geology of Gold Deposits: The Perspective in 1988, Keays, R.R., Ramsay, W.R.H. and Groves, D.I. (eds.), Economic Geology Monograph 6, pp. 424-444.

Burrows, D.R., Wood, P.C. and Spooner, E.T.C., 1986. Carbon isotope evidence for a magmatic origin for Archean gold-quartz vein ore deposits. Nature, v. 321, pp. 851-854.

Campbell, I.H., Naldrett, A.J. and Barnes, S.J., 1983. A model for the origin of the platinum-rich sulfide horizons in the Bushveld and Stillwater Complexes. Journal of Petrology, v. 24, pp. 133-165.

Coleman, R.G. and Peterman, Z.E., 1975. Oceanic plagiogranite. Journal of Geophysical Research, v. 80, pp. 1099-1108.

Collerson, K.D., Jesseau, C.W. and Bridgwater, D., 1976. Contrasting types of bladed olivine in ultramafic rocks from the Archean of Labrador. Canadian Journal of Earth Sciences, v. 13, pp. 442-450.

Colvine, A.C., 1989. An empirical model for the formation of Archean gold deposits: products of final cratonization of the Superior Province, Canada. In: The Geology of Gold Deposits: The Perspective in 1988, Keays, R.R., Ramsay, W.R.H. and Groves, D.I. (eds.), Economic Geology Monograph 6, pp. 37- 53.

Colvine, A.C., Fyon, J.A., Heather, K.B., Marmont, S., Smith, P.M. and Troop, D.G., 1988. Archean lode gold deposits in Ontario: Part I. A depositional model; Part II. A genetic model. Ontario Geological Survey Misc. Paper 139, 136 pp.

Condie, K.C., 1976. Trace-element geochemistry of Archean greenstone belts. Earth Science Reviews, v. 12, pp. 393-417.

Condie, K.C., 1981. Archean Greenstone Belts. Elsevier, Amsterdam, 434 pp.

Condie, K.C., 1985. Secular variation in the composition of basalts: An index of mantle evolution. Journal of Petrology, v. 26, pt. 3, pp. 545-563.

Condie, K.C., 1989. Geochemical changes in basalts and andesites across the Archean-Proterozoic boundary: Identification and significance. Lithos, v. 23, pp. 1-18.

Crow, C. and Condie, K.C., 1988. Geochemistry and origin of late Archean volcanics from the Ventersdorp Supergroup, South Africa. Precambrian Research, v. 42, pp. 19-37.

Deer, W.A., Howie, R.A. and Zussman, J., 1963. Rock-Forming Minerals: Vol. 3, Sheet Silicates. Longmans, Green and Company Limited, London, 270 pp.

Dimroth, E., Imreh, L., Cousineau, P., Leduc, M. and Sanschagrin, Y., 1985. Paleogeographic analysis of mafic submarine flows and its use in the exploration for massive sulphide deposits. In: Evolution of Archean Supracrustal Sequences, Ayres, L.D., Thurston, P.C., Card, K.D. and Weber, W. (eds.), Geological Association of Canada Special Paper 28, pp. 203-222.

Duke, J.M., 1986. The Dumont nickel deposit: a genetic model for disseminated magmatic sulphide deposits of komatiitic affinity. In: Metallogeny of Basic and Ultrabasic Rocks, Gallagher, M.J., Ixer, R.A., Neary, C.R. and Prichard, H.M. (eds.), The Institution of Mining and Metallurgy, pp. 151-160.

Dupuy, C. and Dostal., J., 1984. Trace element geochemistry of some continental tholeiites. Earth and Planetary Science Letters, v. 67, pp. 61-69.

Earthrowl, J.A., 1964. Final Report 1964. Cliffs - BRINEX joint area, Ujuktok Concession, Labrador, Unpublished BRINEX Report.

Ellingwood, S., 1959. Geology of the Ujutok Bay greenstone belt, Labrador. Unpublished BRINEX Report, 3 maps.

Emslie, R.F., Loveridge, W.D., and Stevens, R.D., 1984. The Mealy dykes, Labrador: petrology, age, and tectonic significance. Canadian Journal of Earth Sciences, v. 21, pp. 437-446.

Ermanovics, I., 1980. Geology of the Hopedale Block of Nain Province: Report 2, Nain-Makkovik boundary zone. In: Current Research, Part B, Geological Survey of Canada, Paper 80-1B, pp. 11-15.

Ermanovics, I. and Korstgård, J.A., 1981. Geology of Hopedale block and adjacent areas, Labrador: Report 3. In: Current Research, Part A, Geological Survey of Canada, Paper 81-1A, pp. 69-76.

Ermanovics, I., Korstgård, J.A. and Bridgwater, D., 1982. Structural and lithological chronology of the Archean Hopedale block and the adjacent Proterozoic Makkovik Subprovince, Labrador: Report 4. In: Current Research, Part B, Geological Survey of Canada, Paper 82-1B, pp. 153-165.

Ermanovics, I. and Raudsepp, M., 1979a. Geology of the Hopedale block of eastern Nain Province, Labrador: Report 1. In: Current Research, Part B, Geological Survey of Canada, Paper 79-1B, pp. 341-348.

Ermanovics, I. and Raudsepp, M., 1979b. Adlatok Bay - Florence Lake map-area, (parts of 13N/1,2 and 13K/15). Geological Survey of Canada, Open File 580.

Fodor, R.V. and Vetter, S.K., 1984. Rift-zone magmatism: petrology of basaltic rocks transitional from CFB to MORB, southeastern Brazil margin. Contributions to Mineralogy and Petrology, v. 88, pp. 307-321.

Franklin, J.M., Lydon, J.W. and Sangster, D.F., 1981. Volcanic-associated massive sulphide deposits. Economic Geology, 75th Anniversary Volume, pp. 485-627.

Fyon, J.A., Troop, D.G., Marmont, S. and Macdonald, A.J., 1989. Introduction of gold into Archean crust, Superior Province, Ontario - coupling between mantle-initiated magmatism and lower crustal thermal maturation. In: The Geology of Gold Deposits: The Perspective in 1988, Keays, R.R., Ramsay, W.R.H. and Groves, D.I. (eds.), Economic Geology Monograph 6, pp. 479-490.

Gill, J.B., 1981. Orogenic andesites and plate tectonics. Springer-Verlag, New York, 390 pp.

Glikson, A.Y. and Hickman, A.H., 1981. Geochemistry of Archean volcanic successions, eastern Pilbara block, Western Australia. Australian Bureau of Mineral Resources, Geophysical Rec., 1981/36.

Glikson, A.Y., Pride, C., Jahn, B., Davy, R. and Hickman, A.H., 1986. RE and HFS element evolution of Archean mafic-ultramafic volcanic suites, Pilbara block, Western Australia. Australian Bureau of Mineral Resources, Geophysical Rec., 1986/6.

Gower, C.F., Rivers, T. and Brewer, T.S., in press. Middle Proterozoic mafic magmatism in Labrador, eastern Canada. In: Geological Association of Canada Special Paper.

Grant, N.K., Voner, F.R., Marzano, M.S., Hickman, M.H. and Ermanovics, I.F., 1983. A summary of Rb-Sr isotope studies in the Archaean Hopedale Block and the adjacent Proterozoic Makkovik Subprovince, Labrador: Report 5. In: Current Research, Part B, Geological Survey of Canada, Paper 83-1B, pp. 127-134.

Green, D.H., 1981. Petrogenesis of Archean ultramafic magmas and implications for Archean tectonics. In: Precambrian Plate Tectonics, Kröner, A. (ed.), Elsevier, Amsterdam, pp. 469-489.

Green, D.H., Nicholls, I.A., Viljoen, M.J. and Viljoen, R.P., 1975. Experimental demonstration of the existence of peridotite liquids in earliest Archaean magmatism. Geology, v. 3, pp. 11-14.

Gresham, J.J., 1986. Depositional environments of volcanic peridotite-associated nickel sulphide deposits with special reference to the Kambalda Dome. In: Geology and Metallogeny of Copper Deposits, Friedrich, G.H., Genkin, A.D., Naldrett, A.J., Ridge, J.D., Sillitoe, R.H. and Vokes, F.M. (eds.), Springer-Verlag, Berlin, pp. 63-90.

Groves, D.I., Barley, M.E. and Ho, S.E., 1989. Nature, genesis, and tectonic setting of mesothermal gold mineralization in the Yilgarn Block, Western Australia. In: The Geology of Gold Deposits: The Perspective in 1988, Keays, R.R., Ramsay, W.R.H. and Groves, D.I. (eds.), Economic Geology Monograph 6, pp. 71-85.

Groves, D.I. and Batt, W.D., 1984. Spatial and temporal variations of Archaean metallogenic associations in terms of evolution of granitoid-greenstone terrains with particular emphasis on the western Australian Shield. In: Archaean Geochemistry, Kröner, A., Hanson, G.N. and Goodwin, A.M. (eds.), Springer-Verlag, Berlin, pp. 73-98.

Groves, D.I., Hudson, D.R. and Hack, T.B.C., 1974. Modification of iron-nickel sulfides during serpentinization and talc-carbonate alteration at Black Swan, Western Australia. Economic Geology, v. 69, pp. 1265-1281.

Groves, D.I. and Keays, R.R., 1979. Mobilization of ore-forming elements during alteration of dunites, Mt. Keith-Betheno, Western Australia. Canadian Mineralogist, v. 17, pp. 373-389.

Groves, D.I., Korkiakoski, E.A., McNaughton, N.J., Lesher, C.M. and Cowden, A., 1986. Thermal erosion by komatiites at Kambalda, Western Australia and the genesis of nickel ores. Nature, v. 319, pp. 136-139.

Guthrie, A.E., 1983. Report on exploration in the Florence Lake Greenstone Belt. BP Minerals Ltd. - Billiton Canada Ltd. Joint Venture, 1982. Unpublished BP Minerals Ltd. Report.

Hansuld, J.A., 1959. Geochemical exploration in Ujutok greenstone belt, Asbestos Corporation Joint area, 1959. Unpublished BRINEX Report.

Hargraves, R.B., 1986. Faster spreading or greater ridge length in the Archean? Geology, v. 14, pp. 750-752.

Hawkesworth, C.J. and O'Nions, R.K., 1977. The petrogenesis of some Archaean volcanic rocks from Southern Africa. Journal of Petrology, v. 18, part 3, pp. 487-520.

Helmstaedt, H., Padham, W.A. and Brophy, J.A., 1986. Multiple dikes in Lower Kam Group, Yellowknife greenstone belt: Evidence for Archean sea-floor spreading? Geology, v. 14, pp. 562-566.

Henderson, J.B., 1981. Archean basin evolution in the Slave Province, Canada. In: Plate Tectonics in the Precambrian, Kröner, A. (ed.), Elsevier, Amsterdam, pp. 213-235.

Hoffman, P.F., 1988. United Plates of America, the birth of a craton: early Proterozoic assembly and growth of Laurentia. Annual Reviews in Earth and Planetary Sciences, v. 16, pp. 543-603.

Hofmann, A.W., 1988. Chemical differentiation of the Earth: the relationship between mantle, continental crust, and oceanic crust. Earth and Planetary Science Letters, v. 90, pp. 297-314.

Holm, P.E., 1985. The geochemical fingerprints of different tectonomagmatic environments using hygromagmatophile element abundances of tholeiitic basalts and basaltic andesites. Chemical Geology, v. 51, pp. 303-323.

Hughes, C.J., 1973. Spilites, keratophyres, and the igneous spectrum. Geological Magazine, v. 109, no. 6, pp. 513-527.

Huppert, H.E., Sparks, R.S.J., Turner, J.S. and Arndt, N.T., 1984. emplacement and cooling of komatiite lavas. Nature, v. 309, pp. 19-22.

Hutchinson, R.W., 1982. Syn-depositional hydrothermal processes and Precambrian sulphide deposits. In: Precambrian Sulphide Deposits, Hutchinson, R.W., Spence, C.D. and Franklin, J.M. (eds.), The Geological Association of Canada Special Paper 25, pp. 761-791.

Hutchinson, R.W., 1984. Archaean metallogeny: a synthesis and review. Journal of Geodynamics, v. 1, pp. 339-358.

Irvine, T.N., 1967. Chromian spinels as a petrogenetic indicator. Part II. Petrologic applications. Canadian Journal of Earth Sciences, v. 4, pp. 71-103.

Irvine, T.N., 1975. Crystallisation sequences in the Muskox intrusion and other layered intrusions - II. Origin of chromitite layers and similar deposits of magmatic ores. Geochimica et Cosmochimica Acta, v. 39, pp. 991-1020.

Irvine, T.N., 1977. Origin of chromitite layers in the Muskox intrusion: A new interpretation. Geology, v. 5, pp. 273-277.

Irvine, T.N. and Baragar, W.R.A., 1971. A guide to the chemical classification of the common volcanic rocks. Canadian Journal of Earth Sciences, v. 8, pp. 523-548.

Jagodits, F.L., 1983. Unpublished Excalibur International Consultants Ltd. Report, Submitted to B.P. Minerals Ltd. - Billiton Canada Ltd.

Jahn, B.-M., Auvray, B., Blais, S., Capdevila, R., Cornichet, J., Vidal, F. and Hameurt, J., 1980. Trace element geochemistry and petrogenesis of Finnish greenstone belts. Journal of Petrology, v. 21, pt. 2, pp. 201-244.

Jahn, B.-M., Gruau, G. and Glikson, A.Y., 1982. Komatiites of the Onverwacht Group, S. Africa: REE geochemistry, Sm/Nd age and mantle evolution. Contributions to Mineralogy and Petrology, v. 80, pp. 25-40.

Jensen, L.S., 1976. A new cation plot for classifying subalkalic volcanic rocks. Ontario Division of Mines, Miscellaneous Paper 66.

Jesseau, C.W., 1976. A structural-metamorphic and geochemical study of the Hunt River supracrustal belt, Nain Province, Labrador. Unpublished M.SC. thesis, Memorial University of Newfoundland, St. John's, 211 pp.

Jochum, K.P., Seufert, H.M., Spettel, B. and Palme, H., 1986. The solar system abundances of Nb, Ta and Y and the relative abundances of refractory lithophile elements in differentiated planetary bodies. Geochimica et Cosmochimica Acta, v. 50, pp. 1173-1183.

Korstgård, J.A. and Ermanovics, I., 1984. Archaean and early Proterozoic tectonics of the Hopedale Block, Labrador, Canada. In: Precambrian Tectonics Illustrated, Kröner, A. and Greiling, R. (eds.), E. Scwriz. Verlag, Germany, pp. 295-318.

Korstgård, J. and Ermanovics, I., 1985. Tectonic evolution of the Archean Hopedale Block and the adjacent Makkovik Subprovince, Labrador, Newfoundland. In: Evolution of Archean Supracrustal Sequences, Ayres, L.D., Thurston, P.C., Card, K.D. and Weber, W. (eds.), Geological Association of Canada Special Paper 28, pp. 223-237.

le Roex, A.P., Dick, H.J.B., Erlank, A.J., Reid, A.M., Frey, F.A. and Hart, S.R., 1983. Geochemistry, mineralogy and petrogenesis of lavas erupted along the southwest Indian ridge between the Bouvet triple junction and 11 degrees east. Journal of Petrology, v. 24, pp. 267-318.

Lesher, C.M., Arndt, N.T. and Groves, D.I., 1984. Genesis of komatiite-associated nickel sulphide deposits at Kambalda, Western Australia: A distal volcanic model. In: Sulphide Deposits in Mafic and Ultramafic Rocks, Buchanan, D.L. and Jones, M.J. (eds.), The Institute of Mining and Metallurgy, pp. 70-80.

Lesher, C.M. and Groves, D.I., 1986. Controls on the formation of komatiite-associated nickel-copper sulphide deposits. In: Geology and Metallogeny of Copper Deposits, Friedrich, G.H., Genkin, A.D., Naldrett, A.J., Ridge, J.D., Sillitoe, R.H. and Vokes, F.M. (eds.), Springer-Verlag, Berlin, pp. 43-62.

Lesher, C.M. and Keays, R.R., 1984. Metamorphically and hydrothermally mobilized Fe-Ni-Cu sulphides at Kambalda, Western Australia. In: Sulphide Deposits in Mafic and Ultramafic Rocks, Buchanan, D.L. and Jones, M.J. (eds.), The Institution of Mining and Metallurgy, London, pp. 62-69.

Loveridge, W.D., Ermanovics, I.F. and Sullivan, R.W., 1987. U-Pb ages on zircon from the Maggo Gneiss, the Kanairiktok Plutonic Suite and the Island Harbour Plutonic Suite, coast of Labrador, Newfoundland. In: Radiogenic Age and Isotopic Studies: Report 1, Geological Survey of Canada, Paper 87-2, pp. 59-65.

Lowe, D.R., 1985. Sedimentary environment as a control on the formation and preservation of Archean volcanogenic massive sulphide deposits. In: Evolution of Archean Supracrustal Sequences, Ayres, L.D., Thurston, P.C., Card, K.D. and Weber, W. (eds.), Geological Association of Canada Special Paper 28, pp. 193-201.

Ludden, J. and Hubert, C., 1986. Geologic evolution of the Late Archean Abitibi greenstone belt of Canada. Geology, v. 14, pp. 707-711.

Lydon, J.W., 1984. Ore Deposit Models - 8. Volcanogenic Massive Sulphide Deposits Part I: A Descriptive Model. Geoscience Canada, v. 11, no. 4, pp. 195-202.

Mayor, J.N. and Mann, E.L., 1960. Geological Report of an area to the West of Florence Lake. Unpublished BRINEX Report.

McCallum, M.E., Loucks, R.R., Carlson, R.R., Cooley, E.F. and Doerge, T.A., 1976. Platinum metals associated with hydrothermal copper ores of the New Rambler mine, Medicine Bow Mountains, Wyoming. Economic Geology, v. 71, pp. 1429-1450.

Meschede, M., 1986. A method of discriminating between different types of mid-ocean ridge basalts and continental tholeiites with the Nb-Zr-Y diagram. Chemical Geology, v. 56, pp. 207-218.

Meyers, R.E. and Emslie, R.F., 1977. The Harp dikes and their relationship to the Helikian geological record in central Labrador. Canadian Journal of Earth Sciences, v. 14, pp. 2683-2696.

Moody, J.B., 1976. Serpentinization: a review. Lithos, v. 9, pp. 125-138.

Morris, J.D. and Hart, S.R., 1986. Reply to: Comment on "Isotopic and incompatible element constraints on the genesis of island arc volcanics from Cold Bay and Amak Island, Aleutians, and implications for mantle structure". Geochimica et Cosmochimica Acta, v. 50, pp. 483-487.

Mountain, B.W. and Wood, S.A., 1988. Chemical controls on the solubility, transport, and deposition of platinum and palladium in hydrothermal solutions: a thermodynamic approach. Economic Geology, v. 83, pp. 492-510.

Myers, R.E. and Breitkopf, J.H., 1989. Basalt geochemistry and tectonic settings: a new approach to relate tectonic and magmatic processes. Lithos, v. 23, pp. 53-62.

Naldrett, A.J., 1973. Nickel sulphide deposits - their classification and genesis with special emphasis on deposits of volcanic association. Canadian Institute of Mining and Metallurgy Bulletin, v. 66, pp. 45-63.

Naldrett, A.J., 1981. Platinum-group element deposits. In: Platinum-Group Elements: Mineralogy, Geology, Recovery, Cabri, L.J. (ed.), Canadian Institute of Mining and Metallurgy, Special Volume 23, pp. 197-231.

Naldrett, A.J. and Cabri, L.J., 1976. Ultramafic and related mafic rocks: their classification and genesis with special reference to the concentration of nickel sulfides and platinum-group elements. Economic Geology, v. 71, pp. 1131-1158.

Naldrett, A.J. and Duke, J.M., 1980. Platinum metals in magmatic sulfide ores. Science, v. 208, pp. 1417-1424.

Naldrett, A.J. and Macdonald, A.J., 1980. Tectonic settings of some Ni-Cu sulfide ores: their importance in genesis and exploration. In: The Continental Crust and its Mineral Deposits, Strangway, D.W. (ed.), Geological Association of Canada, Special Paper 20, pp. 633-657.

NEWPET, (1990). A geochemical data plotting program. Department of Earth Sciences - Centre for Earth Resources Research, Memorial University of Newfoundland.

Nisbet, E.G., 1987. The Young Earth: An introduction to Archaean geology. Allen & Unwin, Boston, 402 p.

Nisbet, E.G. and Fowler, C.M.R., 1983. Model for Archean plate tectonics. Geology, v. 11, pp. 376-379.

Nisbet, E.G. and Pearce, J.A., 1977. Clinopyroxene composition in mafic lavas from different tectonic settings. Contributions to Mineralogy and Petrology, v. 63, pp. 149-160.

O'Connor, J.T., 1965. A classification of quartz-rich igneous rocks based on feldspar ratios. U.S. Geological Survey Prof. Paper 525-B.

Pearce, J.A., 1983. Role of sub-continental lithosphere in magma genesis at active continental margins. In: Continental Basalts and Mantle Xenoliths, Hawkesworth, C.J. and Norry, M.J. (eds.), Shiva Publishing Limited, pp. 230-249.

Pearce, J.A. and Cann, J.R., 1973. Tectonic setting of basic volcanic rocks determined using trace element analyses. Earth and Planetary Science Letters, v. 19, pp. 290-300.

Pearce, J.A., Harris, N.B.W. and Tindle, A.G., 1984. Trace element discrimination diagrams for the tectonic interpretation of granitic rocks. Journal of Petrology, v. 25, pt. 4, pp. 956-983.

Pearce, T.H., Gorman, B.E. and Birkett, T.C., 1975. The TiO_2-K_2O-P_2O_5 diagram: a method of discriminating between oceanic and non-oceanic basalts. Earth and Planetary Science Letters, v. 24, pp. 419-426.

Pearton, T.N., 1982. Gold and antimony mineralization in altered komatiites of the Murchison greenstone belt, South Africa. In: Komatiites, Arndt, N.T. and Nisbet, E.G. (eds.), George Allen & Unwin, London, pp. 459-475.

Perfit, M.R. and Kay, R.W., 1986. Comment on "Isotopic and incompatible element constraints on the genesis of island arc volcanics from Cold Bay and Amak Island, Aleutians, and implications for mantle structure". Geochimica et Cosmochimica Acta, v. 50, pp. 477-481.

Piloski, M.J., 1960. Report on exploration in the Asbestos Corporation - BRINEX joint area, Hopedale - Kaipokok area, Labrador, 1960. Unpublished BRINEX Report.

Piloski, M.J., 1962. Report on exploration in the Asbestos Corporation - BRINEX joint area, Hopedale - Kaipokok area, Labrador, 1961. Unpublished BRINEX Report.

Piloski, M.J., 1963. Report on exploration in the Asbestos Corporation - BRINEX joint area, Hopedale - Kaipokok area, Labrador, 1962. Unpublished BRINEX Report.

Reusch, D., 1987. Proposed exploration program for Baikie property, Florence Lake area, Labrador (NTS: 13 K/15). Unpublished Platinum Exploration Canada Inc. Report.

Roberts, R.G., 1987. Ore deposit models #11. Archean lode gold deposits. Geoscience Canada, v. 14, no. 1, pp. 37-52.

Roderick, S., 1959a. Geophysical investigations in the Asbestos Corporation joint area, Labrador, 1959. Unpublished BRINEX Report.

Roderick, S., 1959b. Interpretation of ground magnetometer survey, Ugjuktok Serpentine belt, Asbestos Corporation joint area, Labrador. Unpublished BRINEX Report.

Rowell, W.F. and Edgar, A.D., 1986. Platinum-group element mineralization in a hydrothermal Cu-Ni sulfide occurrence, Rathbun Lake, northeastern Ontario. Economic Geology, v. 81, pp. 1272-1277.

Ryan, B., 1984. Regional geology of the central part of the Central Mineral Belt, Labrador. Newfoundland Department of Mines and Energy Memoir 3, 185 p.

Sangster, D.F. and Scott, S.D., 1976. Precambrian strata-bound, massive Cu-Zn-Pb sulphide ores of North America. In: Handbook of Stratibound and Stratiform Ore Deposits, Wolf, K.H. (ed.), Elsevier, Amsterdam, v. 6, pp. 130-221.

Saunders, A.D. and Tarney, J., 1984. Geochemical characteristics of basaltic volcanism within back-arc basins. In: Marginal Basin Geology. Kokelaar, B.P. and Howells, M.F. (eds.), Geological Society Special Publication, No. 16, Blackwell Scientific, Oxford, pp. 59-76.

Saunders, A.D., Tarney, N.G., Marsh, N.G. and Wood, D.A., 1979. Ophiolites as ocean crust or marginal basin crust: a geochemical approach. In: Ophiolites, Proceedings of the International Ophiolite Symposium, Panayiotou, A. (ed.), Cyprus Geological Survey Department, Nicosia, pp. 193-204.

Sleep, N.H. and Windley, B.F., 1982. Archean plate tectonics: Constraints and inferences. Journal of Geology, v. 90, pp. 363-379.

Stauffer, M.R., Mukherjee, A.C. and Koo, J., 1975. The Amisk Group: an Aphebian (?) island arc deposit. Canadian Journal of Earth Sciences, v. 12, pp. 2021-2035.

Stewart, J.W., 1983. BP Minerals - Billiton joint venture, Florence Lake, Labrador, Summer 1983, Preliminary Report, BP Minerals Ltd. Unpublished BP Minerals Ltd. Report.

Sun, S.-S., 1980. Lead isotopic study of young volcanic rocks from mid-ocean ridges, ocean islands and island arcs. Philosophical Transactions of the Royal Society of London, A 297, pp. 409-446.

Sun, S.-S., 1984. Geochemical characteristics of Archean ultramafic and mafic volcanic rocks: Implications for mantle composition and evolution. In:
Archaean Geochemistry, Kröner, A., Hanson, G.N. and Goodwin, A.M. (eds.), Springer-Verlag, Berlin, pp. 25-46.

Sun, S.-S., 1987. Chemical composition of Archaean komatiites: implications for early history of the Earth and mantle evolution. Journal of Volcanology and Geothermal Research, v. 32, pp. 67-82.

Sutton, J.S., 1970. Geological report - area northwest of Florence Lake, Ugjuktok area, Labrador. Unpublished BRINEX Report.

Sutton, J.S., 1971. Geological report - south end of Ugjuktok Bay, Labrador. Unpublished BRINEX Report.

Tarney, J., 1977. Petrology, mineralogy and geochemistry of the Falkland Plateau basement rocks, Site 330, Deep Sea Drilling Project. In: Initial Reports of the Deep Sea Drilling Project, v. 36, pp. 893-921.

Tarney, J., Dalziel, I.W.D. and de Wit, M.J., 1976. Marginal basin 'Rocas Verdes' complex from S. Chile: A model for Archaean greenstone belt formation. In: The early history of the Earth, Windley, B.F. (ed.), Wiley, London, pp. 131-146.

Tarney, J. and Weaver, B.L., 1987. Geochemistry and petrogenesis of Early Proterozoic dyke swarms. In: Mafic Dyke Swarms, Halls, H.C. and Fahrig, W.F. (eds.), Geological Association of Canada Special Paper 34, pp. 81-94.

Taylor, F.C., 1971. A revision of Precambrian structural provinces in northeastern Quebec and northern Labrador. Canadian Journal of Earth Sciences, v. 8, pp. 579-584.

Taylor, S.R. and McLennan, S.M., 1985. The Continental Crust: its Composition and Evolution. Blackwell Scientific Publications, Oxford, 312 pp.

Thompson, F.J. and Klassen, R.A., 1986. Ice flow directions and drift composition, central Labrador. In: Current Research, Part A, Geological Survey of Canada, Paper 86-1A, pp. 713-717.

Thompson, R.N., Morrison, M.A., Dicken, A.P. and Hendry, G.L., 1983. Continental flood basalts ... arachnids rule OK?. In: Continental Basalts and Mantle Xenoliths, Hawkesworth, C.J. and Norry, M.J. (eds.), Shiva Publishing Limited, pp. 158-185.

Thompson, R.N., Morrison, M.A., Hendry, G.L. and Parry, S.J., 1984. An assessment of the relative roles of crust and mantle in magma genesis: an elemental approach. Philosophical Transactions of the Royal Society of London, v. A310, pp. 549-590.

Thurston, P.C. and Chivers, K.M., 1990. Secular variation in greenstone sequence development emphasizing Superior Province, Canada. Precambrian Research, v. 46, pp. 21-58.

Voner, F.R., 1985. Crustal evolution of the Hopedale Block, Labrador, Canada. Unpublished Ph.D. dissertation, Miami University, Oxford, Ohio.

Wakita, H., Rey, P. and Schmitt, R.A., 1971. Abundances of the 14 rare-earth elements and 12 other trace elements in Apollo 12 samples: five igneous and one breccia rocks and four soils. Proceedings of the Second Lunar Science Conference, pp. 1319-1329.

Wardle, R.J., Rivers, T., Gower, C.F., Nunn, G.A.G. and Thomas, A., 1986. The northeastern Grenville Province: new insights. In: The Grenville Province, Moore, J.M., Davidson, A. and Baer, A.J. (eds.), Geological Association of Canada Special Paper 33, pp. 13-30.

Westoll, N.D.S., 1971. Summary of nickel exploration in southern Labrador. Unpublished BRINEX Report.

Wiebe, R.A., 1985. Proterozoic basalt dikes in the Nain anorthosite complex, Labrador. Canadian Journal of Earth Sciences, v. 22, no. 8, pp. 1149-1157.

Wilson, B.T., 1959. Report on the airborne geophysical survey of the Ujutok Bay area, Labrador, for British Newfoundland Exploration Limited. Unpublished Lundburg Explorations Report.

Wilson, G.C., 1988. A critique of the normalisation of PGE to 100% sulphide. In: The platinum group of elements in Ontario. Ontario Geological Survey Open File Report 5681, pp. 173-176.

Wilton, D.H.C., 1987. Report on the geology and geochemistry of the Baikie Property, northeast of Florence Lake, Labrador. Unpublished Platinum Exploration Canada Inc. Report.

Wilton, D.H.C., in press. Metallogeny of the Labrador Central Mineral Belt. Geological Survey of Canada Paper.

Wilton, D.H.C., MacDougall, C.S., MacKenzie, L.M. and Pumphrey, C., 1988. Stratigraphy and metallogeny of the Moran Lake Group, northeast of Moran Lake. In: Current Research, Part C, Geological Survey of Canada, Paper 88-1C, pp. 277-282.

Winchester, J.A. and Floyd, P.A., 1977. Geochemical discrimination of different magma series and their differentiation products using immobile elements. Chemical Geology, v. 20, pp. 325-343.

Winchester, J.A., Max, M.D. and Long, C.B., 1987. Trace element geochemical correlation in the reworked Proterozoic Dalradian metavolcanic suites of the western Ox Mountains and NW Mayo Inliers, Ireland. In: Geochemistry and Mineralization of Proterozoic Volcanic Suites, Pharaoh, T.C., Beckinsale, R.D. and Rickard, D. (eds.), Geological Society Special Publication No. 33, pp. 489-502.

Winchester, J.A., Park, R.G. and Holland, J.G., 1980. The geochemistry of Lewisian semipelitic schists from the Gairloch District, Wester Ross. Scottish Journal of Geology, v. 16, pp. 165-179.

Winkler, H.G.F., 1979. Petrogenesis of Metamorphic Rocks (Fifth Edition). Springer-Verlag, Berlin, 348 pp.

Wood, D.A., Joron, J.-L and Treuil, M., 1979. A re-appraisal of the use of trace elements to classify and discriminate between magma series erupted in different tectonic settings. Earth and Planetary Science Letters, v. 45, pp. 326-336.

Yagi, K. and Onuma, K., 1967. The join $CaMgSi_2O_6$-$CaTiAl_2O_6$ and its bearing on the titanaugites. Journal of the Faculty of Science Hokkaido University, ser. 4, v. 13, pp. 463-483.

APPENDIX 1

WHOLE ROCK GEOCHEMICAL METHODS

1.1. Sample Preparation

Representative hand-sized grab samples were collected for geochemical analysis. In order to remove weathered surfaces and contaminants such as veins, the samples were cut into small blocks using a rotary rock-cutting diamond table saw. The blocks were then crushed in a steel jaw crusher, and pulverized in a tungsten-carbide bowl and puck assembly to produce a -100 mesh whole rock powder.

1.2. Major Element Analyses

Major element oxides were determined by atomic absorption (AA) spectrometry. Samples were prepared using the methods of Langmhyr and Paus (1968), and analyses were carried out on a Perkin-Elmer Model 370 atomic absorption spectrometer with digital readout. P_2O_5 was analyzed with a Bausch and Lomb Spectronic 20 Colourimeter, based on a modification of the method outlined by Shapiro and Brannock (1962). Aqua-regia dissolution was required for sulphide-rich samples. The precision of the method is shown in Table 1.

Loss on ignition (L.O.I.), which reflects the volatile content of the sample, was determined by weighing an aliquot of rock powder (weighed accurately to 10^{-4} g) into a porcelain crucible, heating the crucible to 1050°C for at least two hours, cooling in a desiccator, and then weighing the de-volatized sample for percent loss of volatiles.

Table 1. Precision of major element analyses based on four analyses of standard G-2.

Element	Published Value	Mean	S.D.	Range Low	Range High
SiO2	69.11	69.70	0.57	68.50	69.96
TiO2	0.50	0.50	0.01	0.47	0.51
Al2O3	15.40	15.10	0.24	14.75	15.60
Fe2O3	2.65	2.60	0.02	2.64	2.74
MnO	0.03	0.03	0.00	---	---
MgO	0.76	0.80	0.005	0.75	0.82
CaO	1.94	0.00	0.10	1.92	2.14
Na2O	4.07	4.30	0.02	4.07	4.21
K2O	4.51	4.56	0.02	4.50	4.57

Published values are from Flanagan (1970).

Table 2. Precision and accuracy of XRF trace element analyses (from Longerich and Veinott, 1986).

	Standard W-1 (N=10)			Standard BCR-1 (N=10)		
Element	Accepted	Determined	%RSD	Accepted	Determined	%RSD
Cr	115	123	2.4	15	40	14.6
Ni	76	77	3.3	10	21	13.9
V	260	252	2.0	420	407	1.5
Cu	110	105	2.5	16	25	5.2
Zn	86	94	3.2	125	126	3.3
Ba	160	181	3.4	680	773	1.8
Ga	16	15	9.4	22	18	11.6
Zr	105	94	2.4	185	193	1.1
Y	25	28	5.8	40	42	6.6

1.3. Trace Element Analyses (XRF Spectrometry)

Trace elements including Cr, Ni, V, Cu, Zn, Ba, Ga, Y and Zr were determined by X-Ray fluorescence (XRF) techniques on pressed whole rock powder pellets using a Phillips 1450 automatic X-Ray fluorescence spectrometer with a rhodium tube. The pellets were made by combining 10 ± 1 g of sample with 1.45 ± 0.05 g of Phenol binding material. The powder was pressed at 30 tonnes psi for 8 seconds, and was then baked for 15 to 20 minutes at 200°C. Data reduction was performed by a Hewlett-Packard 9845B mini computer.

Precision and accuracy for the trace elements are given in Table 2, using the geological reference standards W-1 and BCR-1.

1.4. Trace Element and Rare Earth Element Analyses (ICP-MS)

Trace elements including Sc, Rb, Sr, Nb, Y, Pb, Th and U, and the rare earth elements (REE) were determined by inductively coupled plasma-mass spectrometry (ICP-MS) on a SCIEX ELAN model 250 ICP-MS using a modified standard addition procedure to correct for matrix effects. A comprehensive description of the ICP-MS technique at the Department of Earth Sciences, Memorial University of Newfoundland, is given in Jenner et al. (1990) and Longerich et al. (1990).

Whole rock powders (0.1 g) are dissolved in a small Teflon beaker using HNO_3 and HF. After the HNO_3-HF mixture has evaporated, the sample is taken into solution in HNO3, evaporated to dryness, taken up in 2-3 ml of 8 N HNO_3,

transferred to a 125-ml bottle, and diluted with water to 90 g. A standard run of trace and rare earth element analyses on the ICP-MS consists of 16 unknowns (including 3 duplicates), a reference material (SY-2) and a reagent blank.

The detection limits, and precision and accuracy of the ICP-MS technique are given in Table 3.

1.5. Precious Metal Analyses (Platinum-Group Elements and Gold)

Precious metals including platinum-group elements (PGE) and gold were determined using inductively coupled plasma-mass spectrometry (ICP-MS).

The procedure used for collecting PGE and Au combines the standard NiS fire-assay technique (Robert et al., 1971) accompanied by Te precipitation (Fryer and Kerrich, 1978) which significantly improves recovery of PGE and Au. A NiS button is prepared by fusing 15.0 g of rock powder with a mixture of Ni, S, sodium carbonate, borax and silica. The button is then dissolved in concentrated HCl, and a Te solution is added to form a precipitate which collects the PGE and Au. Concentrated HNO_3 is then added, which dissolves the precipitate, and the solution is analyzed by ICP-MS using two internal standards to correct for instrument drift and matrix effects; Cd for the light metals (Ru, Rh and Pd) and Tl for the heavy metals (Os, Ir, Pt and Au) (Jackson et al., 1990). Minor modifications to the standard preparation procedure are required for samples containing significant concentrations of

Table 3. Detection limits, and precision and accuracy of ICP-MS trace and rare earth element analyses (from Jenner et al., 1990).

	Detection Limits (ppm)			Precision and Accuracy for Standard W-1			
	Mean	Minimum	Maximum	ICP-MS (MUN)* (N=6)	Compiled values	Preferred values	SD (ppm)
Sc	1.7	0.17	4.2	35	35		2
Rb	0.12	0.016	0.4	22	21.4	21.6	2
Sr	0.2	0.03	0.9	191	186	193	5
Nb	0.015	0.0010	0.06	7.5	9.9	7.9	0.5
Y	0.009	0.0017	0.03	21.9	26	22.6	0.8
Pb	0.07	0.011	0.5	7.0	7.5	7.83	0.4
Th	0.013	0.003	0.03	2.21	2.4	2.65	0.07
U	0.014	0.002	0.05	0.57	0.57	0.605	0.02
La	0.011	0.0014	0.03	10.6	11	10.9	0.2
Ce	0.009	0.0020	0.03	23.1	23.5	24.0	0.3
Pr	0.009	0.0011	0.02	2.93	3.2	3.27	0.04
Nd	0.04	0.005	0.14	12.9	14.6	14.4	0.3
Sm	0.03	0.007	0.14	3.3	3.68	3.65	0.1
Eu	0.009	0.0018	0.03	1.16	1.12	1.14	0.02
Gd	0.03	0.003	0.08	3.84	4.01	4.24	0.09
Tb	0.006	0.0009	0.019	0.64	0.63	0.645	0.645
Dy	0.018	0.004	0.07	4.1	3.99	4.18	0.1
Ho	0.006	0.0008	0.020	0.86	0.81	0.803	0.03
Er	0.02	0.006	0.07	2.21	2.3	2.25	0.06
Tm	0.007	0.0014	0.02	0.31	0.34	0.333	0.01
Yb	0.02	0.003	0.10	2.13	2.03	2.17	0.04
Lu	0.006	0.0009	0.03	0.30	0.32	0.34	0.01

* from Jenner et al. (1990).

Preferred values compiled from Jochum et al. (1988, 1989).

Compiled values are from Govindaraju (1989).

one or more of chromite, Ni, S, Cu or Zn.

The measured instrumental detection limits for the four production runs containing samples of this study ranged from 0.12-0.27 ppb (Ru), 0.02-0.28 ppb (Rh), 0.21-0.59 ppb (Pd), 0.05-0.11 ppb (Re), 0.31-0.83 ppb (Os), 0.04-0.07 ppb (Ir), 0.12-0.27 ppb (Pt) and 0.26-5.687 ppb (Au). The precision and accuracy of PGE and Au analyses by the ICP-MS method are given in Table 4 (from Jackson et al., 1990).

Table 4. Precision and accuracy of ICP-MS precious metal analyses for standard SARM-7 (from Jackson et al., 1990).

Element	Certified	ICP-MS (MUN)*	n	RSD (%)	Rel. Diff. (%)
Ru	430 ± 57	397	29	14.0	-7.6
Rh	240 ± 13	212	29	8.6	-11.8
Pd	1,530 ± 32	1,353	29	10.5	-11.5
Os	63 ± 7	53	7	18.0	-15.4
Ir	74 ± 12	71	29	10.0	-3.7
Pt	3,740 ± 45	3,395	29	13.5	-9.2
Au	310 ± 15	253	28**	19.8	-18.3

Certified values are from Steele et al. (1975).
* Values from Jackson et al. (1990).
** One statistically deviant determination of 736 ppb excluded.
n = number of preparations.

APPENDIX 2

MINERAL IDENTIFICATION AND ANALYSES

2.1. Electron Microprobe Analyses

Silicate and carbonate mineral analyses were carried out using a JEOL JXA-50A electron probe microanalyzer with three spectrometers, controlled automatically by a Krisel control and a Digital PDP-11 mini computer. Operating conditions were: accelerating voltage of 15 Kv, beam current approximately 0.22 mA, beam size 1-2 micrometres, and a counting rate up to 60,000 with a default time of 30 seconds. Data reduction was carried out with the Alpha correction program using the method of Bence and Albee (1968). Analyses of anhydrous silicate minerals were considered acceptable if totals fell within the range of 99-101 wt.%.

2.2. Scanning Electron Microscopy

Carbon-coated, polished thin sections were examined using a Hitachi S570 scanning electron microscope at an accelerating voltage of 15-20 Kv. Backscattered electron imaging was obtained with a GW Electronics type 113 solid state Backscattered Electron Detector. X-ray analysis was performed on beam spot mode with a Tracer Northern 5500 Energy Dispersive X-ray spectrometer, Model 70152, with a spectral resolution of 145 eV. Detector/sample positioning was set at a 30° take-off angle.

References Cited in Appendices

Bence, A.E. and Albee, A.L., 1968. Empirical correction factors for the electron microanalysis of silicates and oxides. Journal of Geology, v. 76, pp. 382-403.

Flanagan, F.J., 1970. Sources of geochemical standards - II. Geochimica et Cosmochimica Acta, v. 34, pp. 121-125.

Fryer, B.J. and Kerrich, R., 1978. Determination of precious metals at ppb levels in rocks by a combined wet chemical and flameless atomic absorption method. Atomic Absorption Newsletter, 17, pp. 4-6.

Govindaraju, K., 1989. 1989 compilation of working values and sample description for 272 geostandards. Geostandards Newsletter, 13, pp. 1-114.

Jackson, S.E., Fryer, B.J., Gosse, W., Healey, D.C., Longerich, H.P. and Strong, D.F., 1990. Determination of the precious metals in geological materials by inductively coupled plasma-mass spectrometry (ICP-MS) with nickel sulphide fire-assay collection and tellurium coprecipitation. Chemical Geology, v. 83, pp. 119-132.

Jenner, G.A., Longerich, H.P., Jackson, S.E. and Fryer, B.J., 1990. ICP-MS - A powerful tool for high-precision trace-element analysis in Earth sciences: Evidence from analysis of selected U.S.G.S. reference samples. Chemical Geology, v. 83, pp. 133-148.

Jochum, K.P., Seufert, H.M., Midinet-Best, S., Rettmann, E., Schonberger, K. and Zimmer, M., 1988. Multi-element analysis by isotope dilution-spark source mass spectrometry (ID-SSMS). Fresenius Z. Anal. Chem., v. 331, pp. 104-110.

Jochum, K.P., Seufert, H.M. and Thirlwall, M.F., 1990. High-sensitivity Nb analysis by spark-source mass spectrometry (SSMS) and calibration of XRF Nb and Zr. Chemical Geology, v. 81, pp. 1-16.

Langmhyr, F.J. and Paus, P.E., 1968. The analysis of inorganic siliceous materials by atomic absorption spectrophotometry and the hydrofluoric acid decomposition technique. Pt. I. The analysis of silicate rocks. Anal. Chimica Acta, v. 43, pp. 397-408.

Longerich, H.P. and Veinott, G., 1986. Study of precision and accuracy of XRF data obtained in the Department of Earth Sciences and Centre for Earth Resources Research at Memorial University of Newfoundland. Unpublished Report, Department of Earth Sciences and Centre for Earth Resources Research, Memorial University of Newfoundland.

Longerich, H.P., Jenner, G.A., Fryer, B.J. and Jackson, S.E., 1990. Inductively coupled plasma-mass spectrometric analysis of geological samples: A critical evaluation based on case studies. Chemical Geology, v. 83, pp. 105-118.

Robert, R.V.D., van Wyk, E. and Palmer, R., 1971. Concentration of the nobel metals by a fire-assay technique using NiS as the collector. National Institute of Metallurgy, Johannesburg, Report No. 1371, 15 pp.

Shapiro, L. and Brannock, W.W., 1962. Rapid analysis of silicate, carbonate and phosphate rocks. U.S. Geological Survey Bulletin 1144A, pp. 31-33.

Steele, H.F., Levin, J. and Copelowitz, T., 1975. Preparation and certification of a reference sample of a precious metal ore. National Institute of Metallurgy, Johannesburg, Report No. 1696, 50 pp.

LEGEND

Early Aphebian to Helikian

5 — *Diabase and gabbro dykes*

Late Archean

Kanairiktok Intrusive Suite

4 — *Massive to gneissic, white to pink trondhjemites*

Ultramafic Rocks

3 — *Red, tan and green weathering serpentinized peridotites and talc-carbonate rocks ; 3a, Carbonate-quartz rocks*

Florence Lake Group

2 — *White, pink and pale green felsic volcanogenic tuffs and porpl pelitic and cherty metasedimentary rocks; minor mafic metavo*

1 — *Dark to medium green, mafic metavolcanic schists, flows, pillc and synvolcanic sills; minor felsic volcanosedimentary rocks*

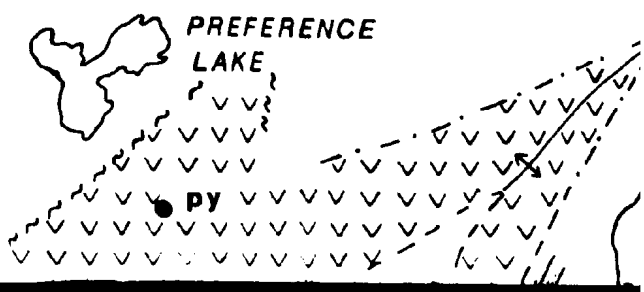

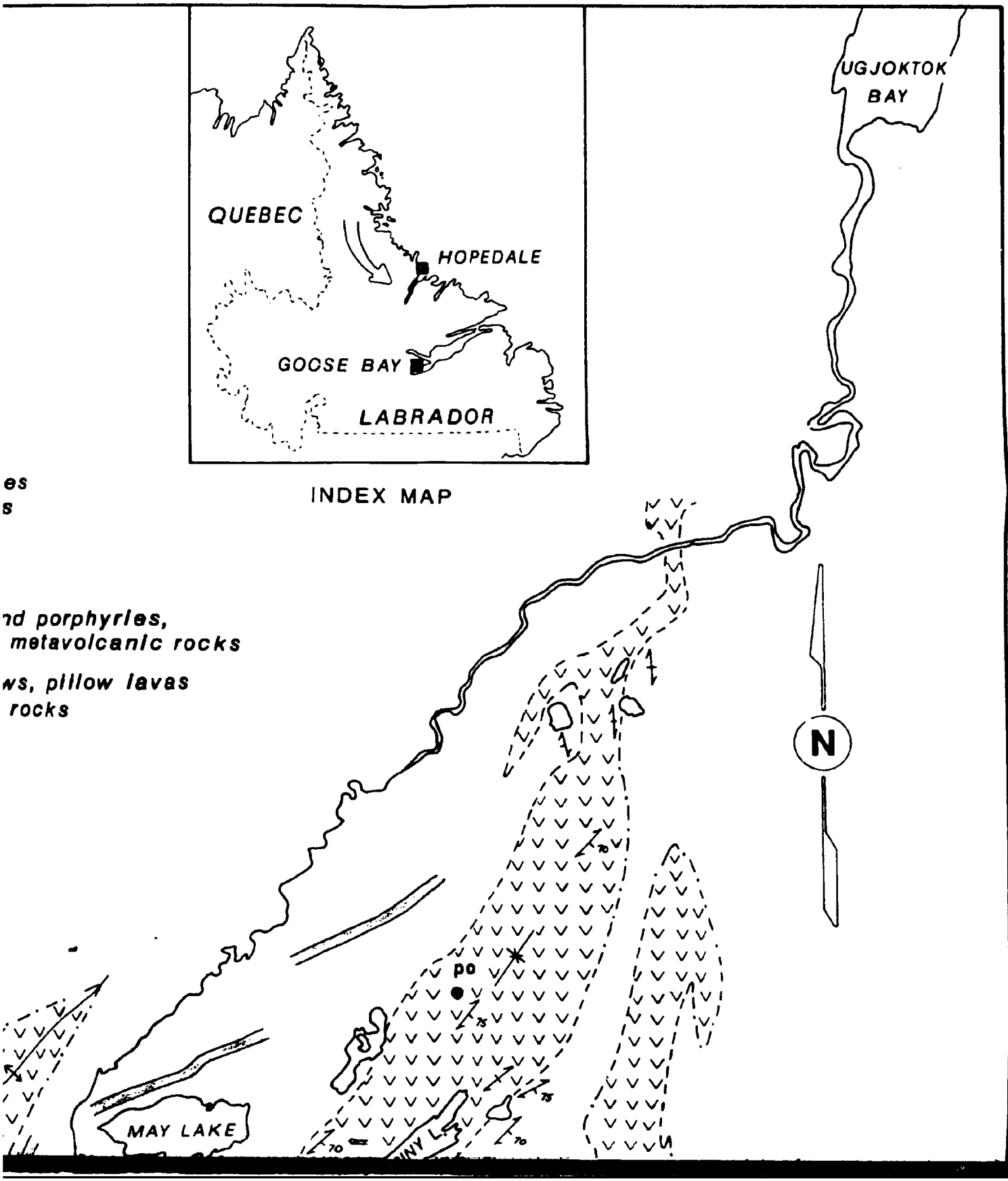

es
s

nd porphyries,
metavolcanic rocks

ws, pillow lavas
rocks

2 *White, pink and pale green felsic volcanogenic tuffs and pelitic and cherty metasedimentary rocks; minor mafic m*

1 *Dark to medium green, mafic metavolcanic schists, flows, and synvolcanic sills; minor felsic volcanosedimentary ro*

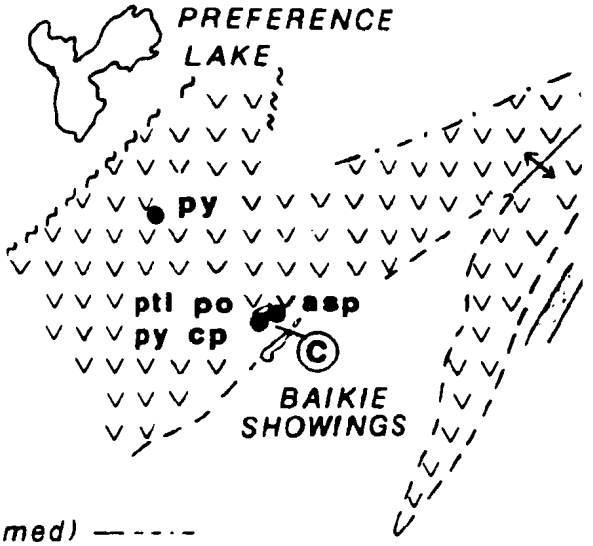

SYMBOLS

Geological boundary (defined, approx., assumed)

Foliation (gneissosity, schistosity, cleavage)

Minor fold (plunge)

Fold (antiform, synform)

Fault

Carbonatization C

MINERAL OCCURRENCE ABBREVIATIONS

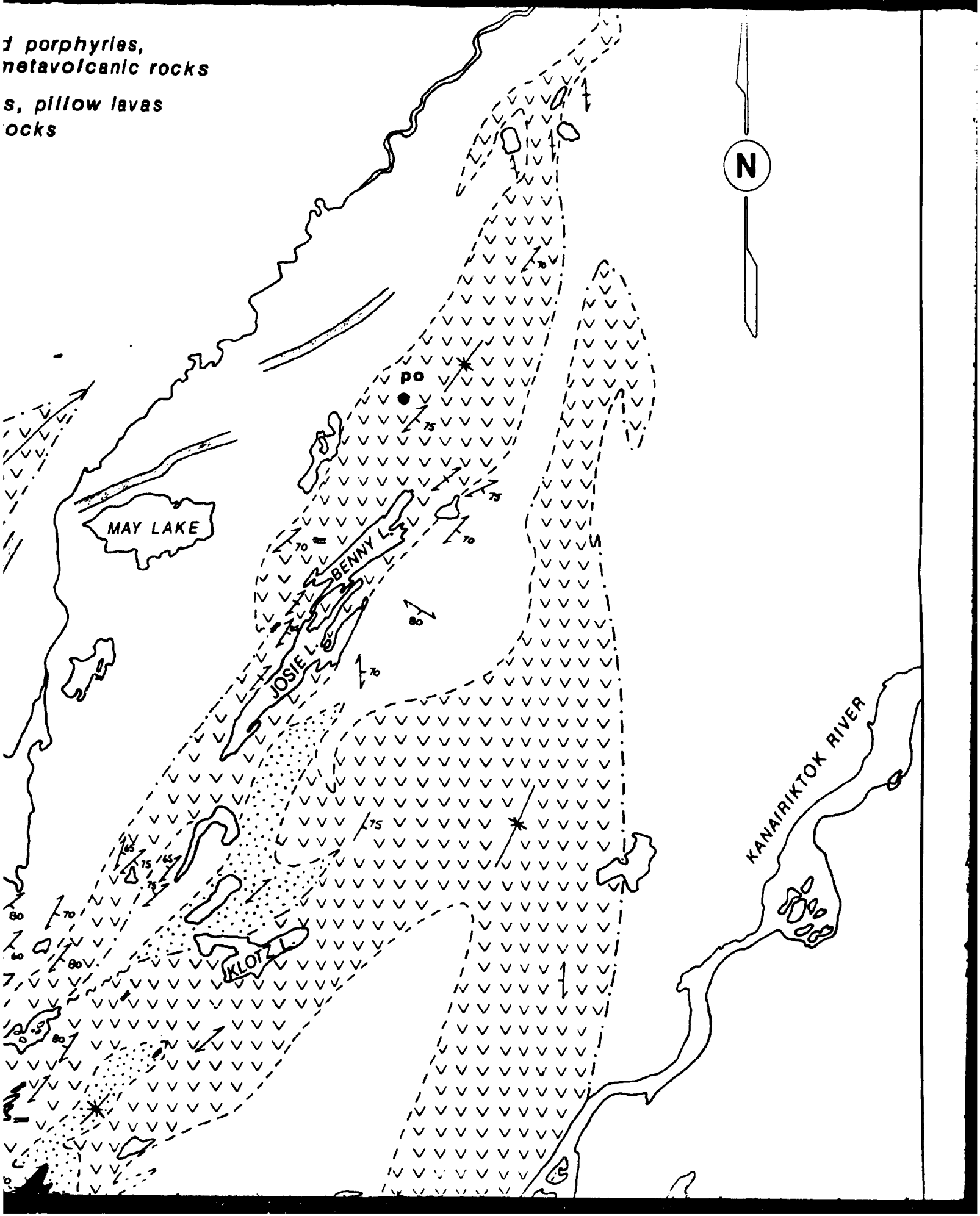
d porphyries,
netavolcanic rocks
s, pillow lavas
ocks
N
po
MAY LAKE
BENNY L.
JOSIE L.
KLOTZ L.
KANAIRIKTOK RIVER

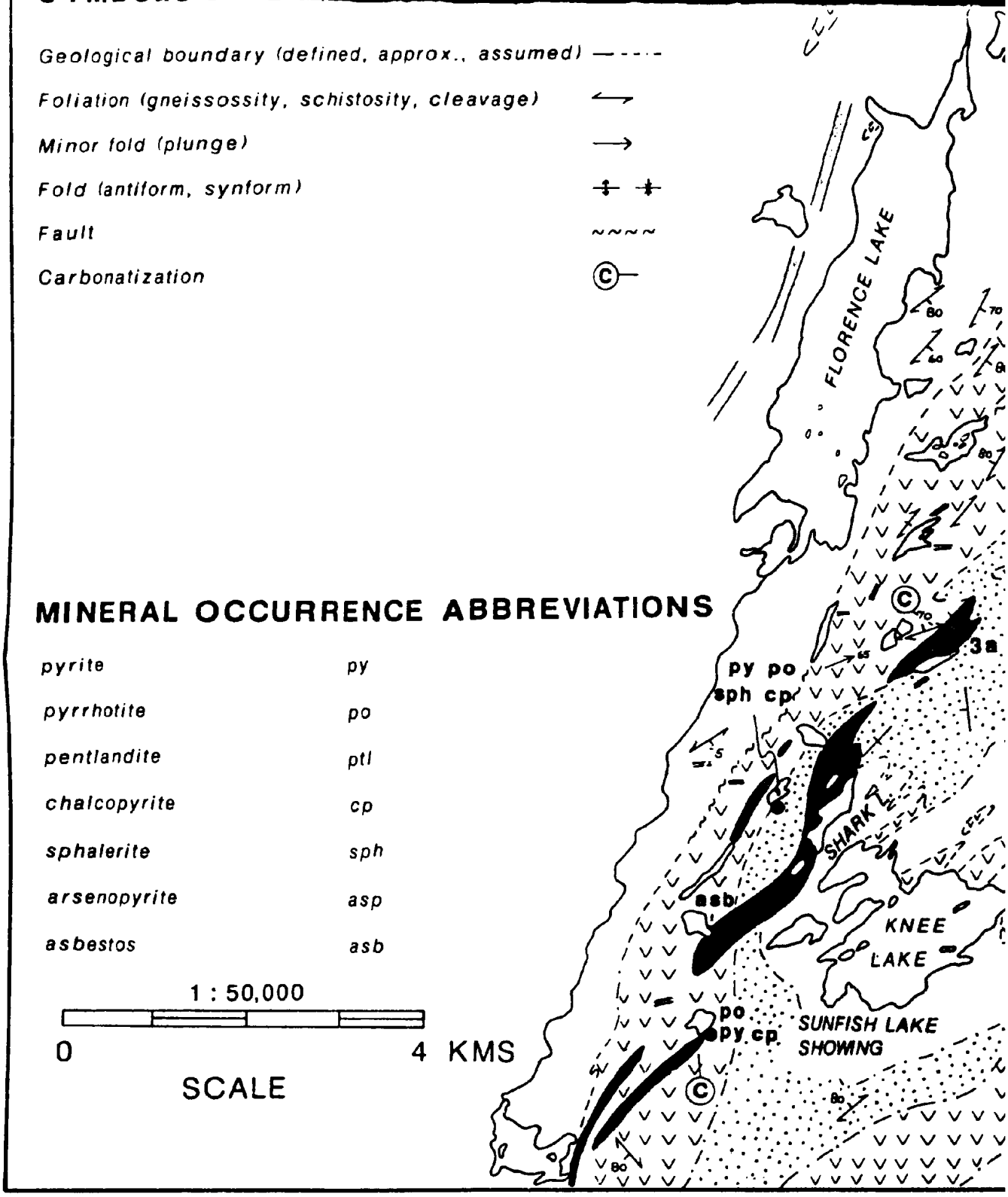

Geology modified after Ermanovics and Raudsepp (1979)

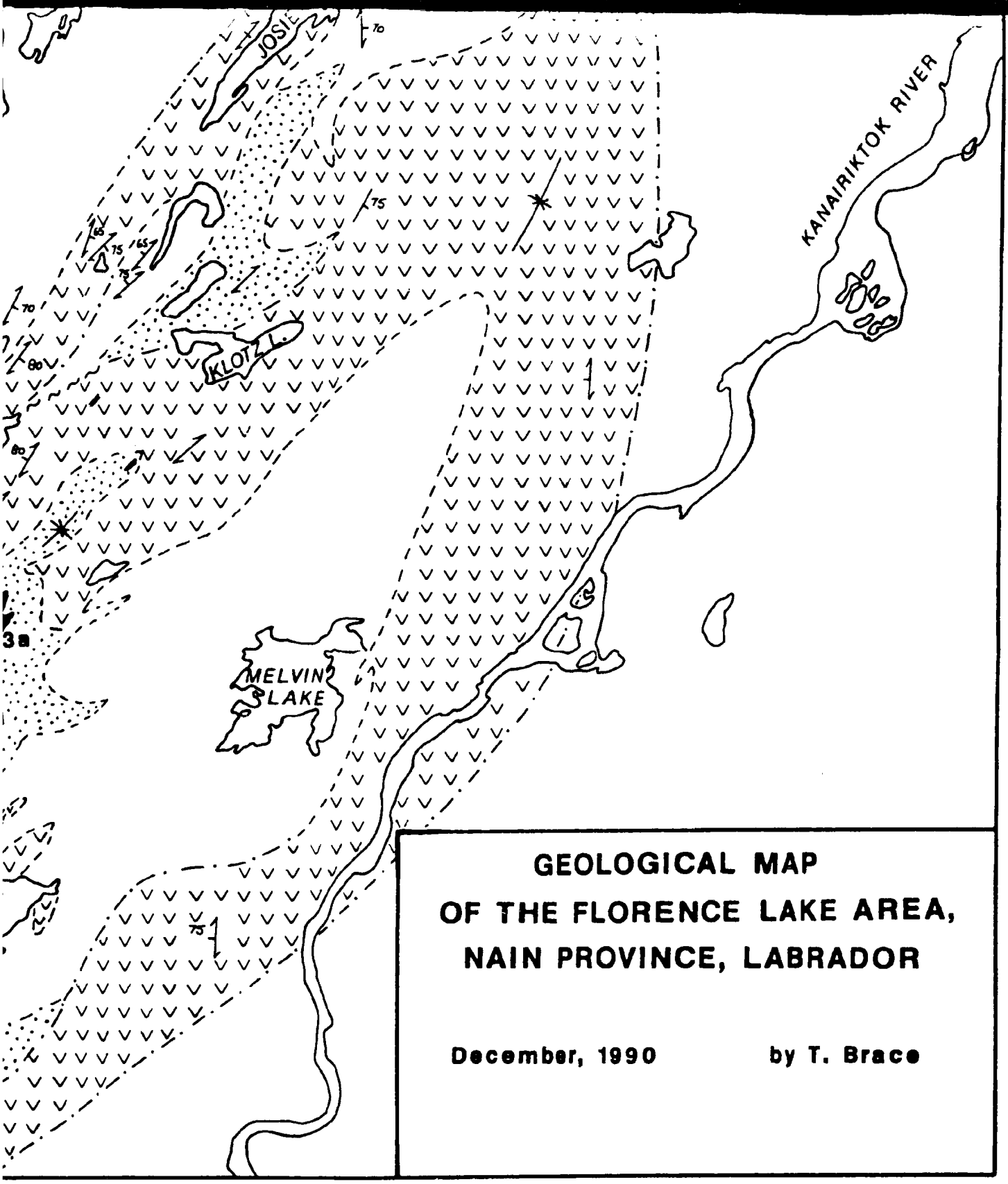

GEOLOGICAL MAP OF THE FLORENCE LAKE AREA, NAIN PROVINCE, LABRADOR

December, 1990

by T. Brace

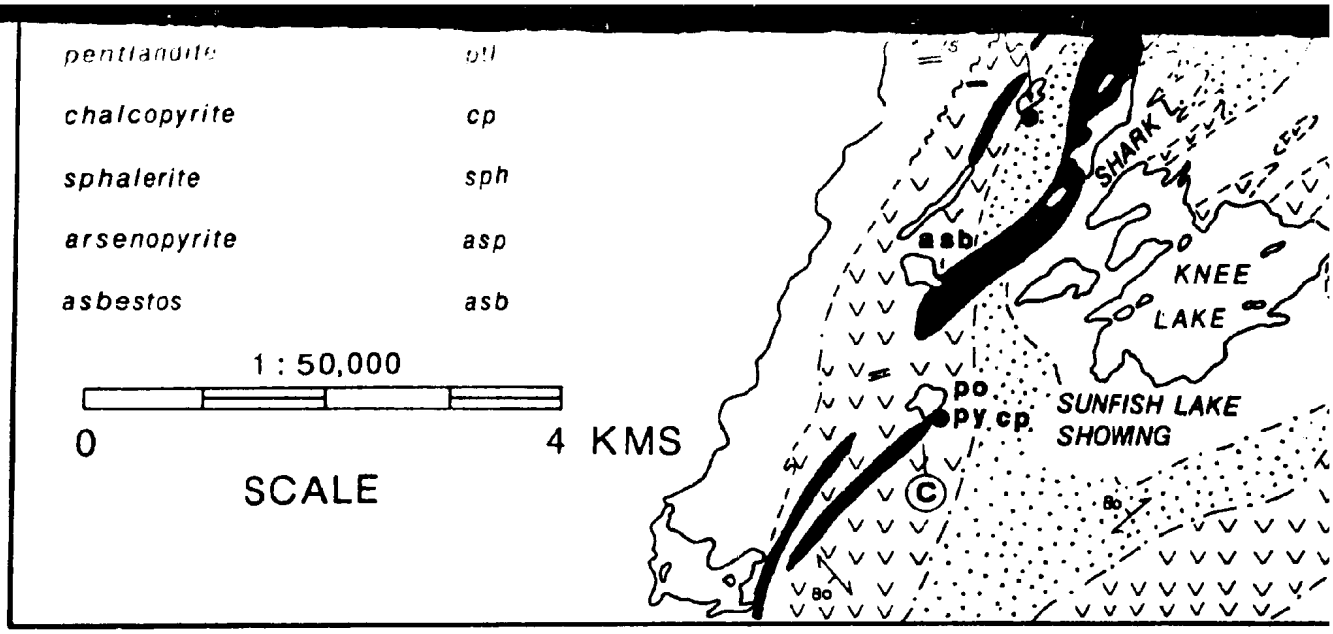

Geology modified after Ermanovics and Raudsepp (1979)

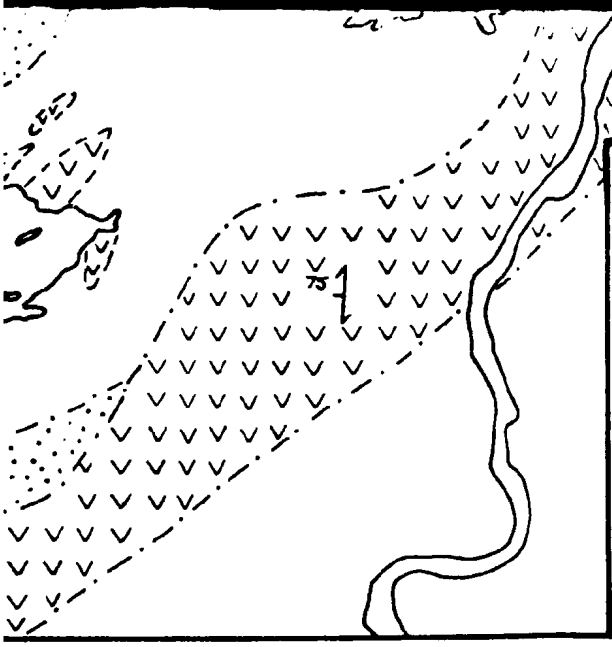

GEOLOGICAL MAP OF THE FLORENCE LAKE AREA, NAIN PROVINCE, LABRADOR

December, 1990

by T. Brace